



**NTNU – Trondheim**  
Norwegian University of  
Science and Technology

# Robotic Assembly Using a 3D Camera

**Martin Morland**

**Geir Ole Tysse**

Subsea Technology

Submission date: June 2015

Supervisor: Olav Egeland, IPK

Norwegian University of Science and Technology  
Department of Production and Quality Engineering



# Robotic assembly using a 3D camera

Martin Morland & Geir Ole Tysse

Spring 2015

PROJECT / MASTER THESIS

Department of Production and Quality Engineering  
Norwegian University of Science and Technology

Supervisor 1: Professor Olav Egeland



---

## MASTEROPPGAVE VÅREN 2015

Martin Morland og Geir Ole Tysse

**Tittel: Robotisert montasje ved bruk av 3D-kamera**

**Tittel (engelsk): Robotic Assembly Using a 3D Camera**

**Oppgavens tekst:**

Ved robotisert montasje i småserieproduksjon kan det være hensiktsmessig å identifisere delenes posisjon og orientering med robotsyn for å sikre korrekt griping og sammensetning. I industriell produksjon med deler i metall vil det være problemer med refleksjon av lys fra metalloverflater, og dette gjør det vanskelig på benytte *key-point descriptors* som SIFT og SURF med vanlige 2D-kamera i stereoarrangement. Videre er stereosyn relativt komplisert å implementere og krever gjerne spesialtilpasning til den konkrete anvendelsen. Det er derfor interessant å studere bruk av 3D-kamera, som er enklere å bruke, og som gir punktskyer som kan være mer robuste enn stereodata. I denne oppgaven skal dette gjøres for sammensetning av bildeler i et eksperiment i instituttets robotlaboratorium. Det skal benyttes et enkelt Asus 3D-kamera.

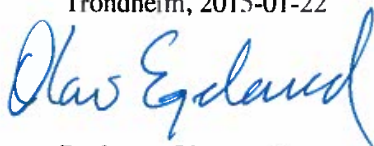
1. Presenter geometrisk algebra og gi et enkelt eksempel på hvordan dette kan brukes i oppgaven.
2. Beskriv kalibrering av interne og eksterne parametere for et 3D-kamera.
3. Beskriv hvordan et 3D-kamera kan benyttes til å bestemme posisjon og orientering av et objekt.
4. Hvis hvordan orientering om lengdeaksen for en sylindrisk del kan bestemmes med et vanlig 2D-kamera.
5. Lag en demonstrasjon av robotisert montasje ved bruk av 3D-kamera.

**Oppgave utlevert: 2015-01-22**

**Innlevering: 2015-06-10**

Utført ved Institutt for produksjons- og kvalitetsteknikk

Trondheim, 2015-01-22



Professor Olav Egeland  
Faglærer



## **Preface**

This is the concluding Master's thesis in the study program Subsea Technology at NTNU. The work was carried out between January and June 2015. The reader should have some elementary knowledge about robotic systems and computer vision.

Trondheim, 2015-06-10

Martin Morland and Geir Ole Tysse





## Acknowledgment

We would like to thank our supervisor Olav Egeland for the lectures given in geometric algebra. We would also like to thank Ph.D. candidate Adam Leon Kleppe for getting us started using Ubuntu, ROS and the robots in this project.

O.N.



## Summary and Conclusions

In this thesis we explain how two parts from the automotive industry can be assembled using an RGB-D camera providing colour (RGB) and depth (D) as a combined RGB-D image, and two KUKA Agilus manipulators with six revolute joints. The RGB-D camera is presented and calibrated, and AR-tags were used to efficiently transform the coordinate frame of the RGB-D camera to a table with the parts. In relation to this, it is shown how geometric algebra can be used to make an orthonormal coordinate frame on the table. Several different methods are presented and evaluated for obtaining the position of the parts, based on data from the RGB-D camera. This includes, a C++ program for segmentation of the scene based on the orientation of the surface normals in the point cloud, and a program based on the geometry of the parts. A method for determining the orientation of the parts, using SIFT (Scale Invariant Feature Transform) and homography based on data from a 2D camera is proposed. We present ROS (Robot Operating System) and how it interacts with the RGB-D camera, 2D camera and the robots. In addition, the forward kinematics of the robots are explained and implemented in ROS.

The experiment was performed as follows: An RGB-D camera positioned at a random place with the AR-tags in the field of view. An algorithm automatically determines the pose of the RGB-D camera with respect to a known coordinate frame. The RGB-D camera was used to measure the coordinates of the parts with respect to the known coordinate frame. A robot with a 2D camera connected to the end-effector, moved to a pose where the 2D camera was vertically above the parts, one at a time. Data from the 2D camera were used in an algorithm for estimating the orientation of the parts. A robot with a gripper connected to the end-effector used the position and orientation of the parts to assemble them.

The results obtained were adequate to perform a simplified assembly task for the parts which require an accuracy of 4 mm. Two demonstration videos have been made. One video demonstrates the estimation of the orientation of the parts. The other video demonstrates how the position of the parts are estimated and how the robot performs the simplified assembly task.



## Sammendrag

Denne rapporten forklarer hvordan to deler fra bilindustrien kan monteres sammen ved bruk av et RGB-D-kamera, som kombinerer farge (RGB) og dybde (D) sammen til et RGB-D-bilde, og to KUKA Agilus manipulatorer med seks roterende ledd. RGB-D-kameraet blir presentert og kalibrert, og AR-merker ble brukt til å effektivt transformere koordinatsystemet til RGB-D-kameraet til et bord med delene på. Med tanke på dette presenteres det også hvordan geometrisk algebra kan benyttes for å lage en ortonormal koordinatsystem på bordet. Flere forskjellige metoder for å innhente posisjonen til delene presenteres og evalueres basert på data fra RGB-D-kameraet. Blant annet, et C++ program som segmenterer scenen basert på orienteringen til overflatenormalene i punktskyen, og et program som baserer seg på delenes geometri. En metode for å bestemme orienteringen til delene, ved å bruke SIFT og homografi basert på data fra 2D-kameraet blir foreslått. Vi presenterer ROS (Robot Operating System) og måten det samhandler med RGB-D-kameraet, 2D-kameraet og robotene. I tillegg, blir robotdirektekinematikken forklart og implementert i ROS.

Eksperimentet ble utført på følgende måte: Et RGB-D-kamera plasseres et tilfeldig sted med AR-merkene på bordet i synsfeltet. En algoritme beregner automatisk posituren til RGB-D-kameraet med hensyn på et kjent koordinatsystem. RGB-D-kameraet ble brukt til å måle koordinatene til delene med i forhold til det kjente koordinatsystemet. En robot med et 2D-kamera festet til end-effektoren flytter 2D kameraet til en positur som er vinkelrett over en av delene, etter tur. Data fra 2D-kameraet benyttes i en algoritme for å estimere orienteringen til delene. En robot med en "griper" påmontert end-effektoren, benytter posisjonen og orienteringen til delene for å montere de sammen.

Resultatene som ble oppnådd var tilstrekkelig for å utføre en forenklet montering av delene, som krevde en nøyaktighet på 4 mm. To demonstrasjonsvideoer har blitt laget. En video demonstrerer hvordan orienteringen bestemmes. Den andre viser hvordan posisjonen til delene blir funnet og hvordan den forenklete monteringen utføres.

# Contents

Preface . . . . .	i
Acknowledgment . . . . .	iii
Summary and Conclusions . . . . .	v
Sammendrag . . . . .	vii
<b>1 Introduction</b>	<b>3</b>
1.1 Background . . . . .	3
1.2 Structure of the Report . . . . .	4
<b>2 Geometric Algebra</b>	<b>5</b>
2.0.1 Geometric product . . . . .	5
2.0.2 The Outer Product Null Space . . . . .	7
2.0.3 The Inner Product Null Space . . . . .	8
2.0.4 The Dual . . . . .	9
2.0.5 The Vector-Bivector Geometric Product . . . . .	11
<b>3 Camera</b>	<b>13</b>
3.1 Central Projection Model . . . . .	13
3.2 RGB-D Camera . . . . .	16
3.2.1 Calibration of the Asus Xtion PRO LIVE . . . . .	21
<b>4 Computer Vision</b>	<b>25</b>
4.1 Relevant Theoretical Background Information for 2D Camera . . . . .	25
4.1.1 SIFT . . . . .	25
4.1.2 Homography . . . . .	32
4.2 Relevant Theoretical Background Information for RGB-D Camera . . . . .	34
4.2.1 AR-tags . . . . .	34
4.2.2 Estimating Surface Normals in a Point Cloud . . . . .	36
4.2.3 PFH - Point Feature Histogram . . . . .	39
4.2.4 FPFH - Fast Point Feature Histogram . . . . .	43
4.3 Program Code for Depth Camera . . . . .	44
4.3.1 Aligning Object Templates to a Point Cloud . . . . .	44
4.3.2 Region Growing Segmentation . . . . .	46
4.3.3 Statistical Removal of Outliers . . . . .	51
<b>5 Computer Vision Experiments and Results</b>	<b>53</b>

5.1	Experiments based on the RGB-D Camera . . . . .	53
5.1.1	Calibration of AR-tag Coordinate Frame . . . . .	53
5.1.2	Calibration of the Table Coordinate Frame . . . . .	61
5.1.3	Template Alignment . . . . .	65
5.1.4	Region Growing Segmentation . . . . .	72
5.1.5	Segmentation based on known Geometry . . . . .	74
5.1.6	Analysis . . . . .	77
5.2	Experiments based on the 2D Camera . . . . .	84
5.2.1	Orientation of the Objects . . . . .	84
<b>6</b>	<b>Kinematics</b>	<b>94</b>
6.1	Robot Forward Kinematics . . . . .	95
6.2	Kinematics Result . . . . .	100
6.2.1	Robot with a 2D Camera Connected to End-Effector . . . . .	100
6.2.2	Robot with a Gripper Connected to End-Effector . . . . .	104
6.2.3	The Kinematics Sequence . . . . .	106
<b>7</b>	<b>ROS</b>	<b>109</b>
7.1	The Robots . . . . .	109
7.2	Implementation of RGB-D Camera . . . . .	111
7.3	Implementation of Robot with a 2D Camera Connected to End-Effector . . . . .	112
7.4	Implementation of 2D Camera . . . . .	114
7.5	Implementation of Robot with a Gripper Connected to End-Effector . . . . .	115
<b>8</b>	<b>Concluding Remarks</b>	<b>117</b>
8.1	Discussion . . . . .	117
8.2	Summary and Conclusions . . . . .	118
8.3	Recommendations for Further Work . . . . .	118
<b>A</b>	<b>Source Code</b>	<b>121</b>
	<b>Bibliography</b>	<b>200</b>





# Chapter 1

## Introduction

### 1.1 Background

Applications of robots in the industry have widened to ameliorate the complexity of factory automation systems. An increasing interest in regard to robotic material handling have been to reduce the cost of installation of a factory automation system while improving productivity [7]. When using grasping robotic systems to assemble parts, it is convenient to identify the position and orientation of the parts. This task can be solved by obtaining depth images of the operational area of the robot. Conventional 2D cameras in stereo arrangement are able to capture depth information in images, but it is relatively complicated to implement and may need special adjustment for the specific task. Low-cost consumer depth cameras have risen to widespread prevalence across many areas of 3D computer vision [17]. Recent RGB-D cameras (3D cameras), such as the Microsoft Kinect or Asus Xtion PRO LIVE, acquire both visual information (RGB) like regular camera systems, along with per-pixel depth information (D) at high frame rates. In terms of real-time performance and general depth accuracy, RGB-D cameras outperform common stereo vision approaches on texture-less object surfaces [17].

Other research groups have developed systems for detecting and grasping objects using a depth camera. A prominent example is found in a paper by Kim et al. [7], where both 3D point cloud and CAD data are segmented to simple primitives as plane, cylinder and cone for object recognition, pose estimation and object grasping. Stückler et al. [27] describe efficient methods for tackling everyday mobile manipulation tasks that require object pick-up. They have developed scene segmentation methods that process depth images in real-time at high frame rates for 3D perception of objects on planar surfaces. Lin and Setiawan [10] uses Scale Invariant Feature Transform (SIFT) for recognition and Support Vector Machine (SVM) to determine the orientation of an object, using a stereo camera.

In this thesis we will study the use of RGB-D camera in robotic assembly of automotive parts, more particularly a piston and a cylinder as shown in Figure 1.1. The intrinsic parameters of the RGB-D camera is calibrated and an efficient method to transform the coordinate frame of the RGB-D camera on to a table using AR-tags proposed. For this purpose, geometric algebra can be used to easily create an orthogonal coordinate frame. Different approaches for measuring the coordinates of the parts from an RGB-D camera are explained. Analysis of accuracy and repeatability related to these measurements are performed. This includes a scene segmentation

method based on the orientation of the surface normals. We propose a method for determining the orientation around the length axis of the objects using a 2D camera, SIFT and homography. The kinematics for assembling the parts with a robot is explained. ROS (Robot Operating System) and how it is applied to solve the kinematics is presented.

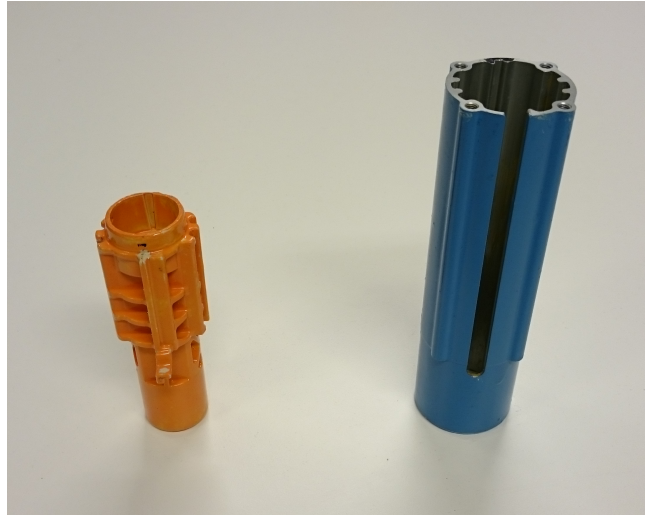


Figure 1.1: The the piston (orange) and cylinder (blue).

The practical work has been performed in the lab at the Department of Production and Quality Engineering, NTNU. Two KUKA Agilus robot cells with six revolute joints and an RGB-D camera (Asus Xtion PRO LIVE) were used in the process of assembling the piston and the cylinder.

## 1.2 Structure of the Report

The rest of the report is organized as follows:

- Chapter 2 gives an introduction to geometric algebra.
- Chapter 3 contains information about the RGB-D camera and calibration.
- Chapter 4 contains theoretical background information relevant for different aspects of computer vision used in the thesis.
- Chapter 5 contains experiments conducted and analysis of the results.
- Chapter 6 addresses the forward kinematics and the homogeneous transformations between robot and camera.
- Chapter 7 presents the implementation in ROS.
- Chapter 8 presents the concluding remarks in form of discussion, conclusion and recommendations for further work.

## Chapter 2

# Geometric Algebra

This chapter will give an introduction to geometric algebra.

Geometric algebra recognise lines, areas, volumes and hyper-volumes as structures with *magnitude* and *orientation*. The foundation of geometric algebra is the *geometric product* [30].

### 2.0.1 Geometric product

Two vectors  $a$  and  $b$  in a 2D Euclidean space  $\mathbb{R}^2$ , can be described as

$$a = a_1e_1 + a_2e_2 \quad , \quad b = b_1e_1 + b_2e_2$$

where  $a_i$  and  $b_i$  are components with respect to the unit basis vectors  $e_1$  and  $e_2$ .

The geometric product of  $a$  and  $b$  is

$$ab = \underbrace{a \cdot b}_{\text{inner product}} + \underbrace{a \wedge b}_{\text{outer product}} \quad (2.1)$$

The inner product of equation (2.1) is

$$\begin{aligned} a \cdot b &= (a_1e_1 + a_2e_2) \cdot (b_1e_1 + b_2e_2) \\ &= a_1b_1e_1 \cdot e_1 + a_1b_2e_1 \cdot e_2 + a_2b_1e_1 \cdot e_2 + a_2b_2e_2 \cdot e_2 \\ &= a_1b_1 + a_2b_2 \end{aligned} \quad (2.2)$$

which gives a scalar. For vectors  $a, b \in \mathbb{R}^n$ , their inner product is just the same as their scalar product, where

$$e_i \cdot e_j = 0 \quad , \quad e_i \cdot e_i = 1$$

The outer product of equation (2.1) is

$$\begin{aligned} a \wedge b &= (a_1e_1 + a_2e_2) \wedge (b_1e_1 + b_2e_2) \\ &= a_1b_1e_1 \wedge e_1 + a_1b_2e_1 \wedge e_2 + a_2b_1e_2 \wedge e_1 + a_2b_2e_2 \wedge e_2 \\ &= (a_1b_2 - a_2b_1)e_1 \wedge e_2 \end{aligned} \quad (2.3)$$

where

$$e_i \wedge e_i = 0 \quad , \quad e_i \wedge e_j = -e_j \wedge e_i$$

Equation (2.3) results in a scalar term  $a_1b_2 - a_2b_1$  that defines a signed area, whilst the unit bivector term  $e_1 \wedge e_2$  identifies a plane associated with the area. The orientation of the plane is defined by its bivector components [30], [28]. The bivector term  $e_1 \wedge e_2$  means that orientation of the surface is anticlockwise, as depicted by the directed circle in figure (2.1).

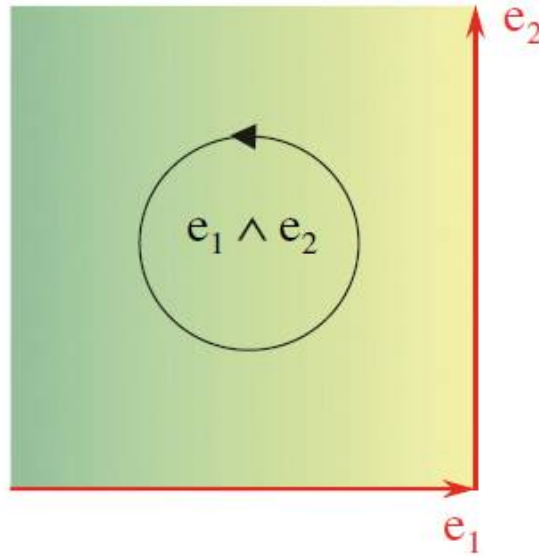


Figure 2.1: Orientation of  $e_1 \wedge e_2$  [30].

For two identical basis vectors, the geometric product is

$$e_i e_i = e_i \cdot e_i + e_i \wedge e_i = e_i^2 = 1$$

and the product of two orthogonal basis vectors is

$$e_i e_j = e_i \cdot e_j + e_i \wedge e_j = e_i \wedge e_j$$

The geometric product of two vectors  $a$  and  $b$

$$a = a_1 e_1 + a_2 e_2 + a_3 e_3 \quad , \quad b = b_1 e_1 + b_2 e_2 + b_3 e_3$$

in a 3D Euclidean space  $\mathbb{R}^3$  with basis vectors  $e_1$ ,  $e_2$  and  $e_3$ , is

$$ab = \underbrace{a \cdot b}_{\text{inner product}} + \underbrace{a \wedge b}_{\text{outer product}} \quad (2.4)$$

where

$$\begin{aligned} a \cdot b &= (a_1e_1 + a_2e_2 + a_3e_3) \cdot (b_1e_1 + b_2e_2 + b_3e_3) \\ a \cdot b &= a_1b_1 + a_2b_2 + a_3b_3 \end{aligned} \quad (2.5)$$

and

$$\begin{aligned} a \wedge b &= (a_1e_1 + a_2e_2 + a_3e_3) \wedge (b_1e_1 + b_2e_2 + b_3e_3) \\ a \wedge b &= (a_1b_2 - a_2b_1)e_1 \wedge e_2 + (a_2b_3 - a_3b_2)e_2 \wedge e_3 + (a_3b_1 - a_1b_3)e_3 \wedge e_1 \\ a \wedge b &= (a_1b_2 - a_2b_1)e_1e_2 + (a_2b_3 - a_3b_2)e_2e_3 + (a_3b_1 - a_1b_3)e_3e_1 \end{aligned} \quad (2.6)$$

The outer product of  $k$  linearly independent vectors is called a  $k$ -blade with the following order:

scalar = 0 – blade  
vector = 1 – blade  
bivector = 2 – blade  
trivector = 3 – blade  
quadvector = 4 – blade

where  $k$  identifies the grade of a blade [30]. Table 2.1 shows the  $k$ -blades in a 3D Euclidean space  $\mathbb{R}^3$ . In such graded algebras it is tradition to call the highest grade element a *pseudoscalar*

$k$	basis $k$ -blades	total
0 (scalar)	{1}	1
1 (vector)	{ $e_1, e_2, e_3$ }	3
2 (bivector)	{ $e_{12}, e_{23}, e_{31}$ }	3
3 (trivector)	{ $e_{123}$ }	1

Table 2.1:  $k$ -blades in  $\mathbb{R}^3$ .

$I$  [30]. In  $\mathbb{R}^3$ , the pseudoscalar is the trivector  $I = e_1e_2e_3 = e_{123}$ .

### 2.0.2 The Outer Product Null Space

The outer product null space  $\text{NO}(a)$  of a vector  $a$  in Euclidean space  $\mathbb{R}^3$  is given by the set of vectors  $x \in \mathbb{R}^3$  that satisfy  $x \wedge a = 0$ . That is,

$$\text{NO}(a) = \{x \in \mathbb{R}^3 : x \wedge a = 0\} = \{x = \alpha a : \alpha \in \mathbb{R}\}$$

The outer product null space of a vector  $a$  is a line through the origin with direction of  $a$ , because  $x \wedge a$  is zero if  $x$  is linearly dependent on  $a$  [28] [3].

Given a 2-blade  $a \wedge b$ , where  $a$  and  $b$  are two vectors in Euclidean space  $\mathbb{R}^3$ . The outer product null space  $\text{NO}(a \wedge b)$  is

$$\text{NO}(a \wedge b) = \{x \in \mathbb{R}^3 : x \wedge (a \wedge b) = 0\} = \{x = \alpha a + \beta b : \alpha, \beta \in \mathbb{R}\}$$

the set of vectors  $x$  satisfying  $x \wedge (a \wedge b) = 0$ . This is a set of vectors  $x$  that are in the plane defined by the bivector  $a \wedge b$ .

In Figure 2.2 the green plane is  $\text{NO}(a \wedge b)$ , where  $a$  and  $b$  are two vectors in  $\mathbb{R}^3$ . The plane goes through origin of the Euclidean space  $\mathbb{R}^3$ .

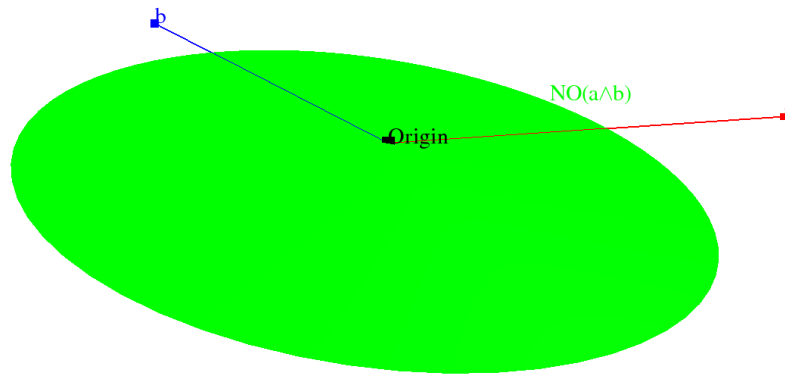


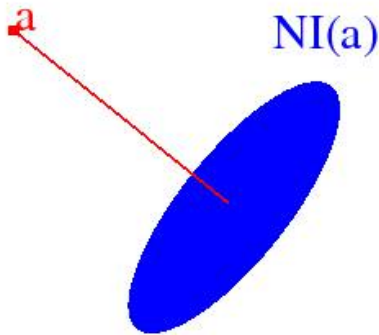
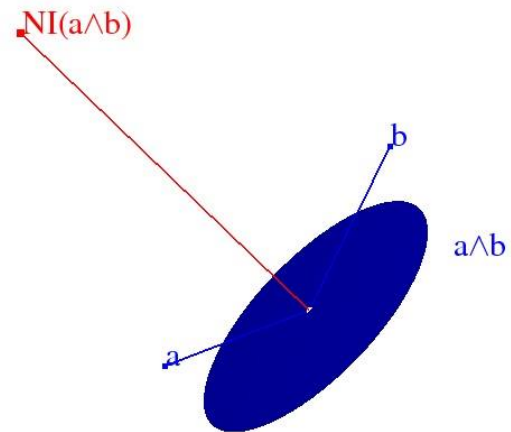
Figure 2.2:  $\text{NO}(a \wedge b)$ .

### 2.0.3 The Inner Product Null Space

The inner product null space  $\text{NI}(a)$  of a vector  $a$  in Euclidean space  $\mathbb{R}^3$  is given by the set of vectors  $x \in \mathbb{R}^3$  that satisfy  $x \cdot a = 0$ , that is

$$\text{NI}(a) = \{x \in \mathbb{R}^3 : x \cdot a = 0\}$$

This implies that the set of vectors  $x$  are orthogonal to  $a$ , which makes  $\text{NI}(a)$  a plane that has  $a$  as the normal vector [28][3]. This is shown in Figure 2.3.

Figure 2.3:  $\text{NI}(a)$ .Figure 2.4:  $\text{NI}(a \wedge b)$ .

The  $\text{NI}(a \wedge b)$  of a blade  $a \wedge b$  is given by the set of vectors  $x$  that satisfy  $x \cdot (a \wedge b) = 0$ , that is,

$$\text{NI}(a \wedge b) = \{x \in \mathbb{R}^3 : x \cdot (a \wedge b) = 0\}$$

This implies that  $x$  must be orthogonal to the plane defined by  $a \wedge b$ . This is shown in Figure 2.4.

#### 2.0.4 The Dual

Let  $\{e_1, e_2, e_3\}$  denote again the orthonormal basis of  $\mathbb{R}^3$ . The  $\text{NI}(e_1)$  is

$$\text{NI}(e_1) = \{\alpha e_2 + \beta e_3 : \alpha, \beta \in \mathbb{R}\}$$

the plane spanned by  $e_2$  and  $e_3$ .

The  $\text{NO}(e_2 \wedge e_3)$  is also

$$\text{NO}(e_2 \wedge e_3) = \{\alpha e_2 + \beta e_3 : \alpha, \beta \in \mathbb{R}\}$$

which implies that it is relation between the concepts of the  $\text{NO}$  and  $\text{NI}$  [28]. This relation is *duality*.

Consider a vector  $a$

$$a = a_1 e_1 + a_2 e_2$$

in a 2D Euclidean space  $\mathbb{R}^2$  with basis vectors  $e_1$  and  $e_2$ . The vector  $a$  in geometric product with the pseudoscalar  $I$  ( $I = e_{12}$  in  $\mathbb{R}^2$ ) gives

$$\begin{aligned}
 aI &= (a_1e_1 + a_2e_2)e_{12} \\
 &= a_1e_{112} + a_2e_{212} \\
 &= -a_2e_1 + a_1e_2
 \end{aligned}$$

a vector  $-a_2e_1 + a_1e_2$  that has been rotated anticlockwise  $90^\circ$ . This is shown in Figure 2.5. The vector  $-a_2e_1 + a_1e_2$  in geometric product with the inverse of the pseudoscalar  $I^{-1} = e_{21}$  gives

$$\begin{aligned}
 (-a_2e_1 + a_1e_2)e_{21} &= -a_2e_{121} + a_1e_{221} \\
 &= a_2e_2 + a_1e_1
 \end{aligned}$$

the original vector  $a$ . The geometric product of the vector  $-a_2e_1 + a_1e_2$  and the inverse of the pseudoscalar  $I^{-1}$ , rotate the vector  $-a_2e_1 + a_1e_2$   $90^\circ$  clockwise back to the original vector  $a$ .

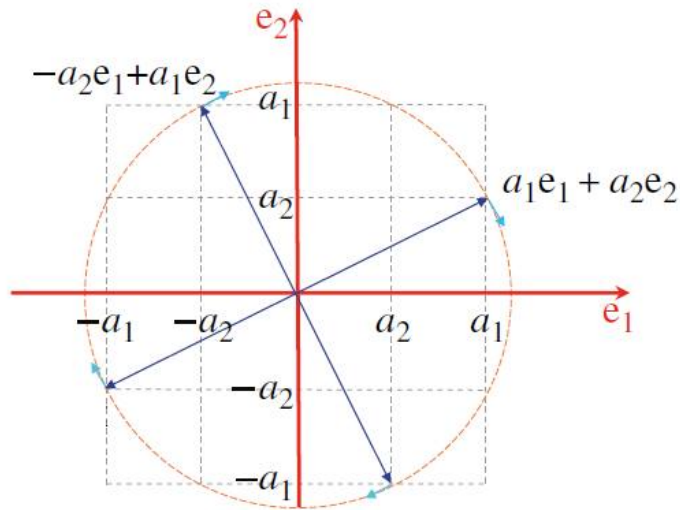


Figure 2.5: Rotation of  $a$  in  $e_{12}$  [30].

The *dual*  $a^*$  of a vector  $a$  is

$$a^* = aI^{-1}$$

In Euclidean space  $\mathbb{R}^3$ , the dual of the basis vectors  $e_1$ ,  $e_2$  and  $e_3$  are

$$\begin{aligned}
 e_1^* &= e_1e_{321} = -e_{1123} = -e_{23} = -e_2 \wedge e_3 \\
 e_2^* &= e_2e_{321} = -e_{3221} = -e_{31} = -e_3 \wedge e_1 \\
 e_3^* &= e_3e_{321} = -e_{3312} = -e_{12} = -e_1 \wedge e_2
 \end{aligned}$$



The dual of the unit bivectors  $e_1 \wedge e_2$ ,  $e_2 \wedge e_3$  and  $e_3 \wedge e_1$  are

$$(e_1 \wedge e_2)^* = e_{12}e_{321} = e_{11223} = e_3$$

$$(e_2 \wedge e_3)^* = e_{23}e_{321} = e_{33221} = e_1$$

$$(e_3 \wedge e_1)^* = e_{31}e_{321} = e_{33112} = e_2$$

[30][28]

In Euclidean space  $\mathbb{R}^3$  the unit bivectors  $e_1 \wedge e_2$  is in the  $x y$  plane. The dual  $(e_1 \wedge e_2)^* = e_3$  is the unit vector in the  $z$  direction, and the normal to the plane. This is shown in Figure 2.6.

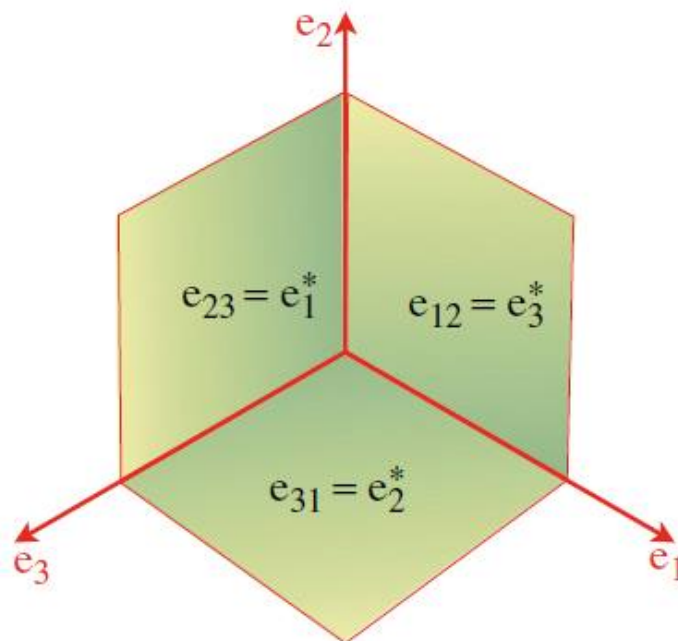


Figure 2.6: Dual [30].

### 2.0.5 The Vector-Bivector Geometric Product

As already mentioned, a pseudoscalar  $I = e_{12}$  in  $\mathbb{R}^2$  rotates a vector  $90^\circ$  when it is in geometric product with the vector.

A vector  $a$  in  $\mathbb{R}^3$

$$a = a_1e_1 + a_2e_2 + a_3e_3$$

in geometric product with a bivector  $e_1 \wedge e_2$  gives

$$\begin{aligned}
 e_{12}a &= a_1e_{121} + a_2e_{12}e_2 + a_3e_{12}e_3 \\
 &= a_1e_{121} + a_2e_{122} + a_3e_{123} \\
 &= a_2e_1 - a_1e_2 + a_3e_{123}
 \end{aligned}$$

a vector  $a_2e_1 - a_1e_2$  and a trivector  $a_3e_{123}$ . These are shown in Figure 2.7. The component of the vector  $a$  contained within the bivector has been rotated clockwise  $90^\circ$  while the vector component orthogonal to the bivector has created a volume. Post-multiplying the vector  $a$  by the same bivector will give a vector that has been rotated anti-clockwise  $90^\circ$  and the same trivector.

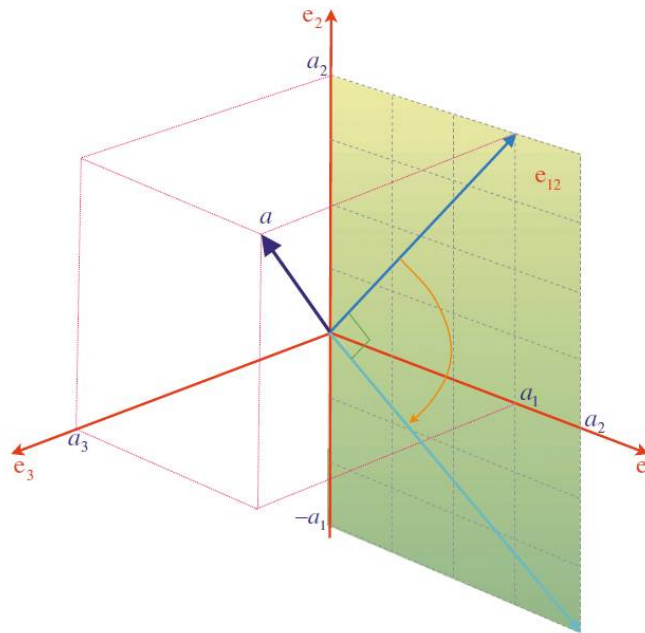


Figure 2.7: Geometric product of a vector  $a$  and a bivector  $e_1 \wedge e_2$  [30].

If the vector  $a$  lies in the plane defined by the bivector  $e_1 \wedge e_2$ , that is

$$a = a_1e_1 + a_2e_2 + 0e_3$$

then the geometric product of the vector  $a$  and the bivector would result in a vector that has been rotated  $90^\circ$  in the plane, and none trivector. The geometric product

$$ae_{12} = \underbrace{a \cdot e_{12}}_{\text{inner product}} + \underbrace{a \wedge e_{12}}_{\text{outer product}}$$

gives a outer product  $a \wedge e_{12} = 0$ , since the vector  $a$  lies in the plane defined by  $e_1 \wedge e_2$ . This means that the inner product part  $a \cdot e_{12}$  is the operation which take the component of the vector  $a$  contained within the bivector, and rotate it  $90^\circ$ .

## Chapter 3

# Camera

### 3.1 Central Projection Model

The central projection model explains fundamental geometry to project three-dimensional points, curves and surfaces on a two-dimensional plane, the image plane. It models a perspective transformation where the image plane is placed in front of the lens. Light rays reflected from objects in the world penetrates the image plane before they converge in the camera center as shown in Figure 3.1 [2]. A point  $P = (X, Y, Z)^T$  with Cartesian coordinates in world is projected on to the image plane

$$x = \frac{fX}{Z} \quad , \quad y = \frac{fY}{Z} \quad (3.1)$$

at the point  $p = (x, y)^T$  given in Cartesian image coordinates.  $f$  is the distance from the camera center to the principal point, known as the focal length. This transformation from three dimensions to two dimensions is called a projective transformation. The consequence of losing a dimension is that angles and distances are not preserved when transformed in to the image plane. A point on the image plane  $p = (x, y)^T$  can be represented by homogeneous coordinates  $\tilde{p} = (x, y, 1)^T$ . A point in the image plane expressed in homogeneous coordinates  $\tilde{p} = (\tilde{x}, \tilde{y}, \tilde{z})^T$  can also be represented by Cartesian coordinates like so

$$x = \frac{\tilde{x}}{\tilde{z}} \quad , \quad y = \frac{\tilde{y}}{\tilde{z}} \quad (3.2)$$

A point in the image plane expressed in homogeneous coordinates  $p = (\tilde{x}, \tilde{y}, \tilde{z})^T$  represents the same point with

$$p = \begin{pmatrix} \tilde{x} \\ \tilde{y} \\ \tilde{z} \end{pmatrix}$$

Equation 3.1 can be derived to

$$\tilde{x} = fX \quad , \quad \tilde{y} = fY \quad , \quad \tilde{z} = Z \quad (3.3)$$

where  $P = (X, Y, Z)^T$  is a point in the world [2]. The use of equation (3.1) with homogeneous coordinates makes a linear transformation which is beneficial in calculations.

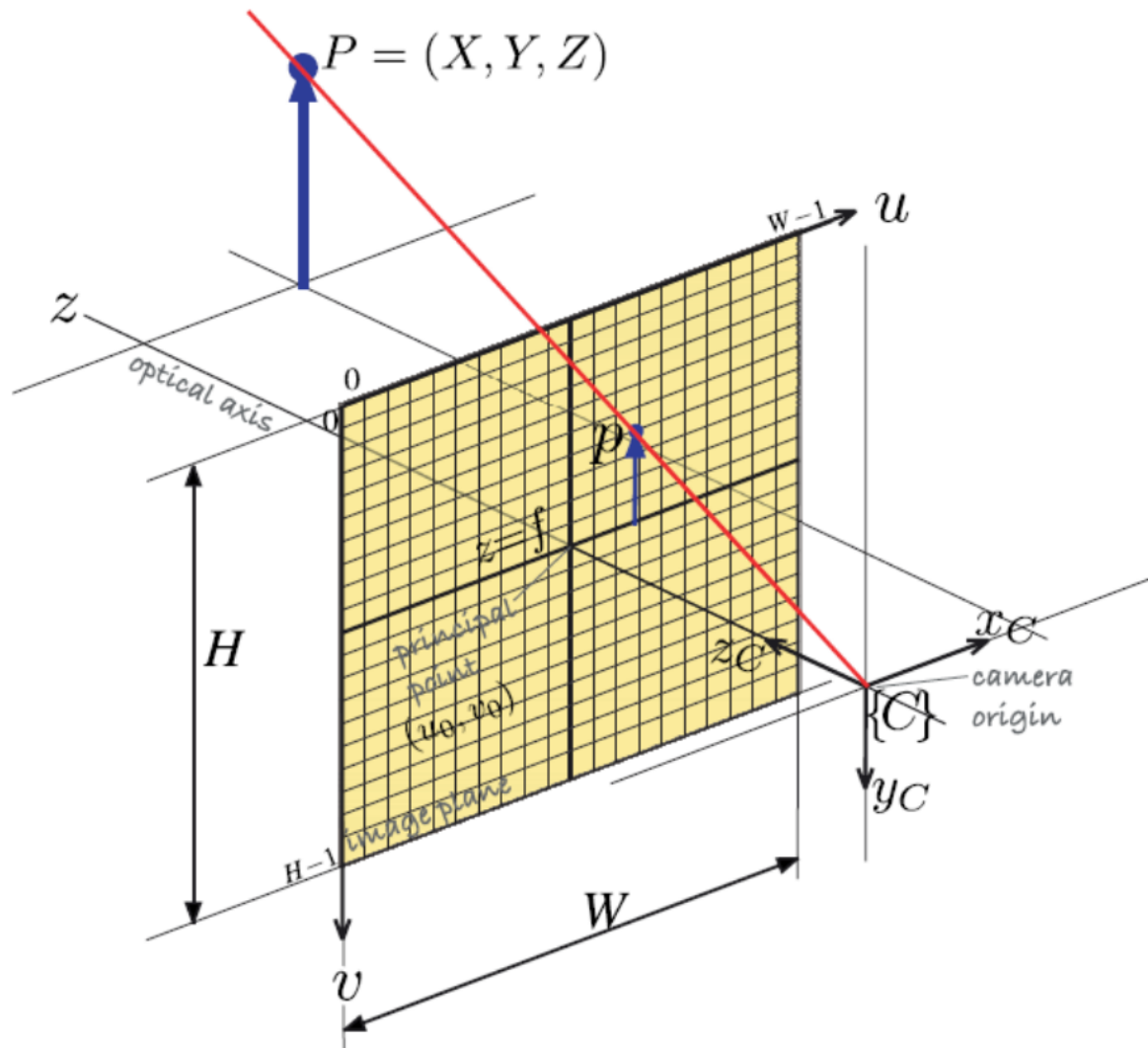


Figure 3.1: The central projection model [2].

In a digital camera, like the Asus Xtion Pro Live and the Logitech HD Pro Webcam C920, the image plane consists of a grid of pixels as shown in Figure 3.1. The pixel coordinates are  $(u, v)$  where  $u$  represents the horizontal axis and  $v$  represents the vertical axis. The coordinates of a point in the world must be scaled down to fit in the image plane. A physical image plane represented in Cartesian coordinates, has its origin in the point where the optical axis penetrates the the image plane. A digital image plane with pixel coordinates on the other hand, have its origin in the upper left corner [2]. A transformation from Cartesian image coordinates  $(x, y)$  to pixel coordinates  $(u, v)$  is

$$u = \frac{x}{\rho_w} + u_0 \quad , \quad v = \frac{y}{\rho_h} + v_0 \quad (3.4)$$

where  $\rho_w$  and  $\rho_h$  is the width and height of a pixel respectively, and  $u_0$  and  $v_0$  are the pixel coordinates where the optical axis penetrates the image plane. The relation between pixel coordinates  $(u, v)$  and homogeneous pixel coordinates  $(\tilde{u}, \tilde{v}, \tilde{w})$  is

$$u = \frac{\tilde{u}}{\tilde{w}} \quad , \quad v = \frac{\tilde{v}}{\tilde{w}} \quad (3.5)$$

Homogeneous pixel coordinates can be expressed by

$$\tilde{u} = \frac{\tilde{x}}{\rho_w} + u_0 \quad , \quad \tilde{v} = \frac{\tilde{y}}{\rho_h} + v_0 \quad , \quad \tilde{w} = \tilde{z} \quad (3.6)$$

Equation (3.6) and equation (3.1) can be derived to

$$\tilde{u} = \frac{fX}{\rho_w} + u_0 \quad , \quad \tilde{v} = \frac{fY}{\rho_h} + v_0 \quad , \quad \tilde{w} = Z \quad (3.7)$$

where the point  $P = (X, Y, Z)$  is given with respect to the position and orientation of camera. Equation (3.7) can be expressed by matrices like so

$$\underbrace{\begin{bmatrix} \tilde{u} \\ \tilde{v} \\ \tilde{w} \end{bmatrix}}_{\tilde{p}} = \underbrace{\begin{bmatrix} \frac{f}{\rho_w} & 0 & u_0 \\ 0 & \frac{f}{\rho_h} & v_0 \\ 0 & 0 & 1 \end{bmatrix}}_K \underbrace{\begin{bmatrix} 1 & 0 & 0 & 0 \\ 0 & 1 & 0 & 0 \\ 0 & 0 & 1 & 0 \end{bmatrix}}_{P_0} \underbrace{\begin{bmatrix} X \\ Y \\ Z \\ 1 \end{bmatrix}}_{{}^C\tilde{P}} \quad (3.8)$$

where  $K$  is a camera parameter matrix with the intrinsic camera parameters  $(f, \rho_w, \rho_h, u_0, v_0)$ .  ${}^C\tilde{P}$  is the point  $P$  with respect to the camera [2].

A point  $P$  with respect to a known world coordinate frame  $\{0\}$ , is shown in Figure 3.2.

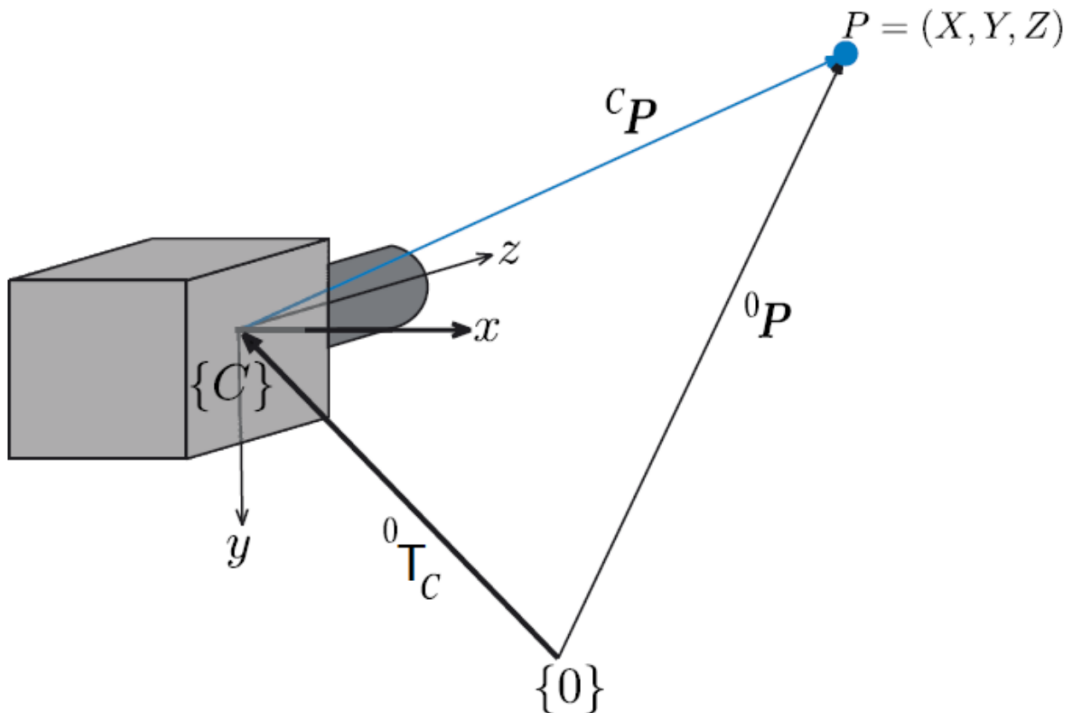


Figure 3.2: Relation between the camera and a point in the world [2].

${}^0 P$  represents the point given in the coordinate frame  $\{0\}$ . The point  $P$  with respect to the

camera frame  $\{C\}$  is

$${}^C\tilde{P} = T_0^C {}^0\tilde{P} \quad (3.9)$$

where  $T_0^C$  is the transformation from  $\{C\}$  to  $\{0\}$ . The inverse of  $T_0^C$  is the transformation from  $\{0\}$  to  $\{C\}$   $T_C^0$  as shown in Equation 3.10.

$$T_0^C = (T_C^0)^{-1} = \begin{bmatrix} (R_C^0)^T & -(R_C^0)^T t_{0C}^0 \\ 0^T & 1 \end{bmatrix} \quad (3.10)$$

Equation 3.8 and Equation 3.10 can be combined to

$$\underbrace{\begin{bmatrix} \tilde{u} \\ \tilde{v} \\ \tilde{w} \end{bmatrix}}_{\tilde{p}} = \underbrace{\begin{bmatrix} \frac{f}{\rho_w} & 0 & u_0 \\ 0 & \frac{f}{\rho_h} & v_0 \\ 0 & 0 & 1 \end{bmatrix}}_K \underbrace{\begin{bmatrix} 1 & 0 & 0 & 0 \\ 0 & 1 & 0 & 0 \\ 0 & 0 & 1 & 0 \end{bmatrix}}_{P_0} \underbrace{\begin{bmatrix} R_0^C & t_{C0}^C \\ 0^T & 1 \end{bmatrix}}_{T_0^C} \underbrace{\begin{bmatrix} X \\ Y \\ Z \\ 1 \end{bmatrix}}_{{}^0\tilde{P}} \quad (3.11)$$

where  $\tilde{p} = (\tilde{u}, \tilde{v}, \tilde{w})$  is a pixel represented in homogeneous coordinates [2]. The pixel  $\tilde{p} = (\tilde{u}, \tilde{v}, \tilde{w})$  represented in pixel coordinates  $p = (u, v)$  is

$$u = \frac{\tilde{u}}{\tilde{w}}, \quad v = \frac{\tilde{v}}{\tilde{w}} \quad (3.12)$$

So that a point  ${}^0P = (X, Y, Z)$  in world is projected on to a image plane as a pixel  $p = (u, v)$ .

## 3.2 RGB-D Camera

As a normal 2D camera captures an image, a depth camera captures a three-dimensional point cloud. A point cloud is a set of data points in a three-dimensional coordinate system. These points are usually defined by  $X$ ,  $Y$ , and  $Z$  coordinates, and they often represent the external surface of an object.

The RGB-D camera used in this project is the Asus Xtion PRO LIVE. It is a structured light based RGB-D (Red Green Blue - Depth) camera as shown in Figure 3.3. Structured light-based depth estimation can be viewed as a specific case of a stereo-vision system where a projector replaces one of the two cameras [26]. Asus Xtion PRO LIVE consists of an infrared camera, a RGB camera and a projector projecting an infrared active pattern.

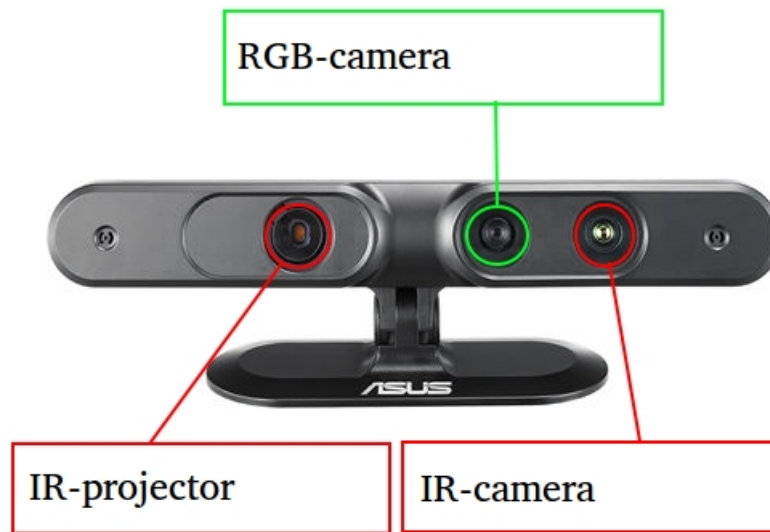


Figure 3.3: Asus Xtion PRO LIVE.

The infrared camera obtains the depth by analyzing the deformation of the pattern projected on to the scene by the projector. Figure 3.4 shows how the light pattern is observed from the IR camera. The lines look straight when projected onto a wall, but are distorted when projected onto people, furniture, or other uneven surfaces.

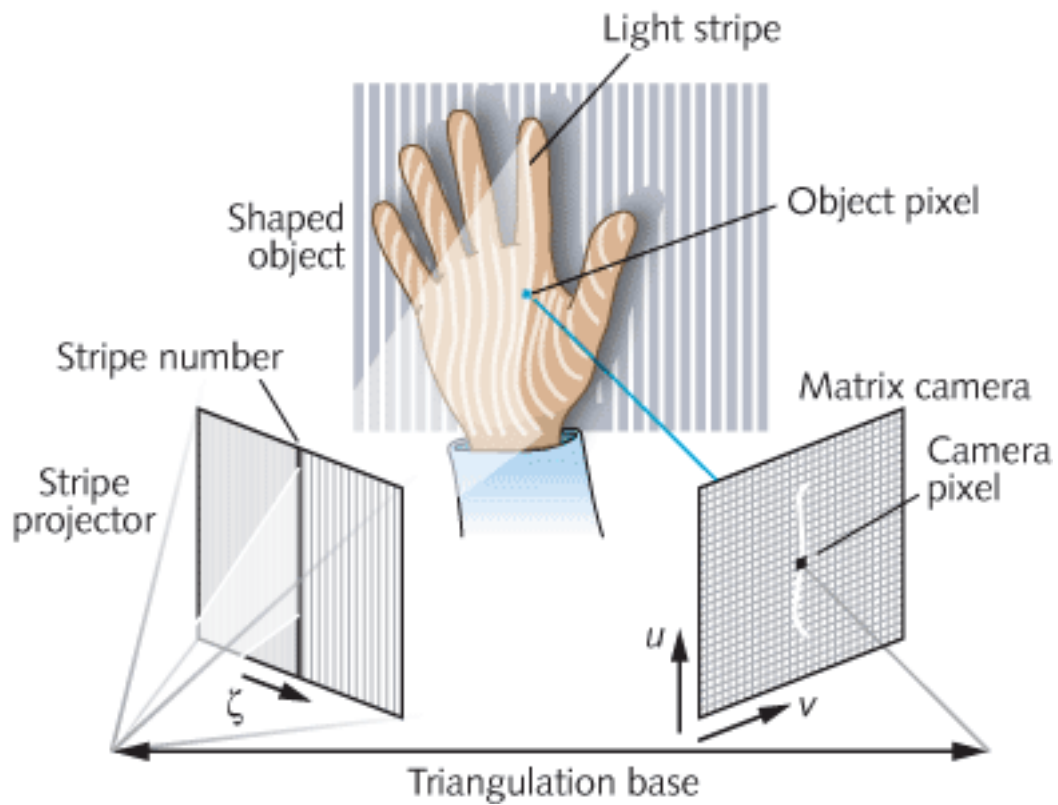


Figure 3.4: Structured light camera [5].

The RGB camera captures the color information and can be aligned with the IR camera by estimating the extrinsic parameters between them. This makes capturing of three-dimensional color point clouds (3D images) possible. Figure 3.5 shows how a three-dimensional point cloud is captured using a structured light camera.



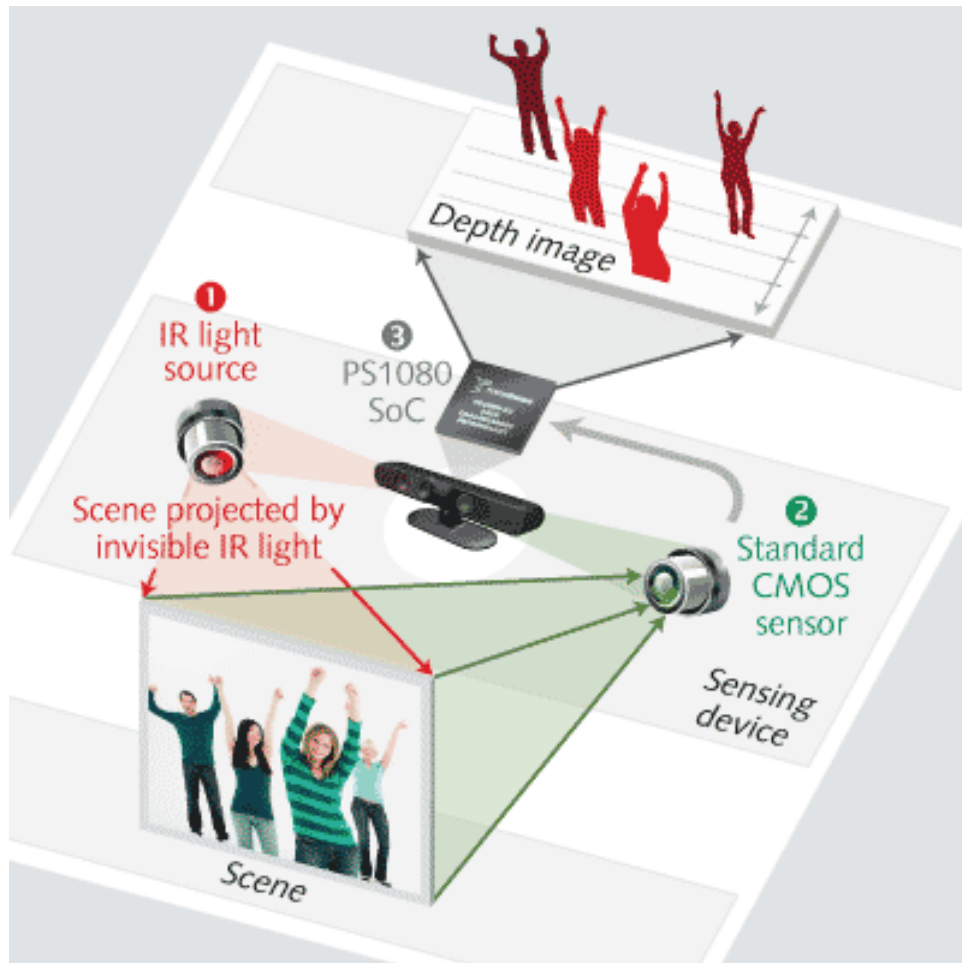


Figure 3.5: Depth image captured with a structured light camera [5].

Structured light based RGB-D cameras have a  $60^\circ$  field of view, which is far less than specialized cameras and laser scanners commonly used for 3D mapping ( $180^\circ$ ). They also provide depth and color information with less depth precision ( $\approx 3$  cm at 3 m depth), and their depth limit is typically 5 m [8]. Another weakness is that the camera does not detect glass doors, mirrors or shiny surfaces for instance. This proved to be a problem for detection of the shiny aluminium cylinder, especially if it was close to the IR-projector. Figure 3.6 shows the point cloud captured by the RGB-D camera. There are only a few points along the edges of the cylinder.

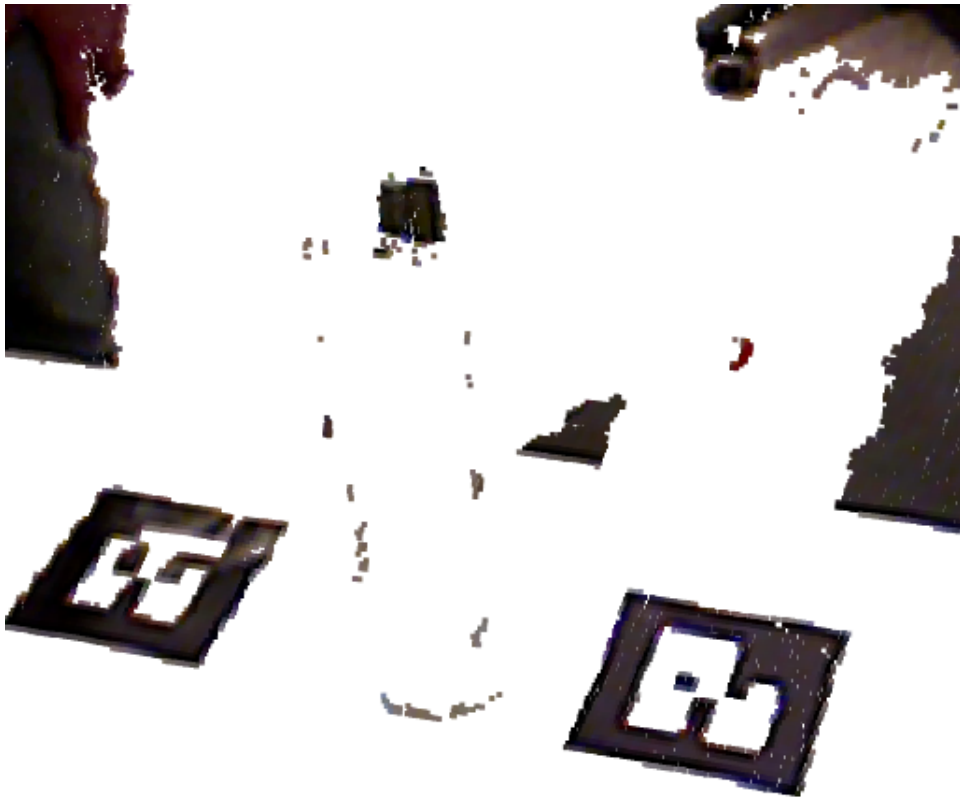


Figure 3.6: The shiny surface of the cylinder reflects the IR pattern so that most points on the cylinder does not show in the point cloud.

To make the camera detect the points, the cylinder was painted blue. As Figure 3.7 shows, the points on the cylinder are now detected much better because the IR pattern is not deflected.



Figure 3.7: The blue cylinder is detected well by the RGB-D camera.

At the macro level, structured light systems are better than other 3D vision technologies at delivering high levels of accuracy with less depth noise in an indoor environment [8].

### 3.2.1 Calibration of the Asus Xtion PRO LIVE

As for any other sensor, and since the manufacturer's parameters (e.g., focal length) might change between different cameras of the same type, calibration is necessary to increase the camera's sensing accuracy.

The intrinsic camera parameters were found by running the *Cameracalibrator* function in *OpenNI* (Open Natural Interaction) in ROS, Figure 3.8. In order to calibrate the RGB camera using *Cameracalibrator*, a large chessboard with known dimensions was used. Calibration uses the interior vertex points of the chessboard pattern as known points. The chessboard was then moved around in front of the camera in different orientations and poses while the camera automatically captured pictures for calibration. When the *Cameracalibrator* had enough good pictures to calibrate, the calibration result could be computed and saved. The saved intrinsic parameters were then used instead of the default parameters from *OpenNI*. This calibration technique proved to be an efficient way to calibrate the camera as the whole process only lasted about 20 minutes.

The IR camera was calibrated the same way, but with the IR projector covered by a post-it note. The reason for this is that the infrared pattern makes it difficult to detect the chessboard corners accurately in the IR image. Covering the IR projector improves the reliability of the chessboard corner detection. An ideal solution is to block the projector completely and provide

a separate IR light source.

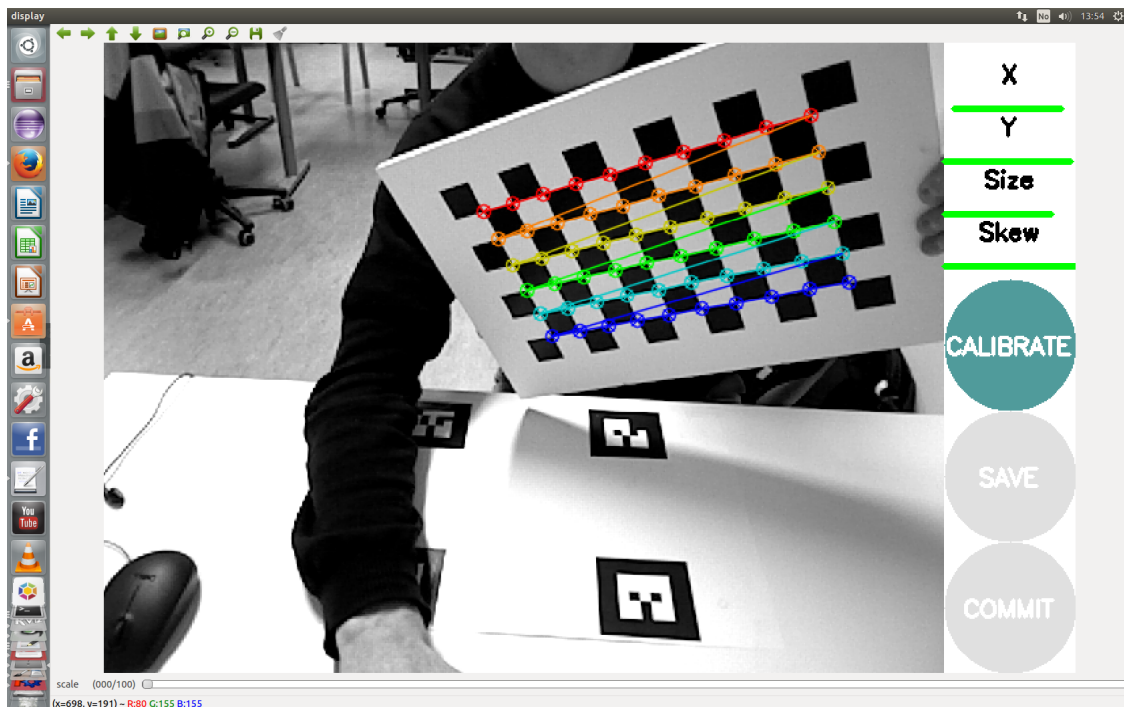


Figure 3.8: Cameracalibrator interface.

The resulting intrinsic parameters for both the RGB and IR camera was given as a camera parameter matrix  $K_{\text{ir}}$  for the IR camera and  $K_{\text{rgb}}$  for the RGB camera.

The depth data  $d$  from the IR camera can be estimated from regression techniques with the linear function [16]:

$$F(d) = ad + b \quad (3.13)$$

where  $a$  and  $b$  are constants from the camera. The depth  $Z$  is

$$Z = \frac{1.0}{F(d)} \quad (3.14)$$

A 3D-point  $(X, Y, Z)^T$  in the world can be approximated from the depth image  $(u, v, Z)$  by using the intrinsic parameters of the IR camera shown in Equation 3.15.

$$K_{\text{ir}} = \begin{bmatrix} f_x & 0 & u_0 \\ 0 & f_y & v_0 \\ 0 & 0 & 1 \end{bmatrix} \quad (3.15)$$

where  $f_x = f/\rho_w$  og  $f_y = f/\rho_h$ . Then the  $X$ ,  $Y$  and  $Z$  coordinates can be calculated as

$$X = \frac{Z(u - u_0)}{f_x} \quad (3.16)$$

$$Y = \frac{Z(v - v_0)}{f_y} \quad (3.17)$$

$$Z = \text{depth} \quad (3.18)$$

where  $u$  and  $v$  are pixels of the depth image and  $Z$  is the distance between the object and the IR camera as shown in Figure 3.9 [16].

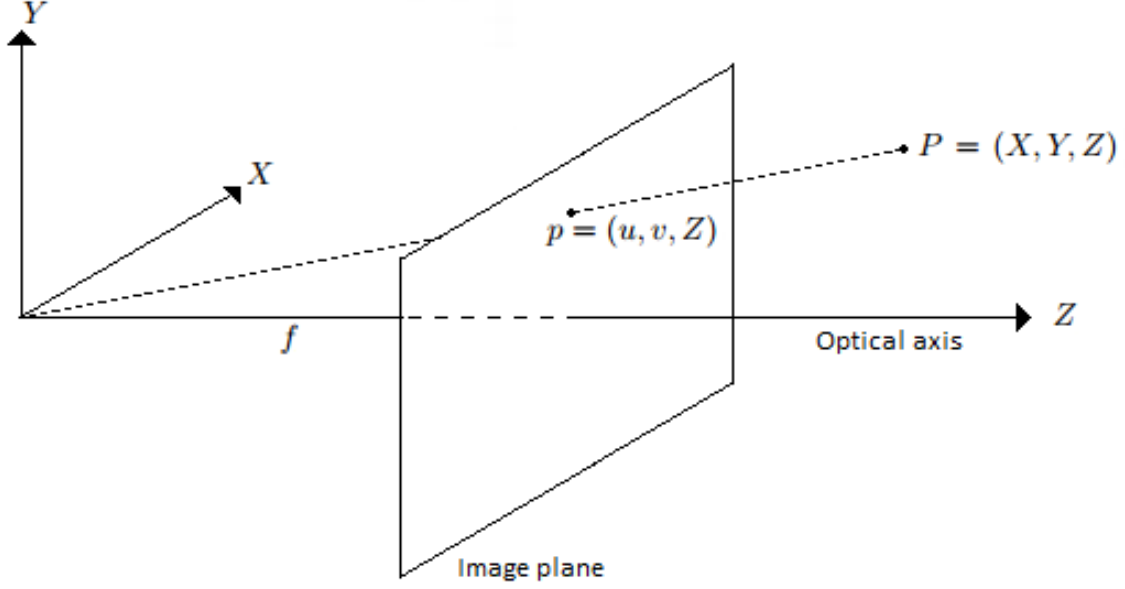


Figure 3.9: A point in the world  $P = (X, Y, Z)^T$  projected on to a corresponding point in the image plane  $p = (u, v, Z)^T$ .

In this project, the default extrinsic camera parameters were used. The extrinsic camera parameters consists of the rotation matrix  $R_{\text{ir}}^{\text{rgb}}$  from RGB camera to IR camera and a translation vector  $t_{\text{ir}}^{\text{rgb}}$  from RGB camera to IR camera. Together they make the homogeneous transformation matrix  $T_{\text{ir}}^{\text{rgb}}$  which can be used to map the images from the IR camera on to the images from the RGB camera. It is possible to compute the depth of the color image from the depth image provided by the IR camera. Consider a pixel  $p_{\text{ir}} = (u_{\text{ir}}, v_{\text{ir}})$  in the IR image. The 3D point  $P_{\text{ir}} = (X_{\text{ir}}, Y_{\text{ir}}, Z_{\text{ir}})$  corresponding to  $p_{\text{ir}}$  can be computed by back-projecting  $p_{\text{ir}}$  in the IR camera's coordinate system [16].

$$P_{\text{ir}} = K_{\text{ir}}^{-1} p_{\text{ir}} \quad (3.19)$$

$P_{\text{ir}}$  can be transformed to the RGB camera's coordinate frame through a relative transformation  $R_{\text{ir}}^{\text{rgb}}$  and  $t_{\text{ir}}^{\text{rgb}}$  like so

$$\underbrace{\begin{bmatrix} X_{\text{rgb}} \\ Y_{\text{rgb}} \\ Z_{\text{rgb}} \end{bmatrix}}_{\tilde{P}_{\text{rgb}}} = R_{\text{ir}}^{\text{rgb}} P_{\text{ir}} + t_{\text{ir}}^{\text{rgb}} \quad (3.20)$$

Figure 3.10 shows the transformation  $T_{\text{ir}}^{\text{rgb}}$  from the RGB camera frame  $\{C_{\text{rgb}}\}$  to the IR camera

frame  $\{C_{ir}\}$ .

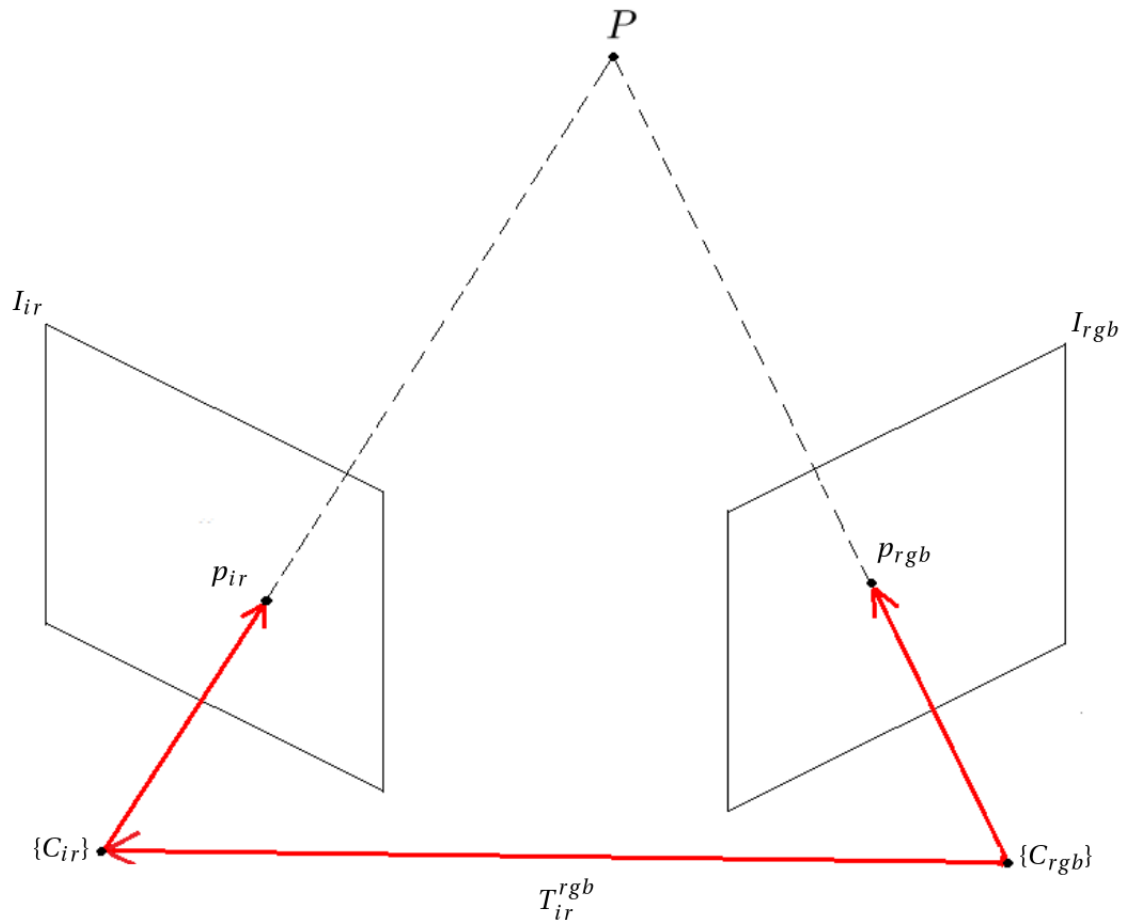


Figure 3.10: Transformation from IR to RGB frame.

Equation (3.21) and equation (3.22) can be used to map the depth images onto the color images [16].

$$u_{rgb} = \frac{X_{rgb}f_x}{Z_{rgb}} + u_0 \quad (3.21)$$

$$v_{rgb} = \frac{Y_{rgb}f_y}{Z_{rgb}} + v_0 \quad (3.22)$$

$p_{rgb} = (u_{rgb}, v_{rgb})$  is a pixel in the image plane of the RGB-camera corresponding to  $P_{ir}$  in equation (3.19).  $f_x$  and  $f_y$  are focal lengths from  $K_{rgb}$  and  $P_{rgb} = (X_{rgb}, Y_{rgb}, Z_{rgb})^T$  is given by equation (3.20).

To see if the newly acquired calibration parameters were different than the default camera parameters included in the driver provided by OpenNI, an experiment was performed. An object was placed directly in front of the camera's optical axis. The  $Z$  coordinate of the closest point were then written to a log file. This result was then compared with the log file from the same experiment but with the default calibration parameters. The result showed that the depth registered only differed with a few micro meters between the result from calibrated parameters and the default parameters.

## Chapter 4

# Computer Vision

This chapter contains some theoretical background information relevant for the computer vision part of this thesis.

### 4.1 Relevant Theoretical Background Information for 2D Camera

Estimating the orientation of the objects is a vital part in the process of assembling the cylinder and the piston.

It was of interest to use a 2D camera to determine the orientation of the parts. This can be achieved by comparing measurements obtained from training images of the parts with measurements from an image stream from a 2D camera. This measurement is called image *features*. Professor David Lowe's SIFT (Scale Invariant Feature Transform) is a method to detect image features that are invariant to image scale and rotation. In other words SIFT is robust when the distance to and the orientation of the objects in the image stream, are different compared to what the objects are in the training images [2].

A feature is a highly distinctive region of an image that can be reliably located in other images of the same scene [20]. This allows a single feature from a training image to be correctly matched with high probability against a feature in the image stream [11].

#### 4.1.1 SIFT

The first stage of feature detection is to identify locations and scales that can be repeatedly assigned under different views of the same object. Consider two images of the same object. The object has varying distance to the camera in the images. Detecting same locations on the object in both images, can be accomplished by searching for stable features across all possible scales, using a continuous function of scale known as *scale space*. The scale space of an input image  $I(u, v)$  in *convolution* (\*) of a Gaussian function  $G(u, v, \sigma)$ , generate a blurred output image  $L(u, v, \sigma)$

$$L(u, v, \sigma) = G(u, v, \sigma) * I(u, v) \tag{4.1}$$

An example of an input image  $I(u, v)$  and a output image  $L(u, v, 1)$ , are shown in Figure 4.1

and Figure 4.2.



Figure 4.1: Input image  $I(u, v)$



Figure 4.2: Output image  $L(u, v, 1)$

Convolution is a linear spatial operator. For every output pixel  $(u, v)$  in  $L(u, v)$  the corresponding window of pixels from  $I(u, v)$  is multiplied element-wise with a kernel [2]. In Figure 4.2 this kernel is the Gaussian function

$$G(u, v, \sigma) = \frac{1}{2\pi\sigma^2} e^{-(u^2+v^2)/2\sigma^2} \quad (4.2)$$

In Figure 4.3 a Gaussian kernel with  $\sigma = 1$  and  $\sigma = 1.2$  is shown.

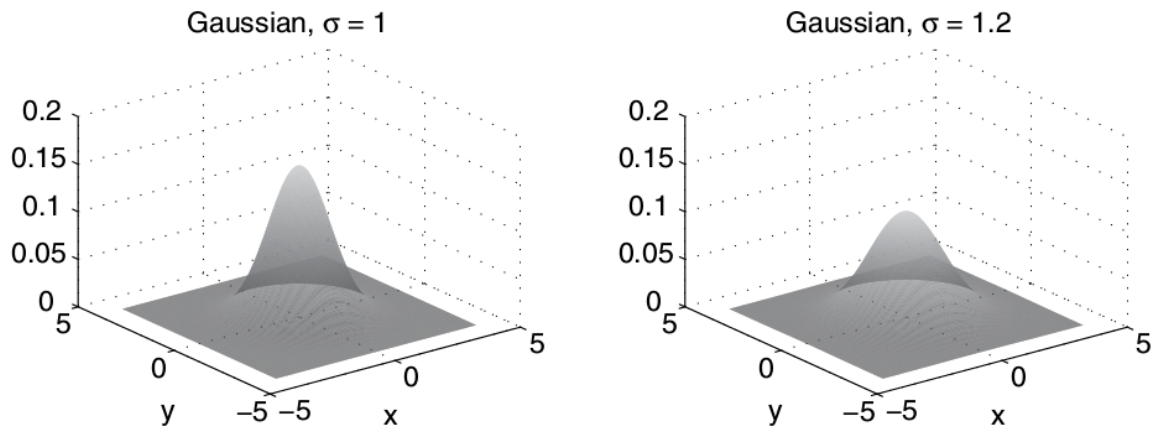


Figure 4.3: Gaussian kernel with  $\sigma = 1$  and  $\sigma = 1.2$  [20]

For detecting stable features, SIFT uses scale-space extrema in a continuous difference-of-Gaussian function convolved with the input image

$$\begin{aligned} D(u, v, \sigma) &= (G(u, v, k\sigma) - G(u, v, \sigma)) * I(u, v) \\ &= L(u, v, k\sigma) - L(u, v, \sigma) \end{aligned} \quad (4.3)$$



SIFT has an octave structure for computing the scale-space difference-of-Gaussian (see Figure 4.4). An octave of a Gaussian scale space is a pair of images whose  $\sigma$  differ by a factor of  $k$ . From equation (4.3)  $k = \frac{1}{s}$  where each set of  $s + 1$  images results in an octave. Lowe suggest  $s = 3$  and  $\sigma = 1.6$  [20]. Once a complete octave has been processed, the next octave re-sample the Gaussian image that has twice the initial value of  $\sigma$  by taking every second pixel  $(u, v)$  in each row and column [20][11].

In Figure 4.4 this process is shown. The white images represent the Gaussian blurred images with the same sequence of scales applied to octaves of images of different resolutions. The Gaussian images at each octave has half the resolution of the images in the octave above. The gray images represents the difference-of-Gaussian images.

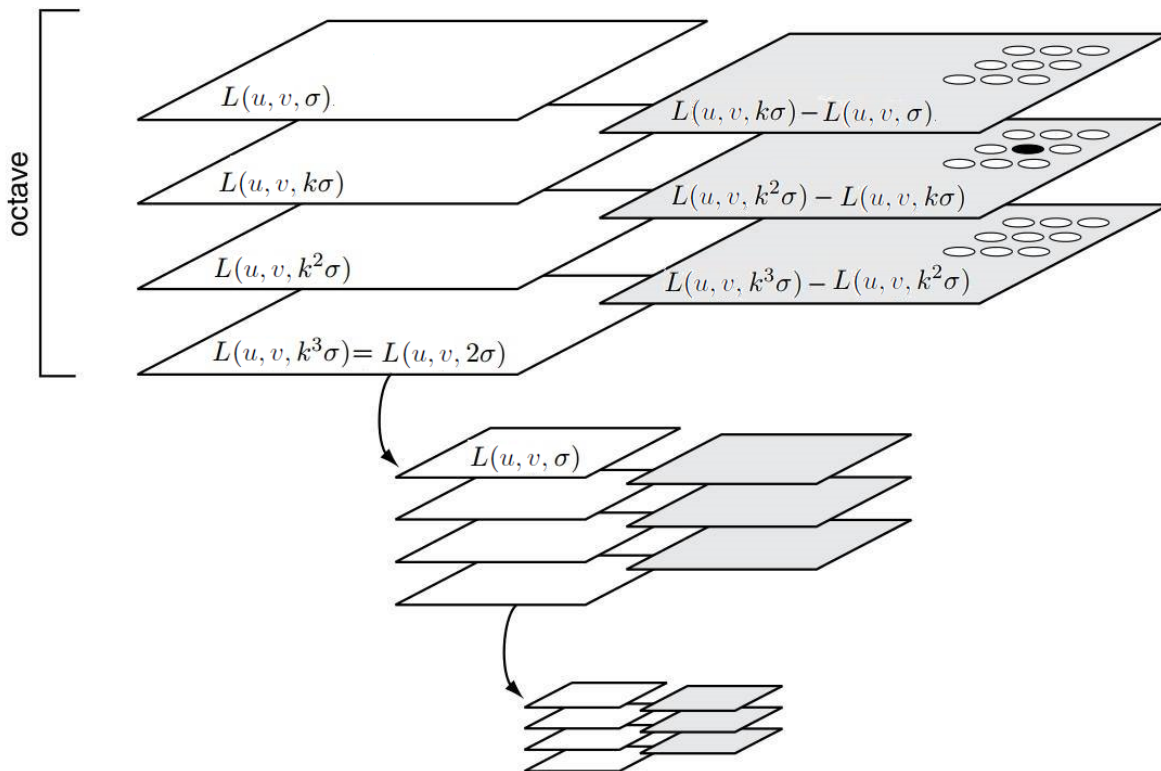


Figure 4.4: Scale-space [20].

The key quantity of difference-of-Gaussian feature detection is the difference of adjacent Gaussians applied to the input image  $I(u, v)$ . The difference-of-Gaussian detection seek for maxima and minima in both the spatial and scale dimensions to detect features. In the difference-of-Gaussian images, local maxima and minima are detected by comparing a pixel to its  $(9+8+9=)$  26 neighbors in  $3 \times 3$  regions at the current and adjacent scales. A candidate for a *keypoint* is accepted if it is larger or smaller than all of its eight neighbors in the current image and the nine neighbors in the scale above and below [11]. This is shown in the top right corner in Figure 4.4 and in Figure 4.5.

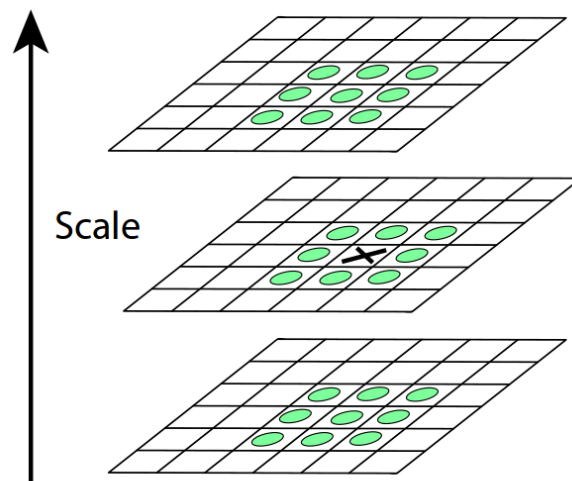


Figure 4.5: Scale-space difference-of-Gaussian [11].

Figure 4.6 shows an example of a difference-of-Gaussian image generated from the input image in Figure 4.1.

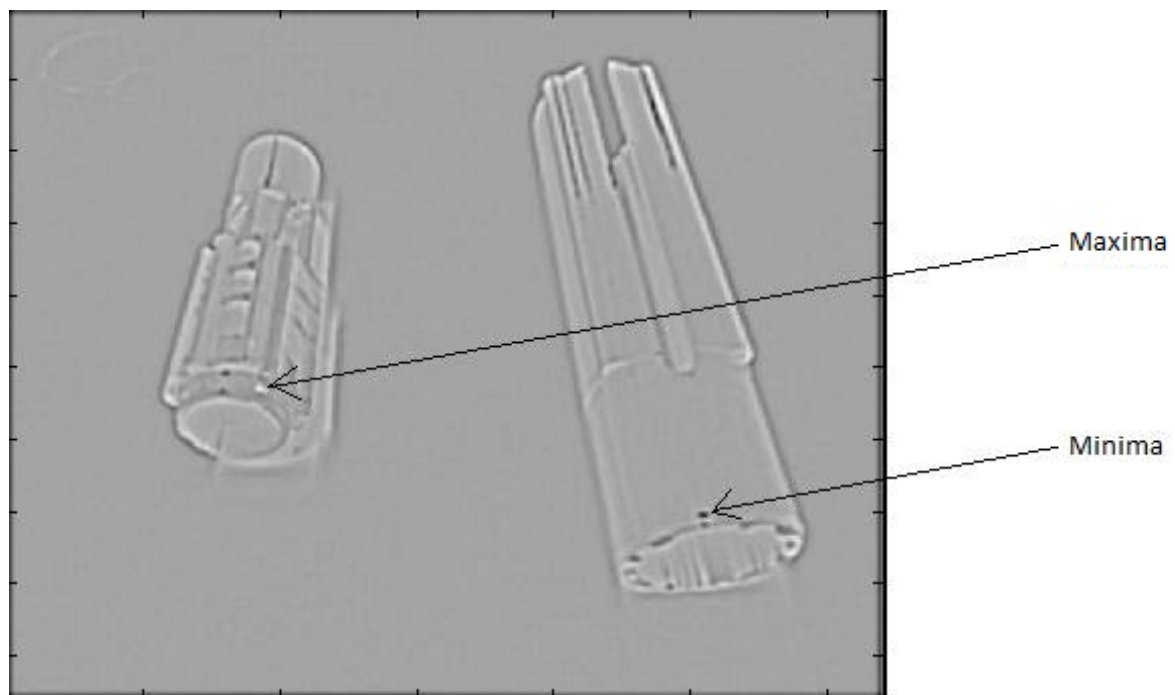


Figure 4.6: Difference-of-Gaussian image.

For some of the candidates of keypoints, there could be some *outliers* because of noise. Example of outliers can be candidates along an edge or low contrast.

An approximation of the difference-of-Gaussian function  $D$  by a Taylor series is

$$D(\mathbf{x}) = D + \frac{\partial D^T}{\partial \mathbf{x}} \mathbf{x} + \frac{1}{2} \mathbf{x}^T \frac{\partial^2 D}{\partial \mathbf{x}^2} \mathbf{x} \quad , \quad \mathbf{x} = (x, y, \sigma)^T \quad (4.4)$$

and an extrema  $\hat{\mathbf{x}}$  is located at

$$\mathbf{x} = -\frac{\partial^2 D^{-1}}{\partial \mathbf{x}^2} \frac{\partial D}{\partial \mathbf{x}} \quad (4.5)$$

The value of  $D(\hat{\mathbf{x}})$  at the location of an extrema  $\hat{\mathbf{x}}$  in equation (4.4), must be lower than a threshold to be accepted as an *inlier*. This process is useful for rejecting outliers that are unstable extrema with low contrast.

The *Hessian* matrix  $H$  of the difference-of-Gaussian function  $D$  is

$$H = \begin{bmatrix} D_{uu} & D_{uv} \\ D_{uv} & D_{vv} \end{bmatrix} \quad (4.6)$$

where  $D_{uu} = \frac{\partial^2 D}{\partial u \partial u}$ ,  $D_{uv} = \frac{\partial^2 D}{\partial u \partial v}$  and  $D_{vv} = \frac{\partial^2 D}{\partial v \partial v}$ . Further outlier rejection can be done by evaluating the *trace* (Tr) and determinant of  $H$

$$\frac{\text{Tr}(H)^2}{\text{Det}(H)} = \frac{(r+1)^2}{r} \quad , \quad r = \frac{\lambda_1}{\lambda_2} \quad (4.7)$$

where

$$\begin{aligned} \text{Tr}(H) &= D_{uu} + D_{vv} = \lambda_1 + \lambda_2 \\ \text{Det}(H) &= D_{uu}D_{vv} - (D_{uv})^2 = \lambda_1\lambda_2 \end{aligned} \quad (4.8)$$

The parameter  $r$  in equation (4.7), must be smaller than a threshold to be accepted as a keypoint. This process is useful for rejecting outliers that are unstable extrema along an edge. At this stage, keypoint have been localised with a pixel  $(u, v)$  and scale [11].

As mentioned, the SIFT features are invariant of orientation. To achieve this orientation invariance, each feature has to be given an orientation assignment. The scale of the keypoint is used to select the Gaussian smoothed image,  $L$ , with the closest scale to the scale of the keypoint, so that all computations are performed in a scale-invariant manner. For the images  $L(u, v)$  at this scale, the gradient magnitude,  $m(u, v)$ , and orientation,  $\theta(u, v)$ , is computed

$$\begin{aligned} m(u, v) &= \sqrt{(L(u+1, v) - L(u-1, v))^2 + (L(u, v+1) - L(u, v-1))^2} \\ \theta(u, v) &= \tan^{-1} \left( \frac{L(u, v+1) - L(u, v-1)}{L(u+1, v) - L(u-1, v)} \right) \end{aligned} \quad (4.9)$$

and used for creating a histogram of the gradient orientation within the scale-covariant circle region around the keypoint. The orientation histogram has 36 bins (one bin for each ten degrees) covering the 360 ° range of orientations. The orientation histogram is weighted by its gradient magnitude and by a Gaussian-weighted circular window with  $1.5\sigma$  where  $\sigma$  is the scale of the

keypoint. That is, for each pixel  $(u, v)$  in the region around the keypoint  $(u_0, v_0, \sigma)$ , the quantity  $m(u, v)G(u - u_0, v - v_0, 1.5\sigma)$  is the quantity incrementing in the bin corresponding to  $\theta(u, v)$  [20].

The highest peak in the histogram and other local peaks that is within 80% of the highest peak, is used to create the orientation of the keypoint. At this stage, the keypoint has an image location  $(u, v)$ , scale  $\sigma$  and orientation  $\theta$ . These parameters are the SIFT feature for a keypoint [11].

The next step is to describe the feature with a 128 number vector called a *SIFT descriptor*.

In Figure 4.7 the input image from Figure 4.1 is shown with a feature. The location of the keypoint is in the center of the green circle, the size of the green circle is corresponding to the scale of the feature, and the green line indicate the orientation of the feature. The descriptor is computed from the pixels inside the blue square in Figure 4.8. The orientation of the square in Figure 4.8 is the same as the orientation of the feature in Figure 4.7. Each side of the square is a multiple of the feature's scale [20].



Figure 4.7: Input image  $I(u, v)$  with one feature. Figure 4.8: Input image  $I(u, v)$  with one descriptor and feature.

The image pixels inside the square are smothered with the appropriate Gaussian for the feature's scale. Then the gradient magnitude and orientation at each pixel is estimated, as shown on the left in Figure 4.9. These are weighted by a Gaussian window (blue circle in Figure 4.9), subdivided into a  $4 \times 4$  grid of smaller squares, and used to create a histogram of eight gradient orientations within each grid square in Figure 4.8. To the right in Figure 4.9 this is also shown.

So for the descriptor in Figure 4.8 there are 8 gradient orientations within each of the  $4 \times 4$  squares, which makes a  $4 \times 4 \times 8 = 128$  element vectors for each feature. The vector is then normalized to unit length. This normalized vector is the descriptor for the feature in Figure 4.7.

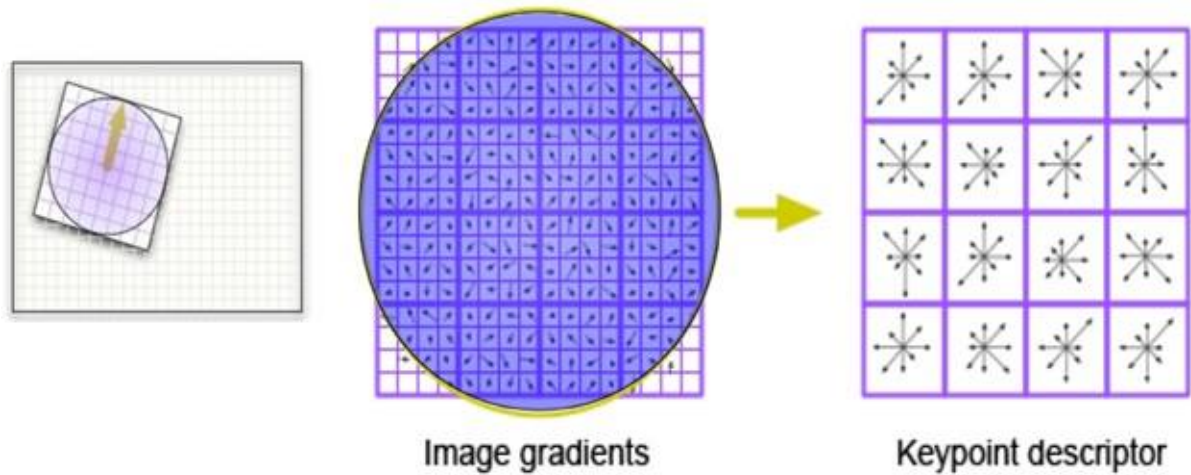
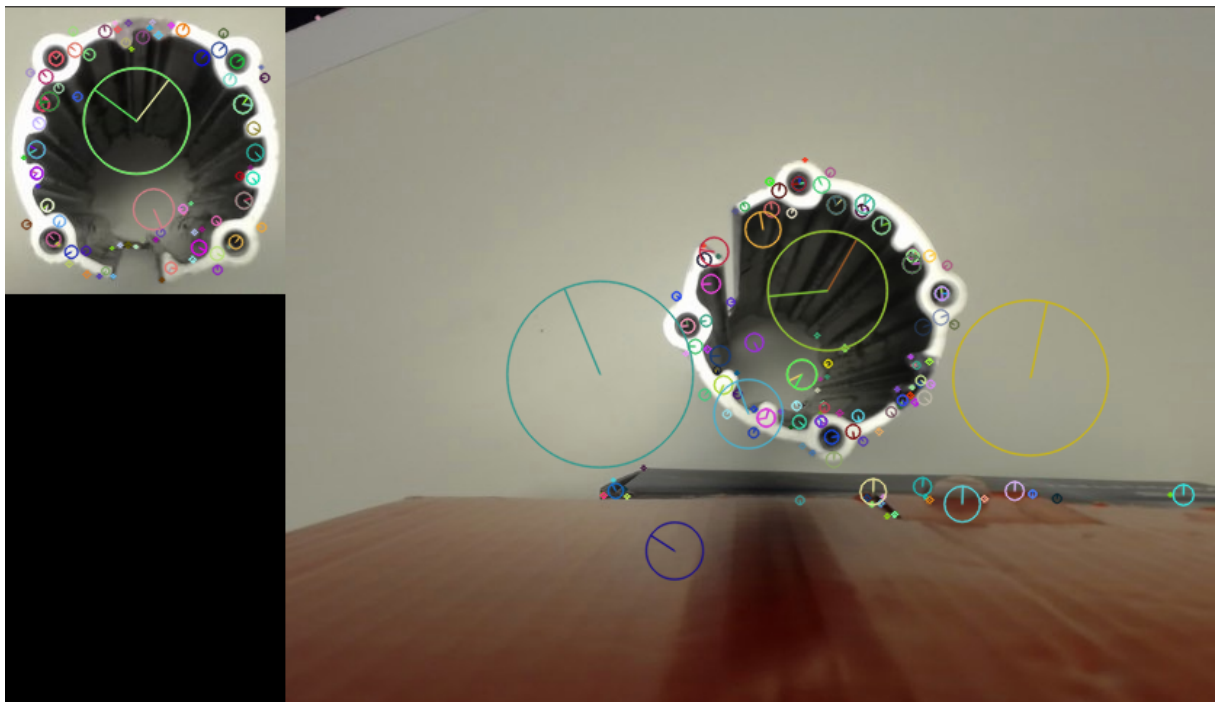


Figure 4.9: Computing a descriptor [1].

In Figure 4.10 there is an image  $I_o$  of an object and an image  $I_s$  of a scene, with some estimated SIFT features (the circles) in both images.

Figure 4.10: From left: Image  $I_o$  of a object and an image  $I_s$  of a scene. The circles are features.

In  $I_o$  there has been computed a set of descriptors  $O = o^1, \dots, o^{N_1}$  for the features, and in  $I_s$  there has been computed a set of descriptors  $S = s^1, \dots, s^{N_2}$  for the features. The next step is to generate a list of *feature correspondences*  $\{(c_o^j, c_s^j), j = 1, \dots, N_3\}$ , which says that  $o^{c_o^j} \in O$  and  $s^{c_s^j} \in S$  are a match. Finding the feature correspondences, can be done by estimating the Euclidean distance between descriptors in  $I_s$  and  $I_o$  and then using the method of nearest neighbor. The euclidean distance  $D$  between a descriptor  $o$  from the set  $O$  in  $I_o$  and  $s$  from the

set  $S$  in  $I_s$  is

$$D(o, s) = \sqrt{\sum_{i=1}^{128} (o_i - s_i)^2} \quad (4.10)$$

(each descriptor vector has 128 element). The match to a descriptor  $o$  from a set of descriptors in  $S$  is computed by use of nearest neighbor

$$s^* = \arg \min_{s \in S} D(o, s) \quad (4.11)$$

A descriptor  $o$  and  $s^*$  are accepted as a match if  $D(o, s^*)$  is below a specified threshold [20].

From the list of feature correspondences, the *corresponding keypoint* are extracted. In the rest of this chapter, the notation  $p = (u, v)^T$  is used for a keypoint in  $I_o$  and  $p' = (u', v')^T$  is used for a keypoint in  $I_s$ . A pair of corresponding keypoints  $p$  and  $p'$ , is the location of a pair of matched features.

In Figure 4.11 some of the corresponding keypoints from Figure 4.10 are shown.

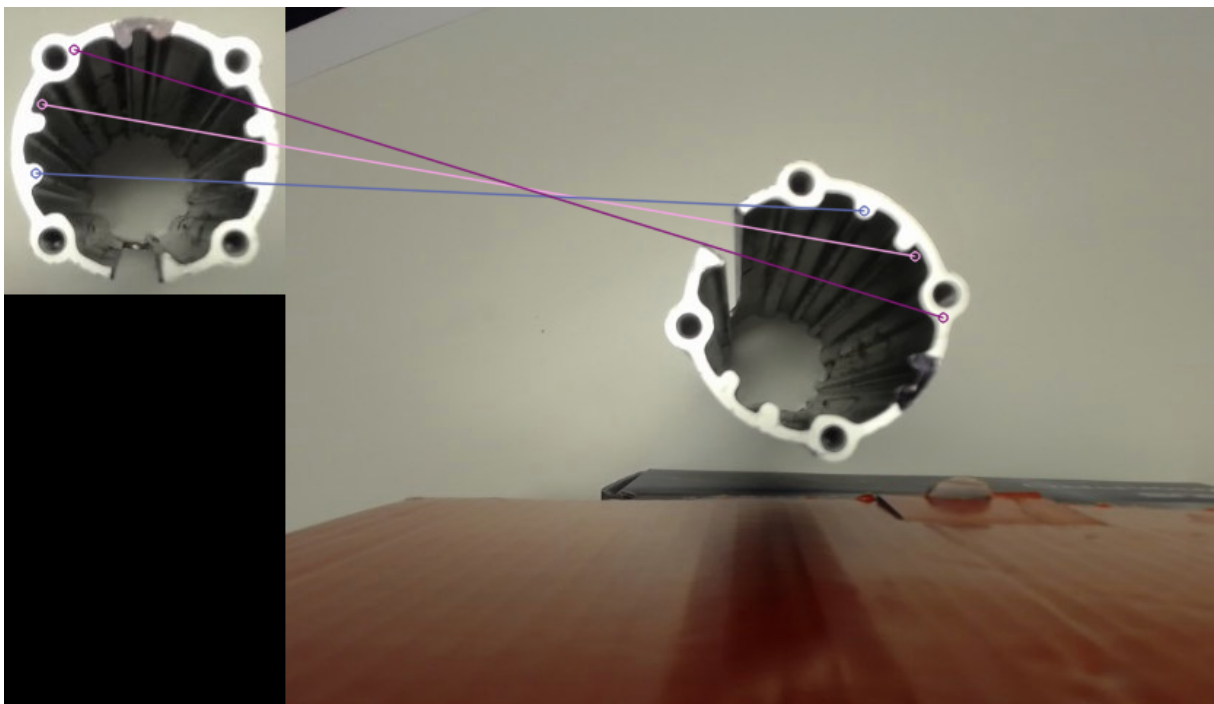


Figure 4.11: From left: Image  $I_o$  with three keypoints (circles) and an image  $I_s$  with three keypoints (circles). The lines indicates that the keypoints are corresponding.

### 4.1.2 Homography

The goal is to find the orientation of the object (in  $I_o$ ) in an image stream (continuous updating of  $I_s$ ). The set of corresponding keypoints (from the set of matched features) can be used to find a perspective transformation between the object in  $I_o$  and  $I_s$ . The projective transformation or homography  $H$  is estimated

$$\underbrace{\begin{bmatrix} u'_i \\ v'_i \\ 1 \end{bmatrix}}_{\tilde{p}'_i} = \underbrace{\begin{bmatrix} h_{11} & h_{12} & h_{13} \\ h_{21} & h_{22} & h_{23} \\ h_{31} & h_{32} & h_{33} \end{bmatrix}}_{\text{homography}} \underbrace{\begin{bmatrix} u_i \\ v_i \\ 1 \end{bmatrix}}_{\tilde{p}_i} \quad (4.12)$$

so that the back-projection error

$$\sum_{i=1} \left( u'_i - \frac{h_{11}u_i + h_{12}v_i + h_{13}}{h_{31}u_i + h_{32}v_i + h_{33}} \right)^2 + \left( v'_i - \frac{h_{21}u_i + h_{22}v_i + h_{23}}{h_{31}u_i + h_{32}v_i + h_{33}} \right)^2 \quad (4.13)$$

is minimized [15]. In equation (4.12),  $p'_i$  are the keypoints  $\{(u'_1, v'_1)^T, \dots, (u'_n, v'_n)^T\}$  in  $I_s$  and  $p_i$  are the keypoints  $\{(u_1, v_1)^T, \dots, (u_n, v_n)^T\}$  in  $I_o$ . However, if not all of the point pairs  $\{p_i, p'_i\}$  are corresponding, the homography matrix can be incorrect.

This is why it is of interest to also include a robust iterative method called RANSAC (RANdom SAMple Consensus) in the estimation of the homography matrix. RANSAC will try many different random subsets of corresponding point pairs (of four pairs each) and the homography matrix  $H$  is estimated on behalf of numbers of *inliers* that fits to the homography matrix. The best subset is then used to estimate the final homography matrix in equation (4.12). The homography is determined up to scale. Therefore it is normalized so that  $h_{33} = 1$  [15][4].

The projective transformation or homography, maps points in a training/object image on the image planes in the image stream. That is, it maps the training/object image plane to the image stream. The orientation of the mapped plane in the image stream is used to determine the orientation of the object.

## 4.2 Relevant Theoretical Background Information for RGB-D Camera

This chapter contains some theoretical background information relevant for the RGB-D camera, followed by an explanation of the different programs for obtaining the position of the piston and the cylinder.

### 4.2.1 AR-tags

AR is an abbreviation for augmented reality and means to make virtual objects appear to enter the real world. AR-markers or AR-tags look like QR-codes and a particular pattern can be recognized in the image from the camera and represent the location of a virtual object. The three-dimensional orientation of the tag can be registered as well as the position of the tag. It is also possible to make digital artificial objects appear on the surface of the tag.

In this project the ROS package `ar_track_alvar` was used to make a coordinate system which is constant regardless of the position of the camera. Figure 4.12 shows AR-tags, and how they are seen from the camera on the computer screen.



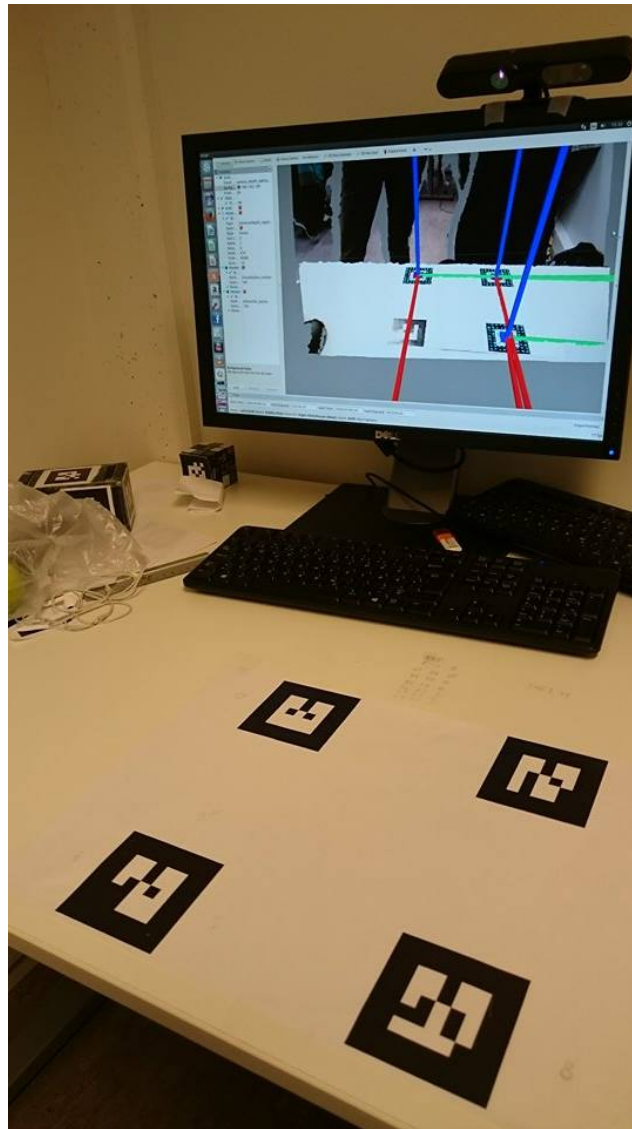


Figure 4.12: AR-tags.

The computer recognizes the AR-tags viewed from the camera and creates an artificial coordinate frame with the origin in the center of three of the four AR-tags.

### 4.2.2 Estimating Surface Normals in a Point Cloud

Local geometric features such as surface normal or curvature at a point form a fundamental basis for extracting semantic information from 3D sensor data. This section explains how to use approximations to infer the surface normals from a point cloud dataset [23].

For a *query point*  $p_q$  its neighboring points  $\mathcal{P}^k = \{p_1, p_2, \dots, p_k\}$  is used in the estimation of a surface normal at  $p_q$ . The problem of determining the normal to a point on a surface can be approximated by the problem of estimating the normal of a plane tangent to the surface, which in turn becomes a least-square plane fitting estimation problem in  $\mathcal{P}^k$ . The plane is represented as a point  $x$  and a normal  $n$ . The distances  $d_i$  from the points  $p_i$ , in the neighborhood  $\mathcal{P}^k$ , to the plane is  $d_i = (p_i - x) \cdot n$ . The point  $x$  and the normal  $n$  are computed in a least-square sense  $d_i = 0$ . That is, the point  $x$  is determined as the 3D centroid of the neighboring points  $\mathcal{P}^k$

$$x = \frac{1}{k} \cdot \sum_{i=1}^k p_i \quad (4.14)$$

and the normal  $n$  is given by analyzing the eigenvalues  $\lambda_j$  and eigenvectors  $v_j$  (or PCA – Principal Component Analysis) of the covariance matrix  $C$

$$C = \frac{1}{k} \sum_{i=1}^k (p_i - x) \cdot (p_i - x)^T, \quad C \cdot v_j = \lambda_j \cdot v_j, \quad j \in \{0, 1, 2\} \quad (4.15)$$

The eigenvectors  $v_j$  form an orthogonal frame, corresponding to the principal components of the query points neighbours. If  $0 \leq \lambda_0 \leq \lambda_1 \leq \lambda_2$ , the eigenvector  $v_0$ , corresponding to the smallest eigenvalue  $\lambda_0$  can be used as an estimate of a normal  $+n = \{n_x, n_y, n_z\}$  or  $-n$  [23]. The ratio between the smallest eigenvalue  $\lambda_0$  and the sum of eigenvalues provides an estimate of the local curvature [6].

There is in general no mathematical way to solve for the sign of the normal  $+n$  or  $-n$  using PCA. The orientation computed is ambiguous and not consistently over an entire point cloud dataset. Figure 4.13 shows a side view of a plane where the normals are pointing both upwards and downwards.

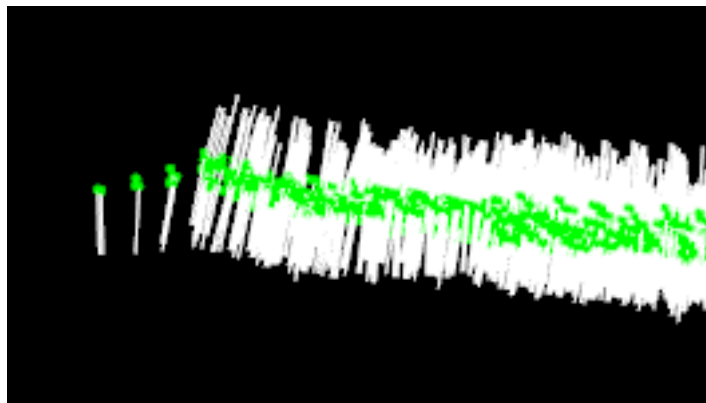


Figure 4.13: Surface normals have ambiguous direction.

The right orientation of the surface normals can be found if the viewpoint  $V_p$  is known. In order for the normals  $n_i$  to be oriented consistently towards the viewpoint, the following equation needs to be satisfied:

$$n_i \cdot (v_p - p_i) > 0 \quad (4.16)$$

where  $p_i$  is the corresponding point to the normal  $n_i$ .

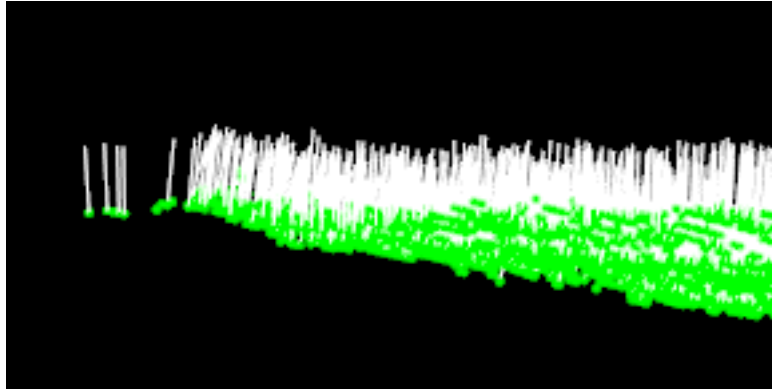


Figure 4.14: Surface normals are oriented in the same direction.

As already mentioned, the surface normal at a point needs to be estimated from the surrounding point neighborhood  $\mathcal{P}^k = \{p_1, p_2, \dots, p_k\}$  support of the point (also called  $k$ -neighborhood). To estimate the nearest neighbours  $\mathcal{P}^k$ , an appropriate scale factor is set either by choosing the radius  $r$  of the sphere containing neighbouring points or the number of  $k$  nearest neighbors to use for the feature estimation. A reasonably chosen scale factor results in estimated surface normals that are approximately perpendicular for planar surfaces. If the scale factor is too big, and the set of neighbors is larger covering points from adjacent surfaces, the estimated point feature representations get distorted, with rotated surface normals at the edges of planar surfaces, and smeared edges and suppressed fine details [23]. Figure 4.15 shows a point cloud with  $r = 0.1$ , which uses all neighbors in a sphere of radius 10 cm around each query point  $p_q$ . The surface normals are pointing downwards and are almost parallel to the surface normals of the table when they should be pointing in the horizontal direction. The scale factor is too high.

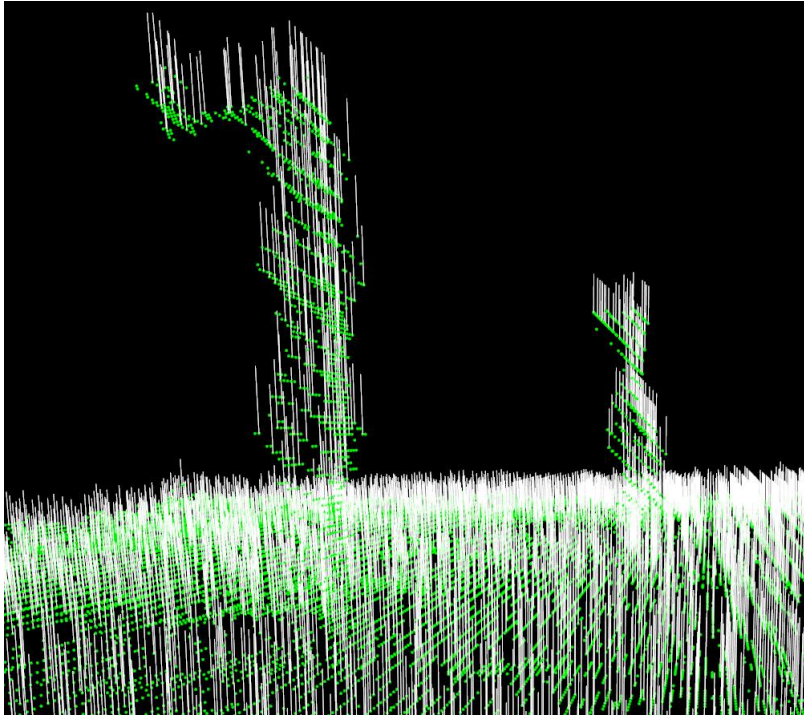


Figure 4.15: Surface normals,  $r = 0.3$ .

Figure 4.16 shows a point cloud with  $r = 0.03$ . Here the normals are pointing more in the horizontal direction, which is what we are looking for.

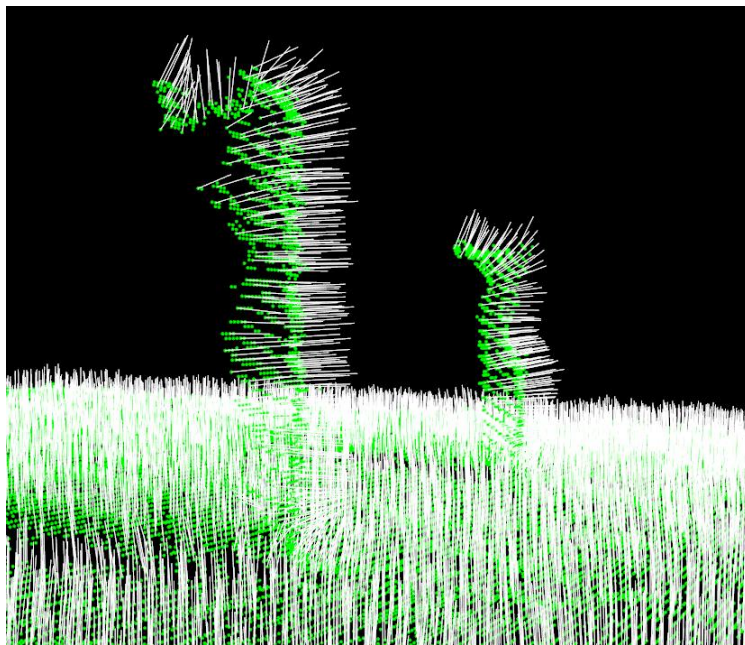


Figure 4.16: Surface normals,  $r = 0.03$ .

After some testing and adjustment  $r = 0.04$  was chosen. The result is shown in Figure 4.17.

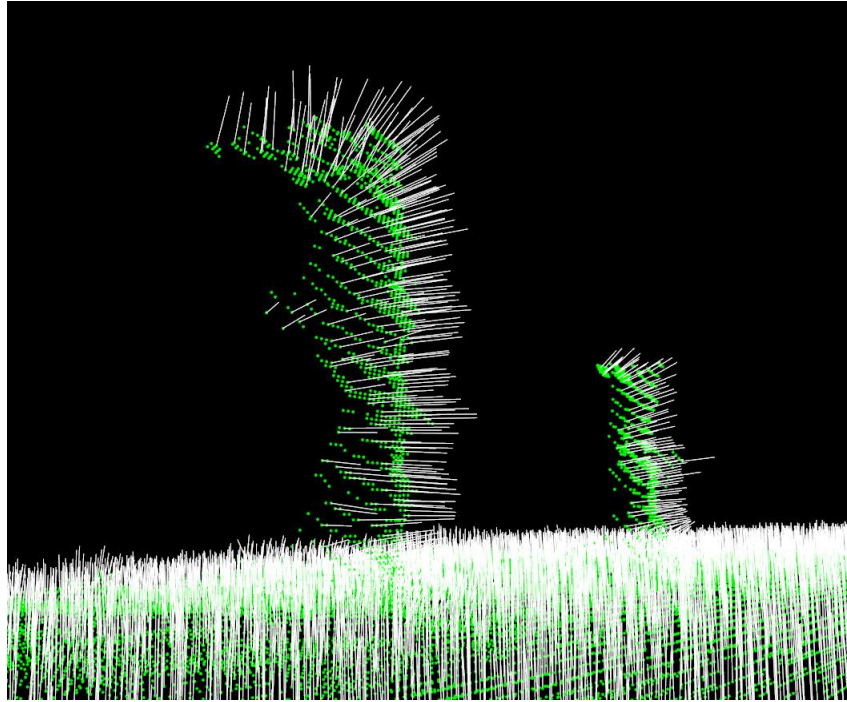


Figure 4.17: Surface normals,  $r = 0.04$ .

The figure clearly shows that the estimated surface normals are approximately perpendicular for the plane and for the objects on it.

The scale factor to choose, depends on the detail level needed in the cloud. Simply put, if the curvature at the edge between the handle of a mug and the cylindrical part is important, the scale factor needs to be small enough to capture those details, and large otherwise [23].

**Estimation of surface normals can be summarized by the following:**

1. Get the nearest neighbors of point cloud  $P$
2. Compute the surface normal  $n$  of the point  $p$
3. Check if  $n$  is consistently oriented towards the viewpoint and flip otherwise

### 4.2.3 PFH - Point Feature Histogram

The characterization of the surface geometry around a point is given through the formulation of a Point Feature Histogram (PFH) 3D feature. This feature space is extremely useful for the problem of finding point correspondences.

Surface normals and curvature estimates are basic in their representation of the geometry around a specific point, as point feature representations. Though extremely fast and easy to compute, they cannot capture too much detail, as they approximate the geometry of a point's neighbouring points ( $k$ -neighborhood) with only a few values [23]. The consequence of this is that the informative characteristics gets reduced because most scenes contains many points with the same or very similar feature values.

Point feature histograms (PFH) are robust multi-dimensional features which describe the local geometry around a point  $p$  for 3D point cloud datasets, and they rely on 3D data  $(X, Y, Z)$  as well as surface normals. The goal of the PFH formulation is to encode a point's  $k$ -neighborhood geometrical properties by generalizing the mean curvature around the point using a multi-dimensional histogram of values. This highly dimensional hyperspace provides an informative signature for the feature representation, is invariant to the 6D pose of the underlying surface, and copes very well with different sampling densities or noise levels present in the neighborhood [23].

The neighborhood  $\mathcal{P}^{k_2}$  used in PFH has larger neighborhood than the neighborhood  $\mathcal{P}^k$  used for estimating the surface normals. That is, it is more points in the neighborhood  $\mathcal{P}^{k_2}$  than  $\mathcal{P}^k$ .

PFH represents the relationship between the points in  $\mathcal{P}^{k_2}$  and their estimated surface normals.

In Chapter 4.2.2 it was described how to estimate a surface normal  $n$  for a point  $p$ . Consider two points  $p_i$  and  $p_j$  in the neighborhood  $\mathcal{P}^{k_2}$ . To compute the relative difference between two points  $p_i$  and  $p_j$  and their surface normals  $n_i$  and  $n_j$ , at either  $p_i$  or  $p_j$ , a fixed *Darboux coordinate frame* is defined. This is shown in Figure 4.18, where

$$p_s = p_i \quad , \quad n_s = n_i \quad , \quad p_t = p_j \quad , \quad n_t = n_j$$

or

$$p_s = p_j \quad , \quad n_s = n_j \quad , \quad p_t = p_i \quad , \quad n_t = n_i$$

The point  $p_s$  is chosen such that the angle between its associated normal  $n_s$  and the line connecting the  $p_i$  and  $p_j$  is minimal.

The Darboux coordinate frame has the axes  $U$ ,  $V$  and  $W$  where:

$$U = n_s \tag{4.17}$$

$$V = U \times \frac{(p_t - p_s)}{d} \tag{4.18}$$

$$W = U \times V \tag{4.19}$$

where  $d = \|p_t - p_s\|_2$  is the Euclidean distance between  $p_s$  and  $p_t$ . [23].

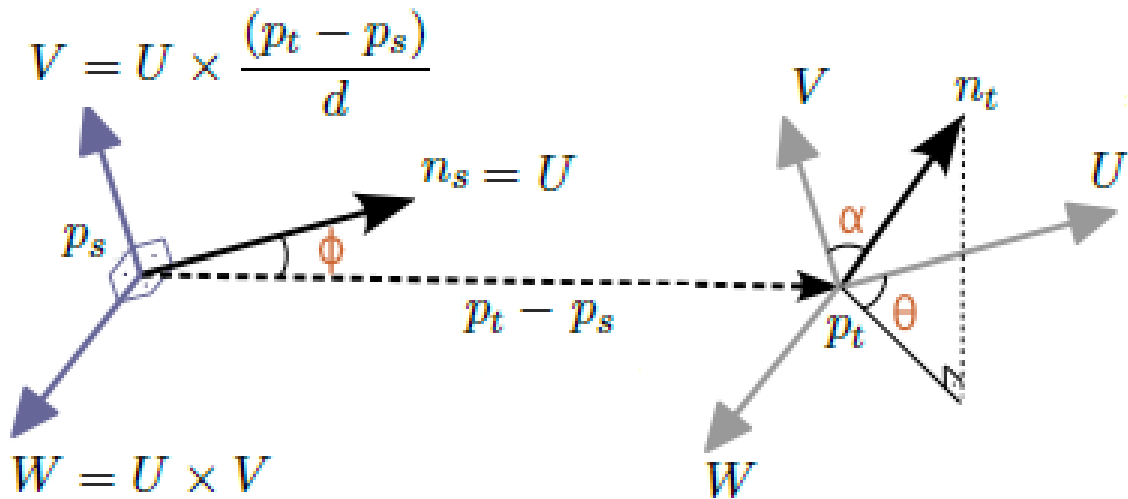


Figure 4.18: A graphical representation of the Darboux frame and the angular PFH features for a pair of points  $p_s$  and  $p_t$  with their associated normals  $n_s$  and  $n_t$  [23].

The angular variation of the two normals  $n_s$  and  $n_t$  can be expressed as follows

$$\begin{aligned}
 \alpha &= V \cdot n_t \\
 \phi &= U \cdot \frac{(p_t - p_s)}{d} \\
 \theta &= \tan^{-1}(W \cdot n_t, U \cdot n_t)
 \end{aligned}
 \tag{4.20}$$

For each pair of points  $p_i$  and  $p_j$  in the neighborhood  $\mathcal{P}^{k_2}$ , the angular variations  $\alpha, \phi$  and  $\theta$  of their normals and the euclidean distance between those points  $d$  are computed. This gives the quadruplet  $\langle \alpha, \phi, \theta, d \rangle$  for each pair of points. This reduces the 12 values ( $X, Y, Z, n_x, n_y, n_z$  for each point) of the two points and their normals to four values [23].

Figure 4.19 presents an influence region diagram of the PFH computation for a query point  $p_q$ .  $p_q$  (red), in the middle of the circle (or sphere in 3D) is interconnected with its  $k$  neighbours (blue) in a mesh.

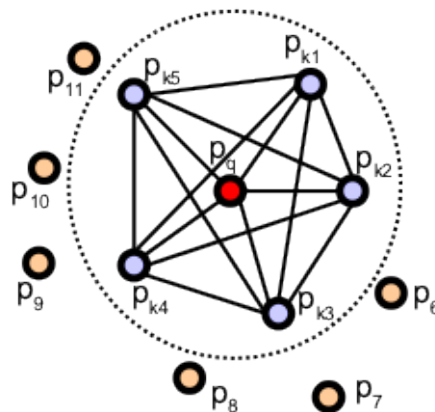


Figure 4.19: The influence region diagram for a Point Feature Histogram. The query point (red) and its  $k$ -neighbours (blue) are fully interconnected in a mesh [23].

To create the final PFH representation for the query point  $p_i$ , the set of all quadruplets is binned into a histogram. The binning process divides each feature's value range into  $b$  subdivisions, and counts the number of occurrences in each sub-interval. Since three out of the four features in the quadruplet are measure of the angles between normals, their values can be normalized to the same interval on the trigonometric circle. A binning example is to divide each feature interval into the same number of equal parts, and therefore create a histogram with  $b^4$  bins in a fully correlated space. In this space, a histogram bin increment corresponds to a point having certain values for all its four features. Figure 4.20 presents examples of Point Feature Histograms representations for different points in a cloud.

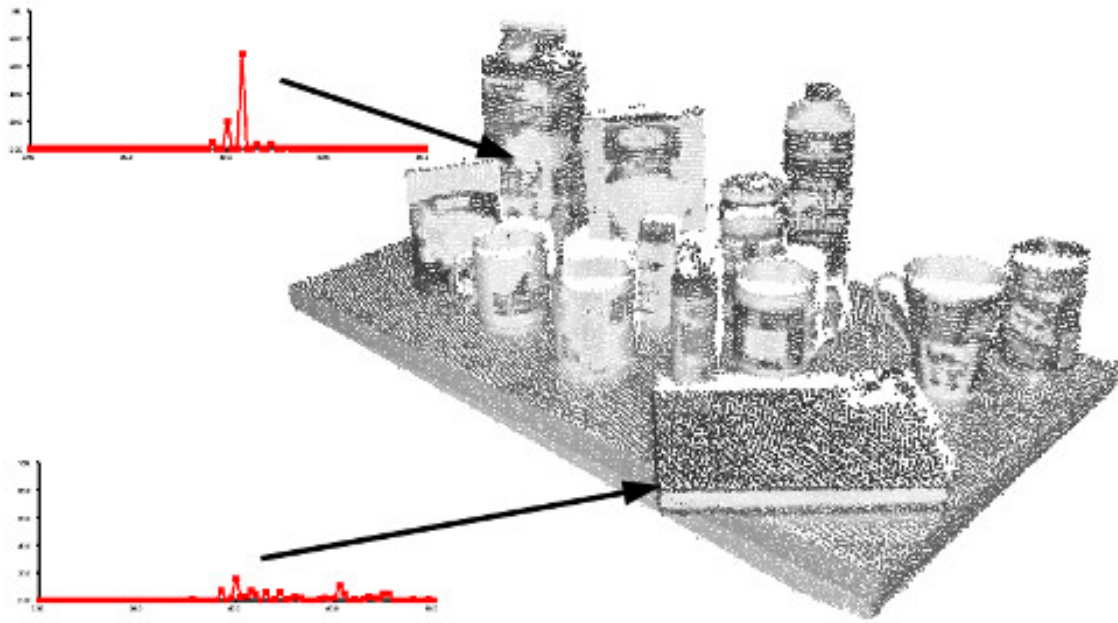


Figure 4.20: Examples of Point Feature Histograms representations for different points in a cloud [23].

In some cases, the fourth feature,  $d$ , does not present an extreme significance for 2.5D datasets captured with one RGB-D camera, as the distance between neighboring points increases from the viewpoint. Therefore, omitting  $d$  for scans where the local point density influences this feature dimension has proved to be beneficial [23].

**PFH can be summarized as follows:**

1. Create normals for all points in point cloud  $P$ .
2. Estimate features for a point  $p_i$  in  $P$ : The set of  $k$ -neighbours in the radius  $r$  around the point  $p_i$  ( $p_{ik}$ ) is taken. Four features are calculated between two points. The corresponding bin is incremented by 1. A point feature histogram (PFH) is generated.
3. The resulting set of histograms can be compared to those of other point clouds in order to find correspondences.



#### 4.2.4 FPFH - Fast Point Feature Histogram

For real-time or near real-time applications, the computation of Point Feature Histograms in dense point neighborhoods can represent one of the major bottlenecks. The theoretical computational complexity of the PFH for a given point cloud  $P$  with  $n$  points is  $O(n \cdot k^2)$ , where  $k$  is the number of neighbors for each point  $p$  in  $P$  [23]. Fast point feature histograms (FPFH) is a simplified version of point feature histograms (PFH) that reduces the computational complexity of the algorithm to  $O(n \cdot k)$ , while still retaining most of the discriminative power of the PFH.

First a set of tuples  $\alpha$ ,  $\phi$  and  $\theta$  are computed (in equation (4.20)) between itself and its neighbours, for each query point  $p_q$ , as described in PFH. This is called the simplified point feature histogram (SPFH). Next, the  $k$  neighbors are re-determined for each point, and the neighboring SPFH values are used to weight the final histogram of  $p_q$  (called FPFH) as follows [23]:

$$\text{FPFH}(p_q) = \text{SPFH}(p_q) + \frac{1}{k} \sum_{i=1}^k \frac{1}{\omega_k} \cdot \text{SPFH}(p_k) \quad (4.21)$$

where the weight  $\omega_k$  represents a distance between the query point  $p_q$  and a neighbor point  $p_k$  in some given metric space. Figure 4.21 presents the influence region diagram for a  $k$ -neighborhood set centered at  $p_q$ .

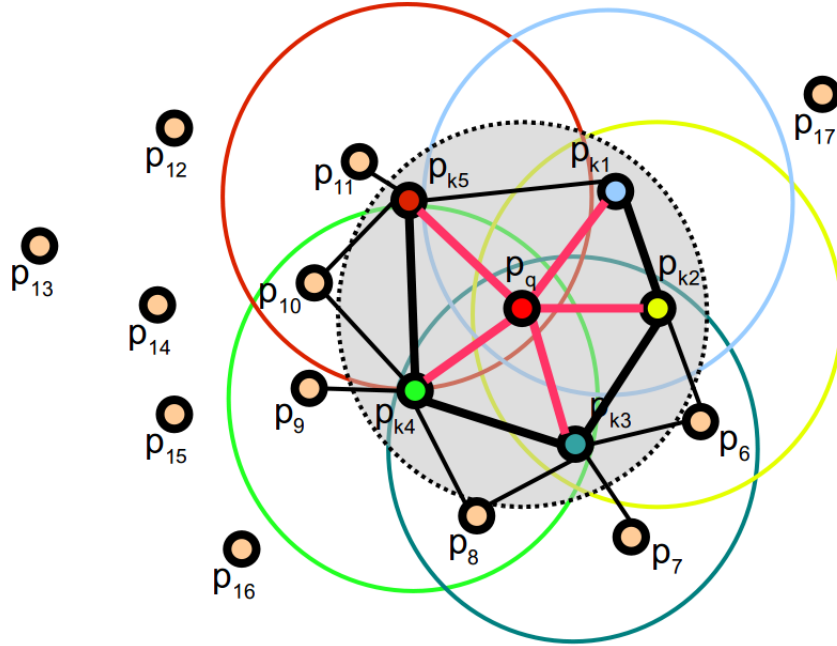


Figure 4.21: The influence region diagram for a Fast Point Feature Histogram. Each query point (red) is connected only to its direct  $k$ -neighbors (enclosed by the gray circle). Each direct neighbor is connected to its own neighbors and the resulted histograms are weighted together with the histogram of the query point to form the FPFH. The connections marked with thicker lines will contribute to the FPFH twice [23].

The algorithm first estimates its SPFH values for a given query point  $p_q$  by creating pairs

between itself and its neighbors (illustrated using red lines). This is repeated for all the points in the dataset, followed by a re-weighting of the SPFH values of  $p_q$  using the SPFH values of its  $p_k$  neighbors. This creates the FPFH for  $p_q$  [23]. The extra FPFH connections, as a result from the additional weighting scheme, are shown with black lines. The connections marked with thicker lines will be counted twice.

**FPFH can be summarized as follows:**

1. Create normals for all points in  $P$
2. Estimate features for a point  $p_i$  in  $P$ : The set of  $k$ -neighbours in the radius  $r$  around the point  $p_i$  ( $p_{ik}$ ) is taken. Three features are calculated between two points (only between  $p_i$  and its neighbours). The corresponding bin is incremented by 1. A simple point feature histogram (SPFH) is generated.
3. To reach more points and connections (up to 2 times  $r$ ) the SPFH of the neighbours are added weighted according to their spatial distance as a last step.
4. The resulting set of histograms can be compared to those of other point clouds in order to find correspondences.

### 4.3 Program Code for Depth Camera

This section explains the principle behind some of the program code used on the data obtained by the depth camera.

#### 4.3.1 Aligning Object Templates to a Point Cloud

To be able to get the pose of an object with respect to a known coordinate frame, some of the example code from Point Cloud Library (PCL) called `template_alignment` was used [18]. `Template_alignment` will, as the name suggests, be used to perform template alignment (also referred to as template fitting/matching/registration). A template is typically a small group of pixels or points that represents a known part of a larger object or scene. The pose of the object in a scene, can be found by registering a template (reference cloud) to a new point cloud (target cloud). That is, the program estimates a transformation  $T_t^r$  from the pose of the object in the reference cloud to the objects' pose in the target cloud.

#### How the program works

The code reads the cloud from the camera and then computes the cloud's surface normals. To do so, the radius  $r_n$  that defines each point's neighborhood must be specified. Then, the feature search radius  $r_f$  is specified so the FPFH-descriptors can be computed.

Once all the descriptors of the two point clouds (target and reference) have been computed, a particular version of the RANSAC algorithm (RANDOM SAMPLE CONSENSUS) is used to find a raw alignment between the clouds [29]. This version is called SAC-IA (SAMPLE CONSENSUS - INITIAL ALIGNMENT) and takes a template as input and aligns it to the target cloud (i.e., the cloud to which the templates will be aligned).

SAC-IA tries to maintain the same geometric relations of the correspondences as the greedy initial alignment method described in [25], without having to try all combinations of a limited set of correspondences (corresponding points). Instead, a large number of correspondence candidates are sampled in a sample  $s$ . The SAC-IA computes the transformation  $T_t^r$  defined by the sample points and their correspondences and compute an error metric for the point cloud that computes the quality of the transformation.

The SAC-IA takes three parameters:

- The minimum distances  $d_{min}$  between samples. That is, the  $s$  samples are selected only if their pairwise distances are greater than  $d_{min}$ .
- The maximum distance threshold  $c_{max}$  between two corresponding points in reference- and target cloud. If the correspondences have larger distances than  $c_{max}$ , the points will be ignored in the alignment process.
- The maximum number of iterations the internal optimization should run for.

The given template is set as the SAC-IA algorithm's source cloud and then it aligns the source to the target [24].

### 4.3.2 Region Growing Segmentation

The purpose of the segmentation is to group points with similar features into segments. Segments are smooth surfaces that are achieved by grouping neighboring points with similarity measures, such as the direction of a locally estimated surface normal.

Point clouds can be segmented into multiple surfaces. The surface growing algorithm starts from the optimal seed points and extend surfaces to neighboring points based on a pre-defined criteria [13]. Selection of the seed point is an important step and the final segmentation results depend on it. First a plane equation, as shown in Figure 4.22, is defined for each seed point and its neighboring points in order to find the optimal seed point. Then, the residuals (orthogonal distances of the point clouds to the best fitted plane) are computed [13]. Figure 4.23 shows a representation of surface normals and segmentation parameters. The point within the fitted plane with lowest square sum of residuals is considered the optimal seed point.

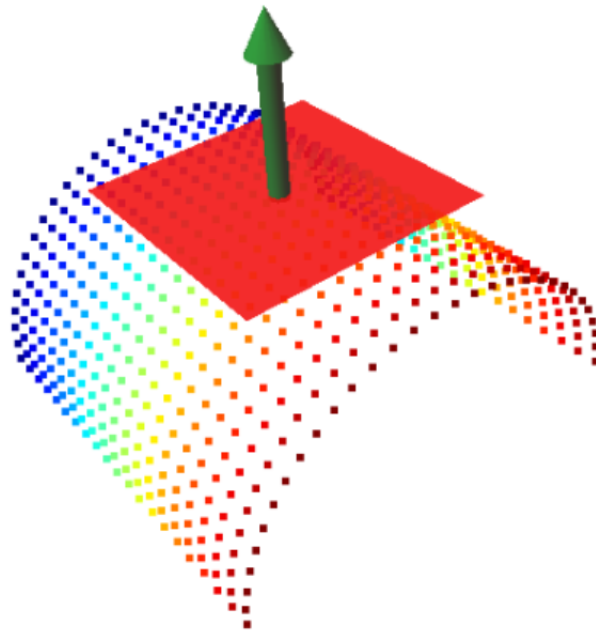


Figure 4.22: Normal estimation by fitting a plane to the points in the neighborhood [19].

The candidate point with a orthogonal distance to the fitted plane (residual) which is below the predefined threshold is accepted as a new surface point. To increase the efficiency of the program while using low accurate point clouds, the plane equation is updated after adding the new candidate point to the corresponding surface points. The neighborhood threshold  $k$  and residual threshold  $r_{th}$  are used to determine the smoothness of the fitted plane [13]. Secondly, the local surface normal at each point is compared with its neighboring points. The neighboring points are accepted if the angle between the surface normal and normal at the neighboring point is below the pre-defined threshold  $\theta_{th}$ .

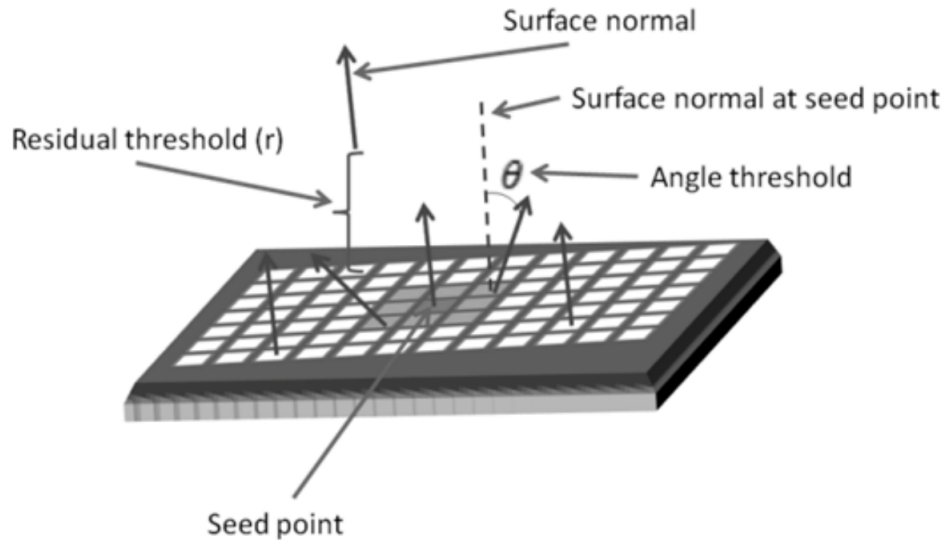


Figure 4.23: Representation of surface normals and segmentation parameters [13].

The process of region growing proceeds in the following steps [19]:

1. Specify a residual threshold  $r_{th}$ .
2. Define a smoothness threshold  $\theta_{th}$  in terms of the angle between the normals of the current seed and its neighbors.
3. If all the points already have been segmented go to step 7. Otherwise select the point with the minimum residual as the current seed.
4. Select the neighboring points of the current seed by using  $k$ -nearest neighbours with specified parameters. Add the points that have normals with smaller angle than the angle threshold to the current region. Add the points whose residuals are less than  $r_{th}$  to the list of potential seed points.
5. If the potential seed point list is not empty, set the current seed to the next available seed, and go to step 4.
6. Add the current region to the segmentation and go to step 3.
7. Return the segmentation result.

A segmented point cloud of the cylinder to the left and the piston to the right is shown in Figure 4.24.

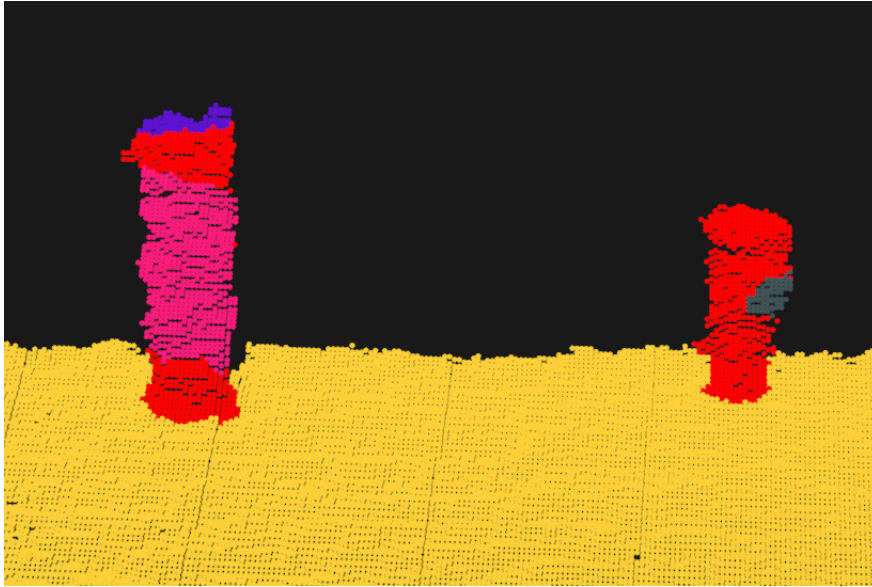


Figure 4.24: A segmented point cloud.

The segment grown on the cylinder is colored pink and the segment grown on the piston is colored dark grey. There is also a purple segment on the top of the cylinder. The color of the segments is randomly generated every time the viewer is run, but the unsegmented points are always red. The table, colored yellow, is separated from the objects by the difference of the angle between the surface normals. If a point's normal has a larger angle difference than the specified threshold  $\theta_{th}$ , the points are not segmented. The flat property of the table makes it a good fit for the plane equation giving the points on the table low residual values. The piston on the other hand is not very well segmented since the plane equation is not ideal for the strong curvature of the piston. The growing region starts its growth where the residuals have the lowest value. For a cylinder shaped object the residual value is high near the top edge and the bottom edge of the object. The segmentation for the piston does not always start from the right side as shown in Figure 4.24, but seed points will always start its growth from somewhere in the middle of the height of the piston if the parameters stays the same. Figure 4.25 shows a segmented point cloud with the same parameters.

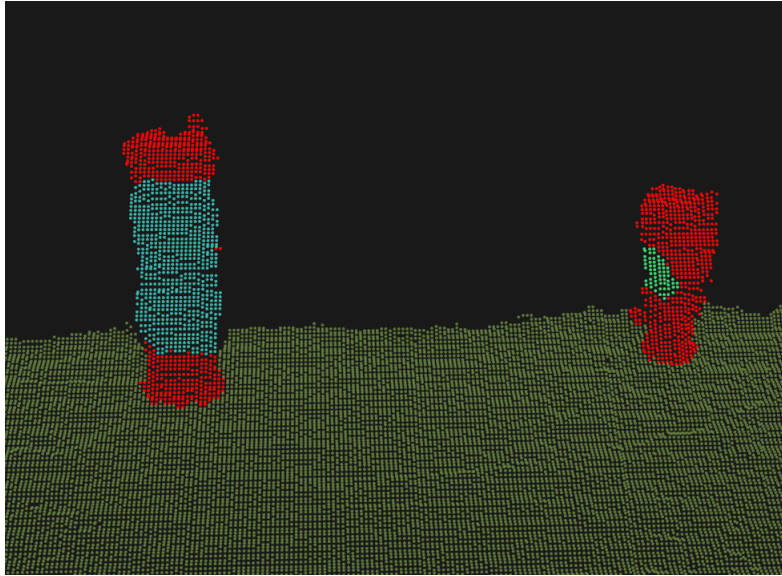


Figure 4.25: A segmented point cloud.

Here the segmentation have started its growth from the left side on the piston. A better segmentation of the piston can be obtained by increasing the residual threshold as shown in Figure 4.26.

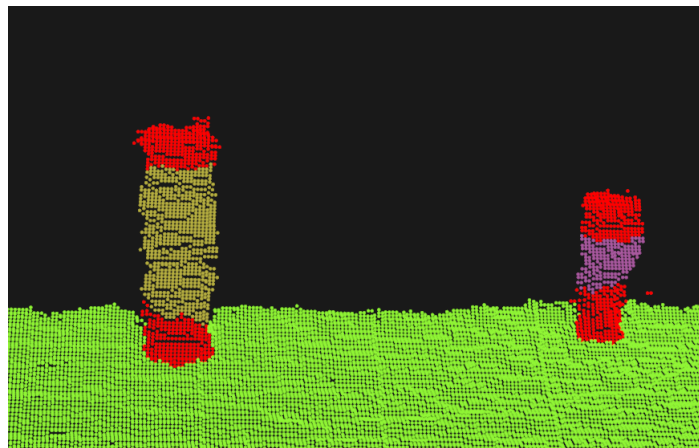


Figure 4.26: A segmented point cloud.

Here the residual threshold is higher so more seed points are found on the piston.

If the  $k$ -nearest neighbours is increased, the the segmented area also increases. Figure 4.27 shows how the point cloud is segmented when searching in a larger neighbourhood.

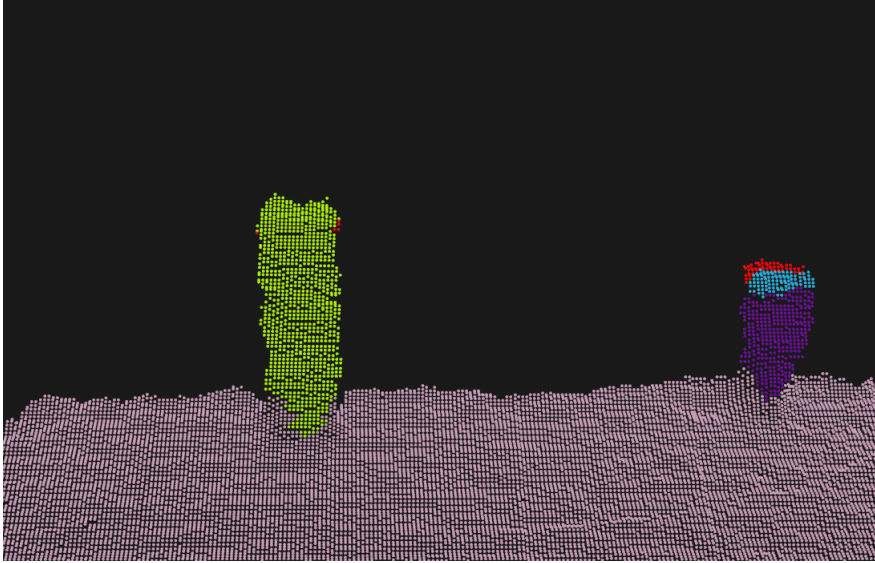


Figure 4.27: A segmented point cloud.

Searching in a larger neighbourhood increases the chance of finding an acceptable seed point to grow from.



### 4.3.3 Statistical Removal of Outliers

Noisy points in the point cloud complicates the estimation of local point cloud characteristics such as surface normals or curvature changes, leading to erroneous values. Some of these irregularities can be solved by performing a statistical analysis on each point's neighborhood, and trimming those which do not meet a certain criteria.

Luckily PCL [18] has developed a filter that removes sparse outliers. The filter is based on the computation of the distribution of point to neighbors distances in the input dataset. The mean distance from a point to all its neighbours is computed for each point. By assuming that the resulted distribution is Gaussian with a mean and a standard deviation, all points whose mean distances are outside an interval defined by the global distances mean and standard deviation can be considered as outliers and trimmed from the dataset.

In this thesis the filter was implemented in the following way. First the excess points (Figure 4.29) are removed from the point cloud (Figure 4.28), leaving only the points of interest (Figure 4.30) in the cloud.

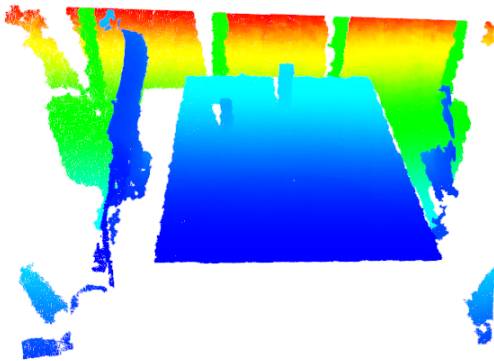


Figure 4.28: Unfiltered point cloud.

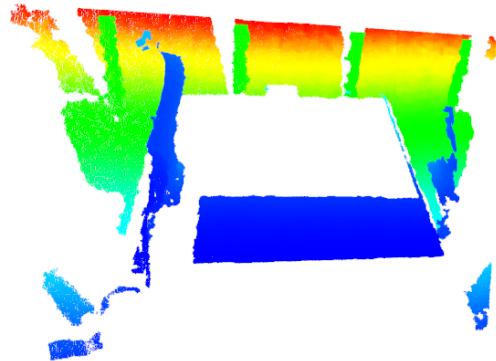


Figure 4.29: Removed part of point cloud.

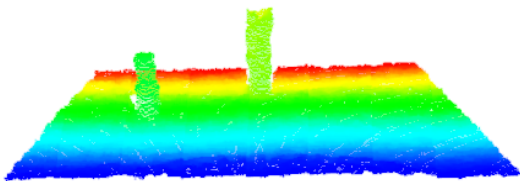


Figure 4.30: Remaining part of point cloud.

Figure 4.31 shows a side view of the cloud in Figure 4.30. By running the statistical outlier removal filter on this cloud, noisy points can be removed from the cloud, leaving only the cloud in Figure 4.33. The trimmed outliers are shown in Figure 4.32.



Figure 4.31: Side view of the point cloud.



Figure 4.32: Noisy points that are trimmed away by the filter.



Figure 4.33: Filtered point cloud.

## Chapter 5

# Computer Vision Experiments and Results

### 5.1 Experiments based on the RGB-D Camera

#### 5.1.1 Calibration of AR-tag Coordinate Frame

This section explains how the coordinate frame of the camera is transformed on to the table. Three AR-tags, ID0, ID2 and ID3 were placed on the table 90 degrees to each other, forming an  $X Y$  plane aligned with the table as shown in Figure 5.1. The  $Z$  axis has its origin in the AR-tag in the middle (ID3) and is set to be orthogonal to the  $X Y$  plane.

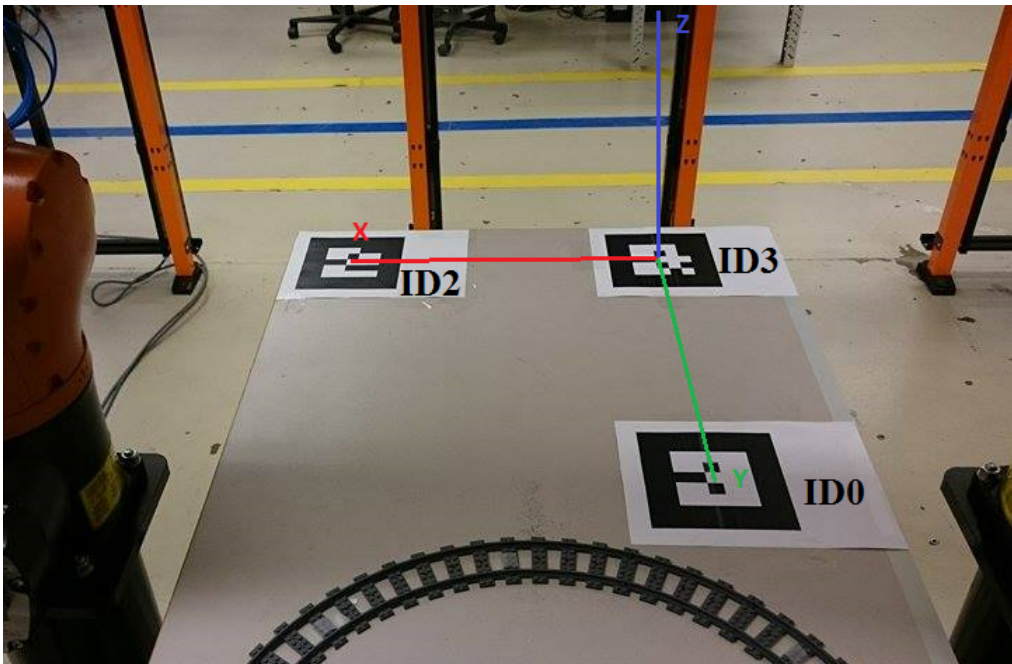


Figure 5.1:  $X Y$  plane is defined between the AR-tags.  $X$  axis is red,  $Y$  axis is green and  $Z$  axis is blue.

The center points  $p_i = (x_i, y_i, z_i)^T$  of each AR-tag  $ID_i$ ,  $i \in \{0, 2, 3\}$  were used in the estimation of transformation  $T_a^c$  from camera to the AR-tags on the table. A problem that occurred was that the coordinates  $x_i$ ,  $y_i$  and  $z_i$  of the AR-tags in the image stream moved randomly with an amplitude of up to 5 millimeters for each frame the camera captured. This was not acceptable

because the work to be done by the robot required high accuracy. Therefore 50 sample points were taken for each of the coordinates  $x_i$ ,  $y_i$  and  $z_i$  for each AR-tag. The median of the samples was used to determine the center points  $p_i$  for each AR-tag ID $i$ ,  $i \in \{0, 2, 3\}$ .

Figure 5.2, Figure 5.3 and Figure 5.4 shows the difference between the coordinates  $x_3$ ,  $y_3$  and  $z_3$  of the AR-tag ID3 fed directly from the camera and the median of 50 frame samples, for  $x_3$ ,  $y_3$  and  $z_3$  respectively. The red curve shows the live coordinate value from the camera and the blue curve shows the improved coordinate value, the median of 50 samples.

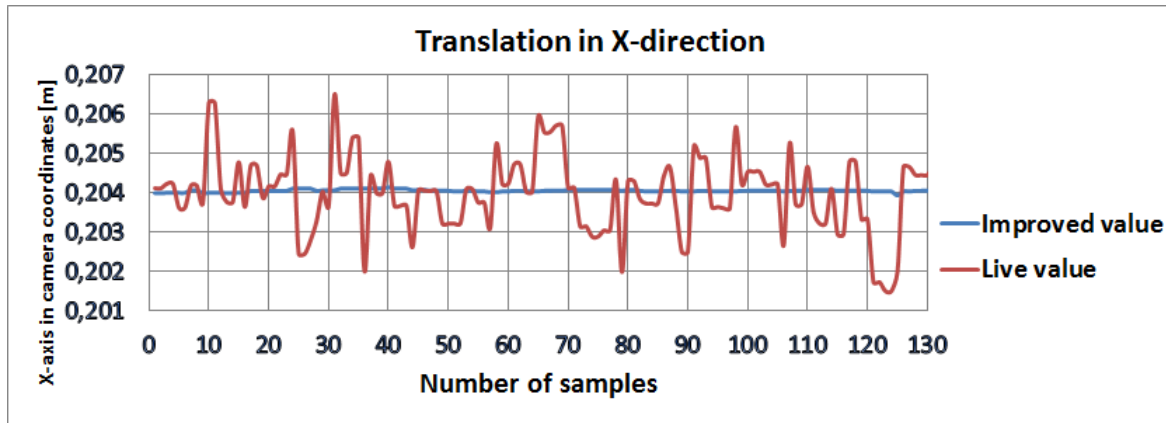


Figure 5.2: The difference between the live value and the improved value of the  $x_3$  coordinate, 1.6 m from the camera.

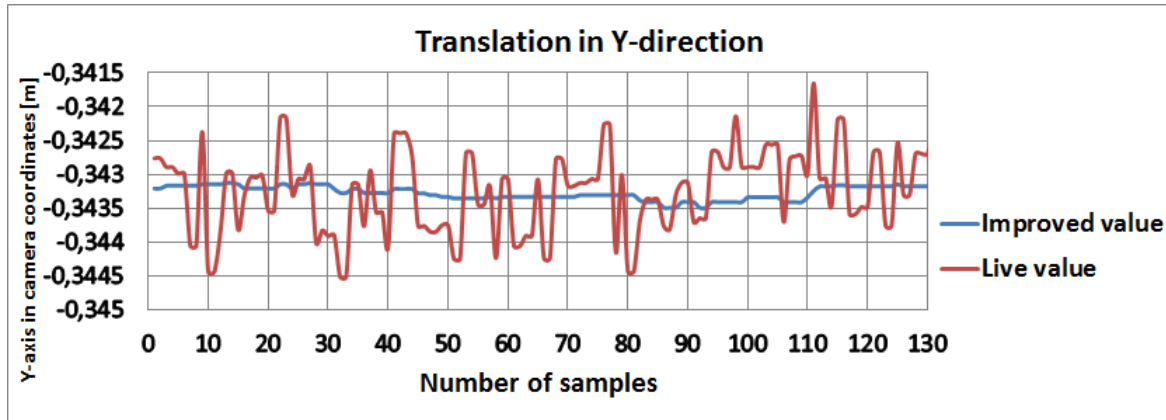


Figure 5.3: The difference between the live value and the improved value of the  $y_3$  coordinate, 1.6 m from the camera.

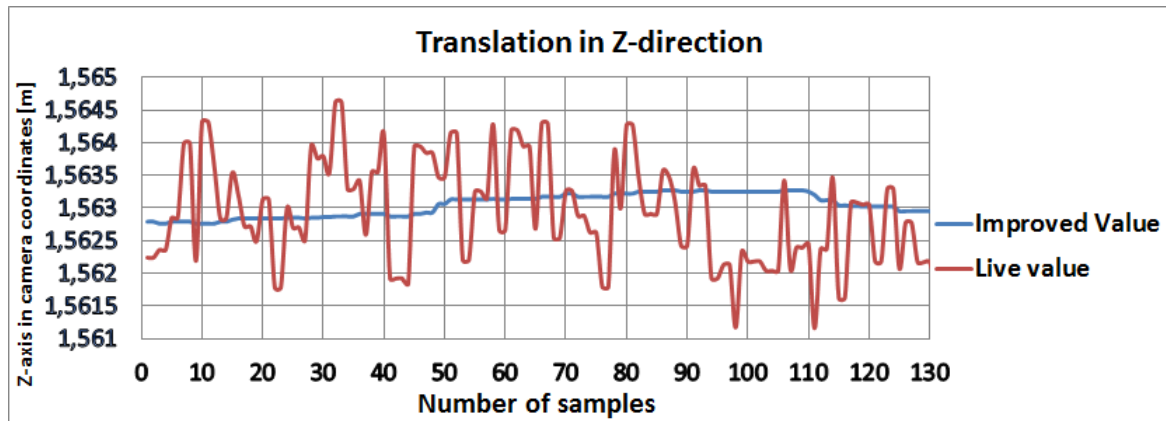


Figure 5.4: The difference between the live value and the improved value of the  $z_3$  coordinate, 1.6 m from the camera.

The graphs shows that the improved value is much more stable and accurate than the live value.

After the improved coordinates are computed, the program defines the axes of the coordinate frame. First, a unit vector  $X$  is defined along the  $X$  axis from  $p_3 = (x_3, y_3, z_3)^T$  (AR-tag ID3) to  $p_2 = (x_2, y_2, z_3)^T$  (AR-tag ID2):

$$X = \frac{p_2 - p_3}{\sqrt{(x_2 - x_3)^2 + (y_2 - y_3)^2 + (z_2 - z_3)^2}} \quad (5.1)$$

Next, a unit vector  $Y$  is defined from  $p_3 = (x_3, y_3, z_3)^T$  (AR-tag ID3) to  $p_0 = (x_0, y_0, z_0)^T$  (AR-tag ID0):

$$Y = \frac{p_0 - p_3}{\sqrt{(x_0 - x_3)^2 + (y_0 - y_3)^2 + (z_0 - z_3)^2}} \quad (5.2)$$

And lastly a unit vector  $Z$  is calculated as the cross product between  $X$  and  $Y$ , rising orthonormal upwards from the  $X Y$  plane:

$$Z = X \times Y \quad (5.3)$$

The three unit vectors  $X$ ,  $Y$  and  $Z$  is then inserted into a  $3 \times 3$  rotation matrix like so:

$$R = \begin{bmatrix} X & Y & Z \end{bmatrix} \quad (5.4)$$

Next, the program repeatedly checks if the determinant of the rotation matrix  $R$  is 1, which means that the  $X$ ,  $Y$  and  $Z$  axes are orthonormal to each other. When  $R$  is 1 ( $1 > R > 0.9999$ ), it is inserted into a homogeneous transformation matrix  $T_a^c$ , which can be used to transform the coordinate frame of the camera  $c$  to the AR-tag  $a$ .

$$T_a^c = \begin{bmatrix} R & p_3 \\ 000 & 1 \end{bmatrix} \quad (5.5)$$

The center point of ID3,  $p_3 = (x_3, y_3, z_3)^T$ , is the origin of the coordinate frame.

For the 50 sample points of each of the coordinates  $x_i$ ,  $y_i$  and  $z_i$  value for each AR-tag, the mode of each sample was also used to make a rotation matrix. Three rotation matrices were estimated, one with the median of the samples, one with the mode of the samples and one with live values from  $x_i$ ,  $y_i$  and  $z_i$  value for each AR-tag. Figure 5.5 shows the result of the determinant values of these rotation matrices.

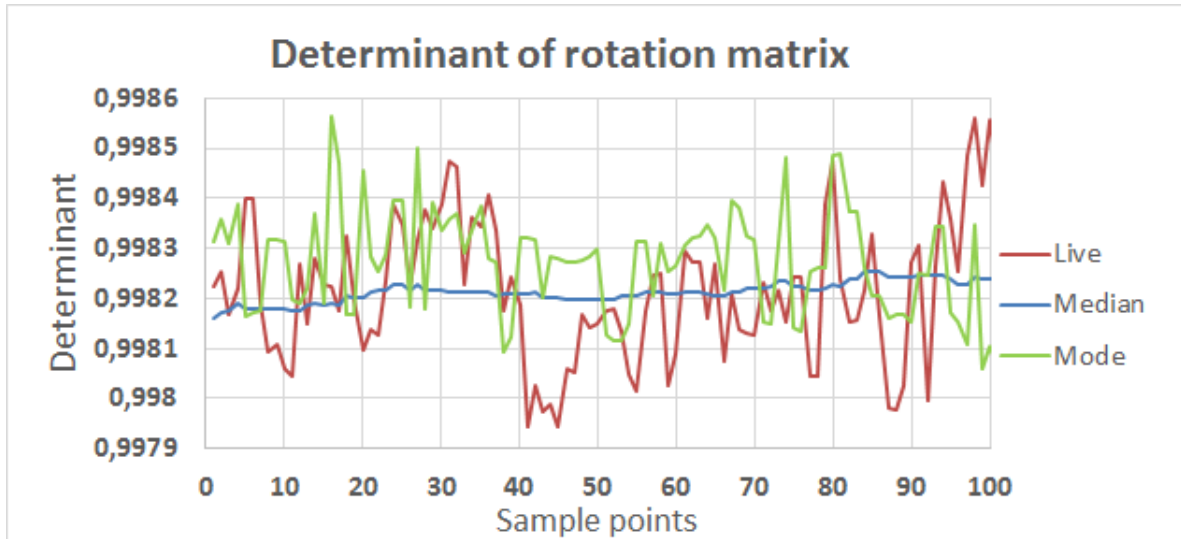


Figure 5.5: The determinant values of the rotation matrix acquired from AR-tag 1.60 m from the camera.

The first rotation matrix to obtain a determinant value between 0.9999 and 1 from either the median- or the mode-value is used in the transformation. In the diagram in Figure 5.5 none of the values would be approved as they are not 0.9999. In order to get the determinant to become 0.9999, one AR-tag had to be moved more than one centimeter away from perpendicular position to the other tags. This was not acceptable, so further experiments had to be conducted.

To see if the accuracy would increase if the AR-tags were closer to the camera, another experiment was conducted. The AR-tags were positioned 0.45 m closer to the camera as shown in Figure 5.6.

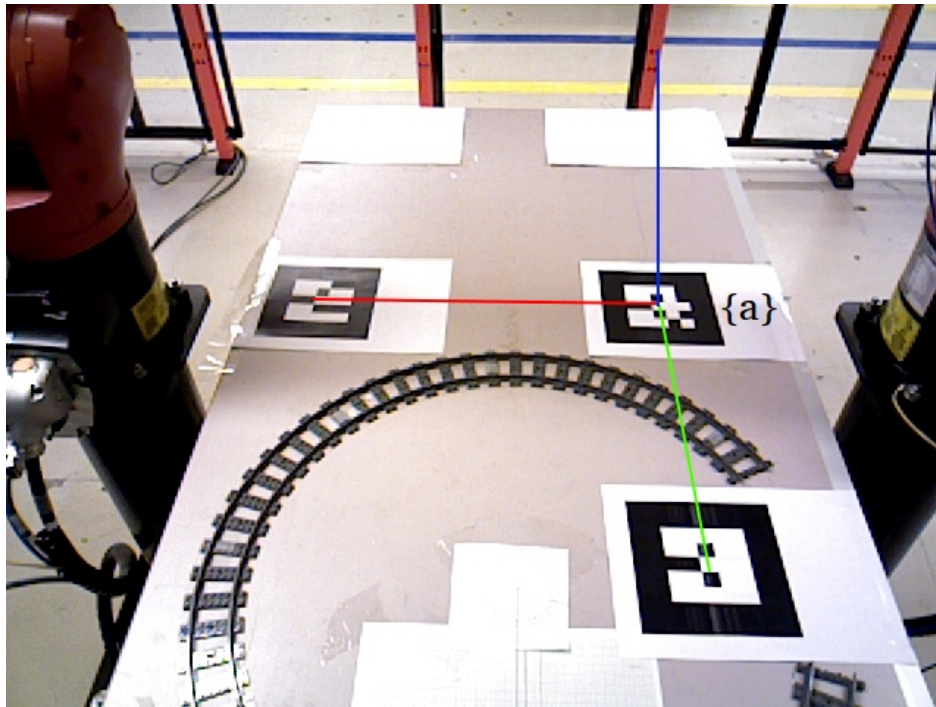


Figure 5.6: AR-tag is 1.15 m from the camera.

The translation  $p_3$  in  $T_a^c$  is shown in Figure 5.7, Figure 5.8 and Figure 5.9 for the  $x_3$ ,  $y_3$  and  $z_3$  coordinate respectively.

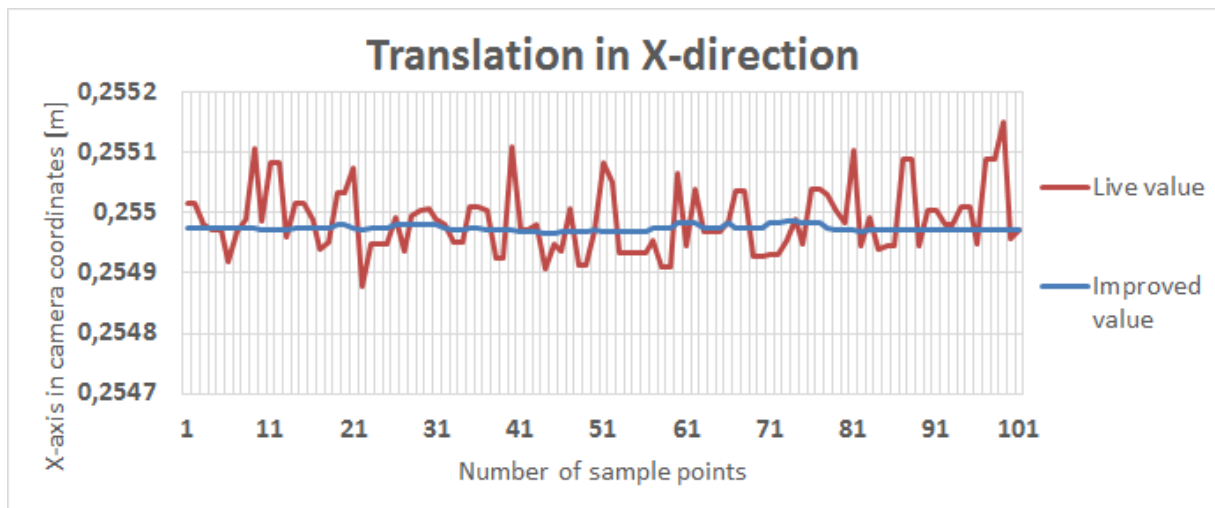


Figure 5.7: The difference between the live value and the improved value of the  $x_3$  coordinate, 1.15 m from the camera.

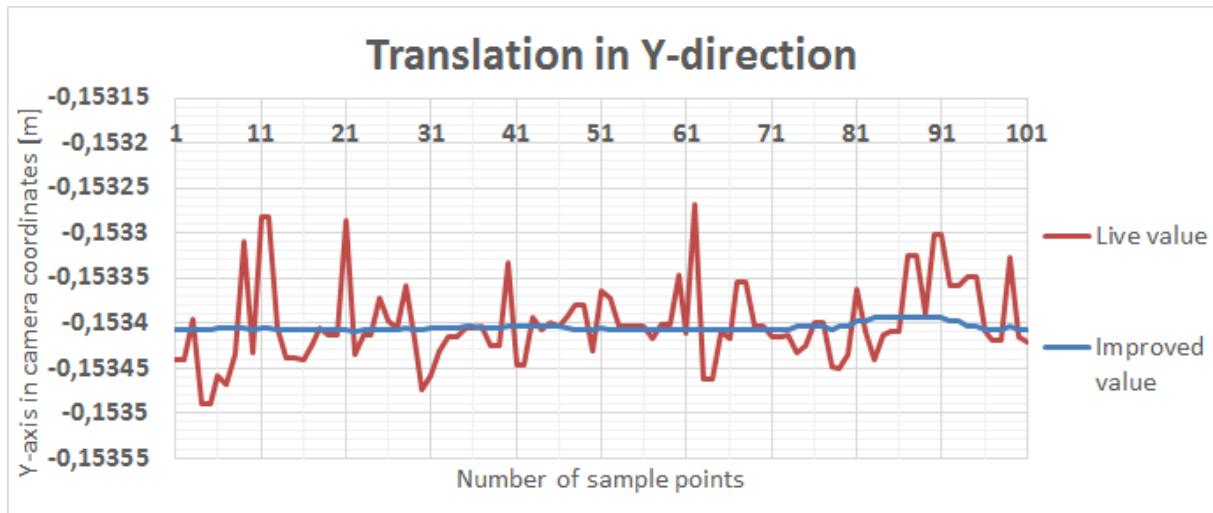


Figure 5.8: The difference between the live value and the improved value of the  $y_3$  coordinate, 1.15 m from the camera.

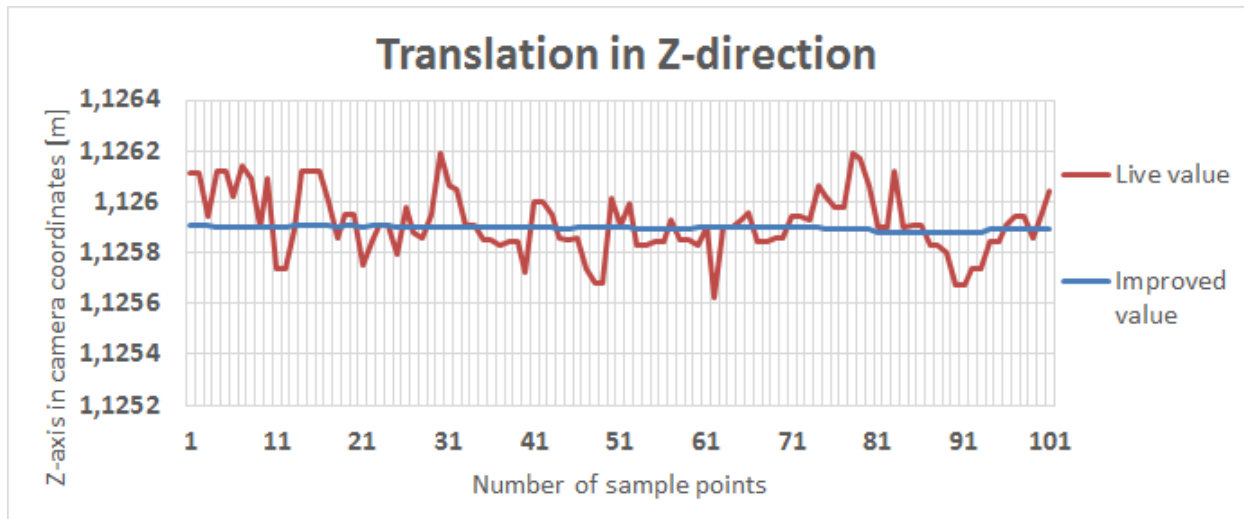


Figure 5.9: The difference between the live value and the improved value of the  $z_3$  coordinate, 1.15 m from the camera.

Figure 5.10 shows the difference between the maximum and minimum value for the new translation  $p_3$  approximately 0.45 m closer to the camera than the original translation.

New	X-live	Y-live	Z-live	X-improved	Y-Improved	Z-improved
Max	0.255151	-0.15327	1.12619	0.254986	-0.15339	1.12591
Min	0.254879	-0.15349	1.12562	0.254967	-0.15341	1.12558
Max - Min	0.000272	0.00022	0.00057	0.000019	0.00002	0.00033

Figure 5.10: The variation of the highest value to the lowest value for the new translation 1.15 m from the camera.

Compared to the original translation, shown in Figure 5.11, the accuracy has improved greatly.



Original	X-live	Y-live	Z-live	X-improved	Y-Improved	Z-improved
Max	0.206503	-0.34214	1.56462	0.20414	-0.343126	1.56327
Min	0.201989	-0.344519	1.56117	0.203991	-0.343494	1.56276
Max - Min	0.004514	0.002379	0.00345	0.000149	0.000368	0.00051

Figure 5.11: The variation of the highest value to the lowest value for the original translation 1.60 m from the camera.

The difference between the original and the new translation is shown in Figure 5.12.

	X-live	Y-live	Z-live	X-improved	Y-Improved	Z-improved
Original variation	0.004514	0.002379	0.00345	0.000149	0.000368	0.00051
New variation	0.000272	0.00022	0.00057	0.000019	0.00002	0.00033
Difference	0.004242	0.002159	0.00288	0.00013	0.000348	0.00018

Figure 5.12: The difference between the original and the new translation.

This shows that better accuracy can be achieved by moving the camera closer to the AR-tag.

The resulting values of the determinant of the new rotation matrix acquired 1.15 m from the camera is shown in the diagram in Figure 5.13.

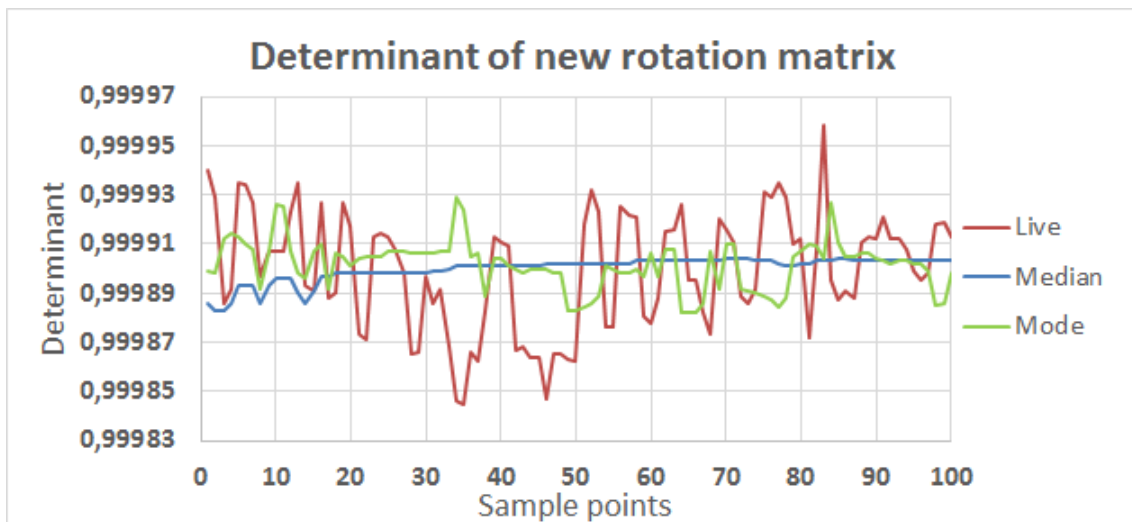


Figure 5.13: The determinant values of the new rotation matrix acquired from an AR-tag 1.15 m from the camera.

The new rotation matrix produced better results than the rotation matrix acquired from 1.60 m from the camera and here the AR-tags were perpendicular to each other.

This result gives us an efficient method to calibrate the camera to a flat surface, and if the camera is moved, all it takes is for the three AR-tags to be in the field of view of the camera. The computation process takes about 25 seconds, but it is only needed once per camera position.

**Calibration of AR-tag-Coordinate Frame using Geometric Algebra**

A unit vector  $X$  (normalized vector from  $p_3$  to  $p_2$ ) was estimated to be

$$X = (-0.9995, 0.0006, 0.0309)$$

and a unit vector  $Y$  (normalized vector from  $p_3$  to  $p_0$ ) was estimated to be

$$Y = (-0.0120, 0.6838, -0.7296)$$

Defining a bivector  $X \wedge Y$  aligned with the table, where

$$\begin{aligned} X &= x_1e_1 + x_2e_2 + x_3e_3 \\ &= -0.9995e_1 + 0.0006e_2 + 0.0309e_3 \end{aligned}$$

and

$$\begin{aligned} Y &= y_1e_1 + y_2e_2 + y_3e_3 \\ &= -0.0120e_1 + 0.6838e_2 - 0.7296e_3 \end{aligned}$$

is

$$X \wedge Y = (x_1e_1 + x_2e_2 + x_3e_3) \wedge (y_1e_1 + y_2e_2 + y_3e_3) = -0.0216e_{23} - 0.73e_{31} - 0.683e_{12}$$

Determine a new  $Y$  axis  $Y_{new}$  with use of the vector  $X$  and bivector  $X \wedge Y$  is done by

$$\begin{aligned} Y_{new} &= X \cdot (X \wedge Y) \\ &= (-0.9995e_1 + 0.0006e_2 + 0.0309e_3) \cdot (-0.0216e_{23} - 0.73e_{31} - 0.683e_{12}) \\ &= -0.0221e_1 + 0.684e_2 + 0.729e_3 \end{aligned}$$

were  $Y_{new}$  is  $X$  rotated  $90^\circ$  anti-clockwise in the bivector  $X \wedge Y$ .

The new  $Z$  axis  $Z_{new}$  is then the normal to  $X \wedge Y$

$$\begin{aligned} Z_{new} &= (X \wedge Y)^* \\ &= (X \wedge Y)I^{-1} \quad \text{where } I^{-1} = e_3 \wedge e_2 \wedge e_1 \\ &= (-0.0216e_{23} - 0.73e_{31} - 0.683e_{12})e_{321} \\ &= -0.0216e_1 - 0.73e_2 - 0.683e_3 \end{aligned}$$

The AR-tag ID3, center point  $p_3$ , was located at

$$p_3 = (0.2293, 0.0011, 1.2589)^T$$

The transformation matrix  $T_a^c$  based on geometric algebra is

$$T_a^c = \begin{bmatrix} X^T & Y_{new}^T & Z_{new}^T & p_3 \\ 0 & 0 & 0 & 1 \end{bmatrix}$$

$$T_a^c = \begin{bmatrix} -0.9995 & -0.0221 & -0.0216 & 0.2293 \\ 0.0006 & 0.684 & -0.73 & 0.0011 \\ 0.0309 & 0.729 & -0.683 & 1.2589 \\ 0 & 0 & 0 & 1 \end{bmatrix}$$

A summary of the geometric algebra calculations is illustrated in Figure 5.14.

Since geometric algebra let us rotate a vector  $90^\circ$  in a plane, the AR-tag ID0 does not necessarily have to be perpendicular to AR-tag ID3. The only information needed is an  $X$  axis defined with ID2 and ID3, as well as ID0 somewhere on the plane of the table.

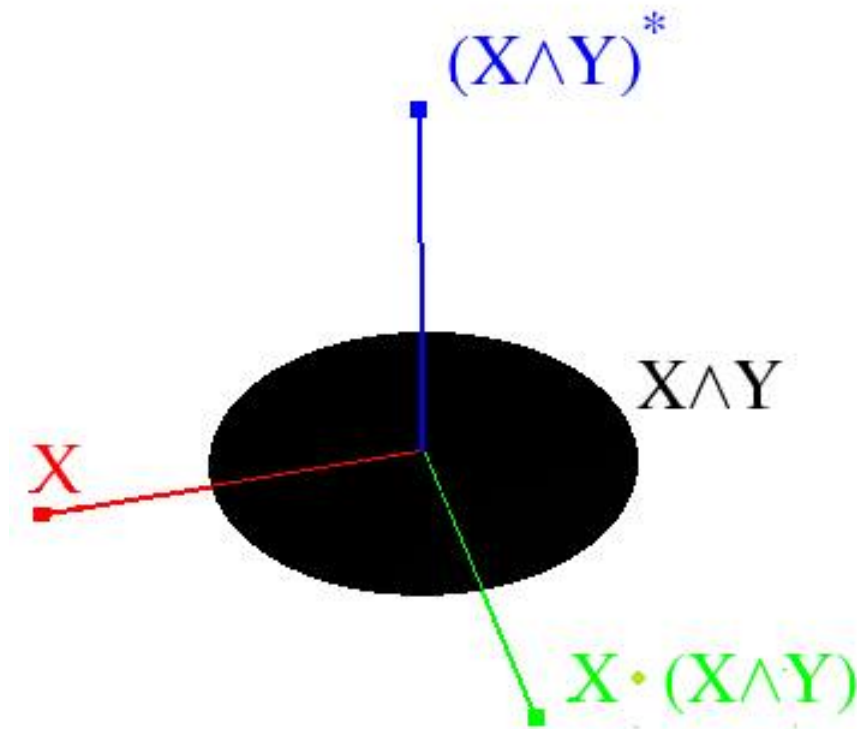


Figure 5.14: Coordinate system  $\{a\}$  estimated with geometric algebra.

### 5.1.2 Calibration of the Table Coordinate Frame

Transformation from the depth camera to the AR-tags  $T_a^c$  has already been described in Chapter 5.1.1. Transformation from the AR-tags  $\{a\}$  to the corner of table  $\{t\}$ ,  $T_t^a$ , is

$$T_t^a = \begin{bmatrix} 1 & 0 & 0 & -0.1905 \\ 0 & 1 & 0 & -0.604 \\ 0 & 0 & 1 & 0 \\ 0 & 0 & 0 & 1 \end{bmatrix} \quad (5.6)$$

and the transformation from the table  $\{t\}$  to the RGB-D camera  $T_c^t$  is

$$T_c^t = (T_t^a)^{-1}(T_a^c)^{-1} \quad (5.7)$$

In Figure 5.15 and Figure 5.16 the different poses  $\{a\}$  and  $\{t\}$  are shown.

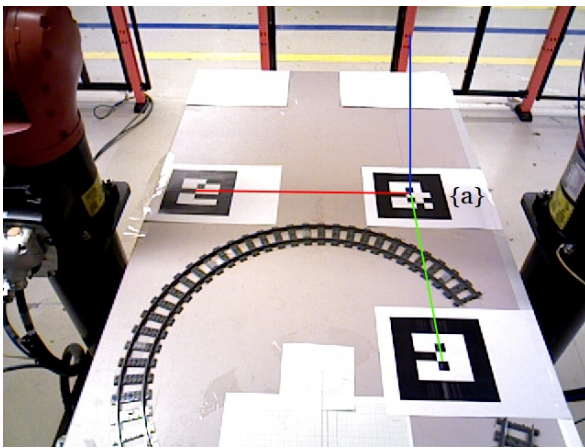


Figure 5.15: The coordinate system  $\{a\}$ .

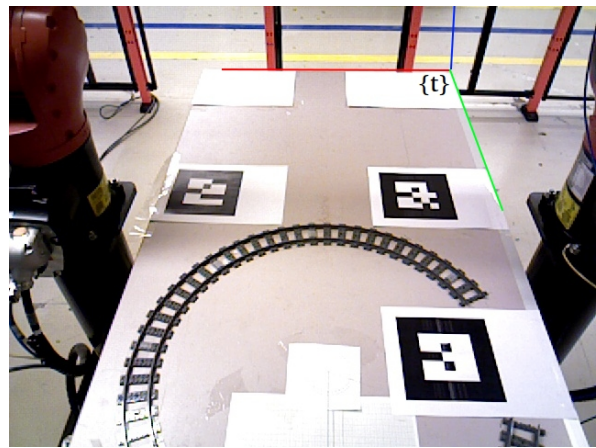


Figure 5.16: The coordinate system  $\{t\}$ .

The points  $p^c$  in the point cloud from the depth camera are transformed to points  $p^t$  given with respect to the table coordinate frame  $\{t\}$  like so

$$\underbrace{\begin{bmatrix} X \\ Y \\ Z \\ 1 \end{bmatrix}}_{\tilde{p}^t} = T_c^t \underbrace{\begin{bmatrix} X \\ Y \\ Z \\ 1 \end{bmatrix}}_{\tilde{p}^c} \quad (5.8)$$

In Figure 5.17 the process so far is shown.

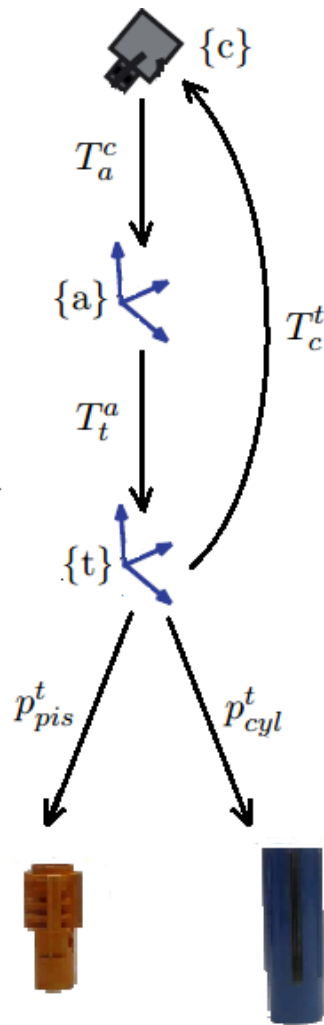


Figure 5.17: Transformation from depth camera  $\{c\}$  to the cylinder and the piston.

In Figure 5.18 the pose of the table frame  $\{t\}$  is shown. Even if the default transformation  $T_{ir}^{rgb}$  from IR camera to RGB camera was used, the final pose of table  $\{t\}$  is correct as shown in Figure 5.18.

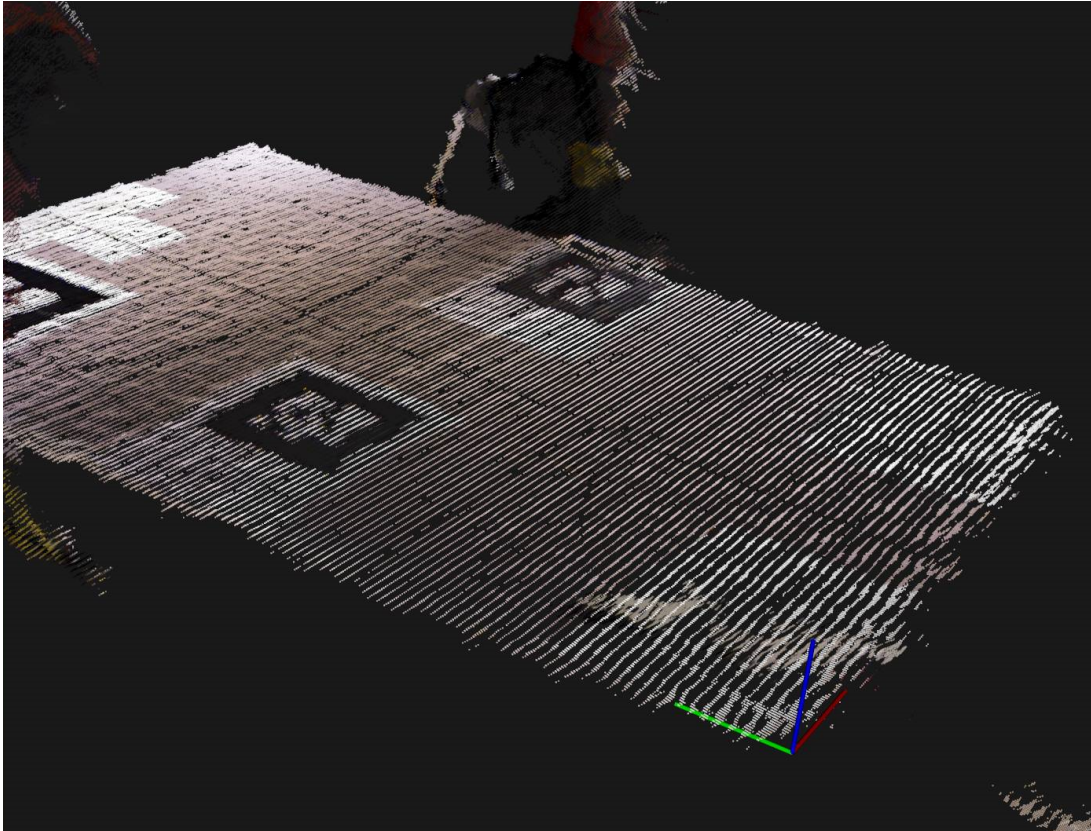


Figure 5.18: The pose of the table  $\{t\}$  is shown in the point cloud.

This coordinate frame is convenient when taking measurements and it is easy to relate to.

### 5.1.3 Template Alignment

This section explains how the code, Template alignment explained in Chapter 4.3.1, was used to locate the pose of the parts. A template cloud was made for the piston and another one for the cylinder. The two templates were then used in the code to align them to the target cloud.

The following parameters were set:

- Estimation of normal search radius  $r_n$
- Feature search radius  $r_f$  (FPFH)
- Minimum sample distance  $d_{\min}$  (SAC-IA)
- Maximum correspondence distance  $c_{\max}$  (SAC-IA)

Default parameters were set to:

- $r_n = 0.02$
- $r_f = 0.02$
- $d_{\min} = 0.05$
- $c_{\max} = 0.0001$

These parameters resulted in a template alignment as shown in Figure 5.19. The purple template is representing the piston and the brown template is representing the cylinder.

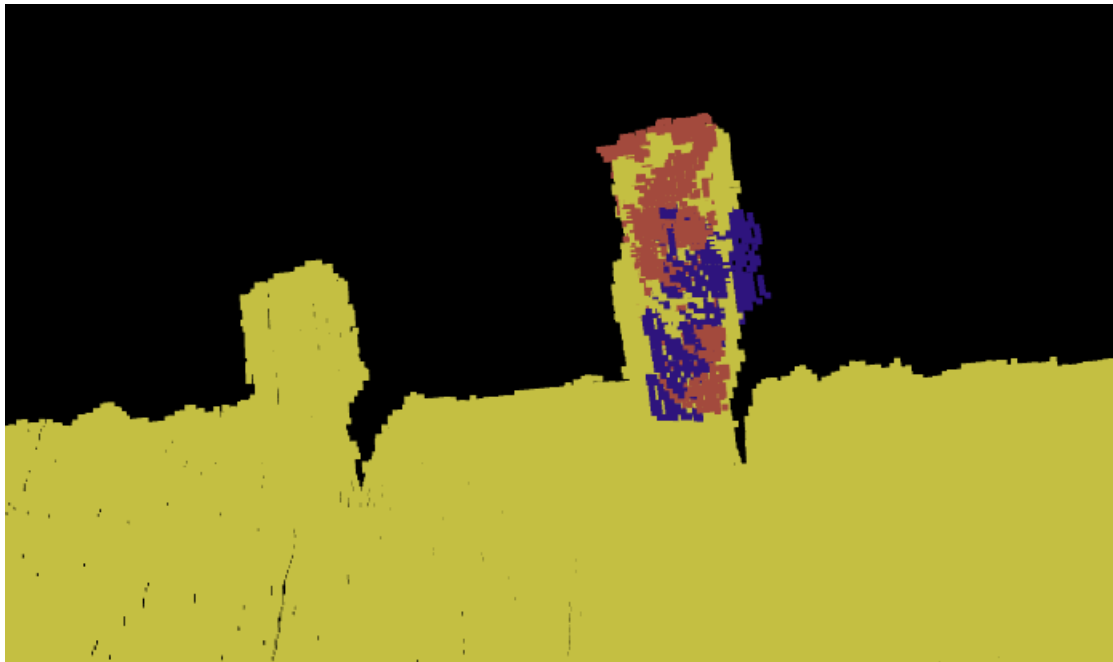


Figure 5.19: Template alignment with initial parameter values.

As shown in Figure 5.19 the initial parameter values did not align the templates correctly to the point cloud.

The best result was obtained by running two independent template alignment programs, one for each of the object. The following parameters were chosen for the program aligning the cylinder:

- $r_n = 0.023$
- $r_f = 0.034$

and for the piston:

- $r_n = 0.02$
- $r_f = 0.025$

Common for both programs:

- $d_{\min} = 0.025$
- $c_{\max} = 0.00005$

These parameter values resulted in an alignment as shown in Figure 5.20.

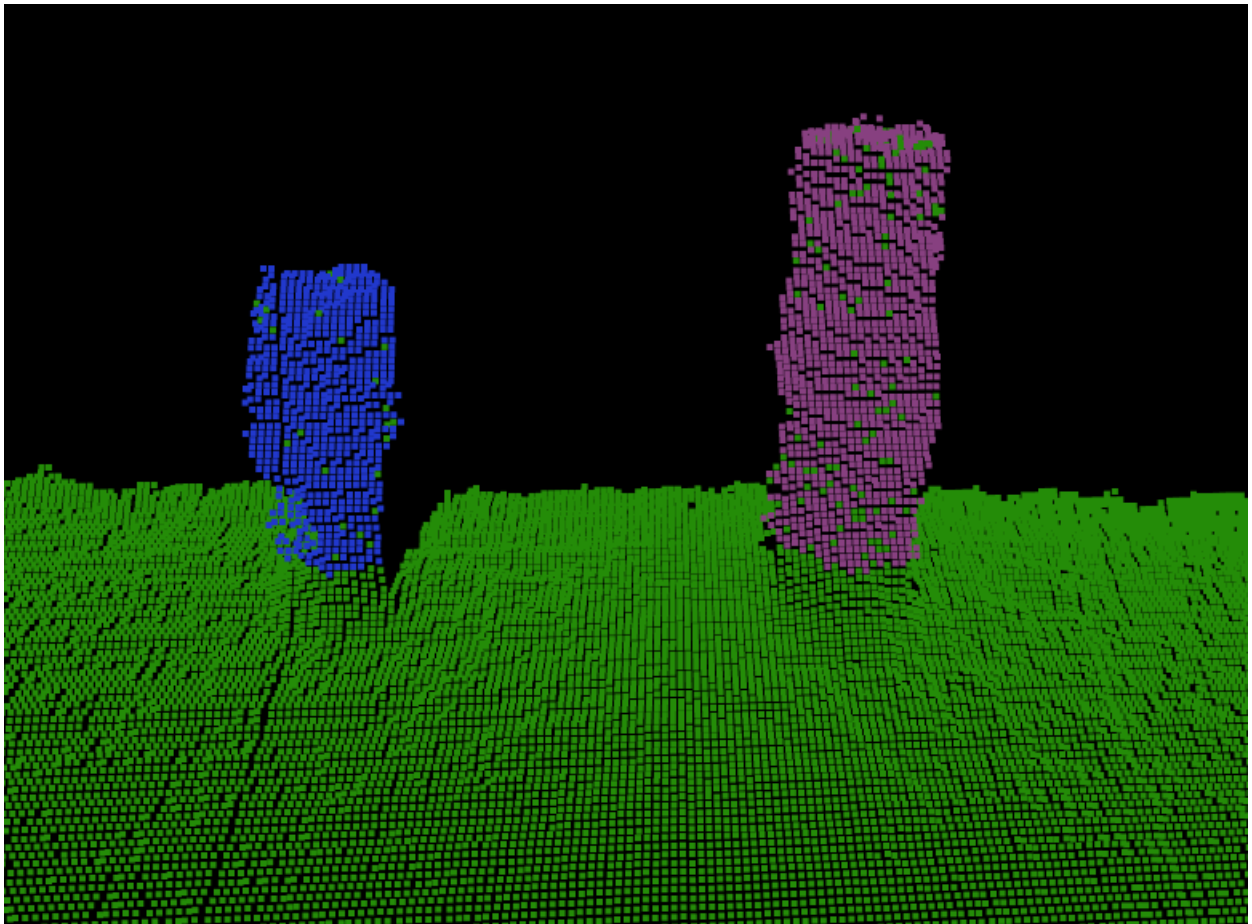


Figure 5.20: Template alignment with new parameter values.

The program estimated a homogeneous transformation from the template to the target cloud. The pose of the objects in the point cloud in Figure 5.20, are the same as the objects pose in the templates. Both the transformation, from the cylinder template to the target cloud and



the transformation from the piston template to the target cloud were estimated to be identity matrix, which is correct.

Running template alignment with live point clouds as input cloud from the camera gave different transformations every time. The alignment of the templates to the live point cloud is shown in Figure 5.21. The objects have the same pose as in Figure 5.20. As shown, the templates have not been aligned as good as in Figure 5.20.

The rotation of the piston template to the live target cloud was estimated to be

$$R = \begin{bmatrix} 0.993 & -0.109 & -0.041 \\ 0.111 & 0.993 & 0.045 \\ 0.036 & -0.050 & 0.998 \end{bmatrix} \quad (5.9)$$

and the cylinder template to the live target cloud

$$R = \begin{bmatrix} 0.991 & 0.093 & 0.094 \\ -0.099 & 0.994 & 0.054 \\ -0.089 & -0.063 & 0.994 \end{bmatrix} \quad (5.10)$$

There was also some movement in the translation part of both the homogeneous transformations. Attempts were made to merge multiple point clouds and use statistical outlier removal, without getting a more stable result.

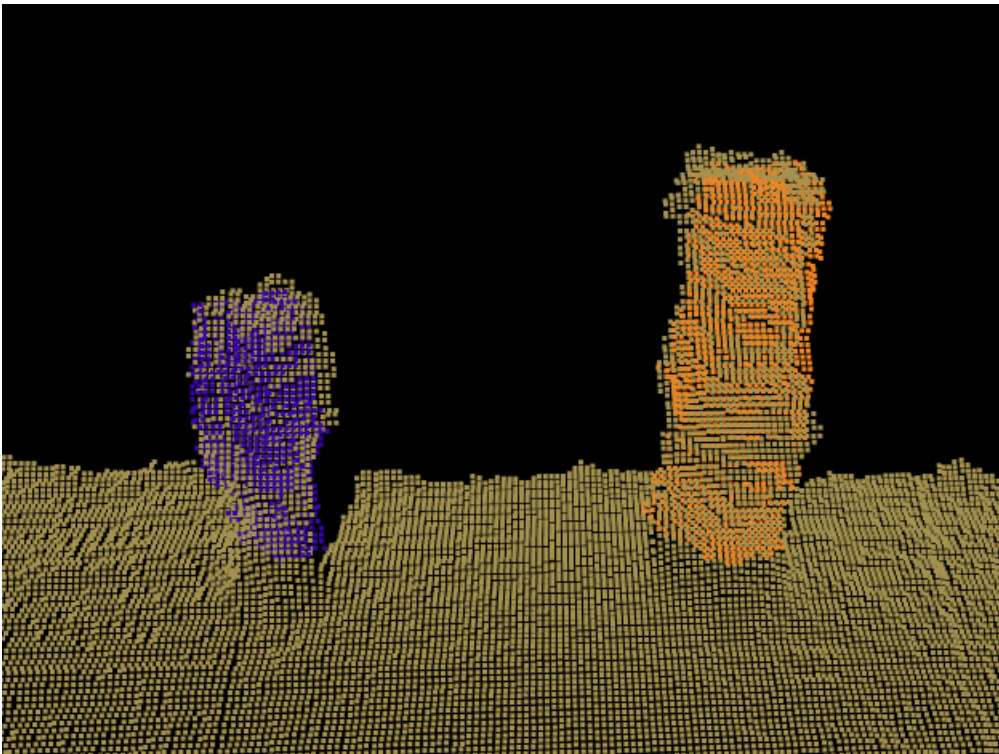


Figure 5.21: Template alignment with a live point cloud.

Next, the objects were oriented  $45^\circ$ . The alignments are shown in Figure 5.22. Until this point

there have only been used one template for each object. Therefore, a test with 8 templates (of the objects oriented  $0^\circ$ ,  $45^\circ$ ,  $90^\circ$ ,  $135^\circ$ ,  $180^\circ$ ,  $225^\circ$ ,  $270^\circ$  and  $315^\circ$ ) captured from different angles of each object was also conducted. The program uses the template (among the 8 templates) with the best *alignment score*. The best alignment score is a representation of how many of the points in the template that were aligned in the point cloud. This proved to work sometimes, but it was more unstable and the program used different templates for each point cloud captured when the objects were in the same pose. Also, the computational time of the program increased when 8 templates were used for each part.

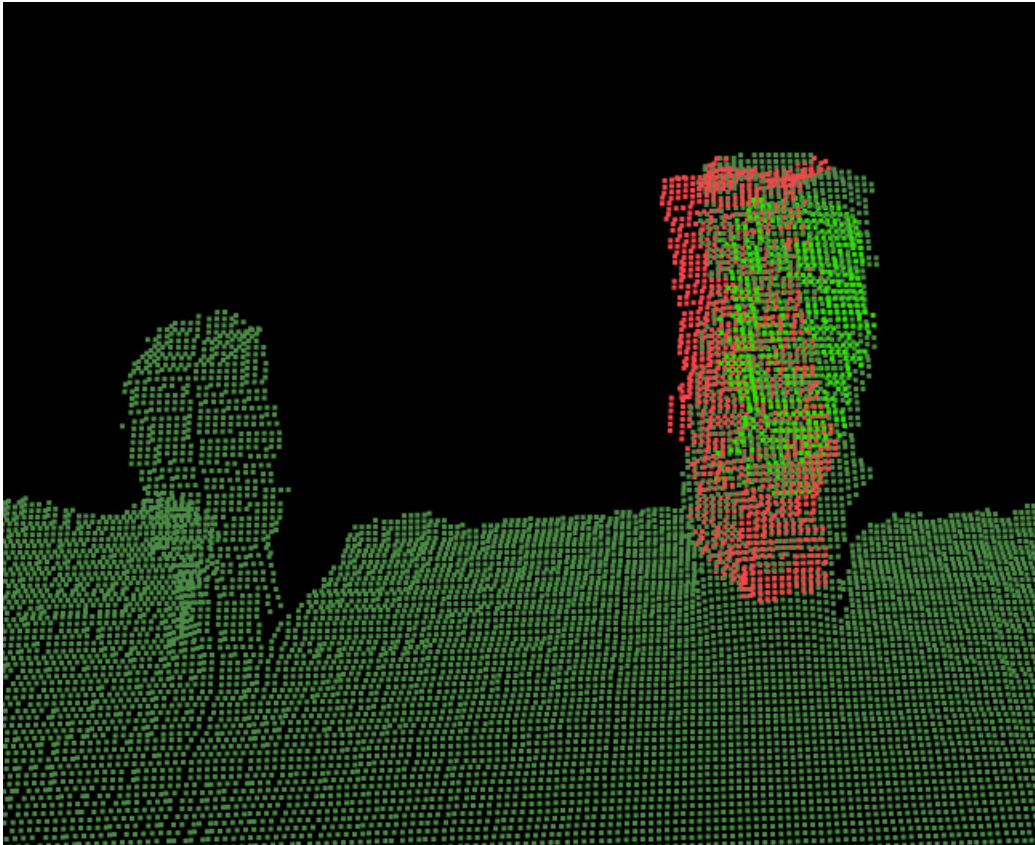


Figure 5.22: Template alignment with  $45^\circ$  oriented objects.

The objects were then moved closer to the camera and oriented  $0^\circ$  (the same as in the templates). The template alignment with two different point clouds are shown in Figure 5.23 and Figure 5.24. As shown, the template alignment differed for every point in the point cloud.

The rotation of the piston template to the target cloud in Figure 5.24 was estimated to be;

$$R = \begin{bmatrix} 0.991 & -0.103 & 0.085 \\ 0.100 & 0.994 & 0.043 \\ -0.089 & -0.034 & 0.995 \end{bmatrix} \quad (5.11)$$

and the cylinder template to the same target cloud

$$R = \begin{bmatrix} 0.996 & 0.054 & 0.073 \\ -0.055 & 0.998 & 0.005 \\ -0.072 & -0.008 & 0.997 \end{bmatrix} \quad (5.12)$$

As shown, the rotation matrices were close to identity matrix. The translation part of the transformations were off with some millimeters. The exception were the cylinder template translation in  $Y$  direction, which was off with almost one centimeter.

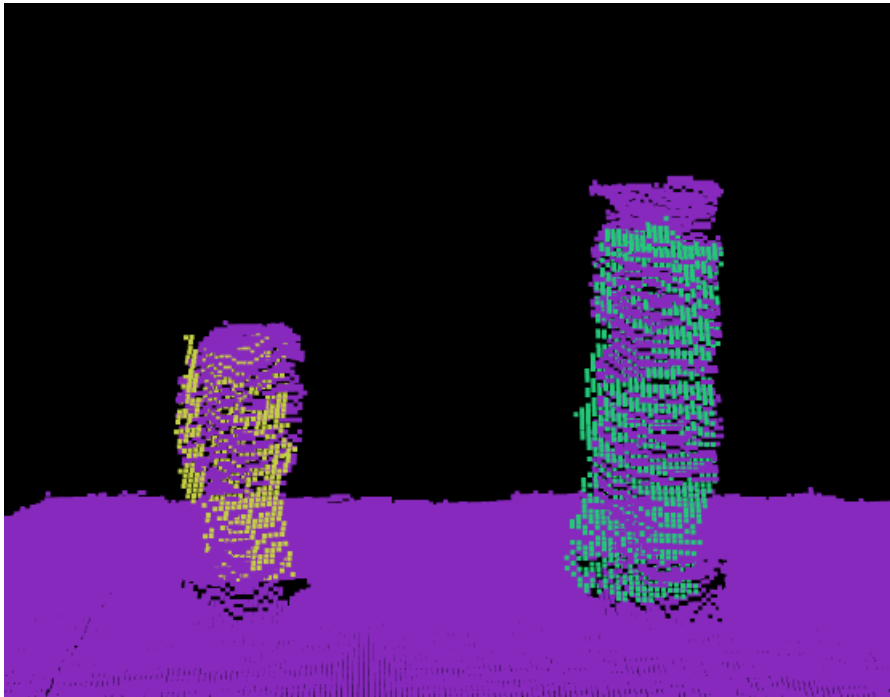


Figure 5.23: Templates alignment with  $0^\circ$  oriented objects closer to camera.

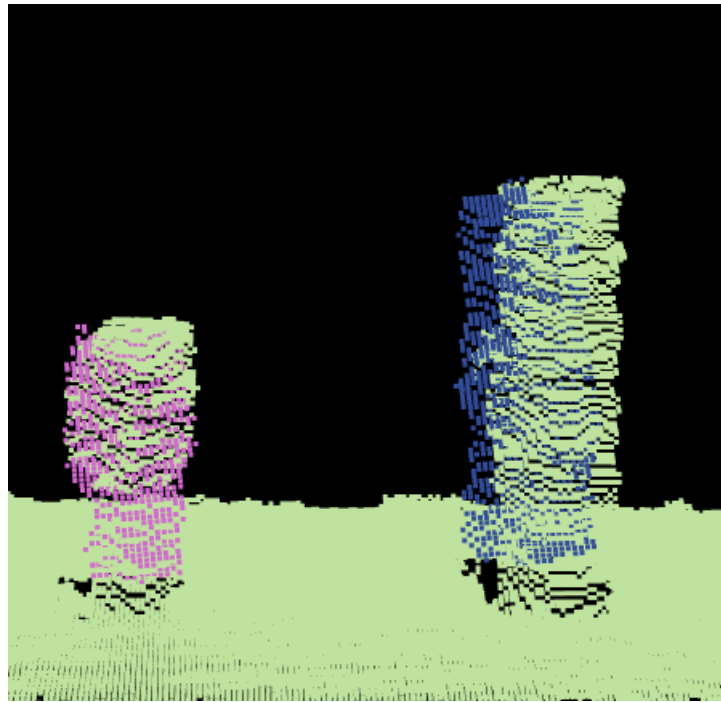


Figure 5.24: Templates alignment with  $0^\circ$  oriented objects closer to camera.

As mentioned, the program did not work better when more templates of each objects were used. It was therefore determined to find the maximal orientation of the objects in the point cloud, while still being able to align the template. The objects could be oriented with a maximum of  $30^\circ$ . Figure 5.25 shows the template alignment when the objects were oriented  $40^\circ$ .

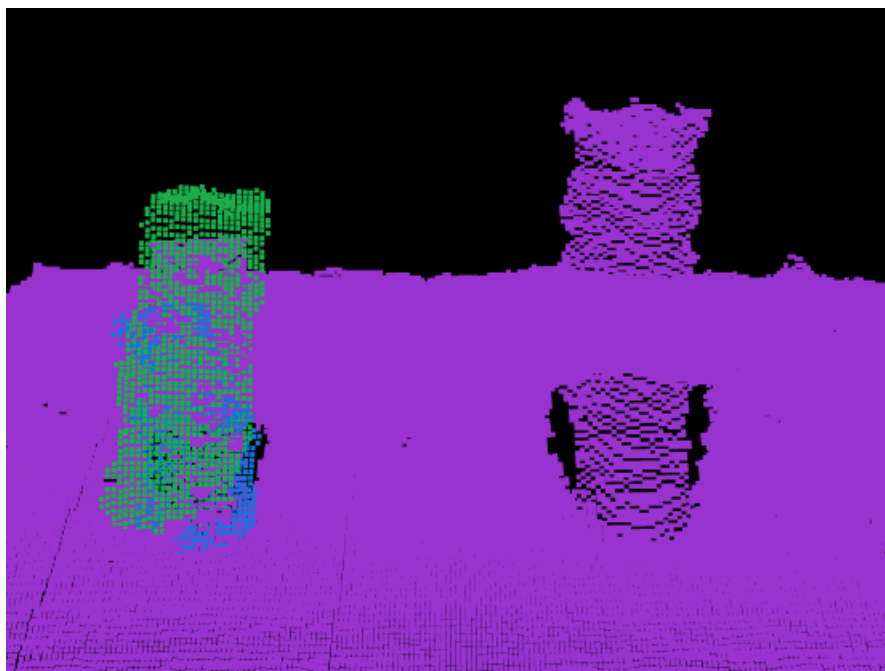


Figure 5.25: The alignment with  $40^\circ$  oriented objects closer to camera.

Still, as the objects were oriented from 0 to  $30^\circ$ , the rotation matrices did not correspond to

the true orientations of the cylinder and the piston. Also the translation part was off with one cm. The algorithm used approximately 25 seconds when running template alignment for the cylinder and piston on a point cloud that only did not include the table.

The template alignment method worked for locating the objects with a maximum error of 1.2 cm, considering that the objects had a maximum orientation of  $30^\circ$  with respect to the orientations of the parts in the templates. The orientation part was difficult to estimate, since the geometry of the objects made it difficult to distinguish between different orientations. Also, the RGB-D camera produces a slightly different point cloud for every frame it captures so the alignment differs for every time the program is run.

### 5.1.4 Region Growing Segmentation

After having tested different ways of determining the position of the piston and the cylinder with respect to the coordinate frame on the table, one of the best results was obtained by a modified version of Region growing segmentation explained in section 4.3.2. This method was not ideal since it was meant for flat and smooth surfaces, but what we were looking for was a segment of the points on the side facing the camera. Region growing segmentation proved to be stable and produced relatively good results repeatedly.

The program reads the point cloud live from the depth camera. Next, the program runs a NaN filter on the point cloud to filter out the NaN values that indicate space locations where the sensor had troubles detecting depth values. This could occur on reflecting surfaces (i.e. metal), surfaces too far away or in areas which are occluded (shadows). Then, the points in the point cloud are transformed from the camera frame  $\{c\}$  to the table frame  $\{t\}$ . Next, the program filters out all the points from the cloud except the points on the table or directly above it.

The surface normals are computed with a scale factor of  $r = 0.04$  m. This value gave good results as shown in Figure 5.26, where the normals on the front of the objects are easily distinguished from the normals on the table.

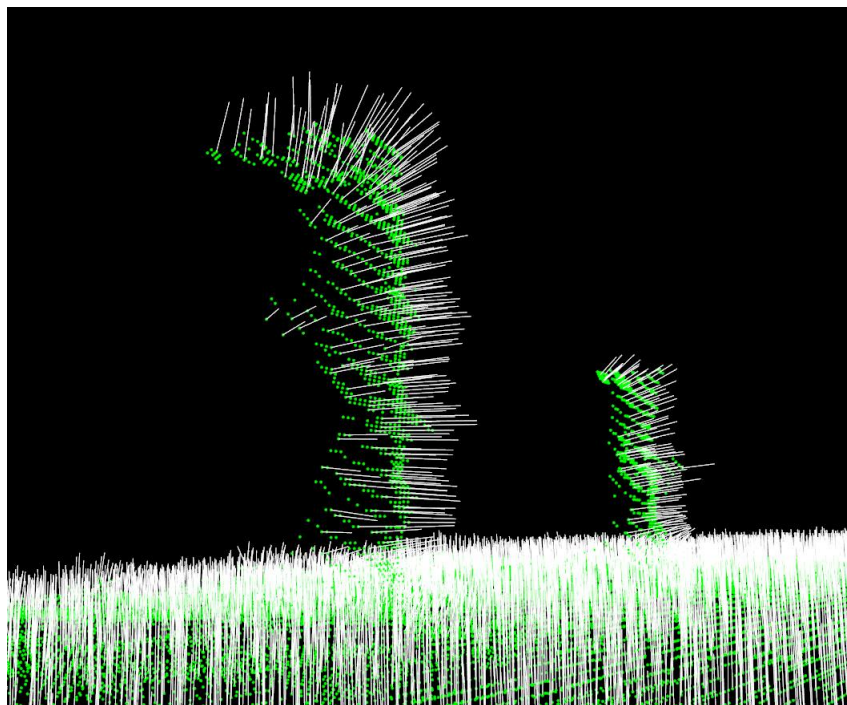


Figure 5.26: Surface normals computed with  $r = 0.04$ .

When the surface normals are computed the segmentation parameters can be set. The residual threshold  $r_{th}$  was set to  $r_{th} = 150$ , the neighborhood threshold  $k$  was set to  $k = 20$  and the smoothness threshold  $\theta_{th}$  was set to  $\theta_{th} = 70^\circ$ . The resulting segmentation is shown in Figure 5.27.

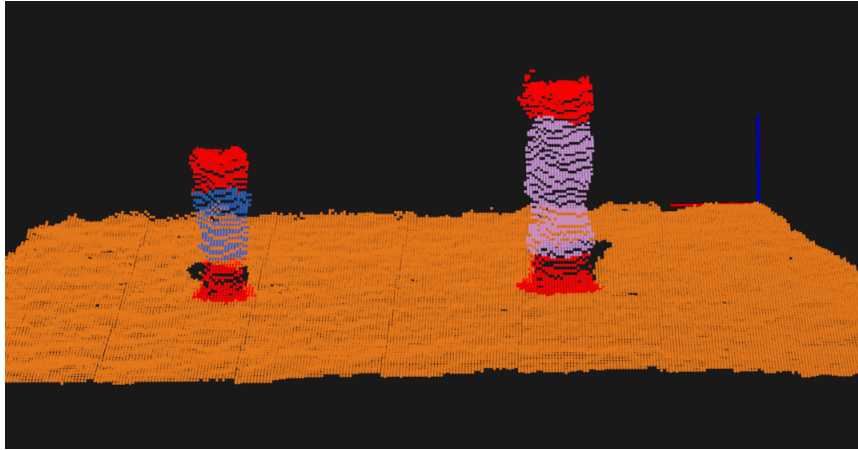


Figure 5.27: Segmentation result. Each segment grown in the cloud gets a random color. Red points are always unsegmented.

The blue segment represents the piston and the purple segment represents the cylinder. There are a lot of noise in the point cloud. The noisy points are normally filtered out with a filter that statistically removes outliers as mentioned in Chapter 4.3.3. This cloud has been captured without the filter to better visualize the scene. The table had not been visible if the filter had been activated. The resulting segments is distinguished by by the number of points and the height of the point cloud. An initial suggestion for the  $X$  and  $Y$  coordinates with respect to the table frame  $\{t\}$ , is then calculated from the median of the coordinates of the points in the segments.

The  $Z$  coordinate is calculated based on the height the gripper is going to grip the object at. From the points  $p^t$  in the point cloud, the coordinates  $(X, Y)$  of the piston  $p_{pis}^t = (X, Y, 0.10)^T$  and the cylinder  $p_{cyl}^t = (X, Y, 0.17)^T$  are extracted.

Figure 5.28 shows the repeatability in the segmentation even if the objects are further away from the camera.

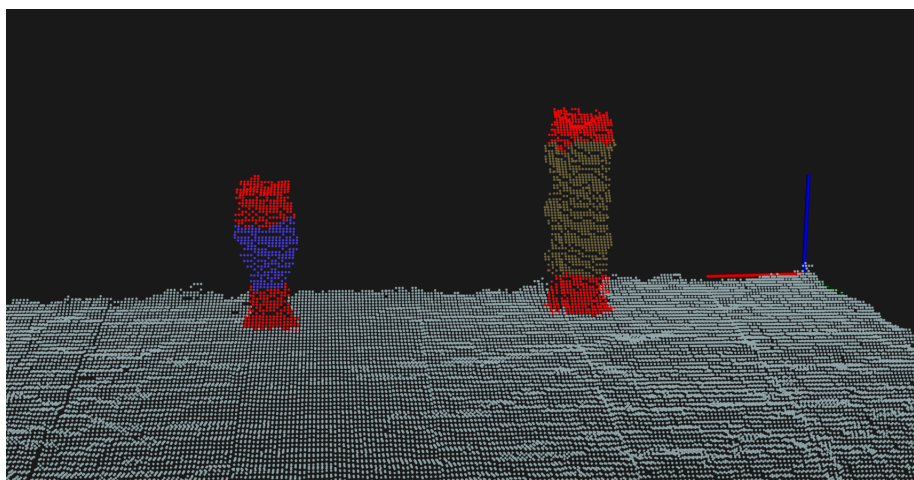


Figure 5.28: Stable segmentation results.

### 5.1.5 Segmentation based on known Geometry

Two programs were made for estimation of the coordinates of the parts based on known geometry of the parts. One program uses one point cloud and another program uses four merged point clouds. The known geometry of the objects are:

- The cylinder is 18.5 cm tall and has a maximum radius of 5 cm.
- The piston is 12.5 cm tall and has a maximum radius of 4.5 cm.

The programs runs as follows:

1. Transform point cloud/point clouds to table coordinates  $\{t\}$ .
2. Statistical removal of outliers.
3. Search for a point  $p$  on the table that has  $Z > 15$  cm.
4. If there are more than 30 points in a cubic volume around  $p$  as shown in Figure 5.29 with  $Z > 3$  cm, save this point. Else, do point 3 again.
5. Segment the points located within a cubic volume around  $p$  shown as the blue cube in Figure 5.29 ( $3 \text{ cm} < Z < 12 \text{ cm}$ ).
6. This segment is saved as the cylinder segment.
7. Search for a new point  $p$  that is  $4 \text{ cm} < Z < 11 \text{ cm}$  and has not already been segmented.
8. If there are more than 10 points in a cubic volume around the new  $p$ , save this point, else do point number 7 again.
9. Segment the points that are in a cubic volume around  $p$  with  $3 \text{ cm} < Z < 8.5 \text{ cm}$ .
10. This segment is saved as the piston segment.



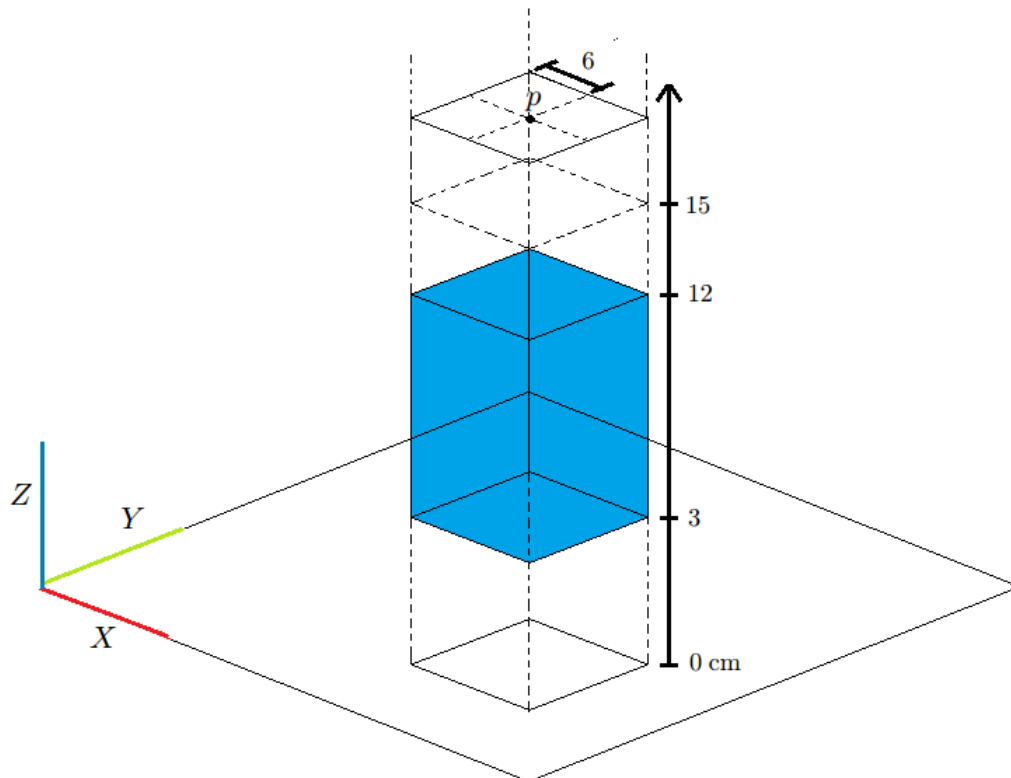


Figure 5.29: Segmentation and search algorithm for the cylinder.

In Figure 5.30 these segments are shown in the program that uses one point cloud at a time.

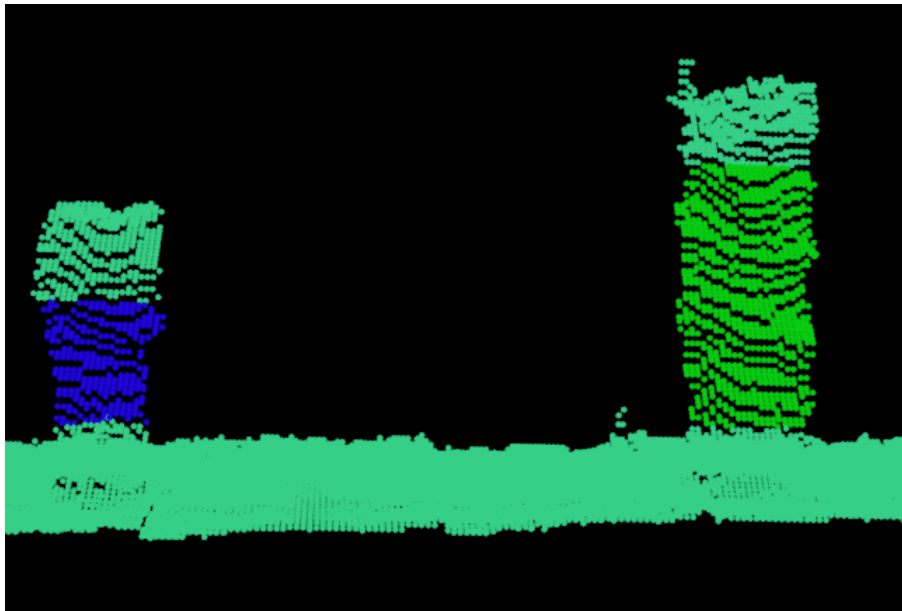


Figure 5.30: One point cloud and segmentation of the cylinder and the piston.

In Figure 5.31 the same segments are shown in the program that uses four point clouds at a time. The segments consist of a more dense point cloud.

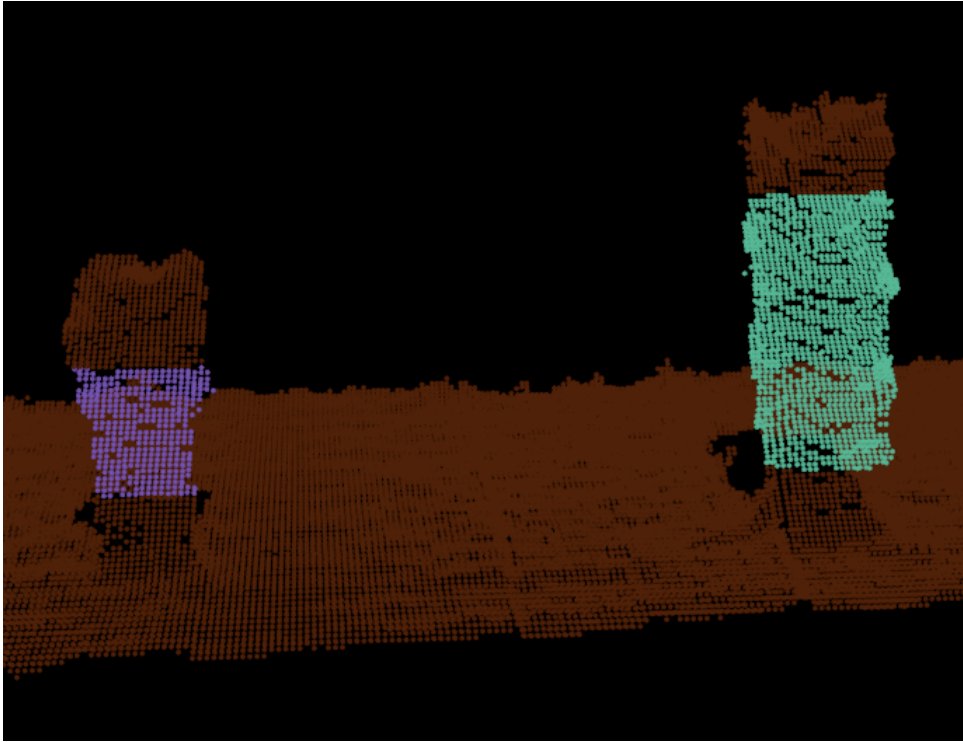


Figure 5.31: Four merged point clouds and segmentation of the cylinder and the piston.

Estimating the coordinates of the cylinder and the piston from the segments, is done in the same way as described in Chapter [5.1.4](#).

### 5.1.6 Analysis

#### Evaluating the Programs for locating the Objects

There are three working programs for estimating the coordinates of the piston and cylinder. These programs are:

- Segmentation based on known geometry using one point cloud.
- Segmentation based on known geometry using 4 point clouds.
- Region growing segmentation.

These programs were tested individually for locating the coordinates of the cylinder and the piston. The tests gave approximately the same result for all the programs. The differences between the programs were the computational time to estimate the coordinates, and the repeatability of the estimations.

Figure 5.32 and Figure 5.33 shows the result from a test where the cylinder was placed at two different locations  $p_{\text{cyl}}^t = (0.25, 0.5)$  and  $p_{\text{cyl}}^t = (0.25, 0.1)$  in the table coordinate frame  $\{t\}$ . For each program there were sampled 29 coordinates for each location of the cylinder. As shown in Figure 5.32 and Figure 5.33, the program *Segmentation based on known geometry using 4 point clouds* is the program that estimates the most stable coordinates and *Segmentation based on known geometry using one point cloud* is the least stable.

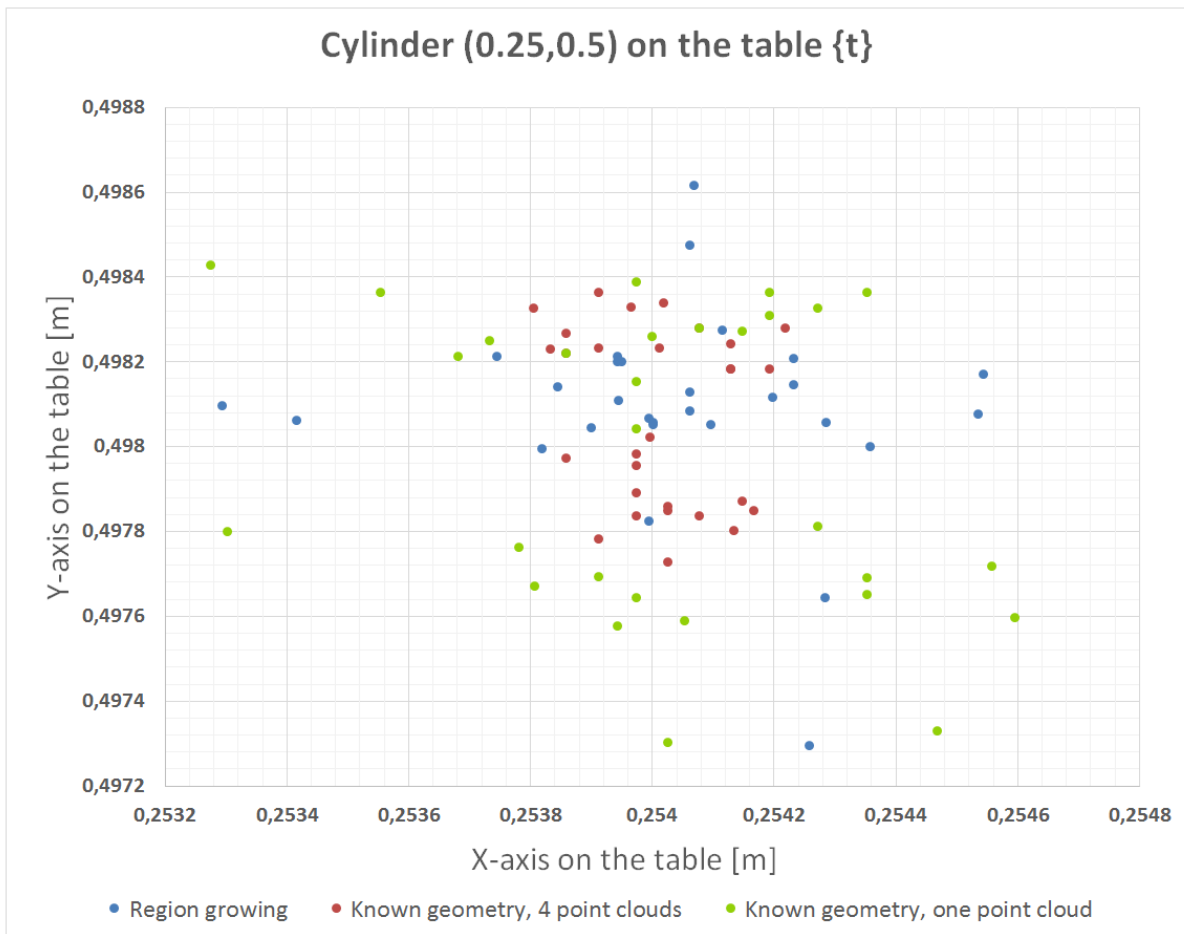


Figure 5.32: 29 samples of the coordinates of the cylinder located at (0.25, 0.5) in  $\{t\}$ .

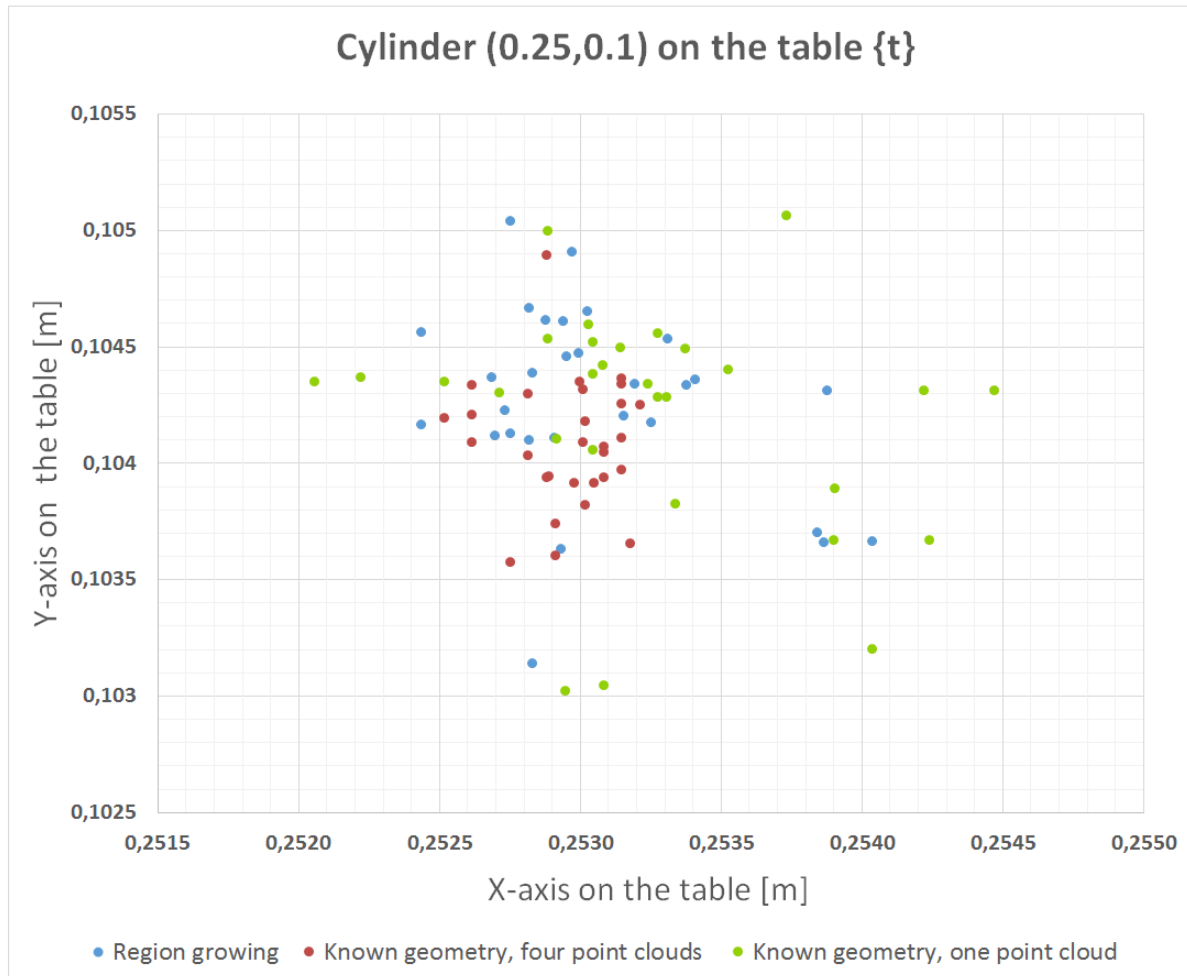


Figure 5.33: 29 samples of the coordinates of the cylinder located at  $(0.25, 0.1)$  in  $\{t\}$ .

The standard deviations with 95% confidence level of the 29 samples, for each of the three different programs, are shown in Figure 5.34.

Method	Cylinder (0.25,0.1)		Cylinder (0.25,0.5)	
	x	y	x	y
Known geometry, one point cloud	0,5745	0,4952	0,3272	0,3539
Region growing	0,4191	0,4091	0,2713	0,2289
Known geometry, 4 point clouds	0,1896	0,2758	0,1143	0,2080

Figure 5.34: Standard deviations (95% confidence level) in millimeters.

As shown in Figure 5.34 the standard deviations varies with the distance from camera. That is, the standard deviations increased the further away from camera the cylinder was. The point  $(0.25, 0.1)$  is further away from the camera than the point  $(0.25, 0.5)$ . Still, the program *Segmentation based on known geometry using one point cloud*, which is the least stable, had at the most a standard deviation (with 95% confidence level) of  $\pm 0.57$  mm in  $X$  direction and  $\pm 0.50$  mm in the  $Y$  direction. This was still acceptable for performing a simplified assembly

task of the parts, assuming that the mean of the samples gives the correct coordinates.

In Figure 5.35 the computation time for the different programs are shown. For the programs *Segmentation based on known geometry using one point cloud* and *Region growing segmentation* there were also implemented an option for sampling 20 coordinates of both parts, and then use the median of those samples as the coordinates.

Method	Live	Median of 20 samples
Known geometry, one point cloud	>1	18
Region growing	2	44
Known geometry, 4 point clouds	23	-

Figure 5.35: Computation time in seconds for the different programs.

Assembling the parts required high accuracy in the measurements of the coordinates. It was therefore of interest to eliminate errors, like the standard deviations, in the estimate of the coordinates. That is why the median of 20 sampled coordinates for the programs *Segmentation based on known geometry using one point cloud* and *Region growing segmentation* were implemented as an option. The median of 20 sampled coordinates with the program *Segmentation based on known geometry using one point cloud* was used in the demo video where a robot assembles the parts. If the demand for fast production is the goal, the *Region growing segmentation* would be a suitable choice.

### Computed Pose VS. Measured Pose

This section will demonstrate the accuracy of the position of the objects seen from the camera with respect to the table coordinate frame. The program code used in this experiment is based on the *Segmentation based on known geometry using one point cloud* with median of 20 sampled coordinates. The objects to detect is the piston and the cylinder, which were placed in nine different positions on the table. For each position, the coordinates in the  $X Y$  plane on the table  $\{t\}$  were measured with a tape measure. These coordinates were then compared with the coordinates from the computer program based on the *Segmentation based on known geometry using one point cloud*. Figure 5.36 and Figure 5.37 shows the difference between the measured coordinates and the computed coordinates for the piston and the cylinder respectively. The axis of the diagram is the  $X$  axis and  $Y$  axis of the table frame  $\{t\}$  in the corner of the table and the unit is in meters. The diagrams clearly show that there is a relatively constant error between the actual coordinates and the computed coordinates.

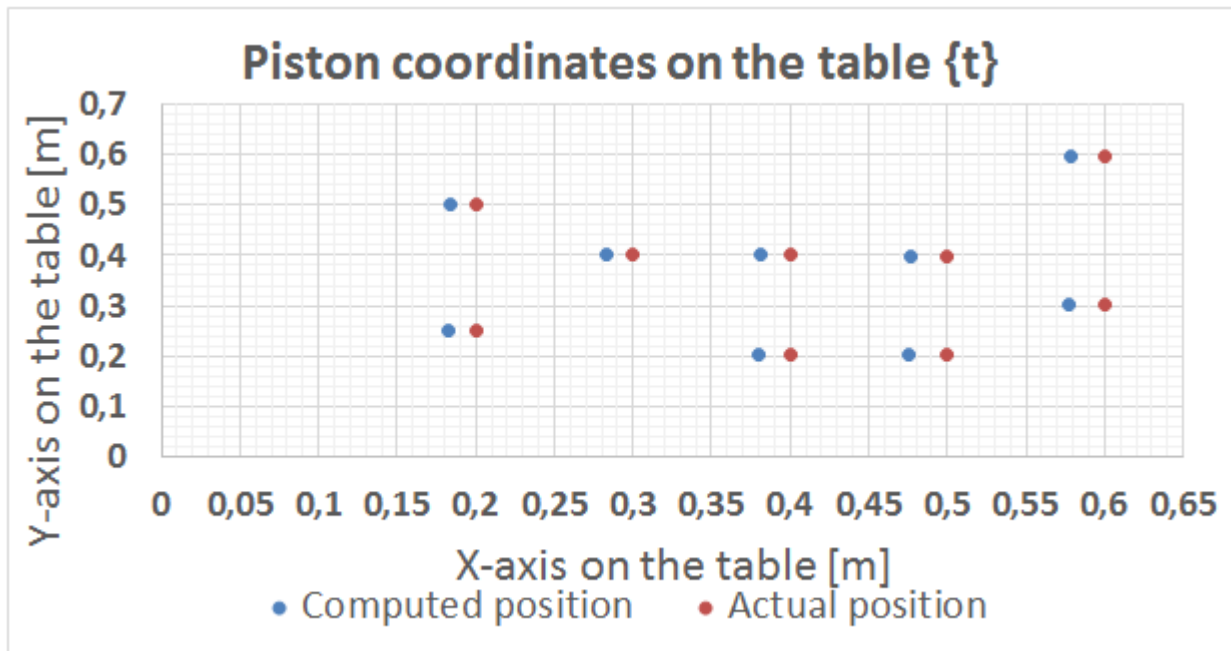


Figure 5.36: Raw coordinates for piston.

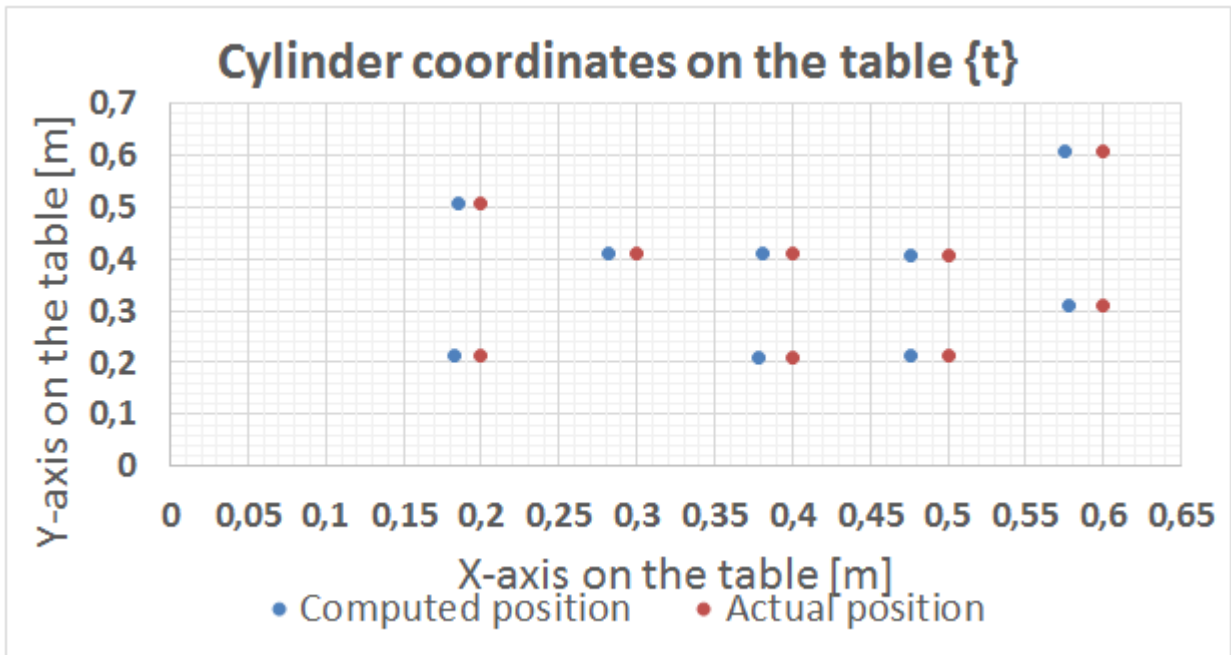


Figure 5.37: Raw coordinates for cylinder.

To compensate for the error, the average error between the actual position and the computed position for the nine samples, were subtracted. The result is shown in Figure 5.38 and Figure 5.39 for the piston and the cylinder respectively.

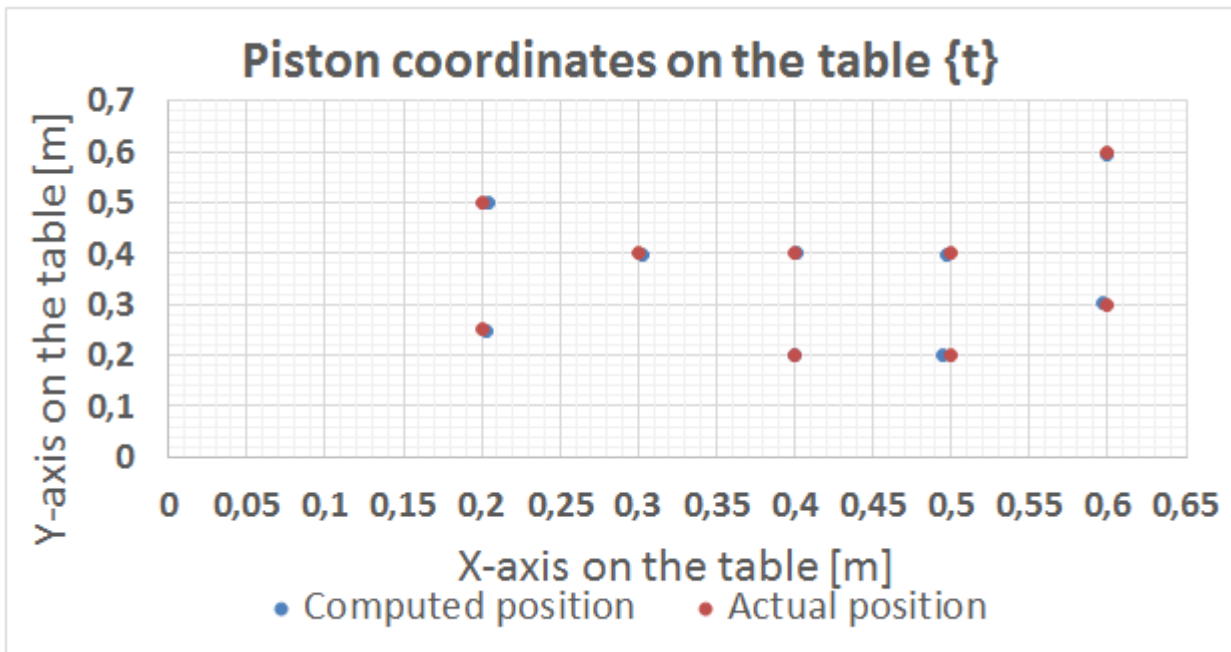


Figure 5.38: Improved coordinates for piston.



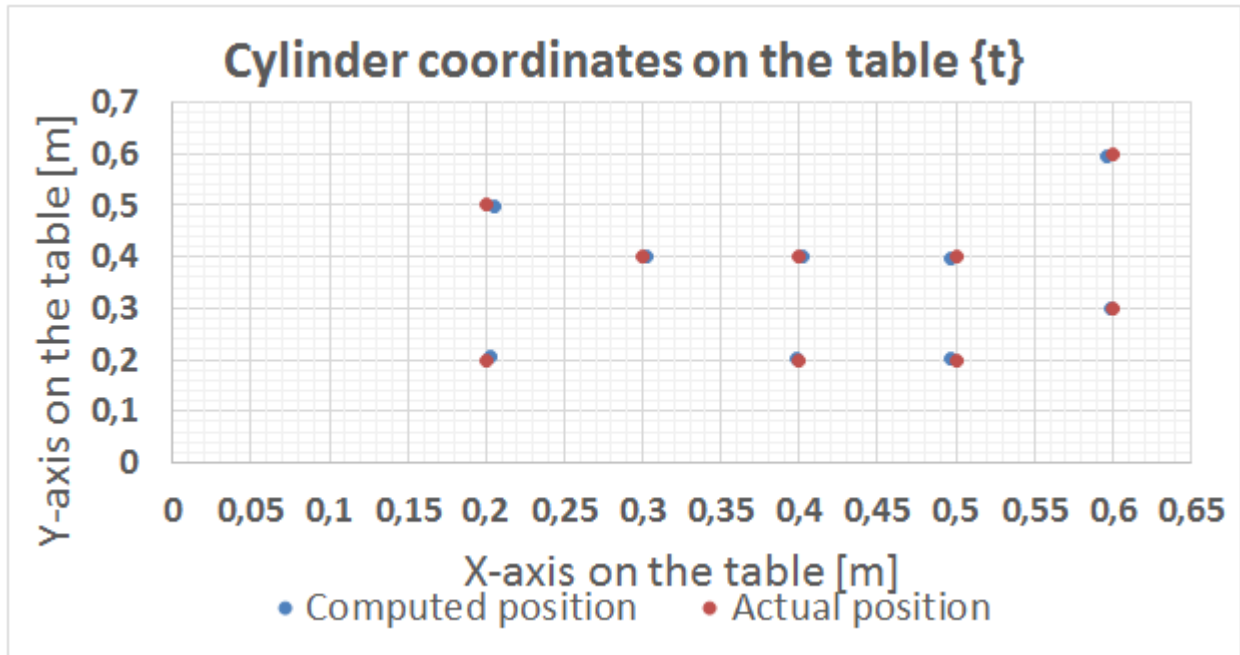


Figure 5.39: Improved coordinates for cylinder.

The result shows that the improved coordinates are much more accurate than before. For the nine samples the piston's average error was 0.0026 m in  $X$  direction and 0.0016 m in  $Y$  direction. The cylinder's average error was 0.0029 m in  $X$  direction and 0.0022 m in the  $Y$  direction. That is, an average error of 3.05 mm for the piston and 3.64 mm for the cylinder. The results obtained were not adequate for the original assembly task which require sub-millimeter accuracy, but it was possible to perform a simplified assembly task requiring 4 mm accuracy. As previously mentioned, the other methods, *Segmentation based on known geometry using 4 point clouds* and *Region growing segmentation* did not produce more accurate coordinates for the parts.

In this test the camera was approximately 1.5 m away from the objects so the results will most likely improve if the camera is mounted closer to the objects of interest. It is also likely that a more thorough and comprehensive calibration technique for the RGB-D camera will increase the accuracy. Also, a calibration of transformation  $T_{ir}^{rgb}$  from RGB camera to IR camera could have improved the transformation  $T_a^c$  from RGB-D camera to the AR-tag pose. This is because the AR-tags are recognized by the RGB camera and the parts location  $(X, Y, Z)$  are given by the IR camera.

## 5.2 Experiments based on the 2D Camera

This chapter presents a program that uses a 2D camera (Logitech HD Pro Webcam C920) to estimate the orientations of the piston and the cylinder. For this purpose a OpenCV program [14] was used and further developed.

### 5.2.1 Orientation of the Objects

The program has four *training images* of each object (the piston and the cylinder). The training images are shown in Figure 5.40 and Figure 5.41 for the piston and the cylinder respectively.

Four training images was necessary because the geometry of the objects made it difficult to estimate an orientation with one, two and three training images. The training images  $I_{o,0}$ ,  $I_{o,90}$ ,  $I_{o,180}$  and  $I_{o,270}$  represents the objects when they are oriented  $0^\circ$ ,  $90^\circ$ ,  $180^\circ$  and  $270^\circ$ .



Figure 5.40: From left: The training images  $I_{o,0}$ ,  $I_{o,90}$ ,  $I_{o,180}$  and  $I_{o,270}$  for the piston.

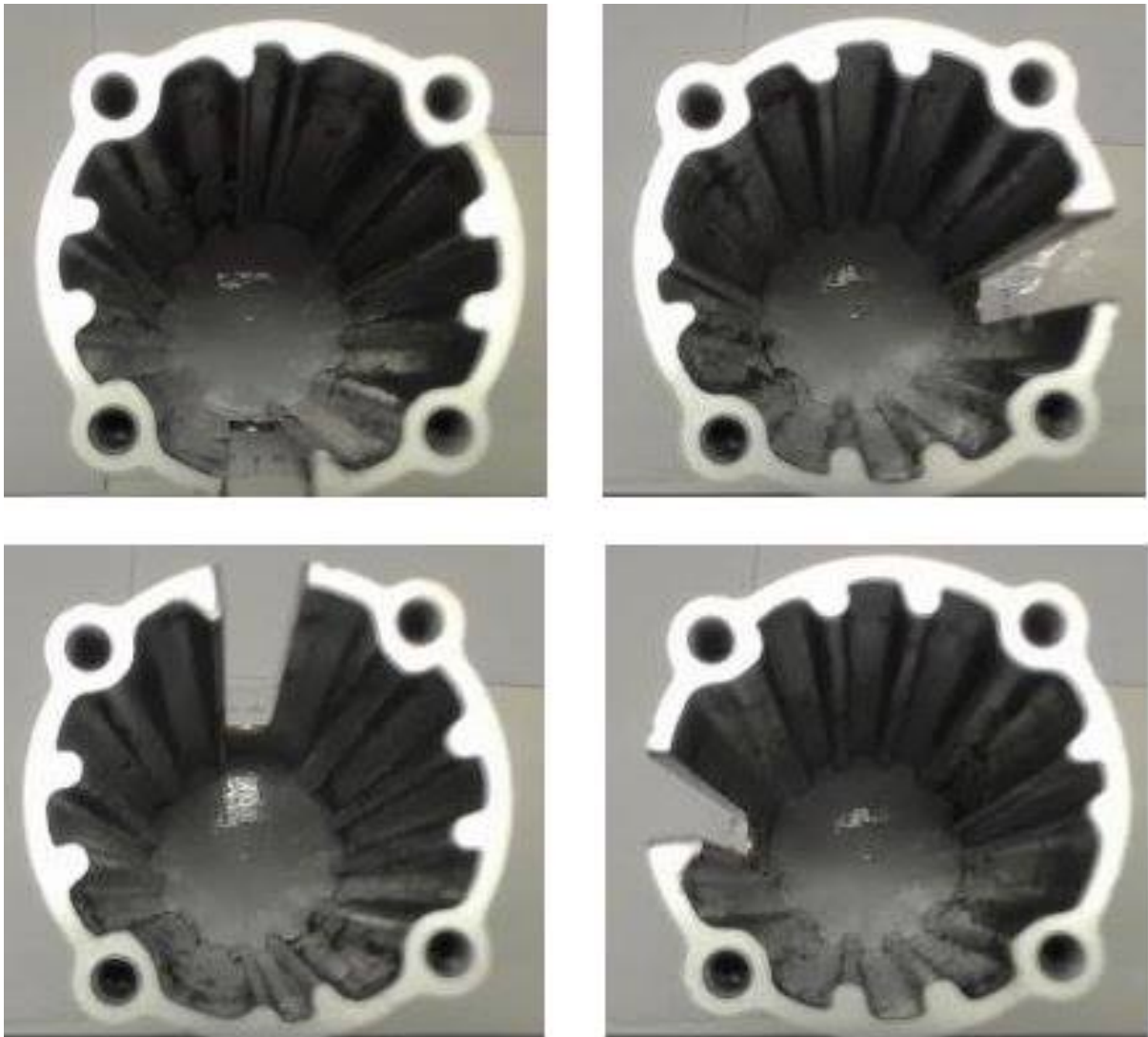


Figure 5.41: From upper left to right: The training images  $I_{o,0}$ ,  $I_{o,90}$ ,  $I_{o,180}$  and  $I_{o,270}$  for the cylinder.

SIFT features are extracted from the training images and the live image stream from the 2D camera and then stored in a database. The threshold for the Hessian matrix in equation (4.7) is set so it approves a maximum of 200 features in each image.

An example of extracted features from two image streams, are shown in Figure 5.43 and Figure 5.43.

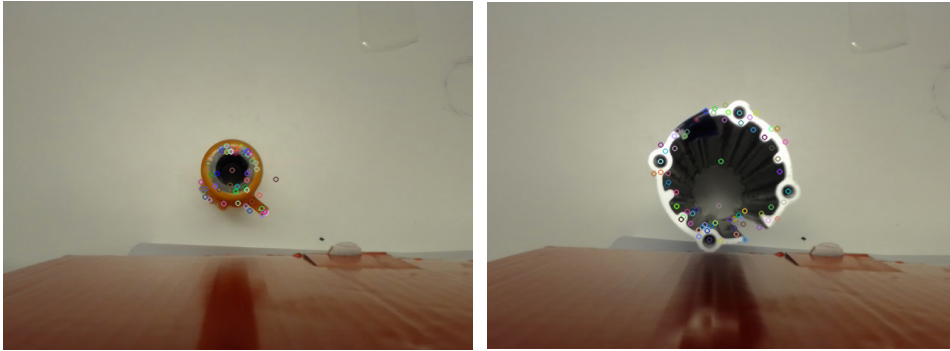


Figure 5.42: Features from the image stream. Figure 5.43: Features from the image stream.

The rest of this chapter, presents the program for determining the orientation of the cylinder.

Examples of accepted matched features in the training image  $I_{o,0}$  in Figure 5.41 and the image stream in Figure 5.43, are shown in Figure 5.44. The matched features have been accepted based on having a Euclidean distance less than 210. As shown in Figure 5.44 not all matched features are consistent.

As mentioned, using RANSAC will improve the estimation of the homography matrix. For the example shown in Figure 5.44, the normalized homography matrix was

$$H = \begin{bmatrix} h_{11} & h_{12} & h_{13} \\ h_{21} & h_{22} & h_{23} \\ h_{31} & h_{32} & h_{33} \end{bmatrix}$$

$$H = \begin{bmatrix} 0.8974 & 0.4594 & 183.271 \\ -0.4714 & 0.8793 & 201.616 \\ 4.958510^{-5} & -3.908810^{-5} & 1 \end{bmatrix} \quad (5.13)$$

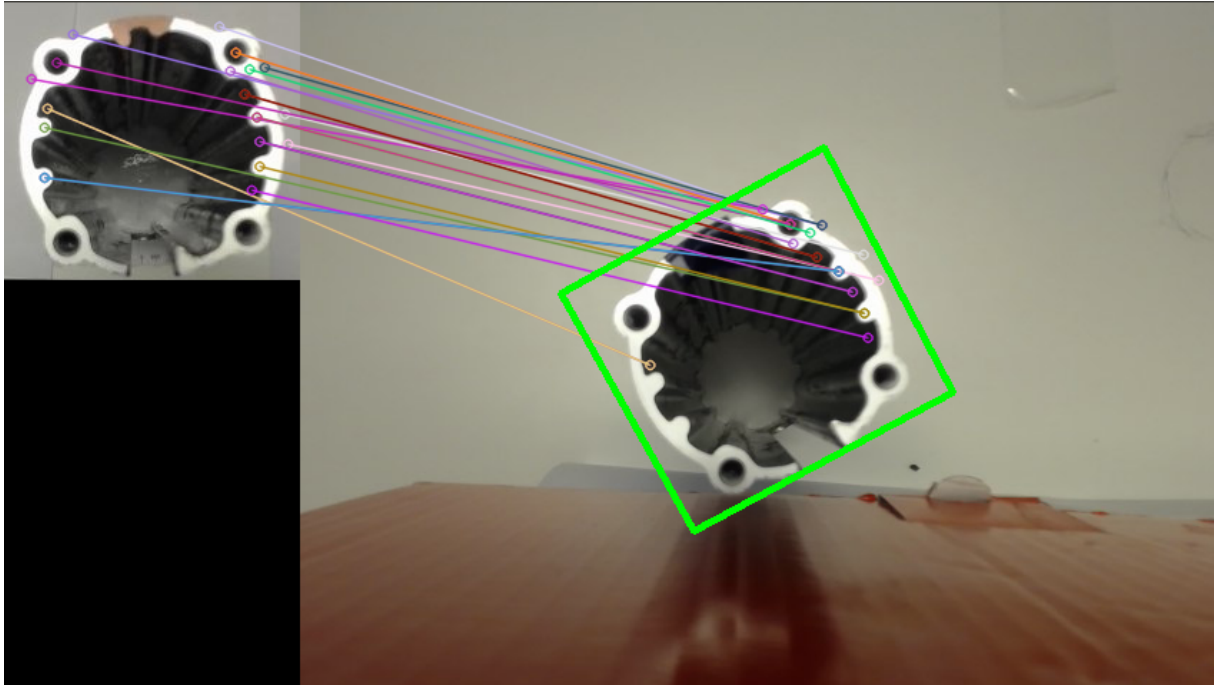


Figure 5.44: Homography to find the orientation of the cylinder.

The camera is perpendicular to the cylinder in the training images and the image stream. The program is designed so the cylinder could be placed in a specified region in the field of view of the camera, as explained in the demo video. The cylinder can be oriented in any direction in the image stream, and there will be an *affine homography* between the training images and the image stream. That is, the projection of the corner points  $p = (u, v)^T$  in the training images, to the corner points  $p' = (u', v')^T$  (the corners of the green square in Figure 5.44) in the image stream

$$u' = \frac{h_{11}u + h_{12}v + h_{13}}{h_{31}u + h_{32}v + h_{33}} \quad v' = \frac{h_{21}u + h_{22}v + h_{23}}{h_{31}u + h_{32}v + h_{33}} \quad (5.14)$$

is an affine transformation with  $h_{31} = h_{32} = 0$  and  $h_{33} = 1$ . The homography in equation (5.13) has  $h_{31} \approx h_{32} \approx 0$  and  $h_{33} = 1$ . The program is designed only to approve a homography matrix if it is an affine transformation. This projective transformation or homography projects the training images into a projectively equivalent figure in the image stream [4].

Examples of corner points (the corners of the image) in the training image  $I_{o,0}$  mapped to an image in the image stream, are shown in Figure 5.45. These mapped corner points are visualized as  $p_0$ ,  $p_1$ ,  $p_2$  and  $p_3$ .

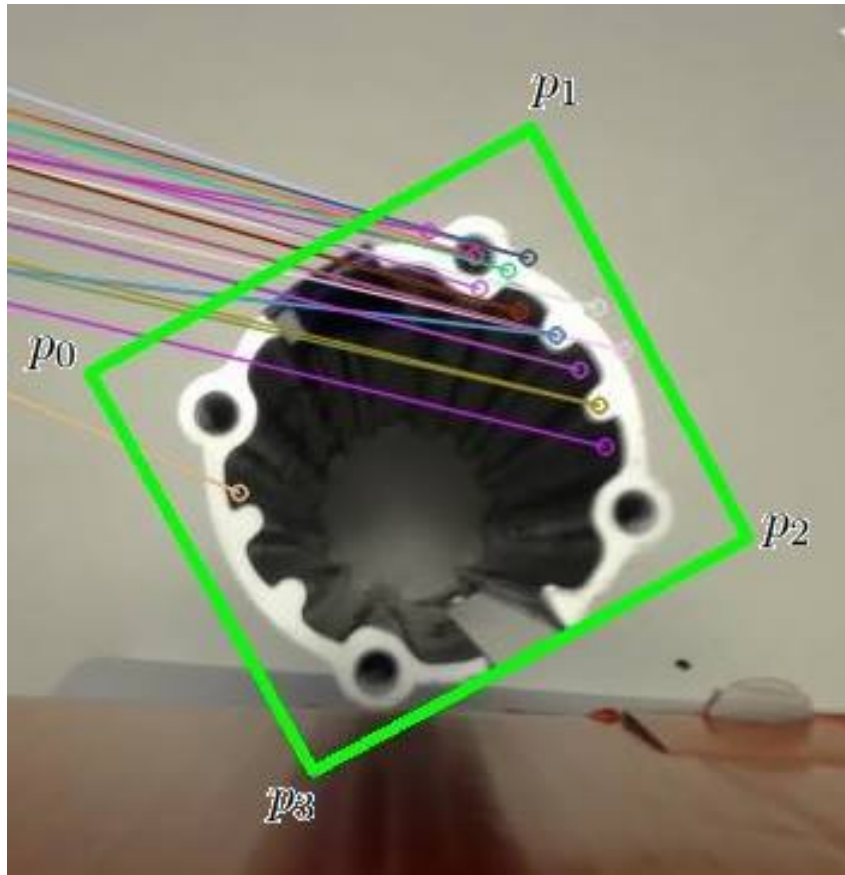


Figure 5.45: Corner points of the affine transformation.

The rotation angle of the cylinder in Figure 5.45 is

$$\begin{aligned}\theta_{p_{12}} &= \cos^{-1} \left( \frac{v_2 - v_1}{\sqrt{(u_2 - u_1)^2 + (v_2 - v_1)^2}} \right) \\ \theta_{p_{03}} &= \cos^{-1} \left( \frac{v_3 - v_0}{\sqrt{(u_3 - u_0)^2 + (v_3 - v_0)^2}} \right)\end{aligned}\tag{5.15}$$

where  $p_i = (u_i, v_i)^T$  and  $\theta_0$  is the estimated orientation of the cylinder from the homography matrix between  $I_{o,0}$  and the image stream. If  $\theta_{p_{12}} \approx \theta_{p_{03}}$ , something it should be since the plane is an affine transformation, then  $\theta_0 = (\theta_{p_{12}} + \theta_{p_{03}})/2$  is an approved orientation.

The program estimates a homography matrix and a  $\theta$  for each of the training images. That is,  $\theta_0$  for the orientation between  $I_{o,0}$  and the image stream,  $\theta_{90}$  for the orientation between  $I_{o,90}$  and the image stream,  $\theta_{180}$  for the orientation between  $I_{o,180}$  and the image stream,  $\theta_{270}$  for the orientation between  $I_{o,270}$  and the image stream. The estimated  $\theta_{90}$ ,  $\theta_{180}$  and  $\theta_{270}$  are computed with use of different points than in the example shown in equation (5.15).

The program estimates which  $\theta_i$ , where  $i \in \{0, 90, 180, 270\}$ , that has a stable value, and which value that dominates in the different  $\theta_i$ .

Figure 5.46 shows the projective transformation of the corner points (corners of the green square)

from the training images ( $I_{o,0}$ ,  $I_{o,90}$ ,  $I_{o,180}$  and  $I_{o,270}$ ) to the image stream. In this case, the homography matrix for  $I_{o,90}$  and  $I_{o,270}$  were rejected and  $\theta_{90}$  and  $\theta_{270}$  were not estimated.  $\theta_0 = 30.674^\circ$  and  $\theta_{180} = 210.942^\circ$  were both stable. That is, the program still does not know what the actual orientation of the cylinder is. For the program to be able to estimate the true orientation of the cylinder, the area on the opposite side of the guiding "slide track" on the cylinder have been marked with a dark color as shown in Figure 5.46.

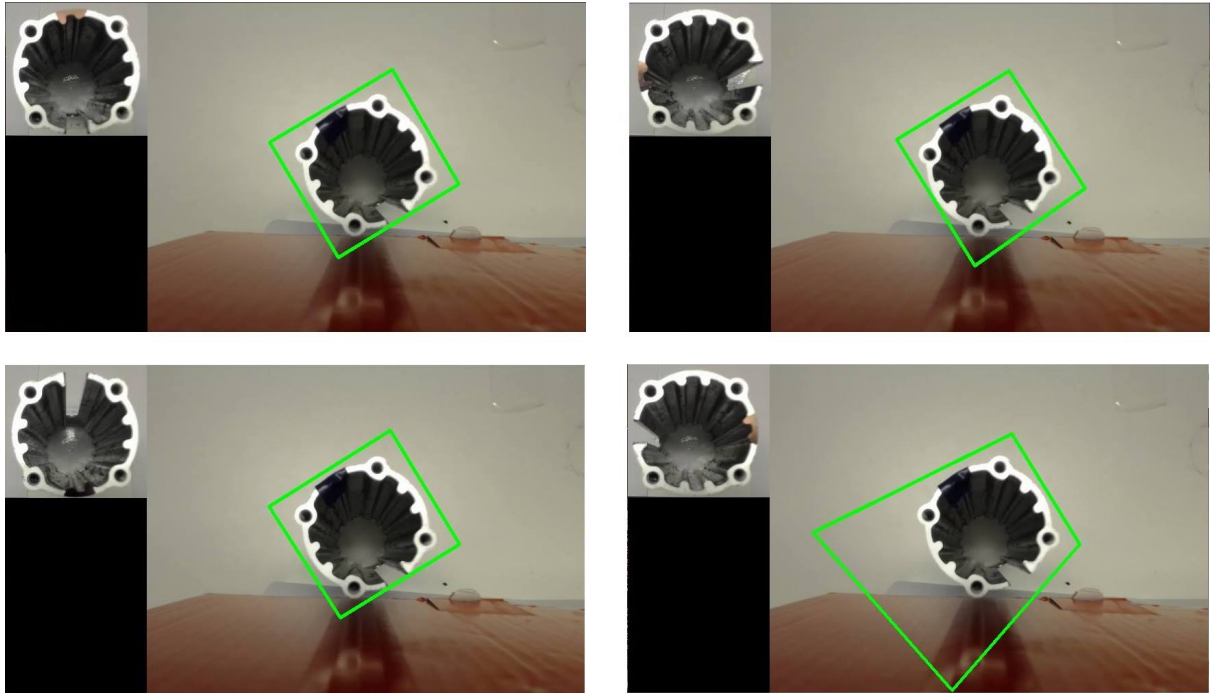


Figure 5.46: The projective transformation of the corner points in the training images to the image stream.

The program reads the grey scale value of three pixels  $p_{180}$  around the edge of the cylinder at  $\theta_{180}$  and three pixels  $p_0$  around  $\theta_0$ , in this case. The pixels  $p_0$  are shown as green squares in Figure 5.47 and the three pixels  $p_{180}$  are shown Figure 5.48.



Figure 5.47: The three pixels  $p_0$  around the edge of the cylinder with orientation equal  $\theta_0$ .





Figure 5.48: The three pixels  $p_{180}$  around the edge of the cylinder with orientation equal  $\theta_{180}$ .

The program need information about the radius  $r$  of the cylinder and the piston, and the distance  $Z$  from the camera center to the top of the objects, to be able to find these pixels.

These pixels represented in normalized image coordinates  $p = (x, y)^T$  are

$$x = \frac{fX}{Z} \quad , \quad y = \frac{fY}{Z} \quad (5.16)$$

where  $X = r \cos(\theta_0 + \delta\theta)$  for the three pixels  $p_0$  and  $X = r \cos(\theta_{180} + \delta\theta)$  for the three pixels  $p_{180}$ . The parameters for the cylinder are  $r = 0.024$  and  $Z = 0.155$ . The focal length  $f = 1$  and  $\delta\theta = 19^\circ, 23^\circ, 27^\circ$ . This is how the six pixels  $p_0$  and  $p_{180}$  (in normalized image coordinates) are obtained. Transforming these pixels  $p = (x, y)^T$  to pixel coordinates  $p = (u, v)^T$  are done by

$$\begin{bmatrix} u \\ v \\ 1 \end{bmatrix} = K \begin{bmatrix} x \\ y \\ 1 \end{bmatrix} \quad (5.17)$$

where  $K$  is the calibrated camera parameter matrix for the 2D camera

$$K = \begin{bmatrix} 540.927271 & 0 & 320 \\ 0 & 540.264582 & 240 \\ 0 & 0 & 1 \end{bmatrix} \quad (5.18)$$

The grey scale values for the pixels  $p_{180}$  were 51, 251 and 250, and the grey scale values for the pixels concerning  $p_0$  were 231, 246 and 230. The program estimates which of the pixels  $p_0$  or  $p_{180}$  that have the most similar grey scale values. In this case the pixels  $p_0$  have the most similar grey scale values (231, 246 and 230) which make the program accept  $\theta_0$  as the true orientation of the cylinder. The program then list an array with the last 7 "true" orientations, and if the estimated orientations are stable, the program approve an orientation  $\theta$  for the cylinder. The final orientation  $\theta$  of the cylinder is equal to the median of the 7 last "true" estimated orientations.

The program estimates that  $\theta = 30.679^\circ$ . This is shown in Figure 5.49 and the green line visualize the estimated orientation  $\theta = 30.679^\circ$ .

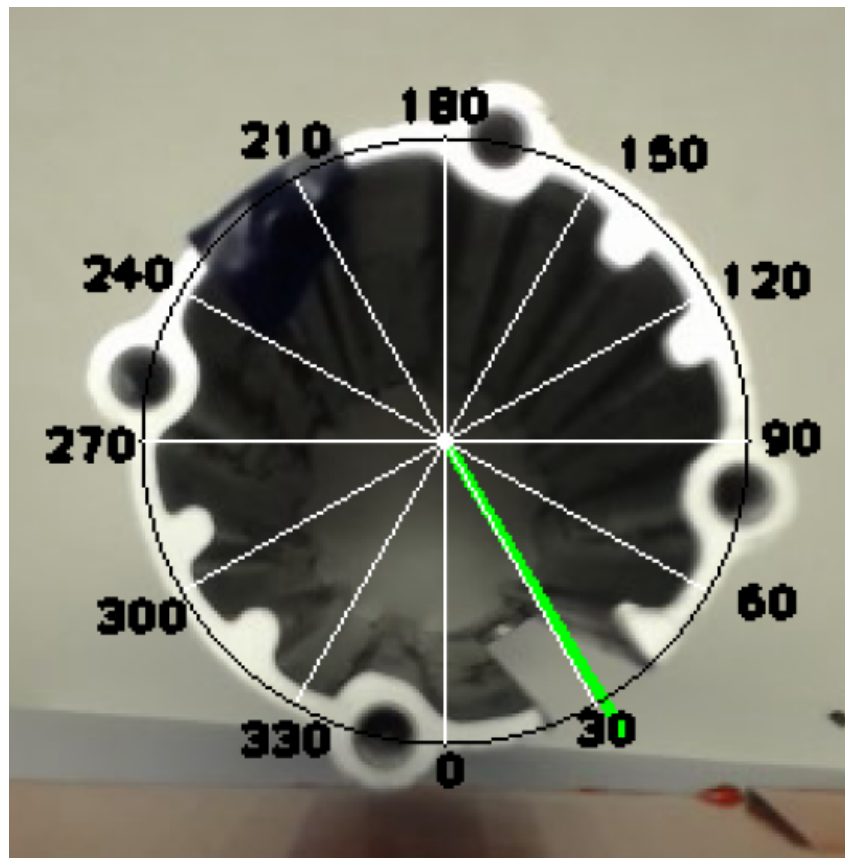


Figure 5.49: Orientation  $\theta = 30.679^\circ$  of the cylinder.

The program for the piston is quite similar to the program that have just been explained except for a few differences. The program for the piston has different training images, distance  $Z$  between the camera center and the object, the radius of the object, how to choose pixels to distinguish between orientations that are true and false ( $180^\circ$  phase shifted) and the visualization part in the program.

A video for demonstrating how these programs work have also been made. In the rest of the thesis, the notations  $\theta_c$  is used for the orientation of the cylinder and  $\theta_p$  for the orientation of the piston. That is, these programs estimates a  $\theta_p$  and a  $\theta_c$ .

It was documented good accuracy of the estimated orientations  $\theta_p$  and  $\theta_c$ . Still, the programs are depending on the parts being in accurate positions with respect to the 2D camera. That is, with a  $Z = 0.155$  for the cylinder and  $Z = 0.205$  for the piston in equation (5.16), which was used in the demo video, the cylinder could have a maximum error (in the  $X Y$  plane) of 2 mm and the piston 4 mm, from the center of the image stream. These maximum allowable errors were measured with a tape measure. Adjusting the distance between the camera and the parts to  $Z = 0.055$  for the cylinder and  $Z = 0.115$  for the piston, allowed the maximum error to be approximately 4.5 mm for the cylinder and 6 mm for the piston.

## Chapter 6

# Kinematics

This chapter presents the kinematics used in this project.

Two identical KUKA AGILUS KR 6 R900 SIXX manipulators have been used in this project. One of the manipulators is used for grasping the objects, while the other manipulator is used for estimating the orientations of the objects. In Figure 6.1 the manipulator used for grasping the objects is shown. This manipulator has a gripper connected to the end-effector.

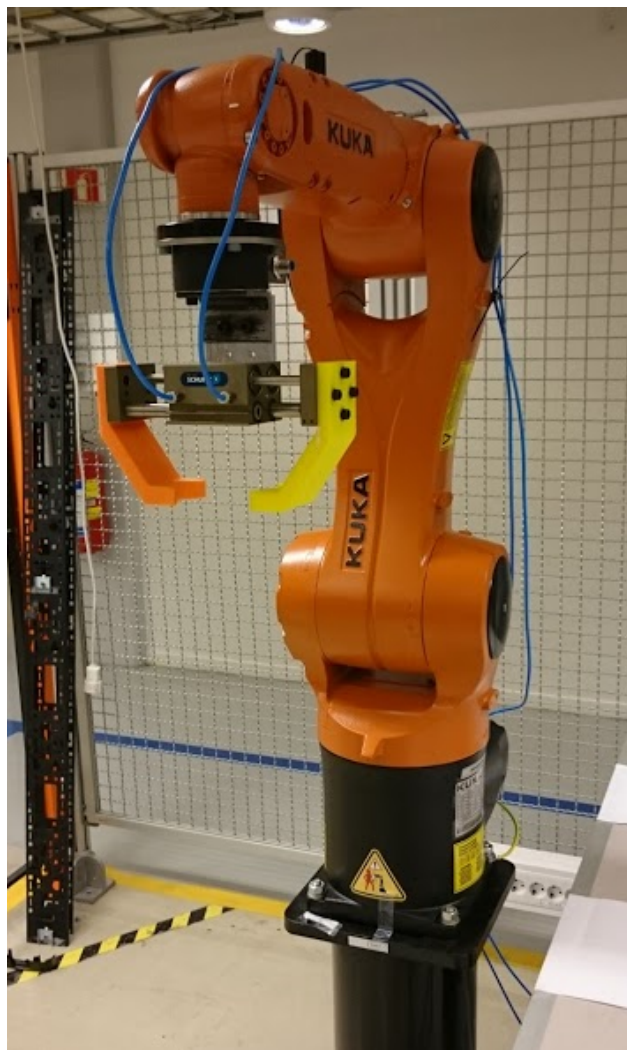


Figure 6.1: Manipulator with a gripper connected to end-effector.

In Figure 6.2 the manipulator used for estimating the orientations of the objects is shown. This manipulator has a 2D camera connected to the end-effector.



Figure 6.2: Manipulator with a 2D camera connected to end-effector.

Only forward kinematics have been used since the program operates in world coordinates. Solving of the inverse kinematics is described in Chapter 7.

## 6.1 Robot Forward Kinematics

A serial-link manipulator comprises a set of bodies, called links, in a chain and connected by joints. Each joint have one degree of freedom, either translation (a prismatic joint) or rotational (a revolute joint).

A systematic way of describing the geometry of a serial chain of links and joints was proposed by Denavit and Hartenberg and is known today as Denavit-Hartenberg notation.

A KUKA Agilus manipulator has 6 revolute joints numbered from 1 to 6, there are 7 links, numbered from 0 to 6. The direction of rotation of the joints, are shown in Figure 6.3.

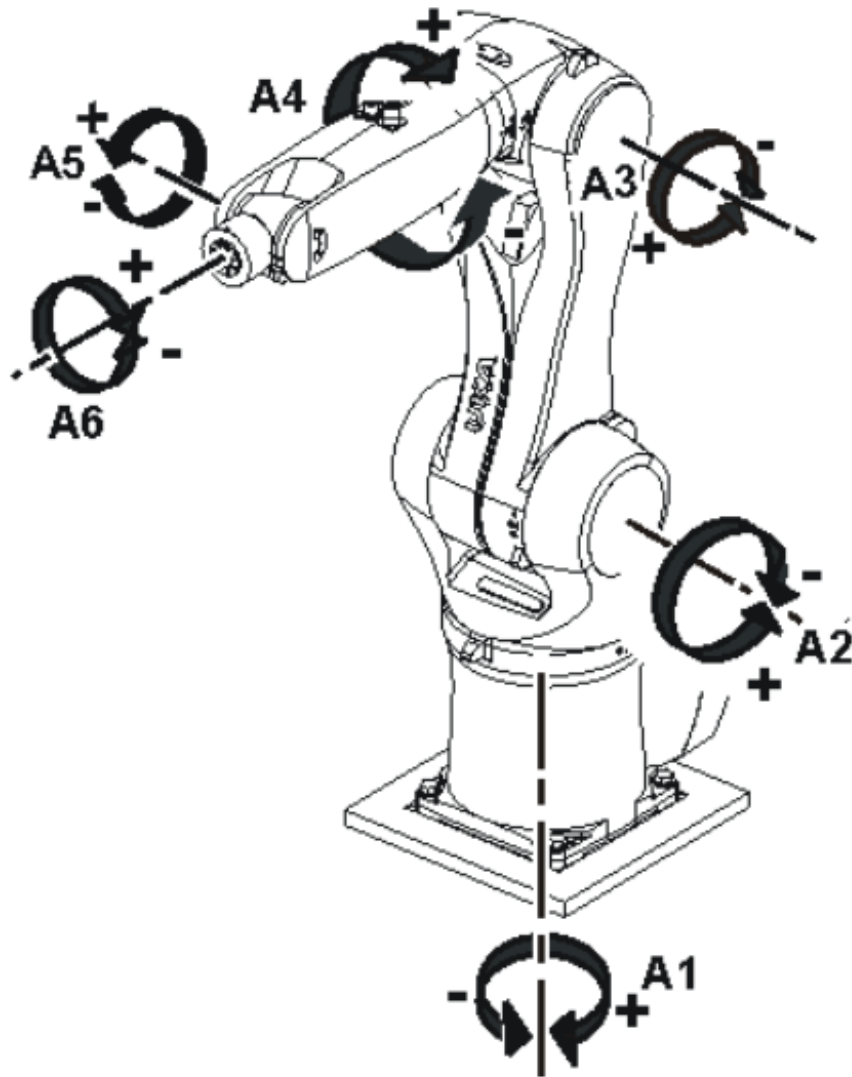


Figure 6.3: Direction of rotation of robot axes [21]

Link 0 is the base of the manipulator and link 6 carries the end effector. Joint  $j$  connects link  $j-1$  to link  $j$  and therefore joint  $j$  moves link  $j$ . This is shown in Figure 6.4. A link can be specified by its length  $a_j$  and its twist  $\alpha_j$ . The link offset  $d_j$  is the distance from one link coordinate frame to the next along the axis of the joint. The joint angle  $\theta_j$  is the rotation of one link with respect to the next about the joint axis. The coordinate frame  $\{j\}$  is attached to the end of link  $j$ . The axis of joint  $j$  is aligned with the  $Z$  axis [2].

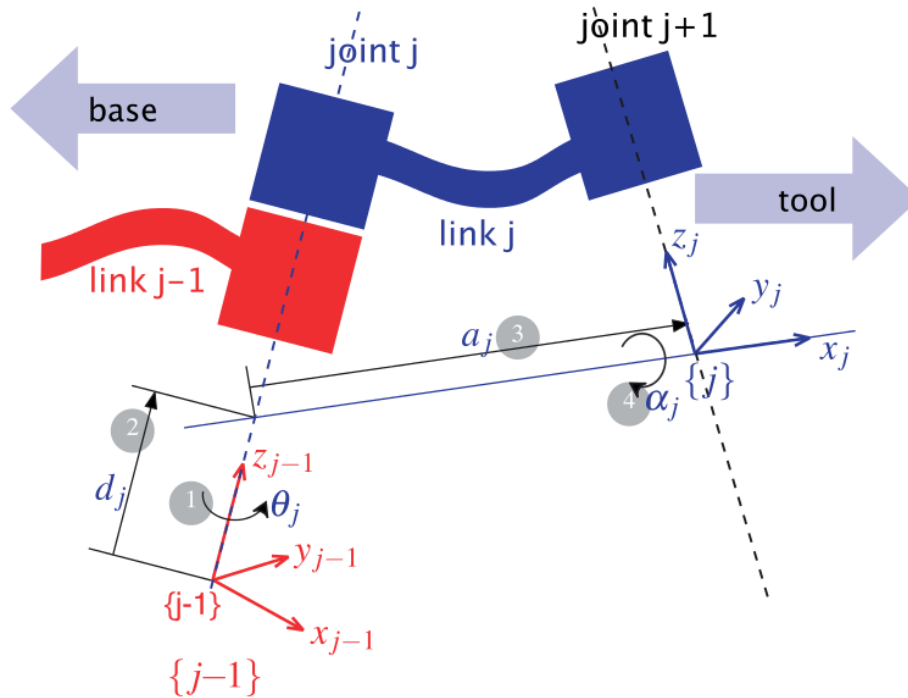


Figure 6.4: Definition of standard Denavit and Hartenberg link parameters [2].

These link and joint parameters are known as Denavit-Hartenberg parameters [2]. The Denavit-Hartenberg parameters for the KUKA Agilus is shown in Table 6.1 and in Figure 6.5. The joint variables  $\theta_j^*$  where  $j \in \{1 \dots 6\}$  are the different joint angles between the  $x_{j-1}$  and  $x_j$  axes about the  $z_{j-1}$  axis in Figure 6.4.

Link	$\theta_j$ [rad]	$d_j$ [mm]	$a_{j-1}$ [mm]	$\alpha_{j-1}$ [rad]
1	$\theta_1^*$	-400	-25	$-\frac{\pi}{2}$
2	$\theta_2^*$	0	315	0
3	$\theta_3^*$	0	35	$\frac{\pi}{2}$
4	$\theta_4^*$	-365	0	$-\frac{\pi}{2}$
5	$\theta_5^*$	0	0	$-\frac{\pi}{2}$
6	$\theta_6^*$	-80	0	$\pi$

Table 6.1: Denavit-Hartenberg parameters for KUKA Agilus.

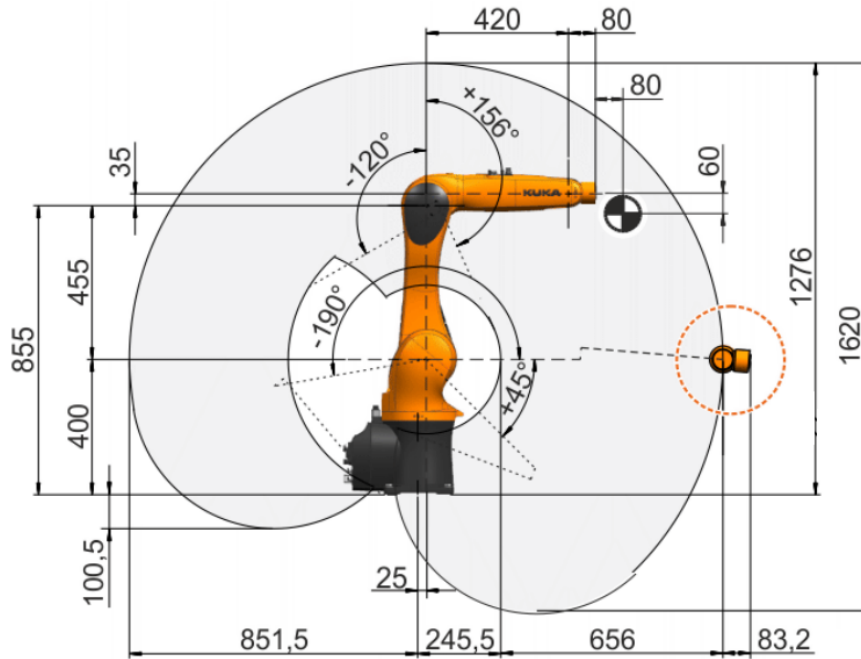


Figure 6.5: KUKA Agilus KR 6 R900 sixx [21].

The transformation from link coordinate frame  $\{j-1\}$  to frame  $\{j\}$  is defined as

$$T_j^{j-1}(\theta_j, d_j, a_j, \alpha_j) = T_{Rz}(\theta_j)T_z(d_j)T_x(a_j)T_{Rx}(\alpha_j) \quad (6.1)$$

which can be expanded as

$$T_j^{j-1} = \begin{bmatrix} \cos\theta_j & -\sin\theta_j\cos\alpha_j & \sin\theta_j\sin\alpha_j & a_j\cos\theta_j \\ \sin\theta_j & \cos\theta_j\cos\alpha_j & -\cos\theta_j\sin\alpha_j & a_j\sin\theta_j \\ 0 & \sin\alpha_j & \cos\alpha_j & d_j \\ 0 & 0 & 0 & 1 \end{bmatrix} \quad (6.2)$$

The forward kinematics  $T_e^0$  is expressed as a function with the end-effectors pose with respect to the base of the robot  $\{0\}$ , as a function of the joint variables

$$T_e^0(\theta_1^*, \theta_2^*, \theta_3^*, \theta_4^*, \theta_5^*, \theta_6^*)$$

Using homogeneous transformations, this is the product of the individual link transformation matrices given by equation (6.2)

$$T_e^0 = T_1^0 T_2^1 T_3^2 T_4^3 T_5^4 T_6^5. \quad (6.3)$$

In ROS (Robot Operating System), both robots operates in a common world coordinate system  $\{w\}$ . That is, there have been implemented transformations from a common world coordinate system  $\{w\}$  to both robots' bases. In ROS, both poses of the end-effector operates with respect



to world coordinate system  $\{w\}$ .

## 6.2 Kinematics Result

### 6.2.1 Robot with a 2D Camera Connected to End-Effector

The robot with a 2D camera attached to the end effector, is the robot that are used in the orientation analysis described in Chapter 5.2.1. The orientation analysis is run when the robot's end effector is at a certain pose with respect to the objects.

#### Pose of the Cylinder

The transformation  $T_{c_{2D}}^e$  from the end-effector to the 2D camera  $\{c_{2D}\}$  is

$$T_{c_{2D}}^e = \begin{bmatrix} 1 & 0 & 0 & 0 \\ 0 & 1 & 0 & -0.028 \\ 0 & 0 & 1 & 0.01 \\ 0 & 0 & 0 & 1 \end{bmatrix} \quad (6.4)$$

Figure 6.6 shows the pose of the 2D camera  $\{c_{2D}\}$  when the program for estimating the orientation  $\theta_c$  of the cylinder is run.  $\theta_c$  and  $\theta_p$  are the orientations around the  $Z$  axis of the objects, which were described in Chapter 5.2. The  $Z$  axis of the objects is parallel to the  $Z$  axis of the table coordinate system  $\{t\}$  shown in Figure 6.6.

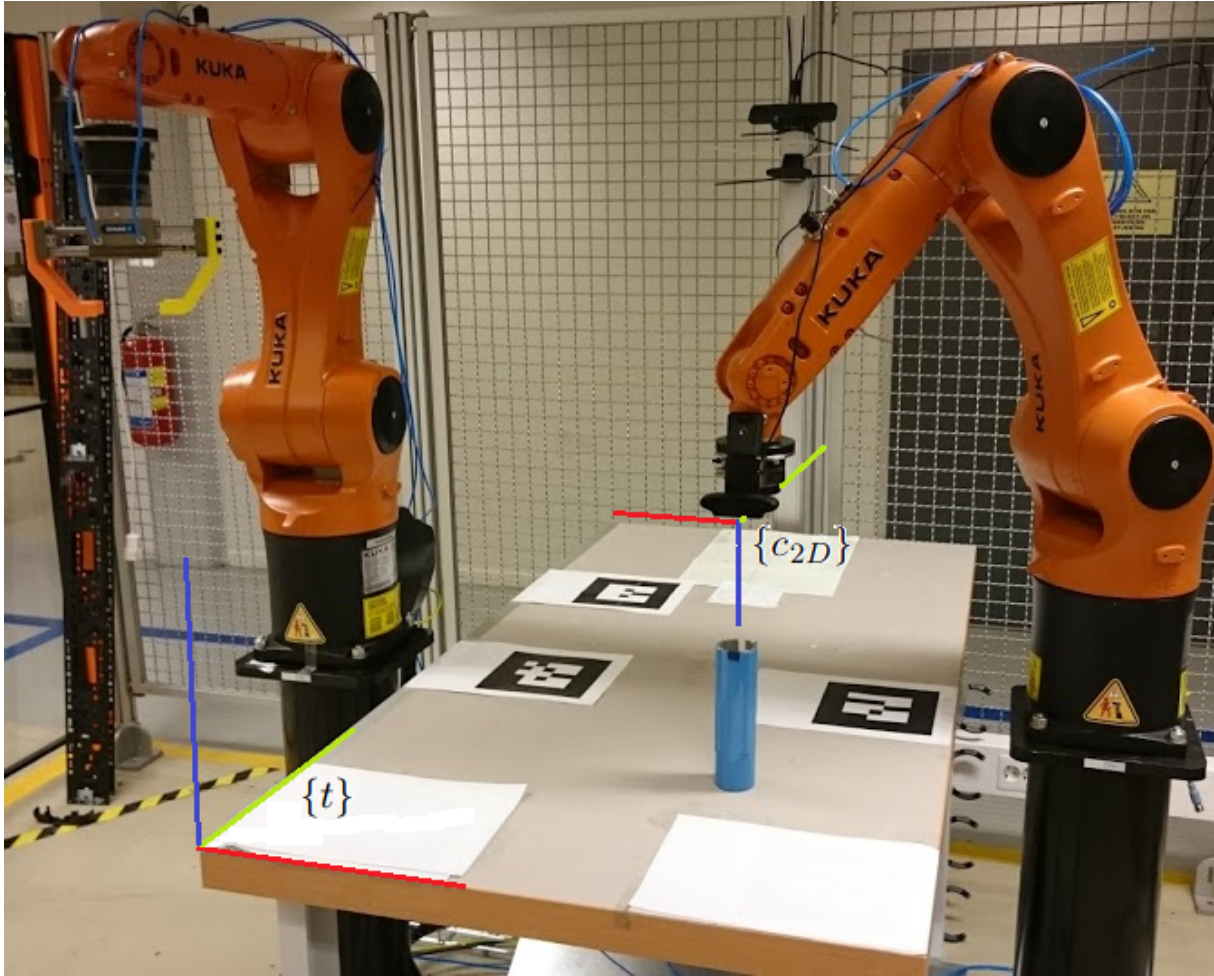


Figure 6.6: The table coordinate system  $\{t\}$  and the 2D camera coordinate system  $\{c_{2D}\}$ .

The rotation matrix  $R_{c_{2D}}^t$  from the table  $\{t\}$  to the 2D camera  $\{c_{2D}\}$  is a  $180^\circ$  rotation around the Y axis as shown in Figure 6.6.

$$R_{c_{2D}}^t = \begin{bmatrix} -1 & 0 & 0 \\ 0 & 1 & 0 \\ 0 & 0 & -1 \end{bmatrix} \quad (6.5)$$

As shown in the Figure 6.7, the transformation  ${}^{\theta_c}T_{c_{2D}}^t$  from table  $\{t\}$  to  $\{c_{2D}\}$  when running the program for estimating  $\theta_c$  is

$${}^{\theta_c}T_{c_{2D}}^t = \begin{bmatrix} R_{c_{2D}}^t & p_{cyl}^t + \delta p_{cyl} \\ 0^T & 1 \end{bmatrix} \quad (6.6)$$

where  $\delta p_{cyl} = (0, 0, 0.055)^T$  is the distance between the top of the cylinder and optical center of the 2D camera. The coordinates  $p_{cyl}^t$  of the cylinder with respect to the table pose  $\{t\}$  was estimated in Chapter 5.1.4.

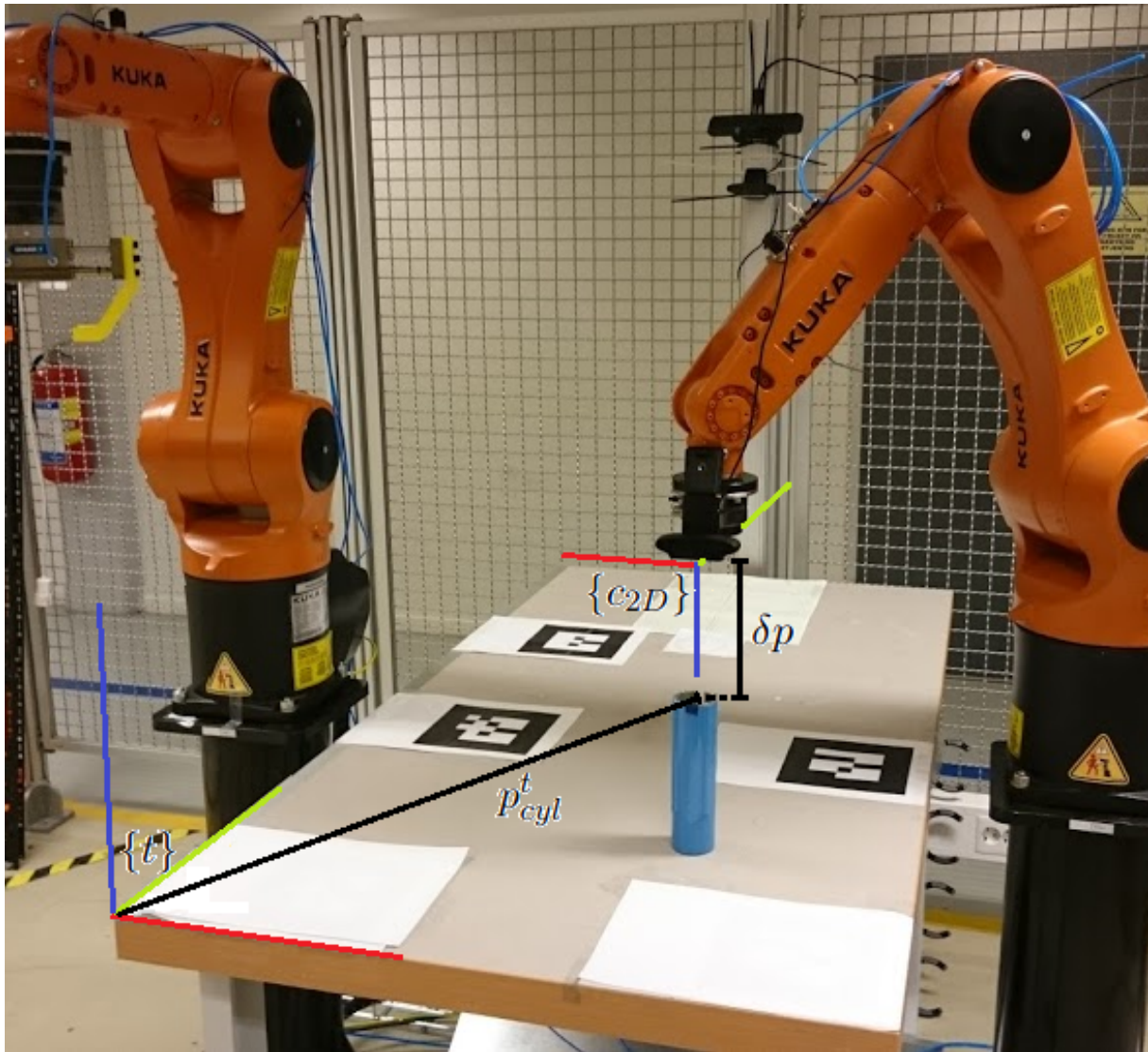


Figure 6.7: Transformation  $T_{c2D}^t$  from table pose  $\{t\}$  to 2D camera pose  $\{c2D\}$ .

The transformation  $T_t^w$  from world  $\{w\}$  (the coordinate system both robots are operating in) to table  $\{t\}$  was measured to be a rotation  $R_z(90^\circ)$  and a translation  $t = (0.67562, -0.39624, 0.938)$ .

$$T_t^w = \begin{bmatrix} 0 & -1 & 0 & 0.67562 \\ 1 & 0 & 0 & -0.39624 \\ 0 & 0 & 1 & 0.938 \\ 0 & 0 & 0 & 1 \end{bmatrix} \quad (6.7)$$

The end-effector pose  $T_{e,\theta_c}^w$  when doing the orientation analysis of the cylinder is

$$T_{e,\theta_c}^w = T_t^w \theta_c T_{c2D}^t (T_{c2D}^e)^{-1} \quad (6.8)$$

were  $T_{c2D}^e$  was estimated in equation (6.4),  $\theta_c T_{c2D}^t$  in equation (6.6) and  $T_t^w$  in equation (6.7).

When the robot's end effector is at  $T_{e,\theta_c}^w$  the program for estimating  $\theta_c$  is run. In Figure 6.8 the  $X$  and  $Y$  axis of the pose of the cylinder is shown. The rotation matrix  $R_{\text{cyl}}^t$  from table  $\{t\}$  to cylinder is an identity matrix when  $\theta_c = 0^\circ$ .

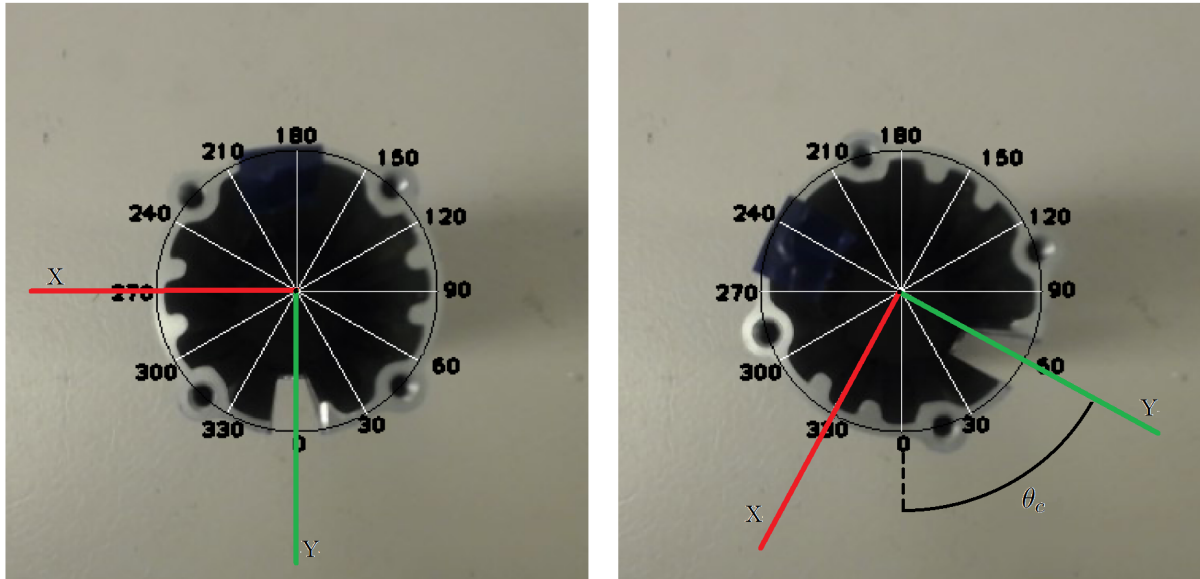


Figure 6.8: From left: Orientation of the cylinder is  $\theta_c = 0^\circ$  and  $\theta_c = 60^\circ$ .

Since the  $Z$  axis of table  $\{t\}$  and the cylinder (and piston) is parallel, the rotation matrix  $R_{\text{cyl}}^t$  is a rotation  $\theta_c$  around the  $Z$  axis

$$R_{\text{cyl}}^t = R_z(\theta_c) \quad (6.9)$$

The pose of the cylinder  $T_{\text{cyl}}^t$  with respect to the table  $\{t\}$  is

$$T_{\text{cyl}}^t = \begin{bmatrix} R_{\text{cyl}}^t & p_{\text{cyl}}^t \\ 0^T & 1 \end{bmatrix} \quad (6.10)$$

The pose of the cylinder  $T_{\text{cyl}}^w$  with respect to the world coordinate system  $\{w\}$  is

$$T_{\text{cyl}}^w = T_t^w T_{\text{cyl}}^t \quad (6.11)$$

were  $T_t^w$  was estimated in equation (6.7) and  $T_{\text{cyl}}^t$  in equation (6.10).

$T_{\text{cyl}}^w$  is the pose of the cylinder with respect to coordinate system both robots are operating in.

### Pose of the Piston

The end-effector pose  $T_{e,\theta_p}^w$  when doing the orientation  $\theta_p$  analysis of the piston is

$$T_{e,\theta_p}^w = T_t^w \underbrace{\begin{bmatrix} R_{c_{2D}}^t & p_{\text{pis}}^t + \delta p_{\text{pis}} \\ 0^T & 1 \end{bmatrix}}_{\theta_p T_{c_{2D}}^t} (T_{c_{2D}}^e)^{-1} \quad (6.12)$$

where  $\delta p_{\text{pis}} = (0, 0, 0.115)$  is the distance between the top of the piston and the optical center of the 2D camera and  $\theta_p T_{c_{2D}}^t$  is the transformation from table  $\{t\}$  to  $\{c_{2D}\}$  when running the program for estimating  $\theta_p$ . The transformation  $T_t^w$  was estimated in equation (6.8),  $T_{c_{2D}}^e$  in equation (6.4) and the rotation matrix  $R_{c_{2D}}^t$  in equation (6.5). The coordinates  $p_{\text{pis}}^t$  of the piston with respect to the table  $\{t\}$  was estimated in Chapter 5.1.4.

When the end-effector is at the pose  $T_{e,\theta_p}^w$  the program for estimating the orientation  $\theta_p$  of the piston is run.

The pose  $T_{\text{pis}}^w$  of the piston with respect to world  $\{w\}$  is

$$T_{\text{pis}}^w = T_t^w \begin{bmatrix} R_z(\theta_{\text{pis}}) & p_{\text{pis}}^t \\ 0^T & 1 \end{bmatrix}$$

The transformations in equations (6.12) and (6.8) are estimated forward kinematics for the robot with 2D camera.

## 6.2.2 Robot with a Gripper Connected to End-Effector

The pose of the parts  $T_{\text{pis}}^w$  and  $T_{\text{cyl}}^w$  are estimated and the robot with a gripper connected to the end-effector, have enough information to assemble the parts.

The transformation  $T_e^g$  from gripper to end-effector is

$$T_e^g = \begin{bmatrix} 1 & 0 & 0 & 0 \\ 0 & 1 & 0 & 0 \\ 0 & 0 & 1 & -0.16 \\ 0 & 0 & 0 & 1 \end{bmatrix} \quad (6.13)$$

In Figure 6.9 the pose of the gripper  $\{g\}$  is shown. The transformation  $T_g^{\text{cyl}}$  from the cylinder to the gripper (when the gripper is grabbing the cylinder) is a  $180^\circ$  rotation around the  $Y$  axis

$$T_g^{\text{cyl}} = \begin{bmatrix} R_y(180^\circ) & 0 \\ 0^T & 1 \end{bmatrix} \quad (6.14)$$

The same applies to the transformation  $T_g^{\text{pis}}$  from the piston to the gripper

$$T_g^{\text{pis}} = \begin{bmatrix} R_y(180^\circ) & 0 \\ 0^T & 1 \end{bmatrix} \quad (6.15)$$

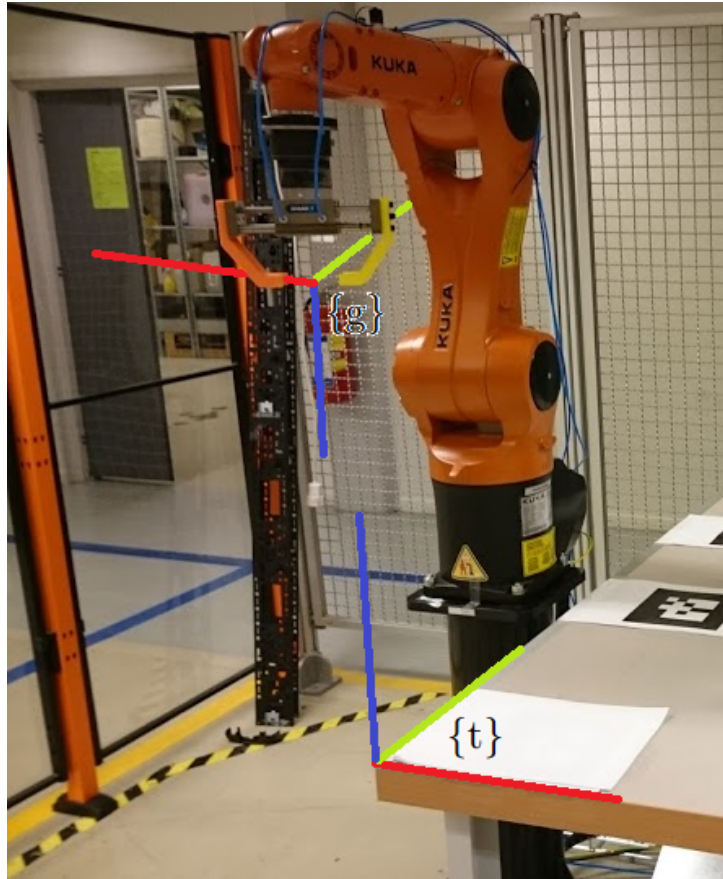


Figure 6.9: The robot gripper pose  $\{g\}$  and the table pose  $\{t\}$ .

The transformation  $T_e^{\text{cyl}}$  from the cylinder to end effector (when the gripper is grabbing the cylinder) is

$$T_e^{\text{cyl}} = T_g^{\text{cyl}} T_e^g \quad (6.16)$$

and transformation  $T_e^{\text{pis}}$  from the piston to end effector is

$$T_e^{\text{pis}} = T_g^{\text{pis}} T_e^g \quad (6.17)$$

The final pose  $T_{e_{\text{pis}}}^w$  of the end-effector with respect to world  $\{w\}$ , when the gripper is grabbing the piston is

$$T_{e_{\text{pis}}}^w = T_{\text{pis}}^w T_e^{\text{pis}} \quad (6.18)$$

and when the gripper  $T_{e_{cyl}}^w$  is grabbing the cylinder is

$$T_{e_{cyl}}^w = T_{cyl}^w T_e^{\text{cyl}} \quad (6.19)$$

This is shown in Figure 6.10. The transformations in equations (6.18) and (6.19) are the estimated forward kinematics for the robot with a gripper connected to end-effector.

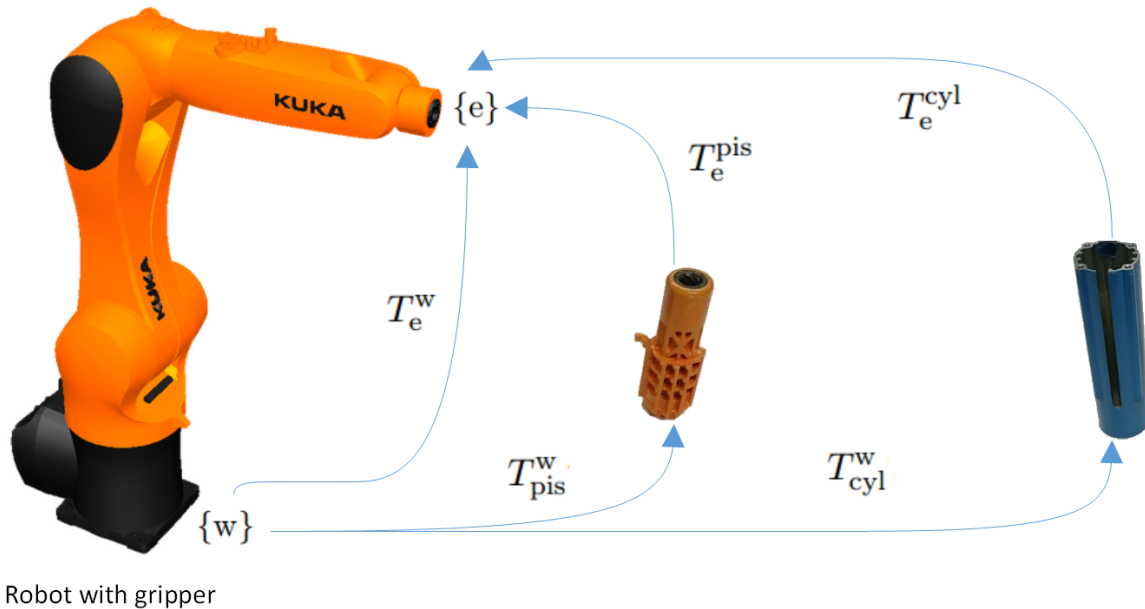


Figure 6.10: Transformations between the robot and the parts (cylinder and piston).

### 6.2.3 The Kinematics Sequence

The sequence of the program runs as follows:

Robot with 2D camera:

1.  $T_e^w = T_{e,\theta_c}^w$  (equation (6.8))
2. Run algorithm for estimating the cylinder orientation  $\theta_c$
3.  $T_e^w = T_{e,\theta_p}^w$  (equation (6.12))
4. Run algorithm for estimating the piston orientation  $\theta_p$
5. Run robot to home position

Robot with gripper:

1. gripper open
2.  $T_e^w = \delta T T_{e_{pis}}^w$
3.  $T_e^w = T_{e_{pis}}^w$  (equation (6.18))
4. gripper close



5.  $T_e^w = \delta T T_{e_{\text{pis}}}^w$
6.  $T_e^w = \delta T T_{e_{\text{cyl}}}^w$
7.  $T_e^w = T_{e_{\text{cyl}}}^w$  (equation (6.19))

where

$$\delta T = \begin{bmatrix} I & t \\ 0^T & 1 \end{bmatrix} \quad \text{and} \quad t = [0, 0, 0.1]^T$$

There have been made a video demonstrating the sequence of the robot assembling the parts with  $\theta_c$  and  $\theta_p$  set equal  $0^\circ$ .

In Figure 6.11 the two robots are shown.

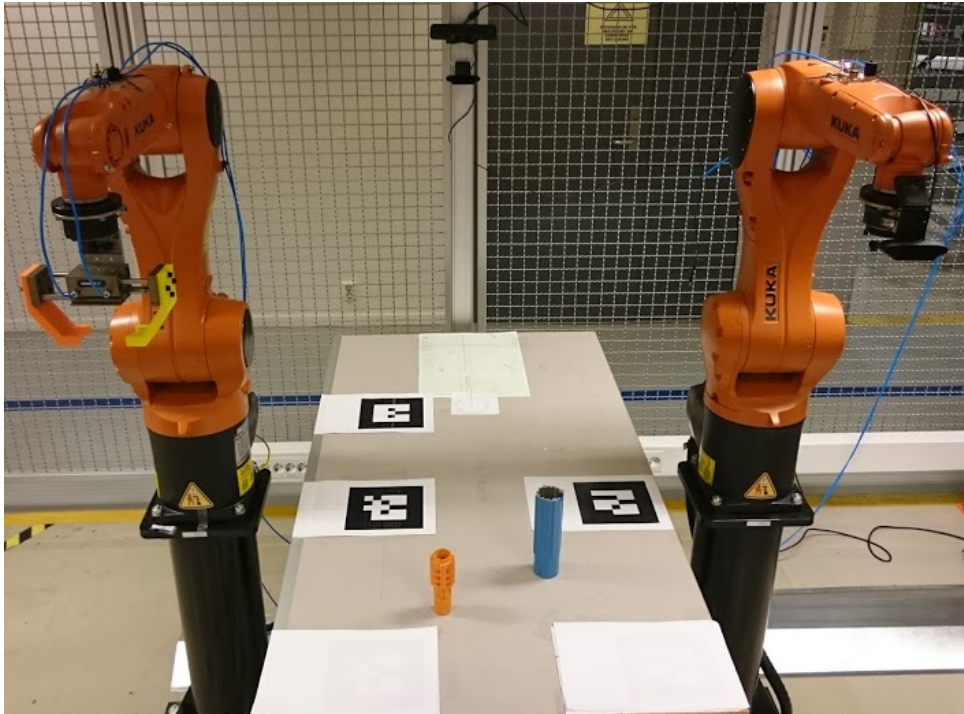


Figure 6.11: The two manipulators and their work space.



## Chapter 7

# ROS

ROS (Robot Operating System) is a framework for writing robot software. It is a collection of tools, libraries, and conventions for creating robot behavior across a wide variety of robotic platforms [22].

### 7.1 The Robots

Figure 7.1 shows a KUKA AGILUS KR 6 R900 SIXX robot. The robot consist of a manipulator (1), a teach pendant (2), connection cable for the teach pendant (3), a KUKA KR C4 controller (4), data cable (5) and motor cable (6).

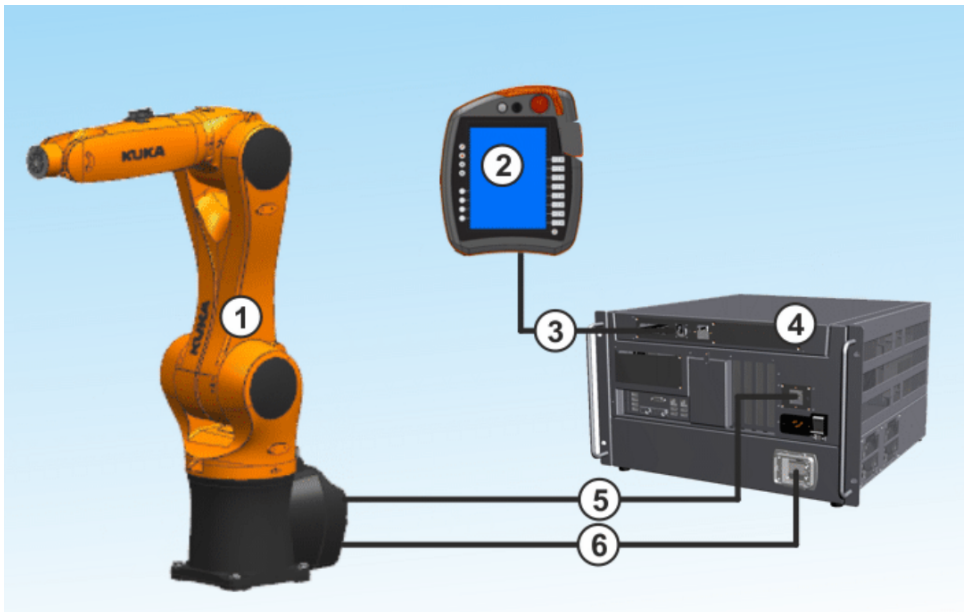
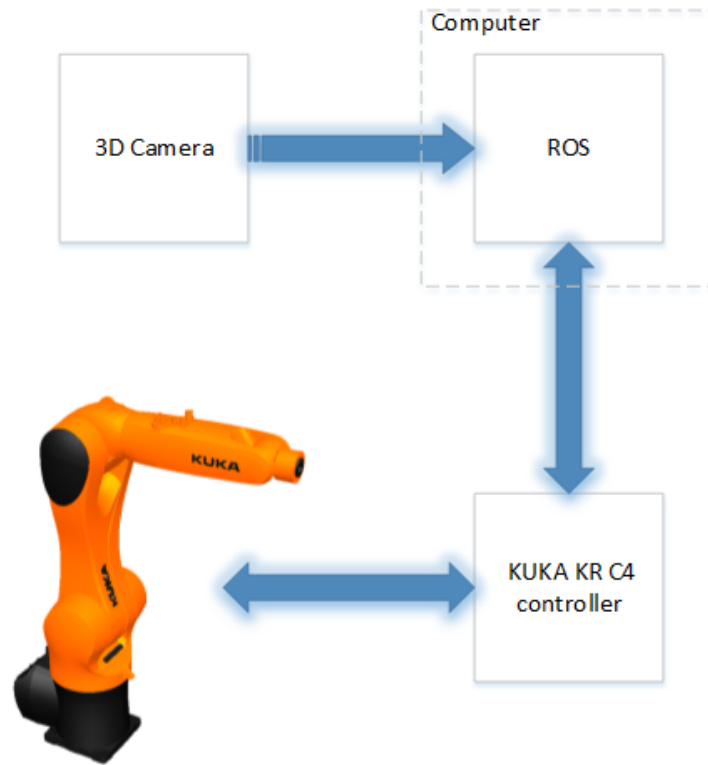


Figure 7.1: Description of the Kuka Agilus robot [9].

The KUKA Robot Sensor Interface (RSI) is the program that passes information between the KUKA KR C4 controller and the computer with ROS. This information is passed over the Ethernet UDP/IP protocol as XML (Extensible Markup Language) strings.

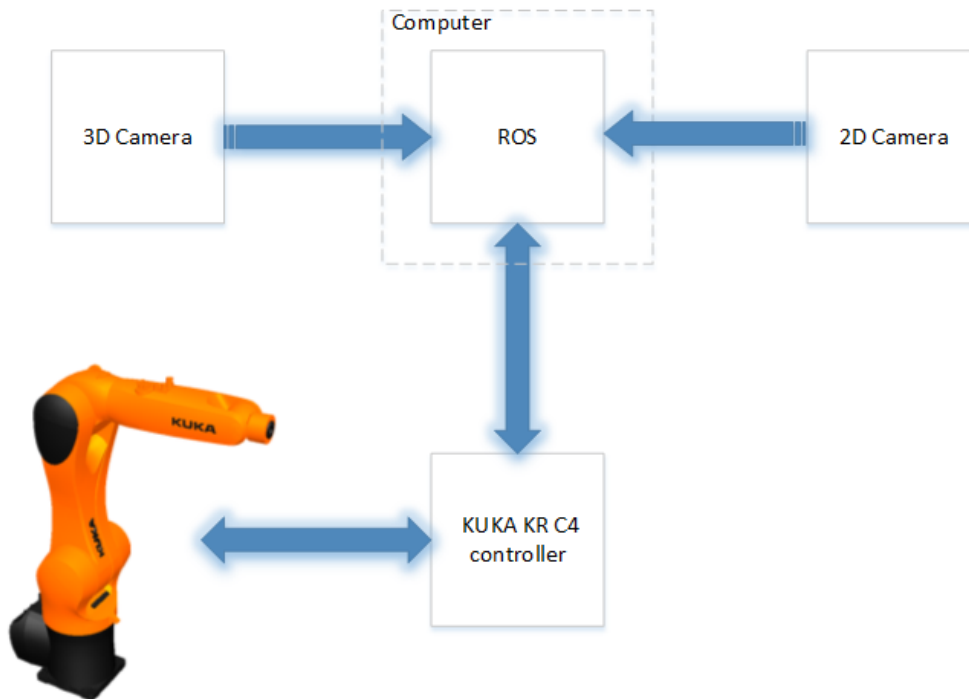
Figure 7.2 shows the information flow for the robot with a 2D camera connected to end-effector.



Agilus 2 – Robot with 2D camera

Figure 7.2: Robot with a 2D camera connected to end-effector.

Figure 7.3 shows the information flow for the robot with a gripper connected to end-effector.



Agilus 1 – Robot with gripper

Figure 7.3: Robot with a gripper connected to end-effector.

## 7.2 Implementation of RGB-D Camera

Software in ROS is organized in *packages*. A package might contain among others, ROS *nodes*, a ROS-independent library, a dataset and configuration files. A node is an executable that uses ROS to communicate with other nodes [22].

In this project the ROS packages *Openni\_camera*, *Openni2\_launch* and *Ar\_track\_alvar* have been used in relation with the depth camera. *openni\_camera* provides a ROS interface to the ASUS Xtion Pro Live. *openni2\_launch* contains launch files for using OpenNI-compliant devices in ROS and *ar\_track\_alvar* is a ROS wrapper for Alvar, an open source AR tag tracking library [22].

Figure 7.4 shows a simplified version of the ROS program for estimating coordinates of the objects. The ellipses are ROS nodes and the rectangles represents ROS topics. A node can publish messages to a topic as well as subscribe to a topic to receive messages. A message is a ROS data type [22]. In this chapter, names for ROS nodes and ROS topics have been simplified in contrast to the names in the program.

The program runs as follows:

1. The node *3D Camera* publishes a point cloud to the topic *Point cloud*.
2. The node *AR TAG* subscribes to *Point cloud* and publishes the center points of the AR-tags on the topic *TAG coordinates*.
3. The node *TF point cloud* subscribes to *TAG coordinates* and publishes a homogeneous transformation from camera frame to table frame on the topic *TF camera table*.
4. The node *Coordinates objects* subscribes to *Point cloud* and *TF point cloud*, and publishes the coordinates of the objects with respect to table coordinate system on the topics *Coordinates cylinder* and *Coordinates piston*.

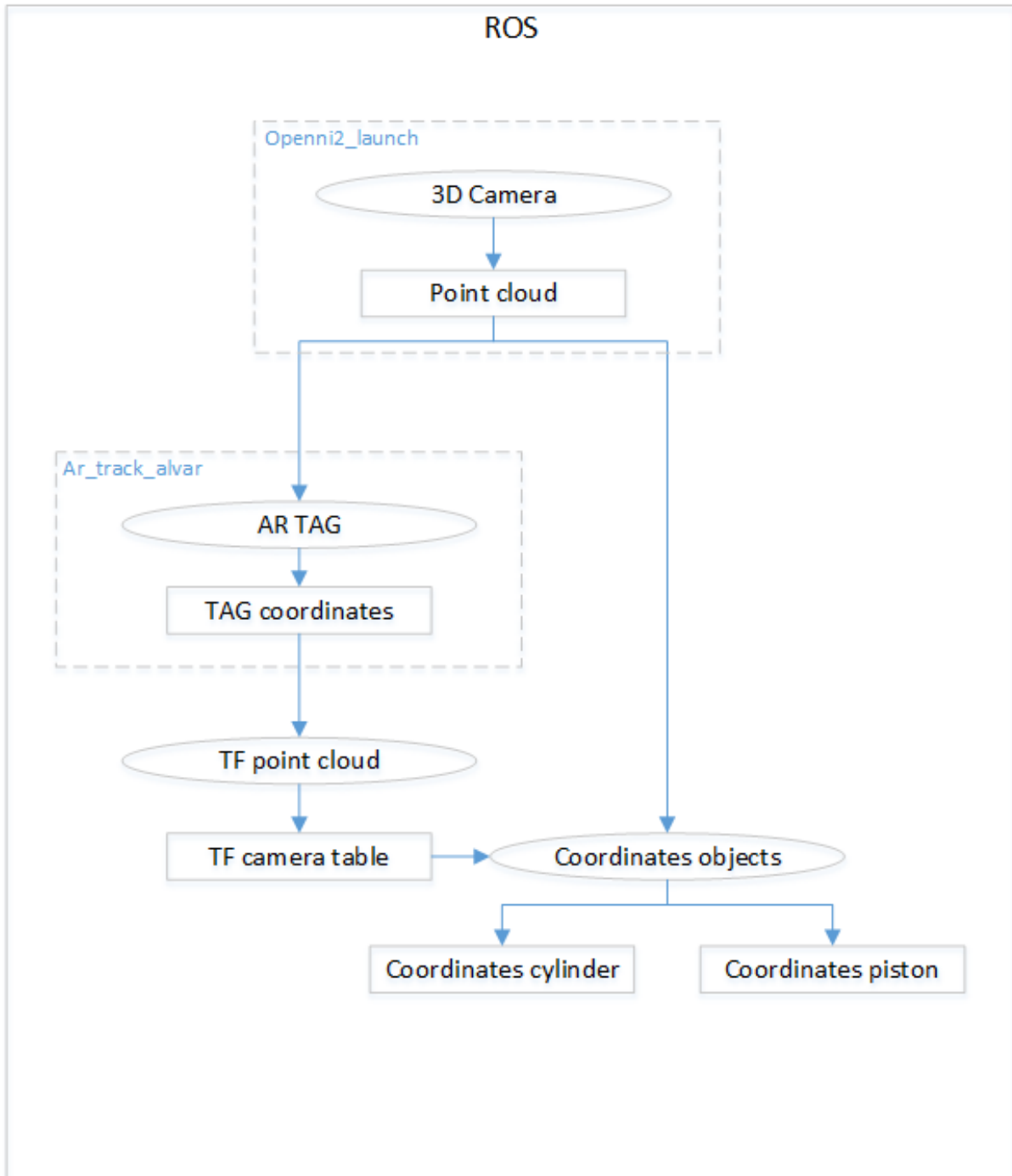


Figure 7.4: RGB-D camera in ROS.

### 7.3 Implementation of Robot with a 2D Camera Connected to End-Effector

Figure 7.5 shows a simplified version of the ROS program for running the robot with 2D camera (The names used in the figure are also simplified). The node *Agilus 2* is the interface to the KUKA KR C4 controller. *Joint trajectory ag2* provides an action interface for tracking trajectory execution.

*MoveIt!* is a program used for planing and execution of trajectories. It will among others

look on joint limits, kinematics and motion planning. MoveIt! talks to the robot through the ROS topics and ROS actions. It communicates with the robot to get current state information (positions of the joints, etc.) to get point clouds and other sensor data from the robot sensors and to talk to the controllers on the robot. [12]. ROS actions is used when someone would like to send a request to a node and also receive a reply to the request. ROS actions also gives the ability to cancel the request if it takes a long time to execute. The ROS actions are visualized (in Figure 7.5) as boxes that are connected to lines with arrows in both ends.

The program runs as follows:

1. The node *Agilus 2* publishes information about the joint angles to the topic *Joint states*.
2. The node *Forward kinematics* subscribes to the topic *Joint states* and publishes the 3D poses of the robot links to the topic *TF*.
3. The node *Moveit* subscribes to the topics *Joint states* and *TF* to determine the current state where each joint of the robot is and the robot's pose.
4. A user defined request is published from the node *Pose objects* to the action topic *New pose end effector*. This user defined request is the kinematics used in points number 1 and 3 in the kinematic sequence "Robot with 2D camera" in Chapter 6.2.3. The topics *Coordinates cylinder* and *Coordinates piston* are the same as the topics shown in Figure 7.4.
5. The node *Moveit* talks to *New pose end effector*, and the KUKA KR C4 controller through the ROS action interface *Joint trajectory ag2*.

MoveIt! will generate a desired trajectory in response to the transformations on *New pose end effector*. Since the robot operates in joint coordinates, the inverse kinematics must be solved. MoveIt! uses a plug-in infrastructure. The default inverse kinematics plug-in for MoveIt! is configured using a numerical jacobian-based solver. This plug-in is automatically configured in MoveIt! [12]. The action topic *Joint trajectory ag2* passes trajectory goals to the node *Agilus 2*, and reports success when they have finished executing. It can also enforce constraints on the trajectory, and abort trajectory execution when the constraints are violated.

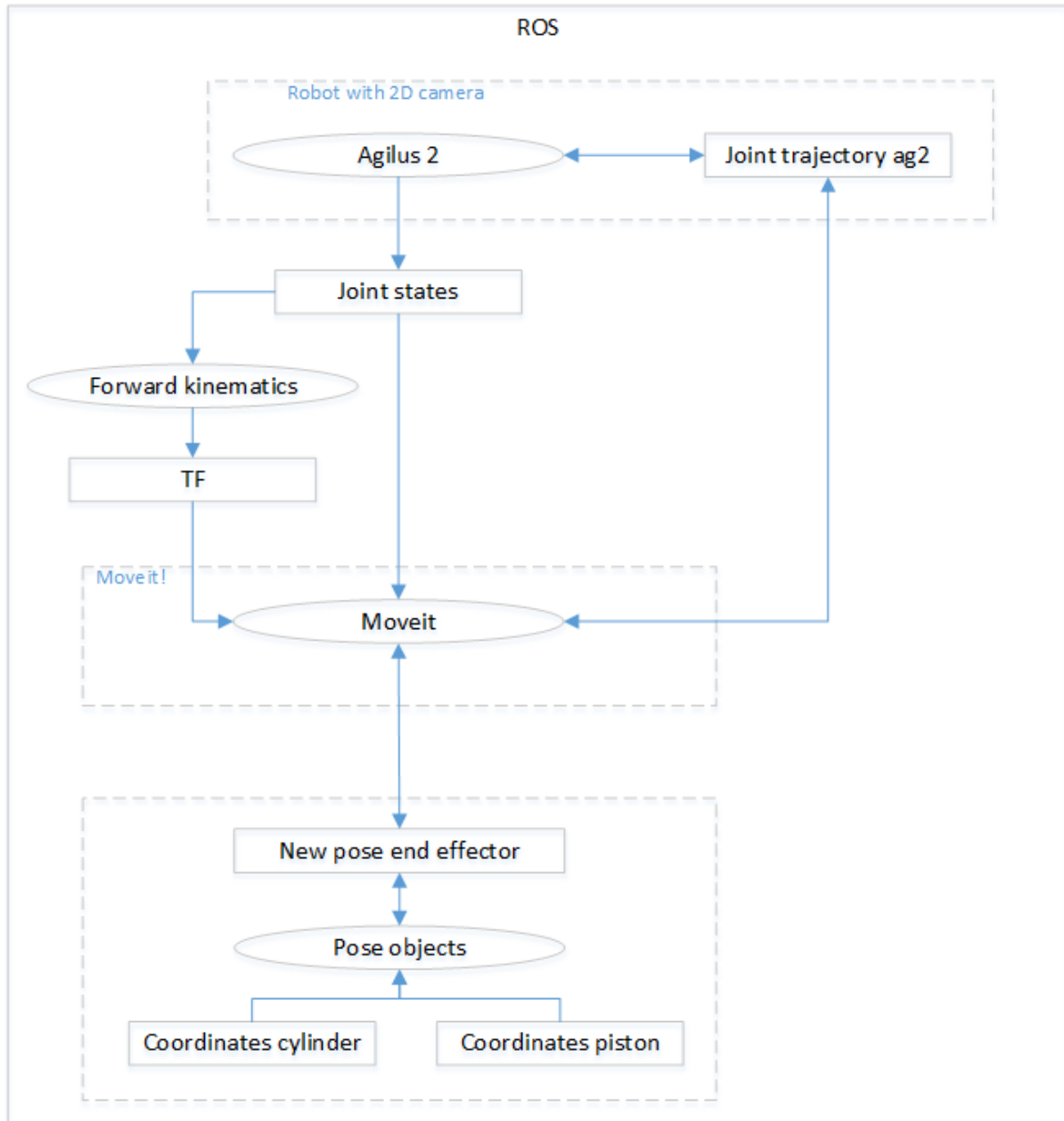


Figure 7.5: Robot with a 2D Camera connected to end-effector.

## 7.4 Implementation of 2D Camera

The ROS package *usb\_camera* was used as ROS interface with the 2D camera. The program for the 2D camera is illustrated in Figure 7.6 and runs as follows:

1. The node *2D camera* publishes images from the 2D camera on the topic *2D image*.
2. The node *Orientation objects* subscribes to *2D image* and publishes the orientations  $\theta_c$  and  $\theta_p$  on the topics *Orientation cylinder* and *Orientation piston*.
3. The node *Pose objects* subscribes to the topics *Orientation piston*, *Orientation cylinder*, *Coordinates piston* and *Coordinates cylinder*. On the basis of this information, the node estimates  $T_{cyl}^w$  and  $T_{pis}^w$ .



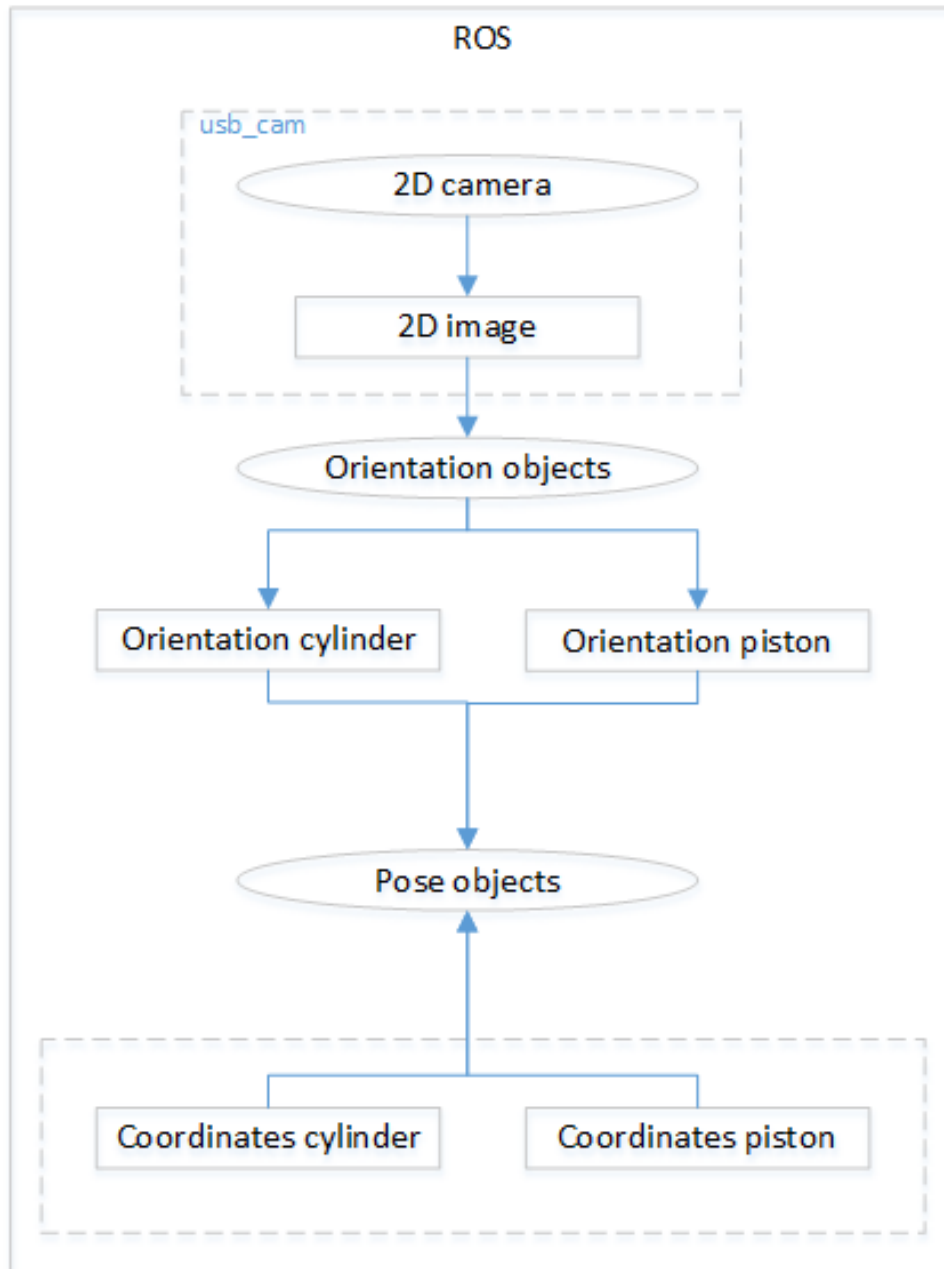


Figure 7.6: 2D camera in ROS

## 7.5 Implementation of Robot with a Gripper Connected to End-Effector

In Figure 7.7 the robot with gripper is shown. The ROS program for this robot is the same as for the robot with the 2D camera. The node *Pose objects* publishes the kinematics estimated in points 2, 3, 5, 6 and 7 in the kinematics sequence "Robot with gripper" in Chapter 6.2.3, to the topic *New pose end effector*.

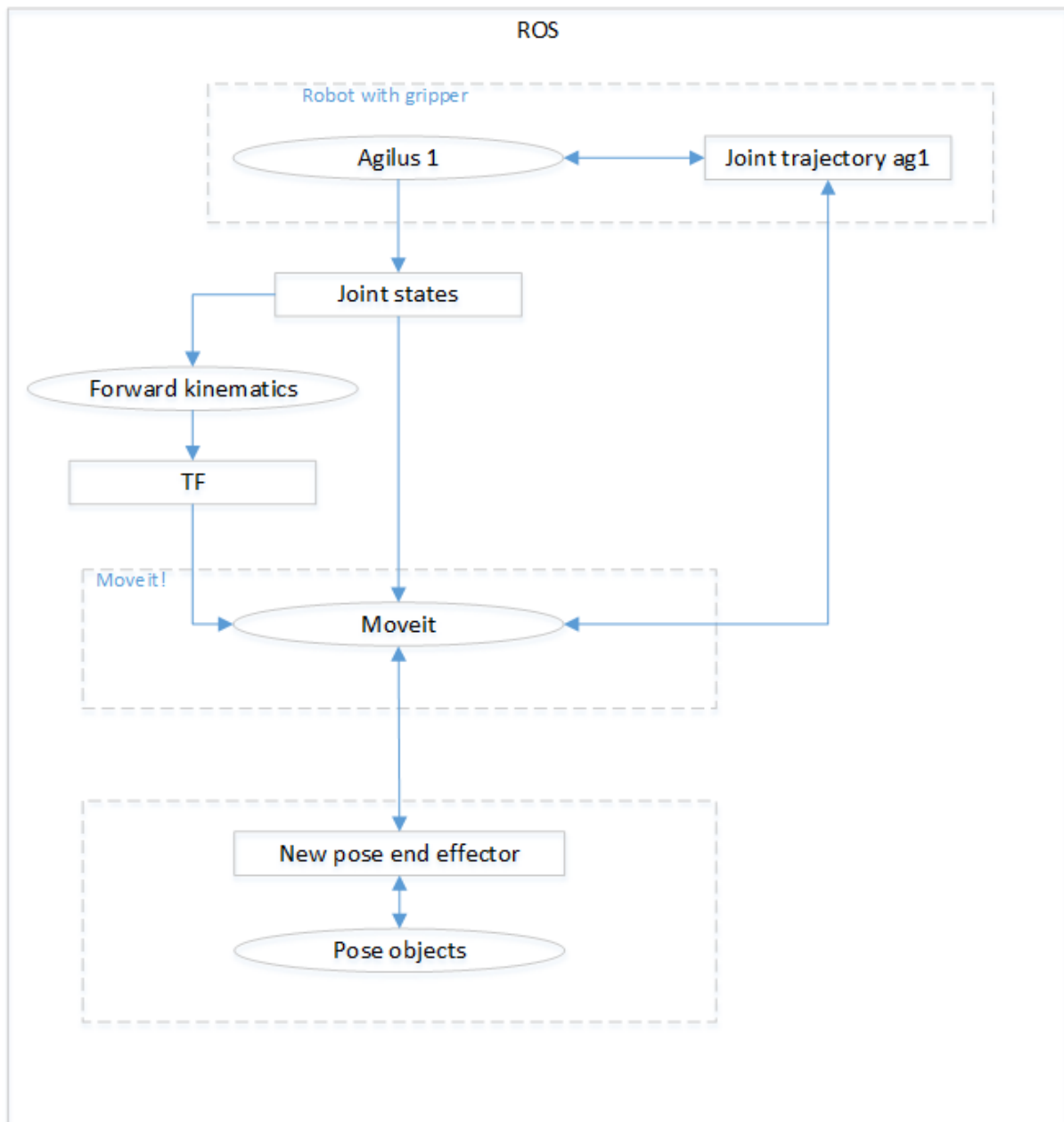


Figure 7.7: Robot with a gripper connected to end-effector

PhD. candidate Adam Leon Kleppe has configured Moveit! and the interfaces for the robots in ROS.

## Chapter 8

# Summary and Recommendations for Further Work

### 8.1 Discussion

Estimating the coordinates of the parts using the RGB-D camera proved to have an accuracy of about 4 mm which was sufficient to perform a simplified assembly task as shown in the video. The program have been further improved since the video was made, introducing a second robot with a 2D camera for estimating the orientation.

Using SIFT and homography on data from the 2D camera to estimate the orientation of the parts proved to work when the objects were placed in a region of stable illumination. The programs developed were quite complex since the geometry of the parts made them difficult to work with. The programs require the 2D camera to be vertically above the part, which can be challenging if the estimated coordinates of the parts are not correct. The maximum possible deviation of the position of the 2D camera was found to be 4.5 mm for the cylinder and 6 mm for the piston. The accuracy of the coordinates of the parts were estimated to an average error of 3.05 mm and 3.64 mm for the piston and the cylinder, respectively. The physical positions were measured using a tape measure with millimeter resolution, which adds some uncertainty. Also, the effect the illumination from the light source in the ceiling had on the objects, changed when the parts were moved around on the table. This created difficulties for the program to estimate the orientation of the parts when they were positioned on certain locations on the table.

A calibrated transformation from the IR camera to the RGB camera could have improved the calibration of the transformation  $T_a^c$  from camera to AR-tags. Still, the transformation from RGB camera to the IR camera was not calibrated due to limited information about how to do this for the ASUS Xtion PRO LIVE. Methods have been developed for calibrating this transformation for the Microsoft Kinect, but they proved not to work for the ASUS Xtion PRO LIVE. Different methods for estimating the transformation from RGB camera to the IR camera were tested without getting better results. We also tried to use different methods for localizing the objects based on the RGB data, but the RGB data for the parts was not perfectly aligned with the depth image from the IR camera so we decided to mainly use the depth data from the IR camera in the experiments. The AR-tags are the only part of the project where the RGB data have been used. The estimation of the coordinates could have been more accurate if the camera had been mounted closer to the objects of interest.

The template alignment method could have been used in combination with a method called ICP (Iterative Closest Point). The ICP algorithm can determine if the aligned template (after template alignment) is just a rigid transformation of the template by minimizing the distances between the points in the template and the corresponding points in the target cloud, and rigidly transforming them. This was not done since the template alignment program had problems to distinguish the parts.

## 8.2 Summary and Conclusions

In this thesis we have presented how two parts from the automotive industry can be assembled using an RGB-D camera, a 2D camera and two KUKA Agilus manipulators with six revolute joints. The RGB-D camera have been presented and calibrated, and AR-tags have been used to efficiently transform the coordinate frame of the RGB-D camera to a table. In relation to this, the use of geometric algebra to make an orthonormal coordinate frame on the table was presented. Several different methods for obtaining the position of the parts, based on data from the RGB-D camera, have been presented and evaluated. This includes a C++ program segmenting the scene based on the orientation of the surface normals in the point cloud, and a program based on known geometry of the parts. The accuracy of the coordinates of the parts were estimated to an average error of 3.05 mm and 3.64 mm for the piston and the cylinder respectively. The results obtained were not adequate for the original assembly task which require sub-millimeter accuracy, but it was possible to perform a simplified assembly task requiring 4 mm accuracy. A method for determining the orientation of the parts, using SIFT and homography, based on data from a 2D camera was presented. Two demonstration videos were made, one determining the orientation, and another one where the parts are assembled using a robot.

### **The final operation runs as follows:**

1. The RGB-D camera is positioned at a random place with the AR-tags in the field of view.
2. An algorithm automatically determines the pose of the RGB-D camera with respect to a known coordinate frame.
3. Data from the RGB-D camera is used to estimate the coordinates of the parts with respect to the known coordinate frame.
4. A robot with a 2D camera connected to the end-effector, moves to a pose where the 2D camera is vertically above the parts, one at a time.
5. Data from the 2D camera is used in an algorithm to estimate the orientation of the parts.
6. A robot with a gripper connected to the end-effector uses the information about the positions and orientations of the parts to assemble them.

## 8.3 Recommendations for Further Work

For future work we would recommend to have one separate computer for the computer vision part and one for robot control. There were problems where the robot would stop in the middle of

a trajectory. The computer did computations for both computer vision and the robots simultaneously, and the computer could not keep up with the updated information from the controllers. This led the program to interrupt the trajectory since it did not get the vital information about trajectory goals from the controllers in time.

We also recommend to develop a method for calibrating the transformation between the IR camera and the RGB camera in the Asus Xtion PRO LIVE. This could improve the estimations of the coordinates of the parts.

Using several RGB-D cameras with different view points and a more comprehensive calibration technique for the RGB-D camera could also improve the result. Using several RGB-D cameras will generate a more dense point cloud and get a point cloud of the entire parts as opposed to one side of the parts, as done in this project.

For the orientation part, we would recommend to store a set of training images of different locations of the parts. Depending on what coordinates the RGB-D camera estimates for the parts, the program can then choose the training images most appropriate for that location. We would also recommend to use the 2D camera to find the final coordinates of the parts. That is, use RGB-D camera to find approximately coordinates, and then run a robot with 2D camera perpendicular to the parts and use the homography matrix to determine more accurate coordinates.

The computational time for the different programs used in this project could most likely be reduced if the program code was optimized.



## Appendix A

### Source Code

The C++ programs explained in the Chapter "ROS" are in the appendix. They are also in the digital appendix. There are 8 programs: three for estimating the coordinates of the parts, two for estimating the orientations and two for the kinematics.

```

1
2 //-----
3 //-----Node run for publishing transformation from camera to table -----
4 //-----
5 //-----
6 //-----Authors: Geir Ole Tysse and Martin Morland -----
7 //-----NINU 2015-----
8 //-----
9
10 #include "ros/ros.h"
11 #include <vector>
12 #include <geometry_msgs/Pose.h>
13 #include <geometry_msgs/Vector3.h>
14 #include <std_msgs/ColorRGBA.h>
15 #include <geometry_msgs/Point.h>
16 #include <std_msgs/ColorRGBA.h>
17 #include "visualization_msgs/Marker.h"
18 #include <iostream>
19 #include <complex>
20 #include "/usr/include/math.h"
21 #include <fstream>
22 #include <sstream>
23 #include "std_msgs/String.h"
24 #include "std_msgs/Float64MultiArray.h"
25 #include <stdio.h>
26 #include <stdlib.h>
27 #include <Eigen/Eigen>
28 #include "std_msgs/MultiArrayLayout.h"
29 #include "std_msgs/MultiArrayDimension.h"
30 #include "std_msgs/Int32MultiArray.h"
31 #include <armadillo>
32
33 using namespace std;
34
35 string argument_old_tags ("table_old_tags");
36 string argument_new_tags ("table_new_tags");
37 int use_old_or_new_tags=0;
38 int ready_for_publish=0;
39 int number_of_extracted_coordinates_from_id0;
40 int number_of_extracted_coordinates_from_id2;
41 int number_of_extracted_coordinates_from_id3;
42 std_msgs::Float64MultiArray Transformation_in_array_list;
43 int size=50;
44 std::vector<float> vec_0;
45 std::vector<float> vec_3;
46 std::vector<float> vec_3_0;
47 std::vector<float> vec_2_0;
48 float id0_x_median;
49 float id0_y_median;
50 float id0_z_median;
51 float id2_x_median;
52 float id2_y_median;
53 float id2_z_median;
54 float id3_x_median;
55 float id3_y_median;
56 float id3_z_median;
57 float id0_x_mode;
58 float id0_y_mode;
59 float id0_z_mode;
60 float id2_x_mode;
61 float id2_y_mode;

```



```

62 float id2_z_mode;
63 float id3_x_mode;
64 float id3_y_mode;
65 float id3_z_mode;
66 float id0_x[50];
67 float id0_y[50];
68 float id0_z[50];
69 float id2_x[50];
70 float id2_y[50];
71 float id2_z[50];
72 float id3_x[50];
73 float id3_y[50];
74 float id3_z[50];
75 int id_nr;
76 geometry_msgs::Pose AR_tags;
77 arma::mat Transformation_camera_AR_tags(4,4);
78 arma::mat Transformation_AR_tags_table(4,4) ;
79 arma::mat Transformation_camera_table(4,4) ;
80 arma::fcolvec translation;
81 arma::fcolvec X_axis_median;
82 arma::fcolvec Y_axis_median;
83 arma::fcolvec Z_axis_median;
84 arma::fcolvec vector_along_x_axis_median;
85 arma::fcolvec vector_along_y_axis_median;
86 arma::fcolvec vector_along_x_axis_mode;
87 arma::fcolvec vector_along_y_axis_mode;
88 arma::fcolvec X_axis_mode;
89 arma::fcolvec Y_axis_mode;
90 arma::fcolvec Z_axis_mode;
91 arma::fcolvec vector_along_x_axis;
92 arma::fcolvec vector_along_y_axis;
93 arma::fcolvec X_axis;
94 arma::fcolvec Y_axis;
95 arma::fcolvec Z_axis;
96
97
98 //— Mode estimation
99 float GetMode(float daArray[], int iSize) {
100     int* ipRepetition = new int[iSize];
101     for (int i = 0; i < iSize; ++i) {
102         ipRepetition[i] = 0;
103         int j = 0;
104         bool bFound = false;
105         while ((j < i) && (daArray[i] != daArray[j])) {
106             if (daArray[i] != daArray[j]) {
107                 ++j;
108             }
109         }
110         ++(ipRepetition[j]);
111     }
112     int iMaxRepeat = 0;
113     for (int i = 1; i < iSize; ++i) {
114         if (ipRepetition[i] > ipRepetition[iMaxRepeat]) {
115             iMaxRepeat = i;
116         }
117     }
118     delete [] ipRepetition;
119     return daArray[iMaxRepeat];
120 }
121
122

```

```

123
124 // — Median estimation
125 float GetMedian(float daArray[], int iSize) {
126     float* dpSorted = new float[iSize];
127     for (int i = 0; i < iSize; ++i) {
128         dpSorted[i] = daArray[i];
129     }
130     for (int i = iSize - 1; i > 0; --i) {
131         for (int j = 0; j < i; ++j) {
132             if (dpSorted[j] > dpSorted[j+1]) {
133                 float dTemp = dpSorted[j];
134                 dpSorted[j] = dpSorted[j+1];
135                 dpSorted[j+1] = dTemp;
136             }
137         }
138     }
139     float dMedian = 0.0;
140     if ((iSize % 2) == 0) {
141         dMedian = (dpSorted[iSize/2] + dpSorted[(iSize/2) - 1])/2.0;
142     } else {
143         dMedian = dpSorted[iSize/2];
144     }
145     delete [] dpSorted;
146     return dMedian;
147 }
148
149
150
151
152 // — The class
153 //-----
154 class SubscribeAndPublish
155 {
156 public:
157     SubscribeAndPublish()
158     {
159
160         //— Subscribe points from the AR-tags and publish transformation from camera to ↔
161         table
162         pub = n_.advertise<std_msgs::Float64MultiArray>("Transformation_from_camera_to_table↔
163             ", 1000);
164         sub = n_.subscribe("visualization_marker", 1, &SubscribeAndPublish::callback, this);
165     }
166     void callback(const visualization_msgs::Marker::ConstPtr& msg)
167     {
168
169         // — Points from the AR-tags
170         AR_tags= msg->pose;
171         id_nr= msg->id;
172
173
174         //— Extract the coordinates of ID0 and save the 50 last coordinates
175         if(id_nr==0){
176             if(!((AR_tags.position.x != AR_tags.position.x) || (AR_tags.position.y != AR_tags.↔
177                 position.y) || (AR_tags.position.z != AR_tags.position.z)))
178             {
179                 number_of_extracted_coordinates_from_id0++;
180                 for(int x = size-1;x>=0;x--){
181                     id0_x[x+1]=id0_x[x];

```

```

181     id0_y[x+1]=id0_y[x];
182     id0_z[x+1]=id0_z[x];
183     if(x==0){
184         id0_x[x]=AR_tags.position.x;
185         id0_y[x]=AR_tags.position.y;
186         id0_z[x]=AR_tags.position.z;
187     }
188 }
189
190 //— Mode and Median of 50 last coordinates
191 if(number_of_extracted_coordinates_from_id0>49)
192 {
193     //— Median of the points
194     id0_x_median=GetMedian(id0_x,50);
195     id0_y_median=GetMedian(id0_y,50);
196     id0_z_median=GetMedian(id0_z,50);
197
198     //— Mode of the points
199     id0_x_mode=GetMode(id0_x,50);
200     id0_y_mode=GetMode(id0_y,50);
201     id0_z_mode=GetMode(id0_z,50);
202 }
203 }
204 }
205
206
207
208 //— Extract the coordinates of ID2 and save the 50 last coordinates
209 if(id_nr==2){
210     if(!((AR_tags.position.x != AR_tags.position.x) || (AR_tags.position.y != AR_tags.↵
                position.y) || (AR_tags.position.z != AR_tags.position.z)))
211     {
212         number_of_extracted_coordinates_from_id2++;
213         for(int x = size-1;x>=0;x--){
214             id2_x[x+1]=id2_x[x];
215             id2_y[x+1]=id2_y[x];
216             id2_z[x+1]=id2_z[x];
217             if(x==0){
218                 id2_x[x]=AR_tags.position.x;
219                 id2_y[x]=AR_tags.position.y;
220                 id2_z[x]=AR_tags.position.z;
221             }
222         }
223
224     //— Mode and Median of 50 last coordinates
225     if(number_of_extracted_coordinates_from_id2>49)
226     {
227         //— Median of the points
228         id2_x_median=GetMedian(id2_x,50);
229         id2_y_median=GetMedian(id2_y,50);
230         id2_z_median=GetMedian(id2_z,50);
231
232         //— Mode of the points
233         id2_x_mode=GetMode(id2_x,50);
234         id2_y_mode=GetMode(id2_y,50);
235         id2_z_mode=GetMode(id2_z,50);
236     }
237 }
238 }
239
240

```

```

241
242 //— Extract the coordinates of ID3 and save the 50 last coordinates
243 if(id_nr==3){
244     if(!((AR_tags.position.x != AR_tags.position.x) || (AR_tags.position.y != AR_tags.↵
           position.y) || (AR_tags.position.z != AR_tags.position.z)))
245     {
246         number_of_extracted_coordinates_from_id3++;
247         for(int x = size-1;x>=0;x--){
248             id3_x[x+1]=id3_x[x];
249             id3_y[x+1]=id3_y[x];
250             id3_z[x+1]=id3_z[x];
251             if(x==0){
252                 id3_x[x]=AR_tags.position.x;
253                 id3_y[x]=AR_tags.position.y;
254                 id3_z[x]=AR_tags.position.z;
255             }
256         }
257
258 //— Mode and Median of 50 last coordinates
259 if(number_of_extracted_coordinates_from_id3>49)
260 {
261     //— Median of the points
262     id3_x_median=GetMedian(id3_x,50);
263     id3_y_median=GetMedian(id3_y,50);
264     id3_z_median=GetMedian(id3_z,50);
265
266     //— Mode of the points
267     id3_x_mode=GetMode(id3_x,50);
268     id3_y_mode=GetMode(id3_y,50);
269     id3_z_mode=GetMode(id3_z,50);
270 }
271 }
272 }
273
274
275
276 if(number_of_extracted_coordinates_from_id3>49 && ↵
       number_of_extracted_coordinates_from_id2>49 && ↵
       number_of_extracted_coordinates_from_id0>49)
277 {
278     //— Translation
279     translation << id3_x_median << id3_y_median <<id3_z_median;
280
281
282     vector_along_y_axis_median << id0_x_median-id3_x_median << id0_y_median-↵
           id3_y_median <<id0_z_median-id3_z_median;
283     vector_along_x_axis_median << id2_x_median-id3_x_median << id2_y_median-↵
           id3_y_median << id2_z_median-id3_z_median;
284     vector_along_y_axis_mode << id0_x_mode-id3_x_mode << id0_y_mode-id3_y_mode <<↵
           id0_z_mode-id3_z_mode;
285     vector_along_x_axis_mode << id2_x_mode-id3_x_mode << id2_y_mode-id3_y_mode << ↵
           id2_z_mode-id3_z_mode;
286     vector_along_y_axis << id0_x[49]-id3_x[49] << id0_y[49]-id3_y[49] <<id0_z[49]-id3_z↵
           [49];
287     vector_along_x_axis<< id2_x[49]-id3_x[49] << id2_y[49]-id3_y[49] << id2_z[49]-id3_z↵
           [49];
288
289
290 //— The axes estimated with median of points
291 Y_axis_median = arma::normalise(vector_along_y_axis_median);
292 X_axis_median = arma::normalise(vector_along_x_axis_median);

```

```

293     Z_axis_median = arma::cross(X_axis_median, Y_axis_median);
294
295     //— The axes estimated with mode of points
296     Y_axis_mode = arma::normalise(vector_along_y_axis_mode);
297     X_axis_mode = arma::normalise(vector_along_x_axis_mode);
298     Z_axis_mode = arma::cross(X_axis_mode, Y_axis_mode);
299
300     //— The axes estimated with live points
301     Y_axis = arma::normalise(vector_along_y_axis);
302     X_axis = arma::normalise(vector_along_x_axis);
303     Z_axis = arma::cross(X_axis, Y_axis);
304
305
306
307     //— Rotation matrix from median of points
308     Eigen::Matrix3f Rotation_matrix_median;
309     Rotation_matrix_median << X_axis_median[0], Y_axis_median[0], Z_axis_median[0],
310         X_axis_median[1], Y_axis_median[1], Z_axis_median[1],
311         X_axis_median[2], Y_axis_median[2], Z_axis_median[2];
312
313     //— Rotation matrix from mode of points
314     Eigen::Matrix3f Rotation_matrix_mode;
315     Rotation_matrix_mode << X_axis_mode[0], Y_axis_mode[0], Z_axis_mode[0],
316         X_axis_mode[1], Y_axis_mode[1], Z_axis_mode[1],
317         X_axis_mode[2], Y_axis_mode[2], Z_axis_mode[2];
318
319     //— Rotation matrix from live points
320     Eigen::Matrix3f Rotation_matrix_live;
321     Rotation_matrix_live << X_axis[0], Y_axis[0], Z_axis[0],
322         X_axis[1], Y_axis[1], Z_axis[1],
323         X_axis[2], Y_axis[2], Z_axis[2];
324
325
326
327
328     //— Determine which of the rotation matrices that are the final rotation matrix
329     if((abs(Rotation_matrix_median.determinant()-1) < 0.0005 || abs(Rotation_matrix_mode.determinant()-1) < 0.0005)&&ready_for_publish==0)
330     {
331         ready_for_publish=1;
332         if(abs(Rotation_matrix_median.determinant()-1)<abs(Rotation_matrix_mode.determinant()-1))
333         {
334             //— Transformation from camera to AR-tags
335             Transformation_camera_AR_tags << X_axis_median[0] << Y_axis_median[0] << Z_axis_median[0] << translation[0] << arma::endr
336                 << X_axis_median[1] << Y_axis_median[1] << Z_axis_median[1] << translation[1] << arma::endr
337                 << X_axis_median[2] << Y_axis_median[2] << Z_axis_median[2] << translation[2] << arma::endr
338             << 0 << 0 << 0 << 1 << arma::endr ;
339         }
340         if (abs(Rotation_matrix_median.determinant()-1)>abs(Rotation_matrix_mode.determinant()-1))
341         {
342             //— Transformation from camera to AR-tags
343             Transformation_camera_AR_tags << X_axis_mode[0] << Y_axis_mode[0] << Z_axis_mode[0] << translation[0] << arma::endr
344                 << X_axis_mode[1] << Y_axis_mode[1] << Z_axis_mode[1] << translation[1] << arma::endr
345                 << X_axis_mode[2] << Y_axis_mode[2] << Z_axis_mode[2] << translation[2] << arma::endr
346             << 0 << 0 << 0 << 1 << arma::endr ;

```

```

347
348 }
349
350
351 //— Transformation from AR-tags to table (old tags)
352 if(use_old_or_new_tags==1)
353 {
354
355 Transformation_AR_tags_table << 1<< 0 << 0 << -0.1905 << arma::endr
356 << 0 << 1 << 0<< -0.104<< arma::endr
357 << 0 << 0 << 1<< 0 << arma::endr
358 << 0 << 0 << 0 << 1 << arma::endr ;
359
360 Transformation_camera_table=Transformation_camera_AR_tags*Transformation_AR_tags_table ;
361
362 Transformation_in_array_list.data.clear() ;
363 for (int i = 0; i < 16; i++)
364 {
365 //assign array a random number between 0 and 255.
366 Transformation_in_array_list.data.push_back(Transformation_camera_table[i]) ;
367 }
368
369 }
370
371 //— Transformation from AR-tags to table (new tags)
372 if(use_old_or_new_tags==2)
373 {
374 Transformation_AR_tags_table << 1<< 0 << 0 << -0.1905 << arma::endr
375 << 0 << 1 << 0<< -0.604<< arma::endr
376 << 0 << 0 << 1<< 0 << arma::endr
377 << 0 << 0 << 0 << 1 << arma::endr ;
378
379 Transformation_camera_table=Transformation_camera_AR_tags*Transformation_AR_tags_table ;
380
381 Transformation_in_array_list.data.clear() ;
382 for (int i = 0; i < 16; i++)
383 {
384 //— Transformation ready for publishing
385 Transformation_in_array_list.data.push_back(Transformation_camera_table[i]) ;
386 }
387 }
388 else{
389 //— Transformation from AR-tags to table (old tags)
390
391 Transformation_in_array_list.data.clear() ;
392 for (int i = 0; i < 16; i++)
393 {
394 //— Transformation ready for publishing
395 Transformation_in_array_list.data.push_back(Transformation_camera_AR_tags[i]) ;
396 }
397 }
398 }
399 }
400
401
402
403 //— Publish transformation from camera to table
404 if(ready_for_publish==1)
405 {
406 pub.publish(Transformation_in_array_list) ;
407 std::cout << "Transformation published!" << endl ;

```

```
408
409 }
410 }
411
412
413
414 private:
415     ros::NodeHandle n_;
416     ros::Publisher pub;
417     ros::Subscriber sub;
418
419 };
420
421 int main(int argc, char **argv)
422 {
423     if(argc !=1)
424     {
425
426         if(argv[1]==argument_old_tags)
427         {
428             use_old_or_new_tags=1;
429             cout << "Align coordinatesystem to the table based on old AR-tags" << endl;
430         }
431
432         if(argv[1]==argument_new_tags)
433         {
434             use_old_or_new_tags=2;
435             cout << "Align coordinatesystem to the table based on new AR-tags" << endl;
436         }
437     }
438
439     //Initiate ROS.
440     ros::init(argc, argv, "Node_Transformation_from_camera_to_table");
441     //Create an object of class SubscribeAndPublish that will take care of everything
442     SubscribeAndPublish SAPObject;
443     ros::spin();
444
445     return 0;
446 }
```

```

1 //-----
2 //-----Node run for Segmentation based on known geometry, one point clouds-----
3 //-----
4 //-----
5 //-----Authors: Geir Ole Tysse and Martin Morland .-----
6 //-----NINU 2015-----
7 //-----
8
9 #include <ros/ros.h>
10 #include <pcl_ros/point_cloud.h>
11 #include <ros/ros.h>
12 #include <iostream>
13 #include <pcl/io/pcd_io.h>
14 #include <pcl/point_types.h>
15 #include <boost/foreach.hpp>
16 #include <sensor_msgs/PointCloud2.h>
17 #include <limits>
18 #include <fstream>
19 #include <vector>
20 #include <Eigen/Core>
21 #include <pcl/point_cloud.h>
22 #include <pcl/kdtree/kdtree_flann.h>
23 #include <pcl/filters/passthrough.h>
24 #include <pcl/filters/voxel_grid.h>
25 #include <pcl/features/normal_3d.h>
26 #include <pcl/features/fpfh.h>
27 #include <pcl/registration/ia_ransac.h>
28 #include <armadillo>
29 #include <sstream>
30 #include "std_msgs/String.h"
31 #include "std_msgs/Float64MultiArray.h"
32 #include <stdio.h>
33 #include <stdlib.h>
34 #include <string>
35 #include "std_msgs/MultiArrayLayout.h"
36 #include "std_msgs/MultiArrayDimension.h"
37 #include "std_msgs/Int32MultiArray.h"
38 #include <armadillo>
39 #include <pcl/filters/filter.h>
40 #include <pcl/filters/statistical_outlier_removal.h>
41
42 using namespace std;
43 using namespace arma;
44
45 float list_with_cylinder_coordinates_y[30];
46 float list_with_cylinder_coordinates_x[30];
47 float list_with_piston_coordinates_y[30];
48 float list_with_piston_coordinates_x[30];
49 int number_of_coordinates_estimated=0;
50 int Transformation_camera_table_ready=0;
51     mat Transformation_table_camera(4,4);
52     mat Transformation_camera_table(4,4);
53     rowvec r;
54     colvec temporary_point_with_respect_to_table;
55     colvec temporary_point;
56     std_msgs::Float64MultiArray publishing_coordinates_cylinder;
57     std_msgs::Float64MultiArray publishing_coordinates_piston;
58
59
60 // --- Get the transformation from camera to table
61     void callbacknh(const std_msgs::Float64MultiArray::ConstPtr& msg)

```



```

62     {
63         Transformation_camera_table << msg->data[0] << msg->data[4] << msg->data[8] << msg->
        ->data[12] << arma::endr
64         << msg->data[1] << msg->data[5] << msg->data[9] << msg->data[13] << arma::endr
65         << msg->data[2] << msg->data[6] << msg->data[10] << msg->data[14] << arma::endr
66         << msg->data[3] << msg->data[7] << msg->data[11] << msg->data[15] << arma::endr;
67         Transformation_camera_table_ready =1;
68
69     }
70
71     //— Remove NAN-points
72     void filterOutNans(const pcl::PointCloud<pcl::PointXYZ>& _inCloud, pcl::PointCloud<pcl::
        ::PointXYZ>& _outCloud) {
73         // Filter out NaNs from data
74         pcl::PassThrough<pcl::PointXYZ> NANRemover;
75         NANRemover.setInputCloud(_inCloud.makeShared());
76         NANRemover.setFilterFieldName("z");
77         NANRemover.setFilterLimits(-0.01, 10.0); /// Get valid range in kinect point cloud ←
        data
78         NANRemover.filter(_outCloud);
79     }
80
81
82
83     //— Estimate the median
84     float GetMedian(float daArray[], int iSize) {
85         double* dpSorted = new double[iSize];
86         for (int i = 0; i < iSize; ++i) {
87             dpSorted[i] = daArray[i];
88         }
89         for (int i = iSize - 1; i > 0; --i) {
90             for (int j = 0; j < i; ++j) {
91                 if (dpSorted[j] > dpSorted[j+1]) {
92                     double dTemp = dpSorted[j];
93                     dpSorted[j] = dpSorted[j+1];
94                     dpSorted[j+1] = dTemp;
95                 }
96             }
97         }
98         double dMedian = 0.0;
99         if ((iSize % 2) == 0) {
100             dMedian = (dpSorted[iSize/2] + dpSorted[(iSize/2) - 1])/2.0;
101         } else {
102             dMedian = dpSorted[iSize/2];
103         }
104         delete [] dpSorted;
105         return dMedian;
106     }
107
108
109     typedef pcl::PointCloud<pcl::PointXYZ> PointCloud;
110     pcl::PointCloud<pcl::PointXYZ> cloud;
111     pcl::PointCloud<pcl::PointXYZ> cloud_table;
112     pcl::PointCloud<pcl::PointXYZ> cloud_cylinder;
113     pcl::PointCloud<pcl::PointXYZ> cloud_piston;
114     pcl::PointCloud<pcl::PointXYZ> cloud_from_camera;
115
116
117     //— The class
118     //—————
119     class SubscribeAndPublish

```

```

120 {
121 public:
122     SubscribeAndPublish()
123     {
124         publisher_cylinder = n_.advertise<std_msgs::Float64MultiArray>("cylinder_coordinates"↵
125         ", 1);
126         publisher_piston = n_.advertise<std_msgs::Float64MultiArray>("piston_coordinates", ↵
127         1);
128         subscriber_point_cloud = n_.subscribe<PointCloud>("/camera/depth_registered/points"↵
129         , 1, &SubscribeAndPublish::callback, this);
130     }
131 void callback(const PointCloud::ConstPtr& msg)
132 {
133     //— Start to run code when transformation from camera to table has been subscribed
134     if(Transformation_camera_table_ready > 0)
135     {
136     //— Point cloud from camera
137     cloud_from_camera =*msg;
138     //— Filters out nan-points
139     filterOutNans(cloud_from_camera, cloud);
140     //— Statistical outliers removal
141     pcl::StatisticalOutlierRemoval<pcl::PointXYZ> statistical_filter;
142     statistical_filter.setInputCloud(boost::make_shared<pcl::PointCloud<pcl::PointXYZ> >(↵
143     cloud));
144     statistical_filter.setMeanK(80);
145     statistical_filter.setStddevMulThresh(2.9);
146     statistical_filter.filter(cloud);
147     //— Transform point cloud to points given with respect to table coordinates
148     temporary_point << 1 << 1 << 1 << 1;
149     Transformation_table_camera=inv(Transformation_camera_table);
150     float cylinder_point_x_coordinate=0;
151     float cylinder_point_y_coordinate=0;
152     int cloud_table_size=0;
153     for (size_t i = 0; i < cloud.points.size (); ++i)
154     {
155     //— Transform every point in point cloud to be given with (X,Y,Z) coordinates with↵
156     //— respect to table
157     temporary_point << cloud.points[i].x << cloud.points[i].y << cloud.points[i].z << 1;
158     temporary_point_with_respect_to_table = Transformation_table_camera* ↵
159     temporary_point;
160     r = temporary_point_with_respect_to_table.t();
161     cloud.points[i].x = r(0);
162     cloud.points[i].y = r(1);
163     cloud.points[i].z = r(2);
164     //— Count number of points on table
165     if((cloud.points[i].z > -0.1)&&(cloud.points[i].x > 0)&&(cloud.points[i].x < 0.7)↵
166     &&(cloud.points[i].y > -0.1)&&(cloud.points[i].y < 0.7))
167     {
168     cloud_table_size++;
169     }
170     }
171 }
172 }
173

```

```

174
175 //— Point cloud on table
176 cloud_table.width = cloud_table_size;
177 cloud_table.height = cloud.height;
178 cloud_table.is_dense = cloud.is_dense;
179 cloud_table.points.resize (cloud_table.width * cloud_table.height);
180 int index_for_points_in_cloud_table=0;
181
182 for (size_t i = 0; i < cloud.points.size (); ++i)
183 {
184     if((cloud.points[i].z > -0.1)&&(cloud.points[i].x > 0)&&(cloud.points[i].x < 0.7)↔
185         &&(cloud.points[i].y > -0.1)&&(cloud.points[i].y < 0.7))
186     {
187         // — A cloud consisting of points on table
188         cloud_table.points[i].x = cloud.points[i].x;
189         cloud_table.points[i].y = cloud.points[i].y;
190         cloud_table.points[i].z = cloud.points[i].z;
191         index_for_points_in_cloud_table++;
192
193         //— Extract a point on the cylinder
194         if((cloud.points[i].z > 0.15)&&(cloud.points[i].z < 0.22))
195         {
196             cylinder_point_x_coordinate= cloud.points[i].x;
197             cylinder_point_y_coordinate = cloud.points[i].y;
198         }
199     }
200
201
202
203     //— Extract a point on the piston
204     float piston_point_x_coordinate=0;
205     float piston_point_y_coordinate=0;
206
207     for (size_t i = 0; i < cloud_table.points.size (); ++i)
208     {
209         if(((abs(cloud_table.points[i].x-cylinder_point_x_coordinate)>0.12) || (abs(↔
210             cloud_table.points[i].y-cylinder_point_y_coordinate)>0.12))&&(cloud_table.↔
211             points[i].z>0.03)&&(cloud_table.points[i].z<0.15))
212         {
213             piston_point_x_coordinate = cloud_table.points[i].x;
214             piston_point_y_coordinate = cloud_table.points[i].y;
215         }
216     }
217
218
219 //— Count number of points on the cylinder and the piston
220 int number_of_points_cylinder=0;
221 int number_of_points_piston=0;
222 for (size_t i = 0; i < cloud_table.points.size (); ++i)
223 {
224     if( (abs(cloud_table.points[i].x-cylinder_point_x_coordinate)<0.07) && (abs(↔
225         cloud_table.points[i].y-cylinder_point_y_coordinate)<0.07)&&(cloud_table.points↔
226         [i].z>0.03)&&(cloud_table.points[i].z<0.14))
227     {
228         number_of_points_cylinder++;
229     }
230
231     if( (abs(cloud_table.points[i].x-piston_point_x_coordinate)<0.06) && (abs(cloud_table↔
232         .points[i].y-piston_point_y_coordinate)<0.06)&&(cloud_table.points[i].z>0.03)&&(↔

```

```

    cloud_table.points[i].z<0.08))
229     {
230         number_of_points_piston++;
231     }
232 }
233
234
235 //— Define a cloud consisting of the cylinder and a cloud consisting of the piston
236     cloud_cylinder.width = number_of_points_cylinder;
237     cloud_cylinder.height = cloud_table.height;
238     cloud_cylinder.is_dense = cloud_table.is_dense;
239     cloud_cylinder.points.resize (cloud_cylinder.width * cloud_cylinder.height);
240
241     cloud_piston.width = number_of_points_piston;
242     cloud_piston.height = cloud_table.height;
243     cloud_piston.is_dense = cloud_table.is_dense;
244     cloud_piston.points.resize (cloud_piston.width * cloud_piston.height);
245
246 int index_for_points_in_cloud_cylinder=0;
247 int index_for_points_in_cloud_piston=0;
248
249 //— A cloud consisting of the cylinder and a cloud consisting of the piston
250     for (size_t i = 0; i < cloud_table.points.size (); ++i)
251     {
252
253         if( (abs(cloud_table.points[i].x-cylinder_point_x_coordinate)<0.07) && (abs(↵
                cloud_table.points[i].y-cylinder_point_y_coordinate)<0.07)&&(cloud_table.points↵
                [i].z>0.03)&&(cloud_table.points[i].z<0.14))
254         {
255             cloud_cylinder.points[index_for_points_in_cloud_cylinder].x = cloud_table.points[i↵
                ].x;
256             cloud_cylinder.points[index_for_points_in_cloud_cylinder].y = cloud_table.points[i↵
                ].y ;
257             cloud_cylinder.points[index_for_points_in_cloud_cylinder].z = cloud_table.points[i↵
                ].z;
258             index_for_points_in_cloud_cylinder++;
259         }
260         else
261         {
262             if( (abs(cloud_table.points[i].x-piston_point_x_coordinate)<0.06) && (abs(↵
                cloud_table.points[i].y-piston_point_y_coordinate)<0.06)&&(cloud_table.points[i↵
                ].z>0.03)&&(cloud_table.points[i].z<0.08))
263             {
264                 cloud_piston.points[index_for_points_in_cloud_piston].x = cloud_table.points[i].x;
265                 cloud_piston.points[index_for_points_in_cloud_piston].y = cloud_table.points[i].y ;
266                 cloud_piston.points[index_for_points_in_cloud_piston].z = cloud_table.points[i].z;
267                 index_for_points_in_cloud_piston++;
268             }
269         }
270     }
271
272
273 //— Save pcd-files of the point clouds
274     pcl::io::savePCDFileASCII ("/home/minions/pcl/build/pcd/cylinder.pcd", cloud_piston)↵
        ;
275     pcl::io::savePCDFileASCII ("/home/minions/pcl/build/pcd/piston.pcd", cloud_cylinder)↵
        ;
276     pcl::io::savePCDFileASCII ("/home/minions/pcl/build/pcd/table.pcd", cloud_table);
277
278
279 //— List the coordinates of the points in point clouds of the piston and the cylinder

```

```

280 float array_cylinder_x_coordinates[index_for_points_in_cloud_cylinder];
281 float array_cylinder_y_coordinates[index_for_points_in_cloud_cylinder];
282
283 for(size_t i =0;i<index_for_points_in_cloud_cylinder;i++)
284 {
285 array_cylinder_x_coordinates[i]= cloud_cylinder.points[i].x ;
286 array_cylinder_y_coordinates[i]= cloud_cylinder.points[i].y ;
287 }
288
289 float array_piston_x_coordinates[index_for_points_in_cloud_piston];
290 float array_piston_y_coordinates[index_for_points_in_cloud_piston];
291
292 for(size_t i =0;i<index_for_points_in_cloud_cylinder;i++)
293 {
294 array_piston_x_coordinates[i]= cloud_piston.points[i].x ;
295 array_piston_y_coordinates[i]= cloud_piston.points[i].y ;
296 }
297
298
299
300
301 //— Coordinates of the piston and the cylinder
302 float piston_coordinate_x = GetMedian(array_piston_x_coordinates ,↔
    index_for_points_in_cloud_piston) -0.011023;
303 float piston_coordinate_y = GetMedian(array_piston_y_coordinates ,↔
    index_for_points_in_cloud_piston) -0.021165;
304 float cylinder_coordinate_x = GetMedian(array_cylinder_x_coordinates ,↔
    index_for_points_in_cloud_cylinder) -0.009983;
305 float cylinder_coordinate_y = GetMedian(array_cylinder_y_coordinates ,↔
    index_for_points_in_cloud_cylinder) -0.026002;
306
307
308 //— Save the last 20 coordinates for both parts
309 for(int x = 20-1;x>=0;x--){
310 list_with_cylinder_coordinates_x[x+1]=list_with_cylinder_coordinates_x[x];
311 list_with_cylinder_coordinates_y[x+1]=list_with_cylinder_coordinates_y[x];
312 list_with_piston_coordinates_x[x+1]=list_with_piston_coordinates_x[x];
313 list_with_piston_coordinates_y[x+1]=list_with_piston_coordinates_y[x];
314     if(x==0){
315 list_with_cylinder_coordinates_x[x]=cylinder_coordinate_x;
316 list_with_cylinder_coordinates_y[x]=cylinder_coordinate_y;
317 list_with_piston_coordinates_x[x]=piston_coordinate_x;
318 list_with_piston_coordinates_y[x]=piston_coordinate_y;
319     }
320 }
321
322 number_of_coordinates_estimated++;
323
324 if(number_of_coordinates_estimated>20)
325 {
326 //— The estimated coordinates for the cylinder and the piston
327 float final_cylinder_coordinate_x=GetMedian(list_with_cylinder_coordinates_x,20);
328 float final_cylinder_coordinate_y=GetMedian(list_with_cylinder_coordinates_y,20);
329 float final_piston_coordinate_x=GetMedian(list_with_piston_coordinates_x,20);
330 float final_piston_coordinate_y=GetMedian(list_with_piston_coordinates_y,20);
331
332 //— Publish cylinder coordinates
333 publishing_coordinates_cylinder.data.clear();
334     for (int i = 0; i < 3; i++)
335 {
336     if(i==0)

```

```

337     {
338     publishing_coordinates_cylinder.data.push_back(final_cylinder_coordinate_x);
339     }
340     if(i==1)
341     {
342         publishing_coordinates_cylinder.data.push_back(final_cylinder_coordinate_y);
343     }
344     if(i==2)
345     {
346         publishing_coordinates_cylinder.data.push_back(0.17);
347     }
348     }
349
350     publisher_cylinder.publish(publishing_coordinates_cylinder);
351
352
353     //— Publish piston coordinates
354     publishing_coordinates_piston.data.clear();
355     for (int i = 0; i < 3; i++)
356     {
357         if(i==0)
358         {
359             publishing_coordinates_piston.data.push_back(final_piston_coordinate_x);
360         }
361         if(i==1)
362         {
363             publishing_coordinates_piston.data.push_back(final_piston_coordinate_y);
364         }
365         if(i==2)
366         {
367             publishing_coordinates_piston.data.push_back(0.10);
368         }
369     }
370     publisher_piston.publish(publishing_coordinates_piston);
371
372     }
373     }
374     }
375
376
377     private:
378     ros::NodeHandle n_;
379     ros::Publisher publisher_cylinder;
380     ros::Publisher publisher_piston;
381     ros::Subscriber subscriber_point_cloud;
382
383
384     };
385
386     int main(int argc, char **argv)
387     {
388
389         //Initiate ROS. The node name is "Pointcloud"
390         ros::init(argc, argv, "Pointcloud");
391         ros::NodeHandle nh;
392
393         //— Subscribe Transformation from camera to table
394         ros::Subscriber subnh = nh.subscribe<std_msgs::Float64MultiArray>("←
           Transformation_from_camera_to_table", 1, callbacknh);
395
396         //Create an object of class SubscribeAndPublish that will take care of everything

```

```
397   SubscribeAndPublish SAPObject;  
398   ros::spin();  
399  
400   return 0;  
401 }
```

```

1 //-----
2 //-----Node run for Segmentation based on known geometry , four point clouds-----
3 //-----
4 //-----
5 //-----Authors: Geir Ole Tysse and Martin Morland .-----
6 //-----NINU 2015-----
7 //-----
8
9 #include <ros/ros.h>
10 #include <pcl_ros/point_cloud.h>
11 #include <ros/ros.h>
12 #include <iostream>
13 #include <pcl/io/pcd_io.h>
14 #include <pcl/point_types.h>
15 #include <boost/foreach.hpp>
16 #include <sensor_msgs/PointCloud2.h>
17 #include <limits>
18 #include <fstream>
19 #include <vector>
20 #include <Eigen/Core>
21 #include <pcl/point_cloud.h>
22 #include <pcl/kdtree/kdtree_flann.h>
23 #include <pcl/filters/passthrough.h>
24 #include <pcl/filters/voxel_grid.h>
25 #include <pcl/features/normal_3d.h>
26 #include <pcl/features/fpfh.h>
27 #include <pcl/registration/ia_ransac.h>
28 #include <armadillo>
29 #include <sstream>
30 #include "std_msgs/String.h"
31 #include "std_msgs/Float64MultiArray.h"
32 #include <stdio.h>
33 #include <stdlib.h>
34 #include <string>
35 #include "std_msgs/MultiArrayLayout.h"
36 #include "std_msgs/MultiArrayDimension.h"
37 #include "std_msgs/Int32MultiArray.h"
38 #include <armadillo>
39 #include <pcl/filters/filter.h>
40 #include <pcl/filters/statistical_outlier_removal.h>
41
42 using namespace std;
43 using namespace arma;
44
45 int index_for_merging_clouds=0;
46 float list_with_cylinder_coordinates_y [30];
47 float list_with_cylinder_coordinates_x [30];
48 float list_with_piston_coordinates_y [30];
49 float list_with_piston_coordinates_x [30];
50 int number_of_coordinates_estimated=0;
51 int Transformation_camera_table_ready=0;
52     mat Transformation_table_camera(4,4);
53     mat Transformation_camera_table(4,4);
54     rowvec r;
55     colvec temporary_point_with_respect_to_table;
56     colvec temporary_point;
57     std_msgs::Float64MultiArray publishing_coordinates_cylinder;
58     std_msgs::Float64MultiArray publishing_coordinates_piston;
59
60
61 // --- Get the transformation from camera to table

```



```

62     void callbacknh(const std_msgs::Float64MultiArray::ConstPtr& msg)
63     {
64         Transformation_camera_table << msg->data[0] << msg->data[4] << msg->data[8] << msg->
        ->data[12] << arma::endr
65         << msg->data[1] << msg->data[5] << msg->data[9] << msg->data[13] << arma::endr
66         << msg->data[2] << msg->data[6] << msg->data[10] << msg->data[14] << arma::endr
67         << msg->data[3] << msg->data[7] << msg->data[11] << msg->data[15] << arma::endr;
68         Transformation_camera_table_ready =1;
69
70     }
71
72     //— Remove NAN-points
73     void filterOutNans(const pcl::PointCloud<pcl::PointXYZ>& _inCloud, pcl::PointCloud<pcl<
        ::PointXYZ>& _outCloud) {
74         pcl::PassThrough<pcl::PointXYZ> NANRemover;
75         NANRemover.setInputCloud(_inCloud.makeShared());
76         NANRemover.setFilterFieldName("z");
77         NANRemover.setFilterLimits(-0.01, 10.0);
78         NANRemover.filter(_outCloud);
79     }
80
81
82
83     //— Estimate the median
84     float GetMedian(float daArray[], int iSize) {
85         double* dpSorted = new double[iSize];
86         for (int i = 0; i < iSize; ++i) {
87             dpSorted[i] = daArray[i];
88         }
89         for (int i = iSize - 1; i > 0; --i) {
90             for (int j = 0; j < i; ++j) {
91                 if (dpSorted[j] > dpSorted[j+1]) {
92                     double dTemp = dpSorted[j];
93                     dpSorted[j] = dpSorted[j+1];
94                     dpSorted[j+1] = dTemp;
95                 }
96             }
97         }
98         double dMedian = 0.0;
99         if ((iSize % 2) == 0) {
100             dMedian = (dpSorted[iSize/2] + dpSorted[(iSize/2) - 1])/2.0;
101         } else {
102             dMedian = dpSorted[iSize/2];
103         }
104         delete [] dpSorted;
105         return dMedian;
106     }
107
108
109     typedef pcl::PointCloud<pcl::PointXYZ> PointCloud;
110     pcl::PointCloud<pcl::PointXYZ> cloud;
111     pcl::PointCloud<pcl::PointXYZ> first_cloud;
112     pcl::PointCloud<pcl::PointXYZ> second_cloud;
113     pcl::PointCloud<pcl::PointXYZ> third_cloud;
114     pcl::PointCloud<pcl::PointXYZ> fourth_cloud;
115     pcl::PointCloud<pcl::PointXYZ> cloud_table;
116     pcl::PointCloud<pcl::PointXYZ> cloud_cylinder;
117     pcl::PointCloud<pcl::PointXYZ> cloud_piston;
118
119
120     //— The class

```

```

121 //-----
122 class SubscribeAndPublish
123 {
124 public:
125     SubscribeAndPublish()
126     {
127         publisher_cylinder = n_.advertise<std_msgs::Float64MultiArray>("cylinder_coordinates"↵
128             ", 1);
129         publisher_piston = n_.advertise<std_msgs::Float64MultiArray>("piston_coordinates", ↵
130             1);
131         subscriber_point_cloud = n_.subscribe<PointCloud>("/camera/depth-registered/points"↵
132             , 1, &SubscribeAndPublish::callback, this);
133     }
134 void callback(const PointCloud::ConstPtr& msg)
135 {
136     //— Start to run code when transformation from camera to table has been subscribed
137     if(Transformation_camera_table_ready > 0)
138     {
139     }
140     unsigned int microseconds=500000;
141     //— Save four point clouds
142     if(index_for_merging_clouds==0)
143     {
144         first_cloud =*msg;
145         usleep(microseconds);
146     }
147     if(index_for_merging_clouds==1)
148     {
149         second_cloud=*msg;
150         usleep(microseconds);
151     }
152     if(index_for_merging_clouds==2)
153     {
154         third_cloud=*msg;
155         usleep(microseconds);
156     }
157     if(index_for_merging_clouds==3)
158     {
159         fourth_cloud=*msg;
160         usleep(microseconds);
161     }
162     index_for_merging_clouds++;
163     if(index_for_merging_clouds>3)
164     {
165         index_for_merging_clouds=0;
166     }
167     //— Four merged point clouds from camera
168     pcl::PointCloud<pcl::PointXYZ> merged_four_clouds = first_cloud;

```

```

179     merged_four_clouds += second_cloud;
180     merged_four_clouds += third_cloud;
181     merged_four_clouds += fourth_cloud;
182
183     //— Filters out nan-points
184     filterOutNans(merged_four_clouds, cloud);
185
186     //— Statistical outliers removal
187     pcl::StatisticalOutlierRemoval<pcl::PointXYZ> statistical_filter;
188     statistical_filter.setInputCloud(boost::make_shared<pcl::PointCloud<pcl::PointXYZ> >(←
        cloud));
189     statistical_filter.setMeanK(80);
190     statistical_filter.setStddevMulThresh(2.9);
191     statistical_filter.filter(cloud);
192
193     //— Transform point cloud to points given with respect to table coordinates
194     temporary_point << 1 << 1 << 1 << 1;
195     Transformation_table_camera=inv(Transformation_camera_table);
196     float cylinder_point_x_coordinate=0;
197     float cylinder_point_y_coordinate=0;
198     int cloud_table_size=0;
199     for (size_t i = 0; i < cloud.points.size (); ++i)
200     {
201         //— Transform every point in point cloud to be given with (X,Y,Z) coordinates with←
            respect to table
202         temporary_point << cloud.points[i].x << cloud.points[i].y << cloud.points[i].z << 1;
203         temporary_point_with_respect_to_table = Transformation_table_camera* ←
            temporary_point;
204         r = temporary_point_with_respect_to_table.t();
205         cloud.points[i].x = r(0);
206         cloud.points[i].y = r(1);
207         cloud.points[i].z = r(2);
208
209         //— Count number of points on table
210         if((cloud.points[i].z > -0.1)&&(cloud.points[i].x > 0)&&(cloud.points[i].x < 0.7)←
            &&(cloud.points[i].y > -0.1)&&(cloud.points[i].y < 0.7))
211         {
212             cloud_table_size++;
213         }
214     }
215
216
217     //— Point cloud on table
218     cloud_table.width = cloud_table_size;
219     cloud_table.height = cloud.height;
220     cloud_table.is_dense = cloud.is_dense;
221     cloud_table.points.resize (cloud_table.width * cloud_table.height);
222     int index_for_points_in_cloud_table=0;
223
224     for (size_t i = 0; i < cloud.points.size (); ++i)
225     {
226         if((cloud.points[i].z > -0.1)&&(cloud.points[i].x > 0)&&(cloud.points[i].x < 0.7)←
            &&(cloud.points[i].y > -0.1)&&(cloud.points[i].y < 0.7))
227         {
228             // — A cloud consisting of points on table
229             cloud_table.points[i].x = cloud.points[i].x;
230             cloud_table.points[i].y = cloud.points[i].y;
231             cloud_table.points[i].z = cloud.points[i].z;
232             index_for_points_in_cloud_table++;
233
234             //— Extract a point on the cylinder

```

```

235     if((cloud.points[i].z > 0.15)&&(cloud.points[i].z < 0.22))
236     {
237         cylinder_point_x_coordinate= cloud.points[i].x;
238         cylinder_point_y_coordinate = cloud.points[i].y;
239     }
240 }
241 }
242
243
244
245     //— Extract a point on the piston
246     float piston_point_x_coordinate=0;
247     float piston_point_y_coordinate=0;
248
249     for (size_t i = 0; i < cloud_table.points.size (); ++i)
250     {
251         if(((abs(cloud_table.points[i].x-cylinder_point_x_coordinate)>0.12) || (abs(↔
                cloud_table.points[i].y-cylinder_point_y_coordinate)>0.12))&&(cloud_table.↔
                points[i].z>0.03)&&(cloud_table.points[i].z<0.15))
252         {
253             piston_point_x_coordinate = cloud_table.points[i].x;
254             piston_point_y_coordinate = cloud_table.points[i].y;
255         }
256     }
257
258
259
260
261     //— Count number of points on the cylinder and the piston
262     int number_of_points_cylinder=0;
263     int number_of_points_piston=0;
264     for (size_t i = 0; i < cloud_table.points.size (); ++i)
265     {
266         if( (abs(cloud_table.points[i].x-cylinder_point_x_coordinate) < 0.07) && (abs(↔
                cloud_table.points[i].y-cylinder_point_y_coordinate) < 0.07)&&(cloud_table.points↔
                [i].z>0.03)&&(cloud_table.points[i].z < 0.14))
267         {
268             number_of_points_cylinder++;
269         }
270         if( (abs(cloud_table.points[i].x-piston_point_x_coordinate) < 0.06) && (abs(cloud_table↔
                .points[i].y-piston_point_y_coordinate) < 0.06)&&(cloud_table.points[i].z > 0.03)&&(↔
                cloud_table.points[i].z < 0.08))
271         {
272             number_of_points_piston++;
273         }
274     }
275
276
277     //— Define a cloud consisting of the cylinder and a cloud consisting of the piston
278     cloud_cylinder.width = number_of_points_cylinder;
279     cloud_cylinder.height = cloud_table.height;
280     cloud_cylinder.is_dense = cloud_table.is_dense;
281     cloud_cylinder.points.resize (cloud_cylinder.width * cloud_cylinder.height);
282
283     cloud_piston.width = number_of_points_piston;
284     cloud_piston.height = cloud_table.height;
285     cloud_piston.is_dense = cloud_table.is_dense;
286     cloud_piston.points.resize (cloud_piston.width * cloud_piston.height);
287
288     int index_for_points_in_cloud_cylinder=0;
289     int index_for_points_in_cloud_piston=0;

```

```

290
291 //— A cloud consisting of the cylinder and a cloud consisting of the piston
292   for (size_t i = 0; i < cloud_table.points.size (); ++i)
293   {
294
295       if( (abs(cloud_table.points[i].x-cylinder_point_x_coordinate)<0.07) && (abs(↔
           cloud_table.points[i].y-cylinder_point_y_coordinate)<0.07)&&(cloud_table.points↔
           [i].z>0.03)&&(cloud_table.points[i].z<0.14))
296       {
297           cloud_cylinder.points[index_for_points_in_cloud_cylinder].x = cloud_table.points[i↔
           ].x;
298           cloud_cylinder.points[index_for_points_in_cloud_cylinder].y = cloud_table.points[i↔
           ].y ;
299           cloud_cylinder.points[index_for_points_in_cloud_cylinder].z = cloud_table.points[i↔
           ].z;
300           index_for_points_in_cloud_cylinder++;
301       }
302       else
303       {
304           if( (abs(cloud_table.points[i].x-piston_point_x_coordinate)<0.06) && (abs(↔
           cloud_table.points[i].y-piston_point_y_coordinate)<0.06)&&(cloud_table.points[i↔
           ].z>0.03)&&(cloud_table.points[i].z<0.08))
305           {
306               cloud_piston.points[index_for_points_in_cloud_piston].x = cloud_table.points[i].x;
307               cloud_piston.points[index_for_points_in_cloud_piston].y = cloud_table.points[i].y ;
308               cloud_piston.points[index_for_points_in_cloud_piston].z = cloud_table.points[i].z;
309               index_for_points_in_cloud_piston++;
310           }
311       }
312   }
313
314
315 //— Save pcd-files of the point clouds
316   pcl::io::savePCDFileASCII ("/home/minions/pcl/build/pcd/cylinder.pcd", cloud_piston)↔
           ;
317   pcl::io::savePCDFileASCII ("/home/minions/pcl/build/pcd/piston.pcd", cloud_cylinder)↔
           ;
318   pcl::io::savePCDFileASCII ("/home/minions/pcl/build/pcd/table.pcd", cloud_table);
319
320
321 //— List the coordinates of the points in point clouds of the piston and the cylinder
322   float array_cylinder_x_coordinates[index_for_points_in_cloud_cylinder];
323   float array_cylinder_y_coordinates[index_for_points_in_cloud_cylinder];
324
325   for(size_t i =0;i<index_for_points_in_cloud_cylinder;i++)
326   {
327       array_cylinder_x_coordinates[i]= cloud_cylinder.points[i].x ;
328       array_cylinder_y_coordinates[i]= cloud_cylinder.points[i].y ;
329   }
330
331   float array_piston_x_coordinates[index_for_points_in_cloud_piston];
332   float array_piston_y_coordinates[index_for_points_in_cloud_piston];
333
334   for(size_t i =0;i<index_for_points_in_cloud_cylinder;i++)
335   {
336       array_piston_x_coordinates[i]= cloud_piston.points[i].x ;
337       array_piston_y_coordinates[i]= cloud_piston.points[i].y ;
338   }
339
340
341

```

```

342
343 //— Coordinates of the piston and the cylinder
344 float piston_coordinate_x = GetMedian(array_piston_x_coordinates, ←
    index_for_points_in_cloud_piston) - 0.011023;
345 float piston_coordinate_y = GetMedian(array_piston_y_coordinates, ←
    index_for_points_in_cloud_piston) - 0.021165;
346 float cylinder_coordinate_x = GetMedian(array_cylinder_x_coordinates, ←
    index_for_points_in_cloud_cylinder) - 0.009983;
347 float cylinder_coordinate_y = GetMedian(array_cylinder_y_coordinates, ←
    index_for_points_in_cloud_cylinder) - 0.026002;
348
349
350 //— Save the last 20 coordinates for both parts
351 for (int x = 20-1; x >= 0; x--){
352 list_with_cylinder_coordinates_x[x+1] = list_with_cylinder_coordinates_x[x];
353 list_with_cylinder_coordinates_y[x+1] = list_with_cylinder_coordinates_y[x];
354 list_with_piston_coordinates_x[x+1] = list_with_piston_coordinates_x[x];
355 list_with_piston_coordinates_y[x+1] = list_with_piston_coordinates_y[x];
356     if (x == 0){
357 list_with_cylinder_coordinates_x[x] = cylinder_coordinate_x;
358 list_with_cylinder_coordinates_y[x] = cylinder_coordinate_y;
359 list_with_piston_coordinates_x[x] = piston_coordinate_x;
360 list_with_piston_coordinates_y[x] = piston_coordinate_y;
361     }
362 }
363
364 number_of_coordinates_estimated++;
365
366 if (number_of_coordinates_estimated > 20)
367 {
368 //— The estimated coordinates for the cylinder and the piston
369 float final_cylinder_coordinate_x = GetMedian(list_with_cylinder_coordinates_x, 20);
370 float final_cylinder_coordinate_y = GetMedian(list_with_cylinder_coordinates_y, 20);
371 float final_piston_coordinate_x = GetMedian(list_with_piston_coordinates_x, 20);
372 float final_piston_coordinate_y = GetMedian(list_with_piston_coordinates_y, 20);
373
374 //— Publish cylinder coordinates
375 publishing_coordinates_cylinder.data.clear();
376     for (int i = 0; i < 3; i++){
377 {
378     if (i == 0)
379     {
380 publishing_coordinates_cylinder.data.push_back(final_cylinder_coordinate_x);
381     }
382     if (i == 1)
383     {
384         publishing_coordinates_cylinder.data.push_back(final_cylinder_coordinate_y);
385     }
386     if (i == 2)
387     {
388         publishing_coordinates_cylinder.data.push_back(0.17);
389     }
390 }
391
392 publisher_cylinder.publish(publishing_coordinates_cylinder);
393
394
395 //— Publish piston coordinates
396 publishing_coordinates_piston.data.clear();
397     for (int i = 0; i < 3; i++){
398 {

```

```
399     if(i==0)
400     {
401     publishing_coordinates_piston.data.push_back(final_piston_coordinate_x);
402     }
403     if(i==1)
404     {
405         publishing_coordinates_piston.data.push_back(final_piston_coordinate_y);
406     }
407     if(i==2)
408     {
409         publishing_coordinates_piston.data.push_back(0.10);
410     }
411 }
412 publisher_piston.publish(publishing_coordinates_piston);
413
414 }
415 }
416 }
417 }
418
419 private:
420     ros::NodeHandle n_;
421     ros::Publisher publisher_cylinder;
422     ros::Publisher publisher_piston;
423     ros::Subscriber subscriber_point_cloud;
424
425
426 };
427
428 int main(int argc, char **argv)
429 {
430
431     //Initiate ROS. The node name is "Pointcloud"
432     ros::init(argc, argv, "Pointcloud");
433     ros::NodeHandle nh;
434
435     //— Subscribe Transformation from camera to table
436     ros::Subscriber subnh = nh.subscribe<std_msgs::Float64MultiArray>("↔
437         Transformation_from_camera_to_table", 1, callbacknh);
438
439     //Create an object of class SubscribeAndPublish that will take care of everything
440     SubscribeAndPublish SAPObject;
441     ros::spin();
442
443     return 0;
444 }
```

```

1  //-----
2  //----- Node run for Region Growing Segmentation -----
3  //-----
4  //-----
5  //----- Authors: Geir Ole Tysse and Martin Morland .-----
6  //----- NINU 2015-----
7  //-----
8
9  #include <ros/ros.h>
10 #include <pcl_ros/point_cloud.h>
11 #include <ros/ros.h>
12 #include <iostream>
13 #include <pcl/io/pcd_io.h>
14 #include <pcl/point_types.h>
15 #include <boost/foreach.hpp>
16 #include <sensor_msgs/PointCloud2.h>
17 #include <limits>
18 #include <fstream>
19 #include <vector>
20 #include <Eigen/Core>
21 #include <pcl/point_cloud.h>
22 #include <pcl/kdtree/kdtree_flann.h>
23 #include <pcl/filters/passthrough.h>
24 #include <pcl/filters/voxel_grid.h>
25 #include <pcl/features/normal_3d.h>
26 #include <pcl/features/fpfh.h>
27 #include <pcl/registration/ia_ransac.h>
28 #include <armadillo>
29 #include <sstream>
30 #include "std_msgs/String.h"
31 #include "std_msgs/Float64MultiArray.h"
32 #include <stdio.h>
33 #include <stdlib.h>
34 #include <string>
35 #include <boost/thread/thread.hpp>
36 #include <pcl/common/common_headers.h>
37 #include <pcl/visualization/pcl_visualizer.h>
38 #include <pcl/console/parse.h>
39 #include "std_msgs/MultiArrayLayout.h"
40 #include "std_msgs/MultiArrayDimension.h"
41 #include "std_msgs/Int32MultiArray.h"
42 #include <armadillo>
43 #include <pcl/filters/filter.h>
44 #include <pcl/filters/statistical_outlier_removal.h>
45 #include <pcl/search/search.h>
46 #include <pcl/search/kdtree.h>
47 #include <pcl/segmentation/region_growing_rgb.h>
48 #include <pcl/visualization/cloud_viewer.h>
49 #include <unistd.h>
50
51
52
53 using namespace std;
54 using namespace arma;
55
56 float piston_x_coordinate_list[20];
57 float piston_y_coordinate_list[20];
58 float cylinder_x_coordinate_list[20];
59 float cylinder_y_coordinate_list[20];
60 int number_of_coordinates_to_save=20;
61 int number_of_saved_coordinates=0;

```



```

62 int subscribed_TF_camera_table=0;
63     mat Transformation_table_camera(4,4);
64     mat Transformation_camera_table(4,4);
65     rowvec r;
66     colvec temporary_point_with_respect_to_table;
67     colvec temporary_point;
68 std_msgs::Float64MultiArray publishing_coordinates_cylinder;
69 std_msgs::Float64MultiArray publishing_coordinates_piston;
70
71
72 //— Visualize effects
73     void
74 printUsage (const char* progName)
75 {
76     std::cout << "\n\nUsage: "<<progName<<" [options]\n\n"
77             << "Options:\n"
78             << "-----\n"
79             << "-h           this help\n"
80             << "-s           Simple visualisation example\n"
81             << "-r           RGB colour visualisation example\n"
82             << "-c           Custom colour visualisation example\n"
83             << "-n           Normals visualisation example\n"
84             << "-a           Shapes visualisation example\n"
85             << "-v           Viewports example\n"
86             << "-i           Interaction Customization example\n"
87             << "\n\n";
88 }
89
90
91 // — Visualize point cloud
92 boost::shared_ptr<pcl::visualization::PCLVisualizer> rgbVis (pcl::PointCloud<pcl::PointXYZRGB>::ConstPtr cloud)
93 {
94     boost::shared_ptr<pcl::visualization::PCLVisualizer> viewer (new pcl::visualization::PCLVisualizer ("3D Viewer"));
95     viewer->setBackgroundColor (0, 0, 0);
96     pcl::visualization::PointCloudColorHandlerRGBField<pcl::PointXYZRGB> rgb(cloud);
97     viewer->addPointCloud<pcl::PointXYZRGB> (cloud, rgb, "sample cloud");
98     viewer->setPointCloudRenderingProperties (pcl::visualization::PCL_VISUALIZER_POINT_SIZE, 3, "sample cloud");
99     viewer->addCoordinateSystem (5.0);
100    viewer->initCameraParameters ();
101    return (viewer);
102 }
103
104
105
106 // — Visualize normals
107 boost::shared_ptr<pcl::visualization::PCLVisualizer> normalsVisRGB (
108     pcl::PointCloud<pcl::PointXYZRGB>::ConstPtr cloud, pcl::PointCloud<pcl::Normal>::ConstPtr normals)
109 {
110     boost::shared_ptr<pcl::visualization::PCLVisualizer> viewer (new pcl::visualization::PCLVisualizer ("3D Viewer"));
111     viewer->setBackgroundColor (0, 0, 0);
112     pcl::visualization::PointCloudColorHandlerCustom<pcl::PointXYZRGB> rgb(cloud, 0, 255, 0);
113     viewer->addPointCloud<pcl::PointXYZRGB> (cloud,rgb, "sample cloud");
114     viewer->setPointCloudRenderingProperties (pcl::visualization::PCL_VISUALIZER_POINT_SIZE, 3, "sample cloud");

```

```

115     viewer->addPointCloudNormals<pcl::PointXYZRGB, pcl::Normal> (cloud, normals, 5, 0.02, ←
        "normals");
116     viewer->initCameraParameters ();
117     return (viewer);
118 }
119
120
121
122 // —Visualize viewport
123 boost::shared_ptr<pcl::visualization::PCLVisualizer> viewportsVis (
124     pcl::PointCloud<pcl::PointXYZRGB >::ConstPtr cloud, pcl::PointCloud<pcl::Normal>::←
        ConstPtr normals1, pcl::PointCloud<pcl::Normal>::ConstPtr normals2)
125 {
126     boost::shared_ptr<pcl::visualization::PCLVisualizer> viewer (new pcl::visualization::←
        PCLVisualizer ("3D Viewer"));
127     viewer->initCameraParameters ();
128     int v1(0);
129     viewer->createViewPort(0.0, 0.0, 0.5, 1.0, v1);
130     viewer->setBackgroundColor (0, 0, 0, v1);
131     viewer->addText("Radius: 0.01", 10, 10, "v1 text", v1);
132     pcl::visualization::PointCloudColorHandlerRGBField<pcl::PointXYZRGB> rgb(cloud);
133     viewer->addPointCloud<pcl::PointXYZRGB> (cloud, rgb, "sample cloud1", v1);
134     int v2(0);
135     viewer->createViewPort(0.5, 0.0, 1.0, 1.0, v2);
136     viewer->setBackgroundColor (0.3, 0.3, 0.3, v2);
137     viewer->addText("Radius: 0.1", 10, 10, "v2 text", v2);
138     pcl::visualization::PointCloudColorHandlerCustom<pcl::PointXYZRGB> single_color(cloud←
        , 0, 255, 0);
139     viewer->addPointCloud<pcl::PointXYZRGB> (cloud, single_color, "sample cloud2", v2);
140     viewer->setPointCloudRenderingProperties (pcl::visualization::←
        PCL_VISUALIZER_POINT_SIZE, 3, "sample cloud1");
141     viewer->setPointCloudRenderingProperties (pcl::visualization::←
        PCL_VISUALIZER_POINT_SIZE, 3, "sample cloud2");
142     viewer->addCoordinateSystem (1.0);
143     viewer->addPointCloudNormals<pcl::PointXYZRGB, pcl::Normal> (cloud, normals1, 10, ←
        0.05, "normals1", v1);
144     viewer->addPointCloudNormals<pcl::PointXYZRGB, pcl::Normal> (cloud, normals2, 10, ←
        0.05, "normals2", v2);
145     return (viewer);
146 }
147
148
149 //— Effects in visualization window
150 unsigned int text_id = 0;
151 void keyboardEventOccurred (const pcl::visualization::KeyboardEvent &event,
152                             void* viewer_void)
153 {
154     boost::shared_ptr<pcl::visualization::PCLVisualizer> viewer = *static_cast<boost::←
        shared_ptr<pcl::visualization::PCLVisualizer> *> (viewer_void);
155     if (event.getKeySym () == "r" && event.keyDown ())
156     {
157         std::cout << "r was pressed => removing all text" << std::endl;
158
159         char str[512];
160         for (unsigned int i = 0; i < text_id; ++i)
161         {
162             sprintf (str, "text#%03d", i);
163             viewer->removeShape (str);
164         }
165         text_id = 0;
166     }

```

```

167 }
168
169 //— Effects in visualization window
170 void mouseEventOccurred (const pcl::visualization::MouseEvent &event,
171                          void* viewer_void)
172 {
173     boost::shared_ptr<pcl::visualization::PCLVisualizer> viewer = *static_cast<boost::↵
        shared_ptr<pcl::visualization::PCLVisualizer> *> (viewer_void);
174     if (event.getButton () == pcl::visualization::MouseEvent::LeftButton &&
175         event.getType () == pcl::visualization::MouseEvent::MouseButtonRelease)
176     {
177         std::cout << "Left mouse button released at position (" << event.getX () << ", " <<↵
            event.getY () << ")" << std::endl;
178
179         char str[512];
180         sprintf (str, "text#%03d", text_id ++);
181         viewer->addText ("clicked here", event.getX (), event.getY (), str);
182     }
183 }
184
185 //— Effects in visualization window
186 boost::shared_ptr<pcl::visualization::PCLVisualizer> interactionCustomizationVis ()
187 {
188     boost::shared_ptr<pcl::visualization::PCLVisualizer> viewer (new pcl::visualization::↵
        PCLVisualizer ("3D Viewer"));
189     viewer->setBackgroundColor (0, 0, 0);
190     viewer->addCoordinateSystem (1.0);
191
192     viewer->registerKeyboardCallback (keyboardEventOccurred, (void*)&viewer);
193     viewer->registerMouseCallback (mouseEventOccurred, (void*)&viewer);
194
195     return (viewer);
196 }
197
198
199 //— Transformation from camera to table
200 void callbacknh_Tf(const std_msgs::Float64MultiArray::ConstPtr& msg)
201 {
202     Transformation_camera_table << msg->data[0] << msg->data[4] << msg->data[8] << msg↵
        ->data[12] << arma::endr
203     << msg->data[1] << msg->data[5] << msg->data[9] << msg->data[13] << arma::endr
204     << msg->data[2] << msg->data[6] << msg->data[10] << msg->data[14] << arma::endr
205     << msg->data[3] << msg->data[7] << msg->data[11] << msg->data[15] << arma::endr;
206     subscribed_TF_camera_table =1;
207
208 }
209
210 // — Filter out NAN points
211 void filterOutNans(const pcl::PointCloud<pcl::PointXYZRGB>& _inCloud, pcl::PointCloud<↵
    pcl::PointXYZRGB>& _outCloud) {
212     // Filter out NaNs from data
213     pcl::PassThrough<pcl::PointXYZRGB> NANRemover;
214     NANRemover.setInputCloud(_inCloud.makeShared());
215     NANRemover.setFilterFieldName("z");
216     NANRemover.setFilterLimits(-10.0, 10.0); /// Get valid range in kinect point cloud ↵
        data
217     NANRemover.filter(_outCloud);
218 }
219
220
221

```

```

222
223 // — Median estimation
224 float GetMedian(float daArray[], int iSize) {
225     // Allocate an array of the same size and sort it.
226     double* dpSorted = new double[iSize];
227     for (int i = 0; i < iSize; ++i) {
228         dpSorted[i] = daArray[i];
229     }
230     for (int i = iSize - 1; i > 0; --i) {
231         for (int j = 0; j < i; ++j) {
232             if (dpSorted[j] > dpSorted[j+1]) {
233                 double dTemp = dpSorted[j];
234                 dpSorted[j] = dpSorted[j+1];
235                 dpSorted[j+1] = dTemp;
236             }
237         }
238     }
239
240     // Middle or average of middle values in the sorted array.
241     double dMedian = 0.0;
242     if ((iSize % 2) == 0) {
243         dMedian = (dpSorted[iSize/2] + dpSorted[(iSize/2) - 1])/2.0;
244     } else {
245         dMedian = dpSorted[iSize/2];
246     }
247     delete [] dpSorted;
248     return dMedian;
249 }
250
251
252 // — The point clouds used
253 pcl::PointCloud<pcl::PointXYZRGB> cloud_from_camera;
254 pcl::PointCloud<pcl::PointXYZRGB> cloud_table_removed_NAN;
255 pcl::PointCloud<pcl::PointXYZRGB> cloud_table;
256 pcl::PointCloud<pcl::PointXYZRGB> cloud_not_on_table;
257 pcl::PointCloud<pcl::PointXYZRGB> first_cloud_from_camera;
258 pcl::PointCloud<pcl::PointXYZRGB> second_cloud_from_camera;
259 pcl::PointCloud<pcl::PointXYZRGB> third_cloud_from_camera;
260 pcl::PointCloud<pcl::PointXYZRGB> fourth_cloud_from_camera;
261 pcl::PointCloud<pcl::PointXYZ> segment_piston;
262 pcl::PointCloud<pcl::PointXYZ> segment_piston_pcd;
263
264 // — The class
265 //—————
266 class SubscribeAndPublish
267 {
268 public:
269     SubscribeAndPublish()
270     {
271         // The different topics beeing published to and subscribed to
272         publisher_cylinder = n_.advertise<std_msgs::Float64MultiArray>("cylinder_coordinates↵
273         ", 1);
274         publisher_piston = n_.advertise<std_msgs::Float64MultiArray>("piston_coordinates", ↵
275         1);
276         subscribe_point_cloud = n_.subscribe<pcl::PointCloud<pcl::PointXYZRGB> >("/camera/↵
277         depth_registered/points", 1, &SubscribeAndPublish::callbackcolor, this);
278
279     }
280
281 // — The main function
282 void callbackcolor(const pcl::PointCloud<pcl::PointXYZRGB>::ConstPtr& msg)

```

```

280 {
281     //— The live point cloud from camera
282     pcl::PointCloud<pcl::PointXYZRGB> cloud_from_camera=*msg;
283
284     // Visualize the live point cloud
285     pcl::visualization::CloudViewer viewer_in_cloud ("Pointcloud from camera");
286     viewer_in_cloud.showCloud(msg);
287     while (!viewer_in_cloud.wasStopped ())
288     {
289     }
290
291 //— The code starts run when the transformation from camera to table is subscribed
292     if(subscribed_TF_camera_table==1)
293     {
294         temporary_point << 1 << 1 << 1 << 1;
295         q_cloud << 1 << 1 << 1 << 1;;
296         Transformation_table_camera=inv(Transformation_camera_table);
297
298 //—Point cloud given with respect to table
299         for (size_t i = 0; i < cloud_from_camera.points.size (); ++i)
300         {
301             //— Transform every point in point cloud to be given with (X,Y,Z) coordinates ←
with respect to table
302             temporary_point << cloud_from_camera.points[i].x << cloud_from_camera.points[i].y <←
<< cloud_from_camera.points[i].z << 1;
303             temporary_point_with_respect_to_table = Transformation_table_camera* temporary_point<←
;
304             r = temporary_point_with_respect_to_table.t();
305
306             cloud_from_camera.points[i].x = r(0);
307             cloud_from_camera.points[i].y = r(1);
308             cloud_from_camera.points[i].z = r(2);
309
310         }
311
312 //— Visualize the point cloud given with respect to table
313         pcl::PointCloud <pcl::PointXYZRGB >::Ptr show_cloud(&cloud_from_camera);
314         pcl::visualization::CloudViewer viewer_out_cloud ("Pointcloud transformed");
315
316         viewer_out_cloud.showCloud(show_cloud);
317         while (!viewer_out_cloud.wasStopped ())
318         {
319         }
320
321
322 //— Number of points in cloud on the table
323         int number_of_points_on_table =0;
324         int number_of_points_not_on_table=0;
325         for (size_t i = 0; i < cloud_from_camera.points.size (); ++i)
326         {
327             if( (cloud_from_camera.points[i].z>0.01)&&(cloud_from_camera.points[i].x>0)&&(←
cloud_from_camera.points[i].x<0.8)&&(cloud_from_camera.points[i].y>0)&&(←
cloud_from_camera.points[i].y<0.8))
328             {
329                 number_of_points_on_table++;
330             }
331             else
332             {
333                 number_of_points_not_on_table++;
334             }
335

```

```

336     }
337
338 //— Save point cloud
339 pcl::io::savePCDFileASCII ("/home/minions/ff/scene.pcd", cloud_from_camera);
340
341
342 // — Segment the part of the point cloud on the table and the part not on the table
343 cloud_table.clear();
344     cloud_table.width = number_of_points_on_table;
345     cloud_table.height = 1;
346     cloud_table.is_dense = cloud_from_camera.is_dense;
347 cloud_table.points.resize (cloud_table.width * cloud_table.height);
348
349 cloud_not_on_table.clear();
350     cloud_not_on_table.width = number_of_points_not_on_table;
351     cloud_not_on_table.height = 1;
352     cloud_not_on_table.is_dense = cloud_from_camera.is_dense;
353 cloud_not_on_table.points.resize (cloud_not_on_table.width * cloud_not_on_table.↵
    height);
354
355 int index_point_on_table=0;
356 int index_point_not_on_table=0;
357 for (size_t i = 0; i < cloud_from_camera.points.size (); ++i)
358 {
359     if( (cloud_from_camera.points[i].z>0.01)&&(cloud_from_camera.points[i].x>0)&&(↵
        cloud_from_camera.points[i].x<0.8)&&(cloud_from_camera.points[i].y>0)&&(↵
        cloud_from_camera.points[i].y<0.8))
360     {
361         cloud_table.points[index_point_on_table].x = cloud_from_camera.points[i].x;
362         cloud_table.points[index_point_on_table].y = cloud_from_camera.points[i].y ;
363         cloud_table.points[index_point_on_table].z = cloud_from_camera.points[i].z;
364
365         cloud_table.points[index_point_on_table].r = cloud_from_camera.points[i].r;
366         cloud_table.points[index_point_on_table].g = cloud_from_camera.points[i].g ;
367         cloud_table.points[index_point_on_table].b = cloud_from_camera.points[i].b;
368         index_point_on_table++;
369     }
370     else
371     {
372         cloud_not_on_table.points[index_point_not_on_table].x = cloud_from_camera.↵
            points[i].x;
373         cloud_not_on_table.points[index_point_not_on_table].y = cloud_from_camera.points[i↵
            ].y ;
374         cloud_not_on_table.points[index_point_not_on_table].z = cloud_from_camera.points[i↵
            ].z;
375         cloud_not_on_table.points[index_point_not_on_table].r = cloud_from_camera.points[i↵
            ].r;
376         cloud_not_on_table.points[index_point_not_on_table].g = cloud_from_camera.points[i↵
            ].g ;
377         cloud_not_on_table.points[index_point_not_on_table].b = cloud_from_camera.points[i↵
            ].b;
378         index_point_not_on_table++;
379     }
380 }
381
382
383
384
385
386 // — Save those two segments

```

```

387   pcl::io::savePCDFileASCII ("/home/minions/pcl/build/pcl/scene_outlier_not_table.pcd", ←
      cloud_not_on_table);
388   pcl::io::savePCDFileASCII ("/home/minions/pcl/build/pcl/scene_inlier_table.pcd", ←
      cloud_table);
389
390
391   //— Remove remaining NAN-points
392   filterOutNans(cloud_table, cloud_table_removed_NAN);
393
394
395   //— Statistical outliers removal
396   pcl::StatisticalOutlierRemoval<pcl::PointXYZRGB> statistical_filter;
397   statistical_filter.setInputCloud(boost::make_shared<pcl::PointCloud<pcl::PointXYZRGB> ←
      >(cloud_table_removed_NAN));
398   statistical_filter.setMeanK(80);
399   statistical_filter.setStddevMulThresh(2.9);
400   statistical_filter.filter(cloud_table_removed_NAN);
401   pcl::PCDWriter writer;
402   writer.write<pcl::PointXYZRGB> ("/home/minions/pcl/build/pcl/scene_inliers.pcd", ←
      cloud_table_removed_NAN, false);
403   statistical_filter.setNegative (true);
404   statistical_filter.filter (cloud_table_removed_NAN);
405   writer.write<pcl::PointXYZRGB> ("/home/minions/pcl/build/pcl/scene_outliers.pcd", ←
      cloud_table_removed_NAN, false);
406   statistical_filter.setNegative (false);
407   statistical_filter.filter (cloud_table_removed_NAN);
408   pcl::PointCloud<pcl::PointXYZRGB>::Ptr cloud_ptr;
409   cloud_ptr.reset (new pcl::PointCloud<pcl::PointXYZRGB> (cloud_table_removed_NAN));
410
411
412   //— Normal estimation of the cloud on the table
413   pcl::NormalEstimation<pcl::PointXYZRGB, pcl::Normal> ne;
414   ne.setInputCloud (cloud_ptr);
415   pcl::search::KdTree<pcl::PointXYZRGB>::Ptr tree (new pcl::search::KdTree<pcl::←
      PointXYZRGB> ());
416   ne.setSearchMethod (tree);
417   ne.setViewPoint (0.4, 1.1, 0.3);
418   pcl::PointCloud<pcl::Normal>::Ptr cloud_normals (new pcl::PointCloud<pcl::Normal>);
419   ne.setRadiusSearch (0.04);
420   ne.compute (*cloud_normals);
421
422
423   //— Visualize the normals
424   boost::shared_ptr<pcl::visualization::PCLVisualizer> viewer;
425   viewer = normalsVisRGB(cloud_ptr, cloud_normals);
426   while (!viewer->wasStopped ())
427   {
428     viewer->spinOnce (100);
429     boost::this_thread::sleep (boost::posix_time::microseconds (100000));
430   }
431
432
433   //— Segment only those points that are listed in the indices (used for later)
434   pcl::IndicesPtr indices (new std::vector<int>);
435   pcl::PassThrough<pcl::PointXYZRGB> pass;
436   pass.setInputCloud (cloud_ptr);
437   pass.filter (*indices);
438
439
440   //— Region growing segmentations
441   pcl::RegionGrowing<pcl::PointXYZRGB, pcl::Normal> reg;

```

```

442     reg.setResidualThreshold(150);
443     reg.setMinClusterSize (70);
444     reg.setMaxClusterSize (100000);
445     reg.setResidualTestFlag(true);
446     reg.setSearchMethod (tree);
447     reg.setNumberOfNeighbours (20);
448     reg.setInputCloud (cloud_ptr);
449     reg.setIndices (indices);
450     reg.setInputNormals (cloud_normals);
451     reg.setSmoothnessThreshold (70.0 / 180.0 * M_PI);
452     std::vector <pcl::PointIndices> clusters;
453     reg.extract (clusters);
454     pcl::PointCloud <pcl::PointXYZRGB >::Ptr colored_cloud = reg.getColoredCloud ();
455
456
457     //— Visualize the segments from region growing segmentations
458     pcl::visualization::CloudViewer viewer_cloud ("Cluster viewer");
459     viewer_cloud.showCloud(colored_cloud);
460     while (!viewer_cloud.wasStopped ())
461     {
462     }
463
464
465     //— Segment cylinder and piston
466     pcl::PointCloud <pcl::PointXYZRGB> segment_cylinder;
467     pcl::PointCloud <pcl::PointXYZRGB> segment_piston;
468     int j = 0;
469     int size_piston_array=1;
470     int size_cylinder_array=1;
471
472
473     //— loops through the segments from region growing
474     for (std::vector<pcl::PointIndices >::const_iterator it = clusters.begin (); it != ←
         clusters.end (); ++it)
475     {
476         float distance_from_table=0;
477
478         pcl::PointCloud<pcl::PointXYZRGB >::Ptr cloud_cluster (new pcl::PointCloud<pcl::←
             PointXYZRGB>);
479         for (std::vector<int >::const_iterator pit = it->indices.begin (); pit != it->←
             indices.end (); ++pit)
480             cloud_cluster->points.push_back (cloud_ptr->points[*pit]);
481         cloud_cluster->width = cloud_cluster->points.size ();
482         cloud_cluster->height = 1;
483         cloud_cluster->is_dense = true;
484
485         int piston_or_cylinder =0;
486
487         //— Checks the different segments for a match for either beeing the piston or ←
             cylinder
488         for(size_t i = 0; i < cloud_cluster->points.size (); ++i)
489         {
490             if(cloud_cluster->points[i].z >0.05)
491             {
492                 piston_or_cylinder=1;
493             }
494         }
495         if(piston_or_cylinder==1 && cloud_cluster->points.size () >50)
496         {
497             for (size_t i = 0; i < cloud_cluster->points.size (); ++i)
498             {

```



```

499     if (cloud_cluster->points[i].z > distance_from_table)
500     {
501         distance_from_table = cloud_cluster->points[i].z;
502     }
503     }
504     if (distance_from_table > 0.135)
505     {
506         //— Segment cylinder
507         segment_cylinder = *cloud_cluster;
508         size_cylinder_array = cloud_cluster->points.size ();
509     }
510     }
511     else
512     {
513         //— Segment piston
514         segment_piston = *cloud_cluster;
515         size_piston_array = cloud_cluster->points.size ();
516     }
517     j++;
518 }
519 }
520
521
522 float array_cylinder_y_coordinates_in_segment [size_cylinder_array];
523 float array_cylinder_x_coordinates_in_segment [size_cylinder_array];
524 float array_piston_y_coordinates_in_segment [size_piston_array];
525 float array_piston_x_coordinates_in_segment [size_piston_array];
526
527
528 //— Extract the points from the segments
529     for (size_t i = 0; i < segment_piston.points.size () ; ++i)
530     {
531         array_piston_x_coordinates_in_segment [i] = segment_piston.points [i].x;
532         array_piston_y_coordinates_in_segment [i] = segment_piston.points [i].y;
533     }
534
535     for (size_t i = 0; i < segment_cylinder.points.size () ; ++i)
536     {
537         array_cylinder_x_coordinates_in_segment [i] = segment_cylinder.points [i].x;
538         array_cylinder_y_coordinates_in_segment [i] = segment_cylinder.points [i].y;
539     }
540
541
542
543 //— Save the segments of the piston and the cylinder in pcd-files
544 pcl::io::savePCDFileASCII ("/home/minions/pcl/build/pcd/cylinder.pcd", segment_cylinder←
545 );
546 pcl::io::savePCDFileASCII ("/home/minions/pcl/build/pcd/piston.pcd", segment_piston);
547
548
549
550 //— Coordinates are extracted from the segment. That is, the median of the ←
551     coordinates in the segments
552 float piston_x_coordinate = GetMedian (array_piston_x_coordinates_in_segment, ←
553     size_piston_array);
554 float piston_y_coordinate = GetMedian (array_piston_y_coordinates_in_segment, ←
555     size_piston_array);
556 float cylinder_x_coordinate = GetMedian (array_cylinder_x_coordinates_in_segment, ←
557     size_cylinder_array);

```

```

554 float cylinder_y_coordinate = GetMedian(array_cylinder_y_coordinates_in_segment, ←
      size_cylinder_array);
555
556
557
558 //— Write coordinates to txt-files
559     ofstream cylinder_file;
560     cylinder_file.open ("cylinder_coordinates.txt", std::ios_base::app);
561     cylinder_file << cylinder_x_coordinate;
562     cylinder_file << " , ";
563     cylinder_file << cylinder_y_coordinate;
564     cylinder_file << endl;
565     cylinder_file.close();
566
567     ofstream piston_file;
568     piston_file.open ("Piston_coordinates.txt", std::ios_base::app);
569     piston_file << piston_x_coordinate;
570     piston_file << " , ";
571     piston_file << piston_y_coordinate;
572     piston_file << endl;
573     piston_file.close();
574
575
576
577
578 //— Save the last 20 coordinates
579     for(int x = number_of_coordinates_to_save - 1; x >= 0; x--){
580         piston_x_coordinate_list[x+1] = piston_x_coordinate_list[x];
581         piston_y_coordinate_list[x+1] = piston_y_coordinate_list[x];
582         cylinder_x_coordinate_list[x+1] = cylinder_x_coordinate_list[x];
583         cylinder_y_coordinate_list[x+1] = cylinder_y_coordinate_list[x];
584         if(x == 0){
585             piston_x_coordinate_list[x] = piston_x_coordinate;
586             piston_y_coordinate_list[x] = piston_y_coordinate;
587             cylinder_x_coordinate_list[x] = cylinder_x_coordinate;
588             cylinder_y_coordinate_list[x] = cylinder_y_coordinate;
589             number_of_saved_coordinates++;
590         }
591     }
592
593
594     //— Median of the 20 last saved coordinates. These are the accepted coordinates
595     if(number_of_saved_coordinates >= number_of_coordinates_to_save)
596     {
597     float final_piston_x_coordinate = GetMedian(piston_x_coordinate_list, ←
      number_of_coordinates_to_save);
598     float final_piston_y_coordinate = GetMedian(piston_y_coordinate_list, ←
      number_of_coordinates_to_save);
599     float final_cylinder_x_coordinate = GetMedian(cylinder_x_coordinate_list, ←
      number_of_coordinates_to_save);
600     float final_cylinder_y_coordinate = GetMedian(cylinder_y_coordinate_list, ←
      number_of_coordinates_to_save);
601
602
603     //— Print out the coordinates
604     std::cout << "cylinder coordinates: " << final_cylinder_x_coordinate << " , " << ←
      final_cylinder_y_coordinate << endl;
605     std::cout << "piston coordinates: " << final_piston_x_coordinate << " , " << ←
      final_piston_y_coordinate << endl;
606
607

```

```
608 //— Publish cylinder coordinates
609 publishing_coordinates_cylinder.data.clear();
610     for (int i = 0; i < 3; i++)
611     {
612         if(i==0)
613         {
614             publishing_coordinates_cylinder.data.push_back(final_cylinder_x_coordinate);
615         }
616         if(i==1)
617         {
618             publishing_coordinates_cylinder.data.push_back(final_cylinder_y_coordinate);
619         }
620         if(i==2)
621         {
622             publishing_coordinates_cylinder.data.push_back(0.17);
623         }
624     }
625     publisher_cylinder.publish(publishing_coordinates_cylinder);
626
627
628 //— Publish piston coordinates
629 publishing_coordinates_piston.data.clear();
630     for (int i = 0; i < 3; i++)
631     {
632         if(i==0)
633         {
634             publishing_coordinates_piston.data.push_back(final_piston_x_coordinate);
635         }
636         if(i==1)
637         {
638             publishing_coordinates_piston.data.push_back(final_piston_y_coordinate);
639         }
640         if(i==2)
641         {
642             publishing_coordinates_piston.data.push_back(0.10);
643         }
644     }
645     publisher_piston.publish(publishing_coordinates_piston);
646     }
647 }
648 }
649
650
651
652 private:
653     ros::NodeHandle n_;
654     ros::Publisher publisher_cylinder;
655     ros::Publisher publisher_piston;
656     ros::Subscriber subscribe_point_cloud;
657
658 };
659
660 int main(int argc, char **argv)
661 {
662
663     //Initiate ROS. The node name is "Pointcloud"
664     ros::init(argc, argv, "Pointcloud");
665     ros::NodeHandle nh;
666
667     //— Subscribe Transformation from camera to table
```

```
668  ros::Subscriber subnh = nh.subscribe<std_msgs::Float64MultiArray>("↔
    Transformation_from_camera_to_table", 1, callbacknh_Tf);
669
670  //— Create an object of class SubscribeAndPublish that will take care of everything
671  SubscribeAndPublish SAPObject;
672  ros::spin();
673
674  return 0;
675 }
```

```

1  //-----
2  //----- Node run for estimating orientation of cylinder -----
3  //-----
4  //-----
5  //----- Authors: Geir Ole Tysse and Martin Morland .-----
6  //----- NINU 2015-----
7  //-----
8
9  #include <ros/ros.h>
10 #include <image_transport/image_transport.h>
11 #include <cv_bridge/cv_bridge.h>
12 #include <sensor_msgs/image_encodings.h>
13 #include <opencv2/opencv.hpp>
14 #include <opencv2/imgproc/imgproc.hpp>
15 #include <opencv2/highgui/highgui.hpp>
16 #include <opencv2/nonfree/features2d.hpp>
17 #include <opencv2/features2d/features2d.hpp>
18 #include <opencv2/core/core.hpp>
19 #include "opencv2/calib3d/calib3d.hpp"
20 #include <stdio.h>
21 #include <iostream>
22 #include <armadillo>
23 #include <cmath>
24 #include "std_msgs/Float64MultiArray.h"
25 using namespace cv;
26 using namespace std;
27 static const std::string OPENCV_WINDOW = "Image window";
28
29
30 float degree_estimated_for_0;
31 float degree_estimated_for_90;
32 float degree_estimated_for_180;
33 float degree_estimated_for_270;
34 arma::mat camera_matrix(3,3);
35 float true_orientation;
36 int number_of_times_approved_H_0=0;
37 int number_of_times_approved_H_90=0;
38 int number_of_times_approved_H_180=0;
39 int number_of_times_approved_H_270=0;
40 float estimated_orientation;
41 float list_with_last_degrees [7];
42 std_msgs::Float64MultiArray array_orientation_cylinder;
43
44 //--- Estimate the median
45 float GetMedian(float daArray[], int iSize) {
46     double* dpSorted = new double[iSize];
47     for (int i = 0; i < iSize; ++i) {
48         dpSorted[i] = daArray[i];
49     }
50     for (int i = iSize - 1; i > 0; --i) {
51         for (int j = 0; j < i; ++j) {
52             if (dpSorted[j] > dpSorted[j+1]) {
53                 double dTemp = dpSorted[j];
54                 dpSorted[j] = dpSorted[j+1];
55                 dpSorted[j+1] = dTemp;
56             }
57         }
58     }
59     double dMedian = 0.0;
60     if ((iSize % 2) == 0) {
61         dMedian = (dpSorted[iSize/2] + dpSorted[(iSize/2) - 1])/2.0;

```

```

62     } else {
63         dMedian = dpSorted[iSize/2];
64     }
65     delete [] dpSorted;
66     return dMedian;
67 }
68
69
70 class ImageConverter
71 {
72     ros::NodeHandle nh_;
73     image_transport::ImageTransport it_;
74     image_transport::Subscriber image_sub_;
75     image_transport::Publisher image_pub_;
76     ros::Publisher publish_orientation_cylinder;
77 private:
78
79
80
81 public:
82
83
84     ImageConverter()
85         : it_(nh_)
86     {
87         //— Subscribe to input video feed
88         image_sub_ = it_.subscribe("/usb_cam/image-raw", 1,
89             &ImageConverter::imageCb, this);
90         cv::namedWindow(OPENCV_WINDOW, WINDOW_NORMAL);
91
92         //— Publish orientation of the cylinder
93         publish_orientation_cylinder = nh_.advertise<std_msgs::Float64MultiArray>("↔
94             cylinder.orientation", 1);
95
96     }
97
98     ~ImageConverter()
99     {
100         cv::destroyWindow(OPENCV_WINDOW);
101
102     }
103
104     void imageCb(const sensor_msgs::ImageConstPtr& msg)
105     {
106
107         cv_bridge::CvImagePtr cv_ptr;
108         try
109         {
110             cv_ptr = cv_bridge::toCvCopy(msg, sensor_msgs::image_encodings::BGR8);
111         }
112         catch (cv_bridge::Exception& e)
113         {
114             ROS_ERROR("cv-bridge exception: %s", e.what());
115             return;
116         }
117
118         //— Get the live image stream and the training images
119         Mat img_show;
120         Mat img_object = imread("/home/jorge/catkin_ws/syl_0.jpg");
121         Mat img_object_90 = imread("/home/jorge/catkin_ws/syl_90.jpg");

```

```

122 Mat img_object_180 = imread("/home/jorge/catkin_ws/syl_180.jpg");
123 Mat img_object_270 = imread("/home/jorge/catkin_ws/syl_270.jpg");
124 Mat img_scene = cv_ptr->image;
125
126 //— Get gray image from the image stream also, used for reading greyscale values
127 Mat gray_image;
128 cvtColor( img_scene, gray_image, CV_BGR2GRAY );
129
130
131 if( !img_object.data || !img_scene.data )
132 { std::cout<< " --(!) Error reading images " << std::endl; }
133
134 //— Step 1: Detect the keypoints using Sift Detector
135 int minHessian = 200;
136 SiftFeatureDetector detector( minHessian );
137 std::vector<KeyPoint> keypoints_object, keypoints_scene, keypoints_object_90, ←
    keypoints_object_180, keypoints_object_270;
138
139 //— Detection of feature in image stream. Searches within a defined mask
140 Mat mask = Mat::zeros(img_scene.size(), CV_8U);
141 Mat roi(mask, cv::Rect(200,50,220,280));
142 roi = Scalar(255, 255, 255);
143 detector.detect(img_scene, keypoints_scene, mask);
144
145
146 //— Detection of feature in training images
147 detector.detect( img_object, keypoints_object );
148 detector.detect( img_object_90, keypoints_object_90);
149 detector.detect( img_object_180, keypoints_object_180 );
150 detector.detect( img_object_270, keypoints_object_270 );
151
152
153
154
155 //— Step 2: Calculate descriptors
156 SiftDescriptorExtractor extractor;
157
158 Mat descriptors_object, descriptors_scene, descriptors_object_90, ←
    descriptors_object_180, descriptors_object_270;
159
160 extractor.compute( img_object, keypoints_object, descriptors_object );
161 extractor.compute( img_object_90, keypoints_object_90, descriptors_object_90);
162 extractor.compute( img_object_180, keypoints_object_180, descriptors_object_180 );
163 extractor.compute( img_object_270, keypoints_object_270, descriptors_object_270 );
164 extractor.compute( img_scene, keypoints_scene, descriptors_scene );
165
166 //— Step 3: Matching descriptor vectors using FLANN matcher
167 FlannBasedMatcher matcher;
168
169 std::vector< DMatch > matches, matches_90, matches_180, matches_270;
170 matcher.match( descriptors_object, descriptors_scene, matches );
171 matcher.match( descriptors_object_90, descriptors_scene, matches_90 );
172 matcher.match( descriptors_object_180, descriptors_scene, matches_180 );
173 matcher.match( descriptors_object_270, descriptors_scene, matches_270 );
174
175
176 std::vector< DMatch > good_matches, good_matches_90, good_matches_180, good_matches_270←
    ;
177
178 //— Matching descriptor vectors in image stream and training image 0 degree
179 Mat img_matches_0;

```

```

180   drawMatches( img_object, keypoints_object, img_scene, keypoints_scene,
181               good_matches, img_matches_0, Scalar::all(-1), Scalar::all(-1),
182               vector<char>(), DrawMatchesFlags::NOT_DRAW_SINGLE_POINTS );
183
184   //— Matching descriptor vectors in image stream and training image 90 degree
185   Mat img_matches_90;
186   drawMatches( img_object_90, keypoints_object_90, img_scene, keypoints_scene,
187               good_matches_90, img_matches_90, Scalar::all(-1), Scalar::all(-1),
188               vector<char>(), DrawMatchesFlags::NOT_DRAW_SINGLE_POINTS );
189
190   //— Matching descriptor vectors in image stream and training image 180 degree
191   Mat img_matches_180;
192   drawMatches( img_object_180, keypoints_object_180, img_scene, keypoints_scene,
193               good_matches_180, img_matches_180, Scalar::all(-1), Scalar::all(-1),
194               vector<char>(), DrawMatchesFlags::NOT_DRAW_SINGLE_POINTS );
195
196   //— Matching descriptor vectors in image stream and training image 270 degree
197   Mat img_matches_270;
198   drawMatches( img_object_270, keypoints_object_270, img_scene, keypoints_scene,
199               good_matches_270, img_matches_270, Scalar::all(-1), Scalar::all(-1),
200               vector<char>(), DrawMatchesFlags::NOT_DRAW_SINGLE_POINTS );
201
202
203
204   //— Quick calculation of max and min distances between keypoints in 0 degrees ←
training image and image stream
205   double max_dist = 0; double min_dist = 70;
206
207   for( int i = 0; i < descriptors_object.rows; i++ )
208   { double dist = matches[i].distance;
209     if( dist < min_dist ) min_dist = dist;
210     if( dist > max_dist ) max_dist = dist;
211   }
212
213
214
215   for( int i = 0; i < descriptors_object.rows; i++ )
216   { if( matches[i].distance < 3*min_dist )
217     { good_matches.push_back( matches[i]); }
218   }
219
220
221   //— Quick calculation of max and min distances between keypoints in 90 degrees ←
training image and image stream
222   max_dist = 0;
223   min_dist = 70;
224
225   for( int i = 0; i < descriptors_object_90.rows; i++ )
226   { double dist = matches_90[i].distance;
227     if( dist < min_dist ) min_dist = dist;
228     if( dist > max_dist ) max_dist = dist;
229   }
230   for( int i = 0; i < descriptors_object_90.rows; i++ )
231   { if( matches_90[i].distance < 3*min_dist )
232     { good_matches_90.push_back( matches_90[i]); }
233   }
234
235   //— Quick calculation of max and min distances between keypoints in 180 degrees ←
training image and image stream
236   max_dist = 0;
237   min_dist = 70;

```



```

238
239   for( int i = 0; i < descriptors_object_180.rows; i++ )
240   { double dist = matches_180[i].distance;
241     if( dist < min_dist ) min_dist = dist;
242     if( dist > max_dist ) max_dist = dist;
243   }
244   for( int i = 0; i < descriptors_object_180.rows; i++ )
245   { if( matches_180[i].distance < 3*min_dist )
246     { good_matches_180.push_back( matches_180[i] ); }
247   }
248
249   //— Quick calculation of max and min distances between keypoints in 270 degrees ←
      training image and image stream
250   max_dist = 0;
251   min_dist = 70;
252
253   for( int i = 0; i < descriptors_object_270.rows; i++ )
254   { double dist = matches_270[i].distance;
255     if( dist < min_dist ) min_dist = dist;
256     if( dist > max_dist ) max_dist = dist;
257   }
258   for( int i = 0; i < descriptors_object_270.rows; i++ )
259   { if( matches_270[i].distance < 3*min_dist )
260     { good_matches_270.push_back( matches_270[i] ); }
261   }
262
263
264
265
266   //— Localize the object
267   std::vector<Point2f> obj , obj_90 , obj_180 ,obj_270;
268   std::vector<Point2f> scene , scene_90 , scene_180 ,scene_270;
269
270
271   //TRAINING IMAGE 0 DEGREES
272   //—————
273   //—————
274
275
276   //— Get the keypoints from the good matches 0 degree
277   for( int i = 0; i < good_matches.size(); i++ )
278   {
279
280     obj.push_back( keypoints_object[ good_matches[i].queryIdx ].pt );
281     scene.push_back( keypoints_scene[ good_matches[i].trainIdx ].pt );
282   }
283
284   std::vector<Point2f> obj_corners(4);
285   if (good_matches.size() > 3)
286   {
287     // — Estimate the homography between training image 0 degrees and image stream
288     cv::Mat H_0 = findHomography( obj , scene , CV_RANSAC );
289
290     //— Get the corners from the training image 0 degrees ( the object to be "detected" ←
      )
291     obj_corners[0] = cvPoint(0,0); obj_corners[1] = cvPoint( img_object.cols , 0 );
292     obj_corners[2] = cvPoint( img_object.cols , img_object.rows ); obj_corners[3] = ←
      cvPoint( 0 , img_object.rows );
293     std::vector<Point2f> scene_corners(4);
294
295     perspectiveTransform( obj_corners , scene_corners , H_0);

```

```

296
297 //— Draw lines between the corners (the mapped object in the scene – training image ←
    0 degrees)
298 line( img_matches_0, scene_corners[0] + Point2f( img_object.cols, 0), scene_corners←
    [1] + Point2f( img_object.cols, 0), Scalar(0, 255, 0), 4 );
299 line( img_matches_0, scene_corners[1] + Point2f( img_object.cols, 0), scene_corners←
    [2] + Point2f( img_object.cols, 0), Scalar( 0, 255, 0), 4 );
300 line( img_matches_0, scene_corners[2] + Point2f( img_object.cols, 0), scene_corners←
    [3] + Point2f( img_object.cols, 0), Scalar( 0, 255, 0), 4 );
301 line( img_matches_0, scene_corners[3] + Point2f( img_object.cols, 0), scene_corners←
    [0] + Point2f( img_object.cols, 0), Scalar( 0, 255, 0), 4 );
302
303
304
305
306 //— Check if it is an affine transformation (training image 0)
307 if( H_0.at<double>(2,0) < 0.0001 && H_0.at<double>(2,1) < 0.0001)
308 {
309 // check if it is a stable homography (training image 0)
310 number_of_times_approved_H_0++;
311
312 // calculate the orientation of the object (training image 0)
313 float hypotenuse_0 = sqrt((scene_corners [2].x-scene_corners [1].x)*(scene_corners [2].x←
    scene_corners [1].x)+(scene_corners [2].y-scene_corners [1].y)*(scene_corners [2].y←
    scene_corners [1].y));
314 float cathetus_0 = scene_corners [2].y-scene_corners [1].y;
315 degree_estimated_for_0 = acos( cathetus_0/hypotenuse_0)*180/(arma::datum::pi);
316
317
318 if((scene_corners [2].x-scene_corners [1].x) < 0)
319 {
320 degree_estimated_for_0=360-degree_estimated_for_0;
321 }
322 }
323 else
324 {
325 //If it is not an stable homography (training image 0)
326 number_of_times_approved_H_0=0;
327 }
328 }
329
330
331
332
333 //TRAINING IMAGE 90 DEGREES
334 //—————
335 //—————
336
337
338 if (good_matches_90.size() > 3)
339 {
340 //— Get the keypoints from the good matches 90 degree
341 for( int i = 0; i < good_matches_90.size(); i++ )
342 {
343
344 obj_90.push_back( keypoints_object_90[ good_matches_90[i].queryIdx ].pt );
345 scene_90.push_back( keypoints_scene[ good_matches_90[i].trainIdx ].pt );
346 }
347
348 // — Estimate the homography between training image 90 degrees and image stream
349 cv::Mat H_90 = findHomography( obj_90, scene_90, CV_RANSAC );

```

```

350
351     ///— Get the corners from the training image 90 degrees ( the object to be "↔
        detected" )
352     std::vector<Point2f> obj_corners_90(4);
353     obj_corners_90[0] = cvPoint(0,0); obj_corners_90[1] = cvPoint( img_object_90.cols, 0 ↔
        );
354     obj_corners_90[2] = cvPoint( img_object_90.cols, img_object_90.rows ); obj_corners_90↔
        [3] = cvPoint( 0, img_object_90.rows );
355     std::vector<Point2f> scene_corners_90(4);
356
357     ///— Draw lines between the corners (the mapped object in the scene - training ↔
        image 90 degrees)
358     perspectiveTransform( obj_corners_90, scene_corners_90, H_90);
359     line( img_matches_90, scene_corners_90[0] + Point2f( img_object_90.cols, 0), ↔
        scene_corners_90[1] + Point2f( img_object_90.cols, 0), Scalar(0, 255, 0), 4 );
360     line( img_matches_90, scene_corners_90[1] + Point2f( img_object_90.cols, 0), ↔
        scene_corners_90[2] + Point2f( img_object_90.cols, 0), Scalar( 0, 255, 0), 4 );
361     line( img_matches_90, scene_corners_90[2] + Point2f( img_object_90.cols, 0), ↔
        scene_corners_90[3] + Point2f( img_object_90.cols, 0), Scalar( 0, 255, 0), 4 );
362     line( img_matches_90, scene_corners_90[3] + Point2f( img_object_90.cols, 0), ↔
        scene_corners_90[0] + Point2f( img_object_90.cols, 0), Scalar( 0, 255, 0), 4 );
363
364     ///— Check if it is an affine transformation (training image 90)
365     if( H_90.at<double>(2,0) < 0.0001 && H_90.at<double>(2,1) < 0.0001)
366     {
367         /// check if it is a stable homography (training image 90)
368         number_of_times_approved_H_90++;
369
370
371         /// calculate the orientation of the object (training image 0)
372         float hypotenuse_90 = sqrt((scene_corners_90[1].x-scene_corners_90[0].x)*(↔
            scene_corners_90[1].x-scene_corners_90[0].x)+(scene_corners_90[1].y↔
            scene_corners_90[0].y)*(scene_corners_90[1].y-scene_corners_90[0].y));
373         float cathetus_90 = scene_corners_90[1].x-scene_corners_90[0].x;
374         degree_estimated_for_90 = acos(cathetus_90/hypotenuse_90)*180/(arma::datum::pi);
375
376
377         if(scene_corners_90[1].y > scene_corners_90[0].y)
378         {
379             degree_estimated_for_90= 90 - degree_estimated_for_90;
380         }
381         else
382         {
383             degree_estimated_for_90= 90 + degree_estimated_for_90;
384         }
385
386     }
387     else
388     {
389         ///If it is not an stable homography (training image 90)
390         int number_of_times_approved_H_90=0;
391     }
392 }
393
394     ///TRAINING IMAGE 180 DEGREES
395     ///—————
396     ///—————
397
398
399     if (good_matches_180.size() > 3)
400     {

```

```

401 //— Get the keypoints from the good matches 180 degree
402 for( int i = 0; i < good_matches_180.size(); i++ )
403 {
404
405     obj_180.push_back( keypoints_object_180[ good_matches_180[i].queryIdx ].pt );
406     scene_180.push_back( keypoints_scene[ good_matches_180[i].trainIdx ].pt );
407 }
408
409
410 // — Estimate the homography between training image 180 degrees and image stream
411 cv::Mat H_180 = findHomography( obj_180, scene_180, CV_RANSAC );
412
413 //— Get the corners from the training image 180 degrees ( the object to be "↔
414     detected" )
415 std::vector<Point2f> obj_corners_180(4);
416 obj_corners_180[0] = cvPoint(0,0); obj_corners_180[1] = cvPoint( img_object_180.cols,↔
417     0 );
418 obj_corners_180[2] = cvPoint( img_object_180.cols, img_object_180.rows ); ↔
419     obj_corners_180[3] = cvPoint( 0, img_object_180.rows );
420 std::vector<Point2f> scene_corners_180(4);
421
422 perspectiveTransform( obj_corners_180, scene_corners_180, H_180);
423 //— Draw lines between the corners (the mapped object in the scene – training image↔
424     180 degrees)
425 line( img_matches_180, scene_corners_180[0] + Point2f( img_object_180.cols, 0), ↔
426     scene_corners_180[1] + Point2f( img_object_180.cols, 0), Scalar(0, 255, 0), 4 );
427 line( img_matches_180, scene_corners_180[1] + Point2f( img_object_180.cols, 0), ↔
428     scene_corners_180[2] + Point2f( img_object_180.cols, 0), Scalar( 0, 255, 0), 4 );
429 line( img_matches_180, scene_corners_180[2] + Point2f( img_object_180.cols, 0), ↔
430     scene_corners_180[3] + Point2f( img_object_180.cols, 0), Scalar( 0, 255, 0), 4 );
431 line( img_matches_180, scene_corners_180[3] + Point2f( img_object_180.cols, 0), ↔
432     scene_corners_180[0] + Point2f( img_object_180.cols, 0), Scalar( 0, 255, 0), 4 );
433
434 //— Check if it is an affine transformation (training image 0)
435 if( H_180.at<double>(2,0) < 0.0001 && H_180.at<double>(2,1) < 0.0001)
436 {
437     // check if it is a stable homography (training image 0)
438     number_of_times_approved_H_180++;
439
440     // calculate the orientation of the object (training image 0)
441     float hypotenuse_180 = sqrt((scene_corners_180[2].x-scene_corners_180[1].x)*(↔
442     scene_corners_180[2].x-scene_corners_180[1].x)+(scene_corners_180[2].y-↔
443     scene_corners_180[1].y)*(scene_corners_180[2].y-scene_corners_180[1].y));
444     float cathetus_180 = scene_corners_180[2].y-scene_corners_180[1].y;
445     degree_estimated_for_180 = acos(cathetus_180/hypotenuse_180)*180/(arma::datum::pi);
446
447     if(scene_corners_180[2].x < scene_corners_180[1].x)
448     {
449         degree_estimated_for_180 =180-degree_estimated_for_180;
450     }
451     else
452     {
453         degree_estimated_for_180 = 180 +degree_estimated_for_180;
454     }
455     }
456     else
457     {
458         //If it is not an stable homography (training image 0)
459         number_of_times_approved_H_180=0;
460     }
461 }

```

```

452
453     //TRAINING IMAGE 270 DEGREES
454     //—————
455     //—————
456
457
458
459
460
461
462
463
464
465
466     if (good_matches_270.size() > 3)
467     {
468         //— Get the keypoints from the good matches 270 degree
469         for( int i = 0; i < good_matches_270.size(); i++ )
470         {
471
472             obj_270.push_back( keypoints_object_270[ good_matches_270[i].queryIdx ].pt );
473             scene_270.push_back( keypoints_scene[ good_matches_270[i].trainIdx ].pt );
474         }
475
476         // — Estimate the homography between training image 270 degrees and image stream
477         cv::Mat H_270 = findHomography( obj_270, scene_270, CV_RANSAC );
478
479         //— Get the corners from the training image 270 degrees ( the object to be "detected" ←
480         " )
481         std::vector<Point2f> obj_corners_270(4);
482         obj_corners_270[0] = cvPoint(0,0); obj_corners_270[1] = cvPoint( img_object_270.cols, ←
483         0 );
484         obj_corners_270[2] = cvPoint( img_object_270.cols, img_object_270.rows ); ←
485         obj_corners_270[3] = cvPoint( 0, img_object_270.rows );
486         std::vector<Point2f> scene_corners_270(4);
487         perspectiveTransform( obj_corners_270, scene_corners_270, H_270);
488
489         //— Draw lines between the corners (the mapped object in the scene - training ←
490         image 0 degrees)
491         line( img_matches_270, scene_corners_270[0] + Point2f( img_object_270.cols, 0), ←
492         scene_corners_270[1] + Point2f( img_object_270.cols, 0), Scalar(0, 255, 0), 4 );
493         line( img_matches_270, scene_corners_270[1] + Point2f( img_object_270.cols, 0), ←
494         scene_corners_270[2] + Point2f( img_object_270.cols, 0), Scalar( 0, 255, 0), 4 );
495         line( img_matches_270, scene_corners_270[2] + Point2f( img_object_270.cols, 0), ←
496         scene_corners_270[3] + Point2f( img_object_270.cols, 0), Scalar( 0, 255, 0), 4 );
497         line( img_matches_270, scene_corners_270[3] + Point2f( img_object_270.cols, 0), ←
498         scene_corners_270[0] + Point2f( img_object_270.cols, 0), Scalar( 0, 255, 0), 4 );
499
500         //— Check if it is an affine transformation (training image 270)
501         if( H_270.at<double>(2,0) < 0.0001 && H_270.at<double>(2,1) < 0.0001)
502         {
503             // check if it is a stable homography (training image 270)
504             number_of_times_approved_H_270++;
505
506             // calculate the orientation of the object (training image 270)
507             float hypotenuse_270 = sqrt((scene_corners_270[1].x-scene_corners_270[0].x)*( ←
508             scene_corners_270[1].x-scene_corners_270[0].x)+(scene_corners_270[1].y- ←
509             scene_corners_270[0].y)*(scene_corners_270[1].y-scene_corners_270[0].y));
510             float cathetus_270 = scene_corners_270[1].y-scene_corners_270[0].y;
511             degree_estimated_for_270 = acos(cathetus_270/hypotenuse_270)*180/(arma::datum::pi)+180;

```

```

503
504 }
505 else
506 {
507     //If it is not an stable homography (training image 270)
508     number_of_times_approved_H_270=0;
509 }
510
511 }
512
513
514 // CHECK WICH OF THE ESTIMATED "degree_estimated_for_xx" THAT VOTE FOR THE SAME VALUE/↔
    DEGREES
515 // ————
516 //—————
517
518
519 // Votes for training image 0 having the correct orientation
520 int g=0;
521 if( (degree_estimated_for_0 < 45 || degree_estimated_for_0 >315)&& ↔
    number_of_times_approved_H_0>4)
522 {
523     g++;
524     if( (degree_estimated_for_90 < 45 || degree_estimated_for_90 >315) && ↔
    number_of_times_approved_H_90>4)
525     {
526         g++;
527     }
528     if( (degree_estimated_for_180 < 45 || degree_estimated_for_180 >315) && ↔
    number_of_times_approved_H_180>4)
529     {
530         g++;
531     }
532     if( (degree_estimated_for_270 < 45 || degree_estimated_for_270 >270) && ↔
    number_of_times_approved_H_270 >4)
533     {
534         g++;
535     }
536 }
537
538
539
540 // Votes for training image 90 having the correct orientation
541 int g_90=0;
542 if( degree_estimated_for_90 < 135 && degree_estimated_for_90 > 45 && ↔
    number_of_times_approved_H_90>4)
543 {
544     g_90++;
545     if( degree_estimated_for_0 < 135 && degree_estimated_for_0 > 45 && ↔
    number_of_times_approved_H_0>4)
546     {
547         g_90++;
548     }
549     if( degree_estimated_for_180 < 135 && degree_estimated_for_180 >45 && ↔
    number_of_times_approved_H_180>4)
550     {
551         g_90++;
552     }
553     if( degree_estimated_for_270 < 135 && degree_estimated_for_270 >45 && ↔
    number_of_times_approved_H_270 >4)
554     {

```

```

555     g_90++;
556   }
557 }
558
559
560 // Votes for training image 180 having the correct orientation
561 int g_180=0;
562 if( degree_estimated_for_180 < 225 && degree_estimated_for_180 > 135 && ←
    number_of_times_approved_H_180>4)
563 {
564   g_180++;
565   if( degree_estimated_for_0 < 225 && degree_estimated_for_0 > 135 && ←
      number_of_times_approved_H_0>4 )
566   {
567     g_180++;
568   }
569   if( degree_estimated_for_90 < 225 && degree_estimated_for_90 >135&& ←
      number_of_times_approved_H_90>4)
570   {
571     g_180++;
572   }
573   if( degree_estimated_for_270 < 225 && degree_estimated_for_270 >135 && ←
      number_of_times_approved_H_270 >4)
574   {
575     g_180++;
576   }
577 }
578
579
580 // Votes for training image 270 having the correct orientation
581 int g_270=0;
582 if( degree_estimated_for_270 < 315 && degree_estimated_for_270 > 225 && ←
    number_of_times_approved_H_270>4)
583 {
584   g_270++;
585   if( degree_estimated_for_0 < 315 && degree_estimated_for_0 > 225&& ←
      number_of_times_approved_H_0>4 )
586   {
587     g_270++;
588   }
589   if( degree_estimated_for_90 < 315 && degree_estimated_for_90 >225 && ←
      number_of_times_approved_H_90>4)
590   {
591     g_270++;
592   }
593   if( degree_estimated_for_180 < 315 && degree_estimated_for_180 >225&& ←
      number_of_times_approved_H_180>4)
594   {
595     g_270++;
596   }
597 }
598
599
600 // CHECK WHICH OF THE "degree_estimated_for_xx" THAT HAS HIGHEST VOTES
601 if(g > g_90 && g > g_180 && g > g_270 )
602 {
603   estimated_orientation= degree_estimated_for_0;
604 }
605
606 if(g_90 > g && g_90 > g_180 && g_90 > g_270 )
607 {

```

```

608     estimated_orientation= degree_estimated_for_90;
609 }
610
611 if(g_180 > g && g_180 > g_90 && g_180 > g_270 )
612 {
613     estimated_orientation= degree_estimated_for_180;
614 }
615
616 if(g_270 > g && g_270 > g_90 && g_270 > g_180 )
617 {
618     estimated_orientation= degree_estimated_for_270;
619 }
620
621
622 // —CHECK PIXELREGIONS, IS THE ORIENTATION TRUE OR 180 DEGREES PHASE SHIFTED ?
623 // —————
624 //—————
625
626
627 std::vector<Point2f> center_point_image_stream(1);
628 center_point_image_stream[0]=cvPoint((cv_ptr->image.cols)/2,(cv_ptr->image.rows)/2);
629
630
631 // Delta degrees for localizing the pixel region
632 std::vector<Point2f> delta_degree_for_pixels_along_cylinder_edge(5);
633     delta_degree_for_pixels_along_cylinder_edge[0].x= cos((423-estimated_orientation)*(←
        arma::datum::pi)/180)*100;
634 delta_degree_for_pixels_along_cylinder_edge[0].y= sin((423-estimated_orientation)*(arma←
        ::datum::pi)/180)*100;
635     delta_degree_for_pixels_along_cylinder_edge[1].x= cos((452-estimated_orientation)*(←
        arma::datum::pi)/180)*100;
636 delta_degree_for_pixels_along_cylinder_edge[1].y= sin((452-estimated_orientation)*(arma←
        ::datum::pi)/180)*100;
637     delta_degree_for_pixels_along_cylinder_edge[2].x= cos((431-estimated_orientation)*(←
        arma::datum::pi)/180)*100;
638 delta_degree_for_pixels_along_cylinder_edge[2].y= sin((431-estimated_orientation)*(arma←
        ::datum::pi)/180)*100;
639     delta_degree_for_pixels_along_cylinder_edge[3].x= cos((427-estimated_orientation)*(←
        arma::datum::pi)/180)*100;
640 delta_degree_for_pixels_along_cylinder_edge[3].y= sin((427-estimated_orientation)*(arma←
        ::datum::pi)/180)*100;
641
642
643     uint16_t greyscale_values[3];
644     float radius_cylinder =0.055;
645     float distance_from_camera_to_cylinder=0.155;
646     float delta_degree_for_pixelregion_around_cylinder [3] = {423,427,431};
647     std::vector<Point2f> visualize_pixel_region_edge_object(3);
648
649     arma::colvec norm_pix_1, norm_pix_2, norm_pix_3, pix_1, pix_2, pix_3;
650
651     // Camera matrix
652     arma::mat camera_matrix(3,3);
653     camera_matrix << 540.927271 << 0 << 320 <<arma::endr
654     << 0 << 540.264582 << 240 <<arma::endr
655     << 0 << 0 << 1 <<arma::endr;
656
657
658
659 for(int i=0;i<3;i++)
660 {

```



```

661
662  if(i==0)
663  {
664  // Localise one pixel and its greyscale value
665  norm_pix_1 << radius_cylinder*cos((delta_degree_for_pixelregion_around_cylinder[0]-←
      estimated_orientation)*(arma::datum::pi)/180)/distance_from_camera_to_cylinder <<←
      radius_cylinder*sin((delta_degree_for_pixelregion_around_cylinder[0]-←
      estimated_orientation)*(arma::datum::pi)/180)/distance_from_camera_to_cylinder <<←
      1;
666  pix_1=camera_matrix*norm_pix_1;
667  greyscale_values[i] = gray_image.at<uchar>(pix_1[1],pix_1[0]);
668
669  visualize_pixel_region_edge_object[i].x=pix_1[0];
670  visualize_pixel_region_edge_object[i].y=pix_1[1];
671
672  }
673  if(i==1)
674  {
675  // Localise one pixel and its greyscale value
676  norm_pix_2 << radius_cylinder*cos((delta_degree_for_pixelregion_around_cylinder[1]-←
      estimated_orientation)*(arma::datum::pi)/180)/distance_from_camera_to_cylinder ←
      << radius_cylinder*sin((delta_degree_for_pixelregion_around_cylinder[1]-←
      estimated_orientation)*(arma::datum::pi)/180)/distance_from_camera_to_cylinder ←
      << 1;
677  pix_2=camera_matrix*norm_pix_2;
678  greyscale_values[i] = gray_image.at<uchar>(pix_2[1],pix_2[0]);
679
680  visualize_pixel_region_edge_object[i].x=pix_2[0];
681  visualize_pixel_region_edge_object[i].y=pix_2[1];
682
683  }
684  if(i==2)
685  {
686  // Localise one pixel and its greyscale value
687  norm_pix_3 << radius_cylinder*cos((delta_degree_for_pixelregion_around_cylinder[2]-←
      estimated_orientation)*(arma::datum::pi)/180)/distance_from_camera_to_cylinder ←
      << radius_cylinder*sin((delta_degree_for_pixelregion_around_cylinder[2]-←
      estimated_orientation)*(arma::datum::pi)/180)/distance_from_camera_to_cylinder ←
      << 1;
688  pix_3=camera_matrix*norm_pix_3;
689  greyscale_values[i] = gray_image.at<uchar>(pix_3[1],pix_3[0]);
690
691  visualize_pixel_region_edge_object[i].x=pix_3[0];
692  visualize_pixel_region_edge_object[i].y=pix_3[1];
693  }
694  }
695
696  // Visualize the pixels (default:NOT SHOWING)
697  cv::circle(cv_ptr->image, visualize_pixel_region_edge_object[0], 2, CV_RGB(0, 255, ←
      0));
698  cv::circle(cv_ptr->image, visualize_pixel_region_edge_object[1], 2, CV_RGB(0, 255, 0))←
      ;
699  cv::circle(cv_ptr->image, visualize_pixel_region_edge_object[2], 2, CV_RGB(0, 255, ←
      0));
700
701
702  // Check the greyscale values
703  if(abs(greyscale_values[0]-greyscale_values[1])>50 || abs(greyscale_values[0]-←
      greyscale_values[2])>50 || abs(greyscale_values[2]-greyscale_values[1])>50)
704  {

```

```

705 delta_degree_for_pixels_along_cylinder_edge [1].x= cos((450-estimated_orientation-180)*(←
    arma::datum::pi)/180)*100;
706 delta_degree_for_pixels_along_cylinder_edge [1].y= sin((450-estimated_orientation-180)*(←
    arma::datum::pi)/180)*100;
707 estimated_orientation=estimated_orientation+180;
708 }
709
710
711 // Check if the orientation is stable — list the last orientations and check if those ←
    are stable
712 if(estimated_orientation>360)
713 {
714     estimated_orientation=estimated_orientation-360;
715 }
716
717 for(int x = 6-1;x>=0;x--){
718     list_with_last_degrees [x+1]=list_with_last_degrees [x];
719
720     if(x==0){
721         list_with_last_degrees [x]=estimated_orientation;
722     }
723 }
724
725 int i=0;
726 for(int x=0 ;x<6;x++){
727 {
728     if(abs(list_with_last_degrees [x]-list_with_last_degrees [x+1])<2)
729     {
730         i++;
731     }
732 }
733 }
734 if(i>=5)
735 {
736     // Median of the last orientations
737     true_orientation = GetMedian(list_with_last_degrees ,7);
738     sleep(1);
739 }
740
741
742
743 // THIS IS THE ESTIMATED ORIENTATION FOR THE OBJECT
744 std::cout << "Rotation around Z-axis (degrees): " << true_orientation << std::endl;
745
746
747
748 // - Visualize the orientation with a green line
749 std::vector<Point2f> visualize_orientation(3);
750 visualize_orientation [0].x=cos((450-true_orientation)*(arma::datum::pi)/180)*100;
751 visualize_orientation [0].y= sin((450-true_orientation)*(arma::datum::pi)/180)*100;
752 line( cv_ptr->image, center_point_image_stream [0] , center_point_image_stream [0]+←
    visualize_orientation [0], Scalar( 0, 255, 0), 2 );
753
754
755
756
757
758 // - Offset values for where the printed degrees should show in the protractor
759 std::vector<Point2f> offset_text(12);
760 offset_text [0].x=-3; offset_text [0].y=12;
761 offset_text [1].x=-15; offset_text [1].y=15;

```

```

762 offset_text [2].x=-25; offset_text [2].y=12;
763 offset_text [3].x=-28; offset_text [3].y=6;
764 offset_text [4].x=-29; offset_text [4].y=0;
765 offset_text [5].x=-16; offset_text [5].y=-6;
766 offset_text [6].x=-14; offset_text [6].y=-4;
767 offset_text [7].x=5; offset_text [7].y=-2;
768 offset_text [8].x=3; offset_text [8].y=3;
769 offset_text [9].x=3; offset_text [9].y=4;
770 offset_text [10].x=8; offset_text [10].y=7;
771 offset_text [11].x=-6; offset_text [11].y=12;
772
773
774
775 // - Visualize the protractor
776 for( int i = 0; i < 12; i++ )
777 {
778 std::vector<Point2f> visualize_line_in_protractor(1);
779 visualize_line_in_protractor [0].y= sin((30*i+90)*(arma::datum::pi)/180)*89;
780 visualize_line_in_protractor [0].x= cos((30*i+90)*(arma::datum::pi)/180)*89;
781
782
783 cv::circle(cv_ptr->image, center_point_image_stream [0], 89, CV_RGB(0,0,0));
784 line( cv_ptr->image, center_point_image_stream [0], center_point_image_stream [0] +↔
       visualize_line_in_protractor [0], Scalar( 255, 255, 255), 1 );
785
786 int visualize_degrees_in_protractor = 360-30*i;
787
788 if(i==0)
789 {
790     visualize_degrees_in_protractor = 0;
791 }
792
793 string text = static_cast<ostringstream*>( &(ostringstream() << ↔
       visualize_degrees_in_protractor) )->str();
794 int fontFace = FONT_HERSHEY_PLAIN;
795 double fontScale = 0.9;
796 int thickness = 2.5;
797
798
799 int baseline=0;
800 Size textSize = getTextSize(text, fontFace,
801                             fontScale, thickness, &baseline);
802 baseline += thickness;
803
804 // center the text
805 Point textOrg((cv_ptr->image.cols - textSize.width)/2,
806              (cv_ptr->image.rows + textSize.height)/2);
807
808 putText(cv_ptr->image, text, center_point_image_stream [0] +visualize_line_in_protractor↔
       [0]+offset_text [i], fontFace, fontScale,
809         Scalar::all(0), thickness, 8);
810 }
811
812
813
814 // — Visualize results
815 cv::imshow(OPENCV_WINDOW, cv_ptr->image);
816
817 //— Publish orientation
818     array_orientation_cylinder.data.clear();
819 for (int i = 0; i < 2; i++)

```

```
820 {
821   array_orientation_cylinder.data.push_back(true_orientation);
822 }
823   publish_orientation_cylinder.publish(array_orientation_cylinder);
824
825   }
826 };
827
828 int main(int argc, char** argv)
829 {
830     ros::init(argc, argv, "Orientation_cylinder_node");
831     ImageConverter ic;
832
833     ros::spin();
834     return 0;
835 }
836 }
```

```

1  //-----
2  //----- Node run for estimating orientation of piston -----
3  //-----
4  //-----
5  //----- Authors: Geir Ole Tysse and Martin Morland . -----
6  //----- NINU 2015 -----
7  //-----
8
9  #include <ros/ros.h>
10 #include <image_transport/image_transport.h>
11 #include <cv_bridge/cv_bridge.h>
12 #include <sensor_msgs/image_encodings.h>
13 #include <opencv2/opencv.hpp>
14 #include <opencv2/imgproc/imgproc.hpp>
15 #include <opencv2/highgui/highgui.hpp>
16 #include <opencv2/nonfree/features2d.hpp>
17 #include <opencv2/features2d/features2d.hpp>
18 #include <opencv2/core/core.hpp>
19 #include "opencv2/calib3d/calib3d.hpp"
20 #include <stdio.h>
21 #include <iostream>
22 #include <armadillo>
23 #include <cmath>
24 #include "std_msgs/Float64MultiArray.h"
25 using namespace cv;
26 using namespace std;
27 static const std::string OPENCV_WINDOW = "Image window";
28
29 float degree_estimated_for_0;
30 float degree_estimated_for_90;
31 float degree_estimated_for_180;
32 float degree_estimated_for_270;
33 arma::mat camera_matrix(3,3);
34 float true_orientation;
35 int number_of_times_approved_H_0=0;
36 int number_of_times_approved_H_90=0;
37 int number_of_times_approved_H_180=0;
38 int number_of_times_approved_H_270=0;
39 float estimated_orientation;
40 float list_with_last_degrees [7];
41 std_msgs::Float64MultiArray array_orientation_piston;
42
43 //--- Estimate the median
44 float GetMedian(float daArray[], int iSize) {
45     double* dpSorted = new double[iSize];
46     for (int i = 0; i < iSize; ++i) {
47         dpSorted[i] = daArray[i];
48     }
49     for (int i = iSize - 1; i > 0; --i) {
50         for (int j = 0; j < i; ++j) {
51             if (dpSorted[j] > dpSorted[j+1]) {
52                 double dTemp = dpSorted[j];
53                 dpSorted[j] = dpSorted[j+1];
54                 dpSorted[j+1] = dTemp;
55             }
56         }
57     }
58     double dMedian = 0.0;
59     if ((iSize % 2) == 0) {
60         dMedian = (dpSorted[iSize/2] + dpSorted[(iSize/2) - 1])/2.0;
61     } else {

```

```

62         dMedian = dpSorted[iSize/2];
63     }
64     delete [] dpSorted;
65     return dMedian;
66 }
67
68
69
70 class ImageConverter
71 {
72     ros::NodeHandle nh_;
73     image_transport::ImageTransport it_;
74     image_transport::Subscriber image_sub_;
75     image_transport::Publisher image_pub_;
76     ros::Publisher publish_orientation_piston;
77
78
79 private:
80
81
82 public:
83
84
85     ImageConverter()
86     : it_(nh_)
87     {
88         //— Subscribe to input video feed
89         image_sub_ = it_.subscribe("/usb_cam/image_raw", 1,
90             &ImageConverter::imageCb, this);
91         cv::namedWindow(OPENCV_WINDOW, WINDOW_NORMAL);
92
93         //— Publish orientation of the piston
94         publish_orientation_piston= nh_.advertise<std_msgs::Float64MultiArray>("↵
95             piston_orientation", 1);
96
97
98     }
99
100 ~ImageConverter()
101 {
102     cv::destroyWindow(OPENCV_WINDOW);
103
104 }
105
106 void imageCb(const sensor_msgs::ImageConstPtr& msg)
107 {
108
109     cv_bridge::CvImagePtr cv_ptr;
110     try
111     {
112         cv_ptr = cv_bridge::toCvCopy(msg, sensor_msgs::image_encodings::BGR8);
113     }
114     catch (cv_bridge::Exception& e)
115     {
116         ROS_ERROR("cv-bridge exception: %s", e.what());
117         return;
118     }
119
120 //— Get the live image stream and the training images
121 Mat img_show;

```

```

122 Mat img_object = imread("/home/jorge/catkin_ws/piston_0.jpg");
123 Mat img_object_90 = imread("/home/jorge/catkin_ws/piston_90.jpg");
124 Mat img_object_180 = imread("/home/jorge/catkin_ws/piston_180.jpg");
125 Mat img_object_270 = imread("/home/jorge/catkin_ws/piston_270.jpg");
126 Mat img_scene = cv_ptr->image;
127
128 //— Get gray image from the image stream also, used for reading greyscale values
129 Mat gray_image;
130 cvtColor( img_scene, gray_image, CV_BGR2GRAY );
131
132
133 if( !img_object.data || !img_scene.data )
134 { std::cout<< " --(!) Error reading images " << std::endl; }
135
136 //— Step 1: Detect the keypoints using Sift Detector
137 int minHessian = 200;
138 SiftFeatureDetector detector( minHessian );
139 std::vector<KeyPoint> keypoints_object, keypoints_scene, keypoints_object_90, ←
    keypoints_object_180, keypoints_object_270;
140
141 //— Detection of feature in image stream. Searches within a defined mask
142 Mat mask = Mat::zeros(img_scene.size(), CV_8U);
143 Mat roi(mask, cv::Rect(260,50,120,250));
144 roi = Scalar(255, 255, 255);
145 detector.detect(img_scene, keypoints_scene, mask);
146
147
148 //— Detection of feature in training images
149 detector.detect( img_object, keypoints_object );
150 detector.detect( img_object_90, keypoints_object_90);
151 detector.detect( img_object_180, keypoints_object_180 );
152 detector.detect( img_object_270, keypoints_object_270 );
153
154
155
156
157 //— Step 2: Calculate descriptors
158 SiftDescriptorExtractor extractor;
159
160 Mat descriptors_object, descriptors_scene, descriptors_object_90, ←
    descriptors_object_180, descriptors_object_270;
161
162 extractor.compute( img_object, keypoints_object, descriptors_object );
163 extractor.compute( img_object_90, keypoints_object_90, descriptors_object_90);
164 extractor.compute( img_object_180, keypoints_object_180, descriptors_object_180 );
165 extractor.compute( img_object_270, keypoints_object_270, descriptors_object_270 );
166 extractor.compute( img_scene, keypoints_scene, descriptors_scene );
167
168
169
170 //— Step 3: Matching descriptor vectors using FLANN matcher
171 FlannBasedMatcher matcher;
172
173 std::vector< DMatch > matches, matches_90, matches_180, matches_270;
174 matcher.match( descriptors_object, descriptors_scene, matches );
175 matcher.match( descriptors_object_90, descriptors_scene, matches_90 );
176 matcher.match( descriptors_object_180, descriptors_scene, matches_180 );
177 matcher.match( descriptors_object_270, descriptors_scene, matches_270 );
178
179

```

```

180 std::vector< DMatch > good_matches , good_matches_90 , good_matches_180 , good_matches_270←
    ;
181
182 ///— Matching descriptor vectors in image stream and training image 0 degree
183 Mat img_matches_0;
184 drawMatches( img_object , keypoints_object , img_scene , keypoints_scene ,
185             good_matches , img_matches_0 , Scalar::all(-1) , Scalar::all(-1) ,
186             vector<char>() , DrawMatchesFlags::NOT_DRAW_SINGLE_POINTS );
187
188 ///— Matching descriptor vectors in image stream and training image 90 degree
189 Mat img_matches_90;
190 drawMatches( img_object_90 , keypoints_object_90 , img_scene , keypoints_scene ,
191             good_matches_90 , img_matches_90 , Scalar::all(-1) , Scalar::all(-1) ,
192             vector<char>() , DrawMatchesFlags::NOT_DRAW_SINGLE_POINTS );
193
194 ///— Matching descriptor vectors in image stream and training image 180 degree
195 Mat img_matches_180;
196 drawMatches( img_object_180 , keypoints_object_180 , img_scene , keypoints_scene ,
197             good_matches_180 , img_matches_180 , Scalar::all(-1) , Scalar::all(-1) ,
198             vector<char>() , DrawMatchesFlags::NOT_DRAW_SINGLE_POINTS );
199
200 ///— Matching descriptor vectors in image stream and training image 270 degree
201 Mat img_matches_270;
202 drawMatches( img_object_270 , keypoints_object_270 , img_scene , keypoints_scene ,
203             good_matches_270 , img_matches_270 , Scalar::all(-1) , Scalar::all(-1) ,
204             vector<char>() , DrawMatchesFlags::NOT_DRAW_SINGLE_POINTS );
205
206
207
208 ///— Quick calculation of max and min distances between keypoints in 0 degrees ←
training image and image stream
209 double max_dist = 0; double min_dist = 70;
210
211 for( int i = 0; i < descriptors_object.rows; i++ )
212 { double dist = matches[i].distance;
213   if( dist < min_dist ) min_dist = dist;
214   if( dist > max_dist ) max_dist = dist;
215 }
216
217
218
219 for( int i = 0; i < descriptors_object.rows; i++ )
220 { if( matches[i].distance < 3*min_dist )
221   { good_matches.push_back( matches[i]); }
222 }
223
224
225 ///— Quick calculation of max and min distances between keypoints in 90 degrees ←
training image and image stream
226 max_dist = 0;
227 min_dist = 70;
228
229 for( int i = 0; i < descriptors_object_90.rows; i++ )
230 { double dist = matches_90[i].distance;
231   if( dist < min_dist ) min_dist = dist;
232   if( dist > max_dist ) max_dist = dist;
233 }
234 for( int i = 0; i < descriptors_object_90.rows; i++ )
235 { if( matches_90[i].distance < 3*min_dist )
236   { good_matches_90.push_back( matches_90[i]); }
237 }

```



```

238
239 //— Quick calculation of max and min distances between keypoints in 180 degrees ←
      training image and image stream
240     max_dist = 0;
241     min_dist = 70;
242
243     for( int i = 0; i < descriptors_object_180.rows; i++ )
244     { double dist = matches_180[i].distance;
245       if( dist < min_dist ) min_dist = dist;
246       if( dist > max_dist ) max_dist = dist;
247     }
248     for( int i = 0; i < descriptors_object_180.rows; i++ )
249     { if( matches_180[i].distance < 3*min_dist )
250       { good_matches_180.push_back( matches_180[i] ); }
251     }
252
253 //— Quick calculation of max and min distances between keypoints in 270 degrees ←
      training image and image stream
254     max_dist = 0;
255     min_dist = 70;
256
257     for( int i = 0; i < descriptors_object_270.rows; i++ )
258     { double dist = matches_270[i].distance;
259       if( dist < min_dist ) min_dist = dist;
260       if( dist > max_dist ) max_dist = dist;
261     }
262     for( int i = 0; i < descriptors_object_270.rows; i++ )
263     { if( matches_270[i].distance < 3*min_dist )
264       { good_matches_270.push_back( matches_270[i] ); }
265     }
266
267
268
269
270 //— Localize the object
271 std::vector<Point2f> obj , obj_90 , obj_180 ,obj_270;
272 std::vector<Point2f> scene , scene_90 , scene_180 ,scene_270;
273
274
275 //TRAINING IMAGE 0 DEGREES
276 //—————
277 //—————
278
279
280 //— Get the keypoints from the good matches 0 degree
281 for( int i = 0; i < good_matches.size(); i++ )
282 {
283
284     obj.push_back( keypoints_object[ good_matches[i].queryIdx ].pt );
285     scene.push_back( keypoints_scene[ good_matches[i].trainIdx ].pt );
286 }
287
288 std::vector<Point2f> obj_corners(4);
289 if (good_matches.size() > 3)
290 {
291     // — Estimate the homography between training image 0 degrees and image stream
292     cv::Mat H_0 = findHomography( obj , scene , CV_RANSAC );
293
294     //— Get the corners from the training image 0 degrees ( the object to be "detected" ←
      )
295     obj_corners[0] = cvPoint(0,0); obj_corners[1] = cvPoint( img_object.cols , 0 );

```

```

296     obj_corners[2] = cvPoint( img_object.cols, img_object.rows ); obj_corners[3] = ←
        cvPoint( 0, img_object.rows );
297     std::vector<Point2f> scene_corners(4);
298
299     perspectiveTransform( obj_corners, scene_corners, H_0);
300
301     //— Draw lines between the corners (the mapped object in the scene – training image ←
        0 degrees)
302     line( img_matches_0, scene_corners[0] + Point2f( img_object.cols, 0), scene_corners←
        [1] + Point2f( img_object.cols, 0), Scalar(0, 255, 0), 4 );
303     line( img_matches_0, scene_corners[1] + Point2f( img_object.cols, 0), scene_corners←
        [2] + Point2f( img_object.cols, 0), Scalar( 0, 255, 0), 4 );
304     line( img_matches_0, scene_corners[2] + Point2f( img_object.cols, 0), scene_corners←
        [3] + Point2f( img_object.cols, 0), Scalar( 0, 255, 0), 4 );
305     line( img_matches_0, scene_corners[3] + Point2f( img_object.cols, 0), scene_corners←
        [0] + Point2f( img_object.cols, 0), Scalar( 0, 255, 0), 4 );
306
307
308
309
310     //— Check if it is an affine transformation (training image 0)
311     if( H_0.at<double>(2,0) < 0.0001 && H_0.at<double>(2,1) < 0.0001)
312     {
313         // check if it is a stable homography (training image 0)
314         number_of_times_approved_H_0++;
315
316         // calculate the orientation of the object (training image 0)
317         float hypotenuse_0 = sqrt( (scene_corners[2].x-scene_corners[1].x)*(scene_corners[2].x←
            scene_corners[1].x)+(scene_corners[2].y-scene_corners[1].y)*(scene_corners[2].y←
            scene_corners[1].y));
318         float cathetus_0 = scene_corners[2].y-scene_corners[1].y;
319         degree_estimated_for_0 = acos( cathetus_0/hypotenuse_0)*180/(arma::datum::pi);
320
321
322         if( (scene_corners[2].x-scene_corners[1].x) < 0)
323         {
324             degree_estimated_for_0=360-degree_estimated_for_0;
325         }
326     }
327     else
328     {
329         //If it is not an stable homography (training image 0)
330         number_of_times_approved_H_0=0;
331     }
332 }
333
334
335
336
337     //TRAINING IMAGE 90 DEGREES
338     //—————
339     //—————
340
341
342     if (good_matches_90.size() > 3)
343     {
344         //— Get the keypoints from the good matches 90 degree
345         for( int i = 0; i < good_matches_90.size(); i++ )
346         {
347
348             obj_90.push_back( keypoints_object_90[ good_matches_90[i].queryIdx ].pt );

```

```

349     scene_90.push_back( keypoints_scene[ good_matches_90[i].trainIdx ].pt );
350 }
351
352 // — Estimate the homography between training image 90 degrees and image stream
353 cv::Mat H_90 = findHomography( obj_90, scene_90, CV_RANSAC );
354
355 //— Get the corners from the training image 90 degrees ( the object to be "↔
    detected" )
356 std::vector<Point2f> obj_corners_90(4);
357 obj_corners_90[0] = cvPoint(0,0); obj_corners_90[1] = cvPoint( img_object_90.cols, 0 ↔
    );
358 obj_corners_90[2] = cvPoint( img_object_90.cols, img_object_90.rows ); obj_corners_90↔
    [3] = cvPoint( 0, img_object_90.rows );
359 std::vector<Point2f> scene_corners_90(4);
360
361 //— Draw lines between the corners (the mapped object in the scene – training ↔
    image 90 degrees)
362 perspectiveTransform( obj_corners_90, scene_corners_90, H_90);
363 line( img_matches_90, scene_corners_90[0] + Point2f( img_object_90.cols, 0), ↔
    scene_corners_90[1] + Point2f( img_object_90.cols, 0), Scalar(0, 255, 0), 4 );
364 line( img_matches_90, scene_corners_90[1] + Point2f( img_object_90.cols, 0), ↔
    scene_corners_90[2] + Point2f( img_object_90.cols, 0), Scalar( 0, 255, 0), 4 );
365 line( img_matches_90, scene_corners_90[2] + Point2f( img_object_90.cols, 0), ↔
    scene_corners_90[3] + Point2f( img_object_90.cols, 0), Scalar( 0, 255, 0), 4 );
366 line( img_matches_90, scene_corners_90[3] + Point2f( img_object_90.cols, 0), ↔
    scene_corners_90[0] + Point2f( img_object_90.cols, 0), Scalar( 0, 255, 0), 4 );
367
368 //— Check if it is an affine transformation (training image 90)
369 if( H_90.at<double>(2,0) < 0.0001 && H_90.at<double>(2,1) < 0.0001)
370 {
371     // check if it is a stable homography (training image 90)
372     number_of_times_approved_H_90++;
373
374
375     // calculate the orientation of the object (training image 0)
376 float hypotenuse_90 = sqrt((scene_corners_90[1].x-scene_corners_90[0].x)*(↔
    scene_corners_90[1].x-scene_corners_90[0].x)+(scene_corners_90[1].y↔
    scene_corners_90[0].y)*(scene_corners_90[1].y-scene_corners_90[0].y));
377 float cathetus_90 = scene_corners_90[1].x-scene_corners_90[0].x;
378 degree_estimated_for_90 = acos(cathetus_90/hypotenuse_90)*180/(arma::datum::pi);
379
380
381 if(scene_corners_90[1].y > scene_corners_90[0].y)
382 {
383     degree_estimated_for_90= 90 - degree_estimated_for_90;
384 }
385 else
386 {
387     degree_estimated_for_90= 90 + degree_estimated_for_90;
388 }
389
390 }
391 else
392 {
393     //If it is not an stable homography (training image 90)
394     int number_of_times_approved_H_90=0;
395 }
396 }
397
398 //TRAINING IMAGE 180 DEGREES
399 //—————

```

```

400 //-----
401
402
403 if (good_matches_180.size() > 3)
404 {
405 //— Get the keypoints from the good matches 180 degree
406 for( int i = 0; i < good_matches_180.size(); i++ )
407 {
408
409     obj_180.push_back( keypoints_object_180[ good_matches_180[i].queryIdx ].pt );
410     scene_180.push_back( keypoints_scene[ good_matches_180[i].trainIdx ].pt );
411 }
412
413
414 // — Estimate the homography between training image 180 degrees and image stream
415 cv::Mat H_180 = findHomography( obj_180, scene_180, CV_RANSAC );
416
417 //— Get the corners from the training image 180 degrees ( the object to be "↔
418     detected" )
419 std::vector<Point2f> obj_corners_180(4);
420 obj_corners_180[0] = cvPoint(0,0); obj_corners_180[1] = cvPoint( img_object_180.cols,↔
421     0 );
422 obj_corners_180[2] = cvPoint( img_object_180.cols, img_object_180.rows ); ↔
423     obj_corners_180[3] = cvPoint( 0, img_object_180.rows );
424 std::vector<Point2f> scene_corners_180(4);
425
426 perspectiveTransform( obj_corners_180, scene_corners_180, H_180);
427 //— Draw lines between the corners (the mapped object in the scene - training image↔
428     180 degrees)
429 line( img_matches_180, scene_corners_180[0] + Point2f( img_object_180.cols, 0), ↔
430     scene_corners_180[1] + Point2f( img_object_180.cols, 0), Scalar(0, 255, 0), 4 );
431 line( img_matches_180, scene_corners_180[1] + Point2f( img_object_180.cols, 0), ↔
432     scene_corners_180[2] + Point2f( img_object_180.cols, 0), Scalar( 0, 255, 0), 4 );
433 line( img_matches_180, scene_corners_180[2] + Point2f( img_object_180.cols, 0), ↔
434     scene_corners_180[3] + Point2f( img_object_180.cols, 0), Scalar( 0, 255, 0), 4 );
435 line( img_matches_180, scene_corners_180[3] + Point2f( img_object_180.cols, 0), ↔
436     scene_corners_180[0] + Point2f( img_object_180.cols, 0), Scalar( 0, 255, 0), 4 );
437
438 //— Check if it is an affine transformation (training image 0)
439 if( H_180.at<double>(2,0) < 0.0001 && H_180.at<double>(2,1) < 0.0001)
440 {
441     // check if it is a stable homography (training image 0)
442     number_of_times_approved_H_180++;
443
444     // calculate the orientation of the object (training image 0)
445     float hypotenuse_180 = sqrt((scene_corners_180[2].x-scene_corners_180[1].x)*(↔
446     scene_corners_180[2].x-scene_corners_180[1].x)+(scene_corners_180[2].y-↔
447     scene_corners_180[1].y)*(scene_corners_180[2].y-scene_corners_180[1].y));
448     float cathetus_180 = scene_corners_180[2].y-scene_corners_180[1].y;
449     degree_estimated_for_180 = acos(cathetus_180/hypotenuse_180)*180/(arma::datum::pi);
450
451     if(scene_corners_180[2].x < scene_corners_180[1].x)
452     {
453         degree_estimated_for_180 =180-degree_estimated_for_180;
454     }
455     else
456     {
457         degree_estimated_for_180 = 180 +degree_estimated_for_180;
458     }
459 }
460 else

```

```

451 {
452     //If it is not an stable homography (training image 0)
453     number_of_times_approved_H_180=0;
454 }
455 }
456
457     //TRAINING IMAGE 270 DEGREES
458     //—————
459     //—————
460
461
462 if (good_matches_270.size() > 3)
463 {
464     //— Get the keypoints from the good matches 270 degree
465     for( int i = 0; i < good_matches_270.size(); i++ )
466     {
467
468         obj_270.push_back( keypoints_object_270[ good_matches_270[i].queryIdx ].pt );
469         scene_270.push_back( keypoints_scene[ good_matches_270[i].trainIdx ].pt );
470     }
471
472     // — Estimate the homography between training image 270 degrees and image stream
473     cv::Mat H_270 = findHomography( obj_270, scene_270, CV_RANSAC );
474
475     //— Get the corners from the training image 270 degrees ( the object to be "detected" ←
476     " )
477     std::vector<Point2f> obj_corners_270(4);
478     obj_corners_270[0] = cvPoint(0,0); obj_corners_270[1] = cvPoint( img_object_270.cols, ←
479     0 );
480     obj_corners_270[2] = cvPoint( img_object_270.cols, img_object_270.rows ); ←
481     obj_corners_270[3] = cvPoint( 0, img_object_270.rows );
482     std::vector<Point2f> scene_corners_270(4);
483     perspectiveTransform( obj_corners_270, scene_corners_270, H_270);
484
485     //— Draw lines between the corners (the mapped object in the scene - training ←
486     image 0 degrees)
487     line( img_matches_270, scene_corners_270[0] + Point2f( img_object_270.cols, 0), ←
488     scene_corners_270[1] + Point2f( img_object_270.cols, 0), Scalar(0, 255, 0), 4 );
489     line( img_matches_270, scene_corners_270[1] + Point2f( img_object_270.cols, 0), ←
490     scene_corners_270[2] + Point2f( img_object_270.cols, 0), Scalar( 0, 255, 0), 4 );
491     line( img_matches_270, scene_corners_270[2] + Point2f( img_object_270.cols, 0), ←
492     scene_corners_270[3] + Point2f( img_object_270.cols, 0), Scalar( 0, 255, 0), 4 );
493     line( img_matches_270, scene_corners_270[3] + Point2f( img_object_270.cols, 0), ←
494     scene_corners_270[0] + Point2f( img_object_270.cols, 0), Scalar( 0, 255, 0), 4 );
495
496
497     //— Check if it is an affine transformation (training image 270)
498     if( H_270.at<double>(2,0) < 0.0001 && H_270.at<double>(2,1) < 0.0001)
499     {
500         // check if it is a stable homography (training image 270)
501         number_of_times_approved_H_270++;
502
503         // calculate the orientation of the object (training image 270)
504         float hypotenuse_270 = sqrt((scene_corners_270[1].x-scene_corners_270[0].x)*( ←
505         scene_corners_270[1].x-scene_corners_270[0].x)+(scene_corners_270[1].y- ←
506         scene_corners_270[0].y)*(scene_corners_270[1].y-scene_corners_270[0].y));
507         float cathetus_270 = scene_corners_270[1].y-scene_corners_270[0].y;
508         degree_estimated_for_270 = acos(cathetus_270/hypotenuse_270)*180/(arma::datum::pi)+180;
509     }
510 }
511 else

```

```

502 {
503     //If it is not an stable homography (training image 270)
504     number_of_times_approved_H_270=0;
505 }
506
507 }
508
509
510 // CHECK WICH OF THE ESTIMATED "degree_estimated_for_xx" THAT VOTE FOR THE SAME VALUE/↔
    DEGREES
511 // ————
512 //—————
513
514
515 // Votes for training image 0 having the correct orientation
516 int g=0;
517 if( (degree_estimated_for_0 < 45 || degree_estimated_for_0 >315)&& ↔
    number_of_times_approved_H_0>4)
518 {
519     g++;
520     if( (degree_estimated_for_90 < 45 || degree_estimated_for_90 >315) && ↔
        number_of_times_approved_H_90>4)
521     {
522         g++;
523     }
524     if( (degree_estimated_for_180 < 45 || degree_estimated_for_180 >315) && ↔
        number_of_times_approved_H_180>4)
525     {
526         g++;
527     }
528     if( (degree_estimated_for_270 < 45 || degree_estimated_for_270 >270) && ↔
        number_of_times_approved_H_270 >4)
529     {
530         g++;
531     }
532 }
533
534
535
536 // Votes for training image 90 having the correct orientation
537 int g_90=0;
538 if( degree_estimated_for_90 < 135 && degree_estimated_for_90 > 45 && ↔
    number_of_times_approved_H_90>4)
539 {
540     g_90++;
541     if( degree_estimated_for_0 < 135 && degree_estimated_for_0 > 45 && ↔
        number_of_times_approved_H_0>4)
542     {
543         g_90++;
544     }
545     if( degree_estimated_for_180 < 135 && degree_estimated_for_180 >45 && ↔
        number_of_times_approved_H_180>4)
546     {
547         g_90++;
548     }
549     if( degree_estimated_for_270 < 135 && degree_estimated_for_270 >45 && ↔
        number_of_times_approved_H_270 >4)
550     {
551         g_90++;
552     }
553 }

```

```

554
555
556 // Votes for training image 180 having the correct orientation
557 int g_180=0;
558 if( degree_estimated_for_180 < 225 && degree_estimated_for_180 > 135 && ←
    number_of_times_approved_H_180>4)
559 {
560     g_180++;
561     if( degree_estimated_for_0 < 225 && degree_estimated_for_0 > 135 && ←
        number_of_times_approved_H_0>4 )
562     {
563         g_180++;
564     }
565     if( degree_estimated_for_90 < 225 && degree_estimated_for_90 >135&& ←
        number_of_times_approved_H_90>4)
566     {
567         g_180++;
568     }
569     if( degree_estimated_for_270 < 225 && degree_estimated_for_270 >135 && ←
        number_of_times_approved_H_270 >4)
570     {
571         g_180++;
572     }
573 }
574
575
576 // Votes for training image 270 having the correct orientation
577 int g_270=0;
578 if( degree_estimated_for_270 < 315 && degree_estimated_for_270 > 225 && ←
    number_of_times_approved_H_270>4)
579 {
580     g_270++;
581     if( degree_estimated_for_0 < 315 && degree_estimated_for_0 > 225&& ←
        number_of_times_approved_H_0>4 )
582     {
583         g_270++;
584     }
585     if( degree_estimated_for_90 < 315 && degree_estimated_for_90 >225 && ←
        number_of_times_approved_H_90>4)
586     {
587         g_270++;
588     }
589     if( degree_estimated_for_180 < 315 && degree_estimated_for_180 >225&& ←
        number_of_times_approved_H_180>4)
590     {
591         g_270++;
592     }
593 }
594
595
596 // CHECK WHICH OF THE "degree_estimated_for_xx" THAT HAS HIGHEST VOTES
597 if(g > g_90 && g > g_180 && g > g_270 )
598 {
599     estimated_orientation= degree_estimated_for_0;
600 }
601
602 if(g_90 > g && g_90 > g_180 && g_90 > g_270 )
603 {
604     estimated_orientation= degree_estimated_for_90;
605 }
606

```

```

607     if(g_180 > g && g_180 > g_90 && g_180 > g_270 )
608     {
609         estimated_orientation= degree_estimated_for_180;
610     }
611
612     if(g_270 > g && g_270 > g_90 && g_270 > g_180 )
613     {
614         estimated_orientation= degree_estimated_for_270;
615     }
616
617
618     // —CHECK PIXELREGIONS, IS THE ORIENTATION TRUE OR 180 DEGREES PHASE SHIFTED ?
619     // _____
620     //—————
621
622
623     std::vector<Point2f> center_point_image_stream(1);
624     center_point_image_stream[0]= cvPoint((cv_ptr->image.cols)/2,(cv_ptr->image.rows)/2);
625
626
627     // Delta degrees for localizing the pixel region
628     std::vector<Point2f> delta_degree_for_pixels_along_cylinder_edge(5);
629     delta_degree_for_pixels_along_cylinder_edge[0].x= cos((450-estimated_orientation)*(←
        arma::datum::pi)/180)*100;
630     delta_degree_for_pixels_along_cylinder_edge[0].y= sin((450-estimated_orientation)*(arma←
        ::datum::pi)/180)*100;
631     delta_degree_for_pixels_along_cylinder_edge[1].x= cos((270-estimated_orientation)*(←
        arma::datum::pi)/180)*100;
632     delta_degree_for_pixels_along_cylinder_edge[1].y= sin((270-estimated_orientation)*(arma←
        ::datum::pi)/180)*100;
633     delta_degree_for_pixels_along_cylinder_edge[2].x= cos((431-estimated_orientation)*(←
        arma::datum::pi)/180)*100;
634     delta_degree_for_pixels_along_cylinder_edge[2].y= sin((431-estimated_orientation)*(arma←
        ::datum::pi)/180)*100;
635     delta_degree_for_pixels_along_cylinder_edge[3].x= cos((427-estimated_orientation)*(←
        arma::datum::pi)/180)*100;
636     delta_degree_for_pixels_along_cylinder_edge[3].y= sin((427-estimated_orientation)*(arma←
        ::datum::pi)/180)*100;
637
638
639     uint16_t greyscale_values[3];
640     float radius_piston =0.115;
641     float distance_from_camera_to_piston=0.205;
642     float delta_degree_for_pixelregion_around_piston [3] = {423,427,431};
643     std::vector<Point2f> visualize_pixel_region_edge_object(3);
644
645     arma::colvec norm_pix_1, norm_pix_2, norm_pix_3, pix_1, pix_2, pix_3;
646
647     // Camera matrix
648     arma::mat camera_matrix(3,3);
649     camera_matrix << 540.927271 << 0 << 320 <<arma::endr
650     << 0 << 540.264582 << 240 <<arma::endr
651     << 0 << 0 << 1 <<arma::endr;
652
653
654
655     for(int i=0;i<3;i++)
656     {
657
658         if(i==0)
659         {

```



```

660 // Localise one pixel and its greyscale value
661 norm_pix_1 << radius_piston*cos((delta_degree_for_pixelregion_around_piston[0]-←
    estimated_orientation)*(arma::datum::pi)/180)/distance_from_camera_to_piston << ←
    radius_piston*sin((delta_degree_for_pixelregion_around_piston[0]-←
    estimated_orientation)*(arma::datum::pi)/180)/distance_from_camera_to_piston << ←
    1;
662 pix_1=camera_matrix*norm_pix_1;
663 greyscale_values[i] = gray_image.at<uchar>(pix_1[1],pix_1[0]);
664
665 visualize_pixel_region_edge_object[i].x=pix_1[0];
666 visualize_pixel_region_edge_object[i].y=pix_1[1];
667
668 }
669 if(i==1)
670 {
671 // Localise one pixel and its greyscale value
672 norm_pix_2 << radius_piston*cos((delta_degree_for_pixelregion_around_piston[1]-←
    estimated_orientation)*(arma::datum::pi)/180)/distance_from_camera_to_piston <<←←
    radius_piston*sin((delta_degree_for_pixelregion_around_piston[1]-←
    estimated_orientation)*(arma::datum::pi)/180)/distance_from_camera_to_piston <<←←
    1;
673 pix_2=camera_matrix*norm_pix_2;
674 greyscale_values[i] = gray_image.at<uchar>(pix_2[1],pix_2[0]);
675
676 visualize_pixel_region_edge_object[i].x=pix_2[0];
677 visualize_pixel_region_edge_object[i].y=pix_2[1];
678
679 }
680 if(i==2)
681 {
682 // Localise one pixel and its greyscale value
683 norm_pix_3 << radius_piston*cos((delta_degree_for_pixelregion_around_piston[2]-←
    estimated_orientation)*(arma::datum::pi)/180)/distance_from_camera_to_piston <<←←
    radius_piston*sin((delta_degree_for_pixelregion_around_piston[2]-←
    estimated_orientation)*(arma::datum::pi)/180)/distance_from_camera_to_piston <<←←
    1;
684 pix_3=camera_matrix*norm_pix_3;
685 greyscale_values[i] = gray_image.at<uchar>(pix_3[1],pix_3[0]);
686
687 visualize_pixel_region_edge_object[i].x=pix_3[0];
688 visualize_pixel_region_edge_object[i].y=pix_3[1];
689 }
690 }
691
692 // Visualize the pixels (default:NOT SHOWING)
693 cv::circle(cv_ptr->image, visualize_pixel_region_edge_object[0], 2, CV_RGB(0, 255, ←
    0));
694 cv::circle(cv_ptr->image, visualize_pixel_region_edge_object[1], 2, CV_RGB(0, 255, 0))←←
    ;
695 cv::circle(cv_ptr->image, visualize_pixel_region_edge_object[2], 2, CV_RGB(0, 255, ←
    0));
696
697
698 // Check the greyscale values
699 if(abs(greyscale_values[0]-greyscale_values[1])>50 || abs(greyscale_values[0]-←
    greyscale_values[2])>50 || abs(greyscale_values[2]-greyscale_values[1])>50)
700 {
701 delta_degree_for_pixels_along_cylinder_edge[1].x= cos((450-estimated_orientation-180)*(←
    arma::datum::pi)/180)*100;
702 delta_degree_for_pixels_along_cylinder_edge[1].y= sin((450-estimated_orientation-180)*(←
    arma::datum::pi)/180)*100;

```

```

703 estimated_orientation=estimated_orientation+180;
704 }
705
706
707 // Check if the orientation is stable — list the last orientations and check if those ↔
    are stable
708 if(estimated_orientation>360)
709 {
710     estimated_orientation=estimated_orientation-360;
711 }
712
713     for(int x = 6-1;x>=0;x--){
714         list_with_last_degrees [x+1]=list_with_last_degrees [x];
715
716         if(x==0){
717             list_with_last_degrees [x]=estimated_orientation;
718         }
719     }
720
721     int i=0;
722     for(int x=0 ;x<6;x++)
723     {
724         if(abs(list_with_last_degrees [x]-list_with_last_degrees [x+1])<2)
725         {
726             i++;
727         }
728     }
729
730     if(i>=5)
731     {
732         // Median of the last orientations
733         true_orientation = GetMedian(list_with_last_degrees ,7);
734     sleep(1);
735
736     }
737
738
739     // THIS IS THE ESTIMATED ORIENTATION FOR THE OBJECT
740     std::cout << "Rotation around Z-axis (degrees): " << true_orientation << std::endl;
741
742
743
744 // - Visualize the orientation with a green line
745     std::vector<Point2f> visualize_orientation(3);
746     visualize_orientation [0].x=cos((450-true_orientation)*(arma::datum::pi)/180)*100;
747     visualize_orientation [0].y= sin((450-true_orientation)*(arma::datum::pi)/180)*100;
748     line( cv_ptr->image, center_point_image_stream [0] , center_point_image_stream [0]+↔
        visualize_orientation [0], Scalar( 0, 255, 0), 2 );
749
750
751
752
753
754 // - Offset values for where the printed degrees should show in the protractor
755     std::vector<Point2f> offset_text(12);
756     offset_text [0].x=-3; offset_text [0].y=12;
757     offset_text [1].x=-15; offset_text [1].y=15;
758     offset_text [2].x=-25; offset_text [2].y=12;
759     offset_text [3].x=-28; offset_text [3].y=6;
760     offset_text [4].x=-29; offset_text [4].y=0;
761     offset_text [5].x=-16; offset_text [5].y=-6;

```

```

762 offset_text [6].x=-14; offset_text [6].y=-4;
763 offset_text [7].x=5; offset_text [7].y=-2;
764 offset_text [8].x=3; offset_text [8].y=3;
765 offset_text [9].x=3; offset_text [9].y=4;
766 offset_text [10].x=8; offset_text [10].y=7;
767 offset_text [11].x=-6; offset_text [11].y=12;
768
769
770
771 // - Visualize the protractor
772 for( int i = 0; i < 12; i++ )
773 {
774     std::vector<Point2f> visualize_line_in_protractor(1);
775     visualize_line_in_protractor [0].y= sin((30*i+90)*(arma::datum::pi)/180)*89;
776     visualize_line_in_protractor [0].x= cos((30*i+90)*(arma::datum::pi)/180)*89;
777
778
779     cv::circle(cv_ptr->image, center_point_image_stream [0], 21, CV_RGB(0,0,0));
780     line( cv_ptr->image, center_point_image_stream [0], center_point_image_stream [0] +<←
        visualize_line_in_protractor [0], Scalar( 255, 255, 255), 1 );
781
782     int visualize_degrees_in_protractor = 360-30*i;
783
784     if(i==0)
785     {
786         visualize_degrees_in_protractor = 0;
787     }
788
789     string text = static_cast<ostringstream*>( &(ostringstream() <<< ←
        visualize_degrees_in_protractor) )->str();
790     int fontFace = FONT_HERSHEY_PLAIN;
791     double fontScale = 0.9;
792     int thickness = 2.5;
793
794
795     int baseline=0;
796     Size textSize = getTextSize(text, fontFace,
797         fontScale, thickness, &baseline);
798     baseline += thickness;
799
800     // center the text
801     Point textOrg((cv_ptr->image.cols - textSize.width)/2,
802         (cv_ptr->image.rows + textSize.height)/2);
803
804     putText(cv_ptr->image, text, center_point_image_stream [0] +visualize_line_in_protractor<←
        [0]+offset_text [i], fontFace, fontScale,
805         Scalar::all(0), thickness, 8);
806 }
807
808
809
810 // — Visualize results
811 cv::imshow(OPENCV_WINDOW, cv_ptr->image);
812
813
814 //— Publish orientation
815     array_orientation_piston.data.clear();
816     for (int i = 0; i < 2; i++)
817     {
818         //— Transformation ready for publishing
819         array_orientation_piston.data.push_back(true_orientation);

```

```
820 }
821   publish_orientation_piston.publish(array_orientation_piston);
822
823
824   }
825 };
826
827 int main(int argc, char** argv)
828 {
829
830   ros::init(argc, argv, "Orientation_piston_node");
831   ImageConverter ic;
832
833   ros::spin();
834   return 0;
835 }
```

```

1 //-----
2 //----- Node run for estimating kinematics robots -----
3 //-----
4 //-----
5 //----- Authors: Geir Ole Tysse and Martin Morland .-----
6 //----- NINU 2015-----
7 //-----
8
9 #include <ros/ros.h>
10 #include <pcl_ros/point_cloud.h>
11 #include <ros/ros.h>
12 #include <iostream>
13 #include <limits>
14 #include <fstream>
15 #include <vector>
16 #include <armadillo>
17 #include <sstream>
18 #include "std_msgs/String.h"
19 #include "std_msgs/Float64MultiArray.h"
20 #include <stdio.h>
21 #include <stdlib.h>
22 #include <string>
23 #include <cmath>
24 #include "std_msgs/MultiArrayLayout.h"
25 #include "std_msgs/MultiArrayDimension.h"
26 #include "std_msgs/Int32MultiArray.h"
27 #include <armadillo>
28
29 using namespace std;
30 using namespace arma;
31
32
33 float theta_cylinder=0;
34 float theta_piston=0;
35
36 colvec coordinates_piston;
37 colvec coordinates_cylinder;
38   mat Transformation_table_cylinder(4,4);
39   mat Transformation_table_piston(4,4);
40   mat Transformation_world_table(4,4);
41   mat Transformation_world_cylinder(4,4);
42   mat Transformation_world_piston(4,4);
43   mat Transformation_gripper_end_effector(4,4);
44   mat Transformation_parts_gripper(4,4);
45   mat Transformation_parts_end_effector(4,4);
46   mat Transformation_world_end_effector_piston(4,4);
47   mat Transformation_world_end_effector_cylinder(4,4);
48
49   mat Transformation_table_cylinder_none_rotation(4,4);
50   mat Transformation_table_piston_none_rotation(4,4);
51   mat Transformation_world_cylinder_none_rotation(4,4);
52   mat Transformation_world_piston_none_rotation(4,4);
53   mat Transformation_table_webcam_piston(4,4);
54   mat Transformation_table_webcam_cylinder(4,4);
55
56   std_msgs::Float64MultiArray Transformation_cylinder;
57   std_msgs::Float64MultiArray Transformation_piston;
58   std_msgs::Float64MultiArray Transformation_cylinder_none_rotation;
59   std_msgs::Float64MultiArray Transformation_piston_none_rotation;
60   std_msgs::Float64MultiArray array_transformation_table_webcam_piston;
61   std_msgs::Float64MultiArray array_transformation_table_webcam_cylinder;

```

```

62
63
64
65
66 //— The class
67 //—
68 class SubscribeAndPublish
69 {
70 public:
71     SubscribeAndPublish()
72     {
73         //— Topics beeing subscribed and published to
74         sub_coord_cylinder = n.subscribe("cylinder_coordinates", 1, &SubscribeAndPublish::↔
            CallbackcoordCylinder, this);
75         sub_coord_piston = n.subscribe("piston_coordinates", 1, &SubscribeAndPublish::↔
            CallbackcoordPiston, this);
76         sub_orientation_piston = n.subscribe("cylinder_orientation", 1, &SubscribeAndPublish::↔
            CallbackorientationCylinder, this);
77         sub_orientation_piston = n.subscribe("piston_orientation", 1, &SubscribeAndPublish::↔
            CallbackorientationPiston, this);
78         subnh = n.subscribe<std_msgs::Float64MultiArray>("Transformation_from_camera_to_table"↔
            , 1, &SubscribeAndPublish::callbacknh, this);
79         publisher_cylinder = n.advertise<std_msgs::Float64MultiArray>("↔
            cylinder_pose_with_respect_to_word", 1);
80         publisher_piston = n.advertise<std_msgs::Float64MultiArray>("↔
            piston_pose_with_respect_to_world", 1);
81         publisher_cylinder_none_rotation = n.advertise<std_msgs::Float64MultiArray>("↔
            cylinder_pose_none_rotation_with_respect_to_world", 1);
82         publisher_piston_none_rotation = n.advertise<std_msgs::Float64MultiArray>("↔
            piston_pose_none_rotation_with_respect_to_world", 1);
83         publisher_transformation_table_webcam_piston=n.advertise<std_msgs::Float64MultiArray↔
            >("Transformation_table_webcam_piston", 1);
84         publisher_transformation_table_webcam_cylinder=n.advertise<std_msgs::↔
            Float64MultiArray>("Transformation_table_webcam_cylinder", 1);
85     }
86
87
88 void CallbackcoordCylinder(const std_msgs::Float64MultiArray::ConstPtr& msg)
89 {
90     coordinates_cylinder << msg->data[0] << msg->data[1] << msg->data[2];
91
92 }
93
94 void CallbackcoordPiston(const std_msgs::Float64MultiArray::ConstPtr& msg)
95 {
96     coordinates_piston << msg->data[0] << msg->data[1] << msg->data[2];
97 }
98
99 void CallbackorientationCylinder(const std_msgs::Float64MultiArray::ConstPtr& msg)
100 {
101     theta_cylinder=msg->data[0];
102 }
103
104 void CallbackorientationPiston(const std_msgs::Float64MultiArray::ConstPtr& msg)
105 {
106     theta_piston=msg->data[0];
107 }
108
109 void callbacknh(const std_msgs::Float64MultiArray::ConstPtr& msg)
110 {
111     //— Tf from table to cylinder pose

```

```

112 Transformation_table_cylinder << cos(theta_cylinder/180*arma::datum::pi) << -sin(←
      theta_cylinder/180*arma::datum::pi) << 0 << coordinates_cylinder[0] << arma::endr
113 << sin(theta_cylinder/180*arma::datum::pi) << cos(theta_cylinder/180*arma::datum::←
      pi)<< 0 << coordinates_cylinder[1] << arma::endr
114 << 0 << 0 << 1 << coordinates_cylinder[2] << arma::endr
115 << 0 << 0 << 0 << 1 << arma::endr;
116
117 //— Tf from table to piston pose
118 Transformation_table_piston << cos(theta_piston/180*arma::datum::pi) << -sin(←
      theta_piston/180*arma::datum::pi) << 0 << coordinates_piston[0] << arma::endr
119 << sin(theta_piston/180*arma::datum::pi) << cos(theta_piston/180*arma::datum::pi)←
      << 0 << coordinates_piston[1] << arma::endr
120 << 0 << 0 << 1 << coordinates_piston[2] << arma::endr
121 << 0 << 0 << 0 << 1 << arma::endr;
122
123 //— Tf from table to cylinder pose (R=I)
124 Transformation_table_cylinder_none_rotation << 1 << 0 << 0 << coordinates_cylinder←
      [0] << arma::endr
125 << 0<< 1 << 0 << coordinates_cylinder[1] << arma::endr
126 << 0<< 0 << 1 << coordinates_cylinder[2] << arma::endr
127 << 0 << 0 << 0 << 1 << arma::endr;
128
129 //— Tf from table to piston pose (R=I)
130 Transformation_table_piston_none_rotation << 1 << 0 << 0 << coordinates_piston[0] ←
      << arma::endr
131 << 0<< 1 << 0 << coordinates_piston[1] << arma::endr
132 << 0<< 0 << 1 << coordinates_piston[2] << arma::endr
133 << 0 << 0 << 0 << 1 << arma::endr;
134
135 //— Tf from world to table
136 Transformation_world_table << 0 << -1 << 0 << 0.67562 << arma::endr
137 << 1 << 0 << 0 << -0.39624 << arma::endr
138 << 0<< 0<< 1 << 0.938 << arma::endr
139 << 0 << 0 << 0 << 1 << arma::endr;
140
141 //— Tf from table to webcam (orientation analysis cylinder)
142 Transformation_table_webcam_cylinder << -1 << 0 << 0 << coordinates_cylinder[0] << ←
      arma::endr
143 << 0 << 1 << 0 << 0 << coordinates_cylinder[1] << arma::endr
144 << 0<< 0 << -1 << coordinates_cylinder[2]+0.055 << arma::endr
145 << 0 << 0 << 0 << 1 << arma::endr;
146
147 //— Tf from table to webcam (orientation analysis piston)
148 Transformation_table_webcam_piston << -1 << 0 << 0 << coordinates_piston[0] << arma::←
      endr
149 << 0<< 1<< 0 << coordinates_piston[1] << arma::endr
150 << 0<< 0<< -1 << coordinates_piston[2]+0.115 << arma::endr
151 << 0 << 0 << 0 << 1 << arma::endr;
152
153 //— Tf from world to piston
154 Transformation_world_piston = Transformation_world_table*Transformation_table_piston;
155 //— Tf from world to cylinder
156 Transformation_world_cylinder = Transformation_world_table*←
      Transformation_table_cylinder;
157 //— Tf from world to piston (none orientation of piston)
158 Transformation_world_piston_none_rotation = Transformation_world_table*←
      Transformation_table_piston_none_rotation;
159 //— Tf from world to piston (none orientation of cylinder)
160 Transformation_world_cylinder_none_rotation = Transformation_world_table*←
      Transformation_table_cylinder_none_rotation;
161

```

```

162     //—Publish Tf world to cylinder
163     Transformation_cylinder.data.clear();
164     for (int i = 0; i < 16; i++)
165     {
166     Transformation_cylinder.data.push_back(Transformation_world_cylinder[i]);
167     }
168     publisher_cylinder.publish(Transformation_cylinder);
169
170     //—Publish Tf world to piston
171     Transformation_piston.data.clear();
172     for (int i = 0; i < 16; i++)
173     {
174     Transformation_piston.data.push_back(Transformation_world_piston[i]);
175     }
176
177     publisher_piston.publish(Transformation_piston);
178
179
180     //—Publish Tf world to cylinder (none rotation)
181     Transformation_cylinder_none_rotation.data.clear();
182     for (int i = 0; i < 16; i++)
183     {
184     Transformation_cylinder_none_rotation.data.push_back(↔
185         Transformation_world_cylinder_none_rotation[i]);
186     }
187     publisher_cylinder_none_rotation.publish(Transformation_cylinder_none_rotation);
188
189     //—Publish Tf world to piston (none rotation)
190     Transformation_piston_none_rotation.data.clear();
191     for (int i = 0; i < 16; i++)
192     {
193     Transformation_piston_none_rotation.data.push_back(↔
194         Transformation_world_piston_none_rotation[i]);
195     }
196     publisher_piston_none_rotation.publish(Transformation_piston_none_rotation);
197
198     //—Publish Tf world to webcam (cylinder)
199     array_transformation_table_webcam_cylinder.data.clear();
200     for (int i = 0; i < 16; i++)
201     {
202     array_transformation_table_webcam_cylinder.data.push_back(↔
203         Transformation_table_webcam_piston[i]);
204     }
205     publisher_transformation_table_webcam_cylinder.publish(↔
206         array_transformation_table_webcam_cylinder);
207
208     //—Publish Tf world to webcam (piston)
209     array_transformation_table_webcam_piston.data.clear();
210     for (int i = 0; i < 16; i++)
211     {
212     array_transformation_table_webcam_piston.data.push_back(↔
213         Transformation_world_piston_none_rotation[i]);
214     }
215     publisher_transformation_table_webcam_piston.publish(↔
216         array_transformation_table_webcam_piston);

```



```
217
218
219
220
221
222
223 private:
224     ros::NodeHandle n;
225     ros::Publisher publisher_cylinder;
226     ros::Publisher publisher_piston;
227     ros::Subscriber sub_coord_cylinder ;
228     ros::Subscriber sub_coord_piston;
229     ros::Subscriber sub_orientation_piston;
230     ros::Subscriber subnh ;
231     ros::Publisher publisher_cylinder_none_rotation;
232     ros::Publisher publisher_piston_none_rotation;
233     ros::Publisher publisher_transformation_table_webcam_piston;
234     ros::Publisher publisher_transformation_table_webcam_cylinder;
235
236
237 };
238
239 int main(int argc, char **argv)
240 {
241
242     //Initiate ROS. The node name is "Publish_transformations"
243     ros::init(argc, argv, "Publish_transformations");
244
245
246     //Create an object of class SubscribeAndPublish that will take care of everything
247     SubscribeAndPublish SAPObject;
248     ros::spin();
249
250     return 0;
251 }
```

```

1  //-----
2  //----- Node run for publishing the end effector poses for both robots-----
3  //-----
4  //-----
5  //-----Authors: Geir Ole Tysse and Martin Morland .-----
6  //-----NINU 2015-----
7  //-----
8
9  #include <ros/ros.h>
10 #include <pcl_ros/point_cloud.h>
11 #include <ros/ros.h>
12 #include <iostream>
13 #include <limits>
14 #include <fstream>
15 #include <vector>
16 #include <armadillo>
17 #include <sstream>
18 #include "std_msgs/String.h"
19 #include "std_msgs/Float64MultiArray.h"
20 #include <stdio.h>
21 #include <stdlib.h>
22 #include <string>
23 #include <cmath>
24 #include "std_msgs/MultiArrayLayout.h"
25 #include "std_msgs/MultiArrayDimension.h"
26 #include "std_msgs/Int32MultiArray.h"
27 #include <armadillo>
28
29 using namespace std;
30 using namespace arma;
31
32 std_msgs::Float64MultiArray Transformation_cylinder;
33 std_msgs::Float64MultiArray Transformation_piston;
34 std_msgs::Float64MultiArray array_transformation_world_end_effector_webcam_cylinder;
35 std_msgs::Float64MultiArray array_transformation_world_end_effector_webcam_piston;
36 mat Transformation_gripper_end_effector(4,4);
37 mat Transformation_parts_gripper(4,4);
38 mat Transformation_end_effector_web_cam(4,4);
39 mat Transformation_world_table(4,4);
40 mat Transformation_table_webcam_piston(4,4);
41 mat Transformation_table_webcam_cylinder(4,4);
42 mat Transformation_ag2_world_end_effector_cylinder(4,4);
43 mat Transformation_world_end_effector_piston(4,4);
44 mat Transformation_world_cylinder(4,4);
45 mat Transformation_ag2_world_end_effector_piston(4,4);
46 mat Transformation_ag1_world_end_effector_cylinder(4,4);
47 mat Transformation_world_piston(4,4);
48 mat Transformation_ag1_world_end_effector_piston(4,4);
49
50
51 //--- The class
52 //-----
53 class SubscribeAndPublish
54 {
55 public:
56
57
58
59     SubscribeAndPublish()
60     {
61         //--- Tf from gripper to end effector

```

```

62 Transformation_gripper_end_effector << 1 << 0 << 0 << 0 << arma::endr
63     << 0 << 1 << 0 << 0 << arma::endr
64     << 0 << 0 << 1 << -0.16 << arma::endr
65     << 0 << 0 << 0 << 1 << arma::endr;
66
67     //— Tf from gripper to 2D camera
68 Transformation_end_effector_web_cam << 1 << 0 << 0 << 0 << arma::endr
69     << 0 << 1 << 0 << -0.028 << arma::endr
70     << 0 << 0 << 1 << 0.01 << arma::endr
71     << 0 << 0 << 0 << 1 << arma::endr;
72
73     //— Tf from world to table
74 Transformation_world_table << 0 << -1 << 0 << 0.67562 << arma::endr
75     << 1 << 0 << 0 << -0.39624 << arma::endr
76     << 0 << 0 << 1 << 0.938 << arma::endr
77     << 0 << 0 << 0 << 1 << arma::endr;
78
79 //— Topics beeing subscribed and published to
80 subscriber_transformation_table_webcam_piston=n.subscribe("↵
    Transformation_table_webcam_piston", 1,&SubscribeAndPublish::↵
    CallbackWebcam_piston, this);
81 subscriber_transformation_table_webcam_cylinder=n.subscribe("↵
    Transformation_table_webcam_cylinder", 1,&SubscribeAndPublish::↵
    CallbackWebcam_cylinder, this);
82 sub_coord_cylinder = n.subscribe("cylinder_pose_with_respect_to_world", 1, &↵
    SubscribeAndPublish::CallbackCylinder, this);
83 sub_coord_piston = n.subscribe("piston_pose_with_respect_to_world", 1, &↵
    SubscribeAndPublish::CallbackPiston, this);
84 publisher_gripper_cylinder = n.advertise<std_msgs::Float64MultiArray>("↵
    End_Effector_pose_cylinder_ag1", 1);
85 publisher_gripper_piston = n.advertise<std_msgs::Float64MultiArray>("↵
    End_Effector_pose_piston_ag1", 1);
86 publisher_cam_cylinder = n.advertise<std_msgs::Float64MultiArray>("↵
    End_Effector_pose_cylinder_ag2", 1);
87 publisher_cam_piston = n.advertise<std_msgs::Float64MultiArray>("↵
    End_Effector_pose_piston_ag2", 1);
88 }
89
90 void CallbackWebcam_cylinder(const std_msgs::Float64MultiArray::ConstPtr& msg)
91 {
92     //— TF webcam to cylinder when doing orientation analysis
93 Transformation_table_webcam_cylinder << msg->data[0] << msg->data[4] << msg->data[8] <<↵
    msg->data[12] << arma::endr
94     << msg->data[1] << msg->data[5] << msg->data[9] << msg->data[13] << arma::endr
95     << msg->data[2] << msg->data[6] << msg->data[10] << msg->data[14] << arma::endr
96     << msg->data[3] << msg->data[7] << msg->data[11] << msg->data[15] << arma::endr;
97
98     //— TF world to end-effector when doing orientation analysis
99 Transformation_ag2_world_end_effector_cylinder=Transformation_world_table*↵
    Transformation_table_webcam_cylinder*inv(Transformation_end_effector_web_cam);
100
101 //— Publish TF world to end-effector when doing orientation analysis
102 array_transformation_world_end_effector_webcam_cylinder.data.clear();
103 for (int i = 0; i < 16; i++)
104 {
105
106 array_transformation_world_end_effector_webcam_cylinder.data.push_back(↵
    Transformation_ag2_world_end_effector_cylinder[i]);
107 }
108 publisher_cam_cylinder.publish(array_transformation_world_end_effector_webcam_cylinder↵
    );

```

```

109
110 }
111
112
113 void CallbackWebcam_piston(const std_msgs::Float64MultiArray::ConstPtr& msg)
114 {
115     //— TF webcam to piston when doing orientation analysis
116     Transformation_table_webcam_piston << msg->data[0] << msg->data[4] << msg->data[8] << msg->data[12] << arma::endr
117     << msg->data[1] << msg->data[5] << msg->data[9] << msg->data[13] << arma::endr
118     << msg->data[2] << msg->data[6] << msg->data[10] << msg->data[14] << arma::endr
119     << msg->data[3] << msg->data[7] << msg->data[11] << msg->data[15] << arma::endr;
120
121     //— TF world to end-effector when doing orientation analysis
122     Transformation_ag2_world_end_effector_piston=Transformation_world_table*
123     Transformation_table_webcam_piston*inv(Transformation_end_effector_web_cam);
124
125     //— Publish TF world to end-effector when doing orientation analysis
126     array_transformation_world_end_effector_webcam_piston.data.clear();
127     for (int i = 0; i < 16; i++)
128     {
129     array_transformation_world_end_effector_webcam_piston.data.push_back(
130     Transformation_ag2_world_end_effector_piston[i]);
131     }
132     publisher_cam_piston.publish(array_transformation_world_end_effector_webcam_piston);
133 }
134
135 void CallbackCylinder(const std_msgs::Float64MultiArray::ConstPtr& msg)
136 {
137     //— Tf world to cylinder
138     Transformation_world_cylinder << msg->data[0] << msg->data[4] << msg->data[8] << msg->data[12] << arma::endr
139     << msg->data[1] << msg->data[5] << msg->data[9] << msg->data[13] << arma::endr
140     << msg->data[2] << msg->data[6] << msg->data[10] << msg->data[14] << arma::endr
141     << msg->data[3] << msg->data[7] << msg->data[11] << msg->data[15] << arma::endr;
142
143     //— Tf world to end-effector (cylinder)
144     Transformation_ag1_world_end_effector_cylinder=Transformation_world_cylinder*
145     Transformation_parts_gripper*Transformation_gripper_end_effector;
146
147     //— Publish TF world to end-effector grasping piston
148     Transformation_cylinder.data.clear();
149     for (int i = 0; i < 16; i++)
150     {
151     Transformation_cylinder.data.push_back(Transformation_ag1_world_end_effector_cylinder[i]);
152     }
153     publisher_gripper_cylinder.publish(Transformation_cylinder);
154 }
155
156 void CallbackPiston(const std_msgs::Float64MultiArray::ConstPtr& msg)
157 {
158     //— Tf world to piston
159     Transformation_world_piston << msg->data[0] << msg->data[4] << msg->data[8] << msg->data[12] << arma::endr
160     << msg->data[1] << msg->data[5] << msg->data[9] << msg->data[13] << arma::endr
161     << msg->data[2] << msg->data[6] << msg->data[10] << msg->data[14] << arma::endr
162     << msg->data[3] << msg->data[7] << msg->data[11] << msg->data[15] << arma::endr;

```

```

163     //— Tf world to end-effector (piston)
164     Transformation_ag1_world_end_effector_piston =Transformation_world_piston*←
        Transformation_parts_gripper*Transformation_gripper_end_effector;
165
166     //— Publish TF world to end-effector grasping cylinder
167     Transformation_piston.data.clear();
168     for (int i = 0; i < 16; i++)
169     {
170     Transformation_piston.data.push_back(Transformation_ag1_world_end_effector_piston[i]);
171     }
172
173     publisher_gripper_piston.publish(Transformation_piston);
174
175     }
176
177
178
179
180
181
182
183
184     private:
185     ros::NodeHandle n;
186     ros::Publisher publisher_gripper_cylinder;
187     ros::Publisher publisher_gripper_piston;
188     ros::Subscriber sub_coord_cylinder ;
189     ros::Subscriber sub_coord_piston;
190     ros::Subscriber sub_orientation_piston;
191     ros::Subscriber subnh ;
192     ros::Publisher publisher_cam_cylinder;
193     ros::Publisher publisher_cam_piston;
194     ros::Subscriber subscriber_cylinder_none_rotation;
195     ros::Subscriber subscriber_piston_none_rotation;
196     ros::Subscriber subscriber_transformation_table_webcam_piston;
197     ros::Subscriber subscriber_transformation_table_webcam_cylinder;
198
199
200     };
201
202     int main(int argc, char **argv)
203     {
204
205     //Initiate ROS. The node name is "Pointcloud"
206     ros::init(argc, argv, "Publish_end_effector_poses");
207
208     //Create an object of class SubscribeAndPublish that will take care of everything
209     SubscribeAndPublish SAPObject;
210     ros::spin();
211
212     return 0;
213     }

```

## Bibliography

- [1] Clemons, J. SIFT: Scale invariant feature transform by david lowe. Lecture, Opened 02.10.2014 .
- [2] Corke, P. (2011). *Robotics, Vision and Control*. Springer-Verlag Berlin Heidelberg, 1st edition.
- [3] Dorst, Leo, Fontijne, D. A. M. S. (2007). *Geometric Algebra for Computer Science: An Object-oriented Approach to Geometry*. Morgan Kaufmann Publishers.
- [4] Hartley, R. and Zisserman, A. (2004). *Multiple View Geometry in Computer Vision*. Cambridge University Press, 2nd edition.
- [5] Hecht, J. (2011). Photonic frontiers: Gesture recognition: Lasers bring gesture recognition to the home. <http://www.laserfocusworld.com/articles/2011/01/lasers-bring-gesture-recognition-to-the-home.html>. [Online; accessed 14-April-2015].
- [6] Holz, D., Holzer, S., Rusu, R. B., and Behnke, S. (2012). Real-time plane segmentation using rgb-d cameras. In *RoboCup 2011: Robot Soccer World Cup XV*, pages 306–317. Springer.
- [7] Kim, J., Nguyen, H. H., Lee, Y., and Lee, S. (2013). Structured light camera base 3d visual perception and tracking application system with robot grasping task. In *Assembly and Manufacturing (ISAM), 2013 IEEE International Symposium on*, pages 187–192. IEEE.
- [8] Ko, D.-I. and Agarwal, G. (2012). Gesture recognition: Enabling natural interactions with electronics.
- [9] Kuka (2014). KR C4 compacts. [http://www.kuka-robotics.com/res/sps/94de4d6a-e810-4505-9f90-b2d3865077b6\\_Spez\\_KR\\_C4\\_compact\\_en.pdf](http://www.kuka-robotics.com/res/sps/94de4d6a-e810-4505-9f90-b2d3865077b6_Spez_KR_C4_compact_en.pdf). [Online; accessed 12-March-2015].
- [10] Lin, C.-Y. and Setiawan, E. (2009). Object orientation recognition based on sift and svm by using stereo camera. In *Robotics and Biomimetics, 2008. ROBIO 2008. IEEE International Conference on*, pages 1371–1376. IEEE.
- [11] Lowe, D. (2004). Distinctive image features from scale-invariant keypoints. *International journal of computer vision* 60, no. 2.
- [12] MoveIt! MoveIt! home page. <http://moveit.ros.org/>. [Online; accessed 22-May-2015].

- [13] Omidalizarandi, M. and Saadatseresht, M. (2013). Segmentation and classification of point clouds from dense aerial image matching. *The International Journal of Multimedia & Its Applications*, 5(4):33.
- [14] OpenCV (2014). Features2D + Homography to find a known object. [http://docs.opencv.org/doc/tutorials/features2d/feature\\_homography/feature\\_homography.html](http://docs.opencv.org/doc/tutorials/features2d/feature_homography/feature_homography.html). [Online; accessed 08-April-2015].
- [15] OpenCV (2015). Open Source Computer Vision. <http://opencv.org/>. [Online; accessed 12-March-2015].
- [16] Patnaik, S. and Zhong, B. (2014). *Soft Computing Techniques in Engineering Applications*, volume 543. Springer.
- [17] Payen de La Garanderie, G. and Breckon, T. (2014). Improved depth recovery in consumer depth cameras via disparity space fusion within cross-spectral stereo. In *Proceedings of the British Machine Vision Conference*. BMVA Press.
- [18] PCL (2013). Point Cloud Library. <http://pointclouds.org/>. [Online; accessed 19-May-2015].
- [19] Rabbani, T., van den Heuvel, F., and Vosselmann, G. (2006). Segmentation of point clouds using smoothness constraint. *International Archives of Photogrammetry, Remote Sensing and Spatial Information Sciences*, 36(5):248–253.
- [20] Radke, R. J. (2013). *Computer vision for visual effects*. Cambridge, 1st edition.
- [21] Robots, K. I. (2015). KR AGILUS sixx. [http://www.kuka-robotics.com/res/sps/e6c77545-9030-49b1-93f5-4d17c92173aa\\_Spez\\_KR\\_AGILUS\\_sixx\\_en.pdf](http://www.kuka-robotics.com/res/sps/e6c77545-9030-49b1-93f5-4d17c92173aa_Spez_KR_AGILUS_sixx_en.pdf). [Online; accessed 15-May-2015].
- [22] ROS. ROS home page. <http://wiki.ros.org/>. [Online; accessed 10-May-2015].
- [23] Rusu, R. B. (2009). *Semantic 3D Object Maps for Everyday Manipulation in Human Living Environments*. PhD thesis, Technischen Universität München, München.
- [24] Rusu, R. B., Blodow, N., and Beetz, M. (2009). Fast point feature histograms (fpfh) for 3d registration. In *Robotics and Automation, 2009. ICRA '09. IEEE International Conference on*, pages 3212–3217. IEEE.
- [25] Rusu, R. B., Blodow, N., Marton, Z. C., and Beetz, M. (2008). Aligning point cloud views using persistent feature histograms. In *Intelligent Robots and Systems, 2008. IROS 2008. IEEE/RSJ International Conference on*, pages 3384–3391. IEEE.
- [26] Shao, L., Han, J., Kohli, P., and Zhang, Z. (2014). *Computer Vision and Machine Learning with RGB-D Sensors*. Springer.
- [27] Stückler, J., Steffens, R., Holz, D., and Behnke, S. (2013). Efficient 3d object perception and grasp planning for mobile manipulation in domestic environments. *Robotics and Autonomous Systems*, 61(10):1106–1115.

- [28] Tutorial, A. I., Perwass, C. B., and Hildenbrand, D. (2004). Aspects of geometric algebra in euclidean, projective and conformal space.
- [29] Ugolotti, R., Micconi, G., Aleotti, J., and Cagnoni, S. (2014). Gpu-based point cloud recognition using evolutionary algorithms. In *Applications of Evolutionary Computation*, pages 489–500. Springer.
- [30] Vince, J. (2009). *Geometric Algebra: An Algebraic System for Computer Games and Animation*. Springer, 1st edition.